

UCSF

UC San Francisco Electronic Theses and Dissertations

Title

Molecular genetic analysis of chemosensory behaviors in *C. elegans*

Permalink

<https://escholarship.org/uc/item/44s572rx>

Author

Chou, Joseph H.

Publication Date

1998

Peer reviewed|Thesis/dissertation

Molecular Genetic Analysis of
Chemosensory Behaviors in *C. elegans*

by

Joseph H. Chou

DISSERTATION

Submitted in partial satisfaction of the requirements for the degree of

DOCTOR OF PHILOSOPHY

in

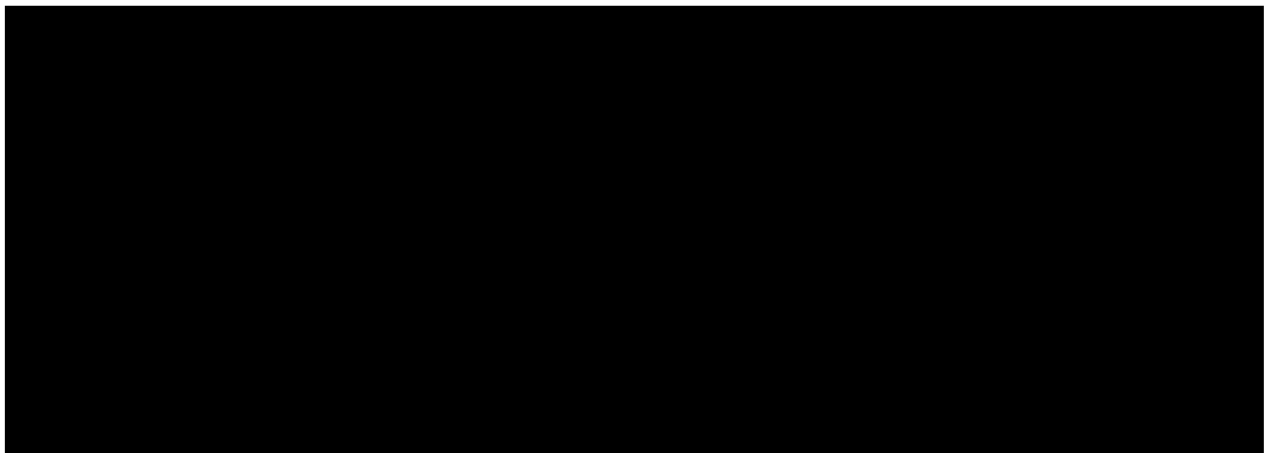
Biochemistry

in the

GRADUATE DIVISION

of the

UNIVERSITY OF CALIFORNIA SAN FRANCISCO



Date

University Librarian

Degree Conferred:

Copyright © 1998

by

Joseph H. Chou

This thesis is dedicated to my wife.

Acknowledgments

So many people have helped me during my graduate training, it is difficult to adequately thank them all. I am immensely indebted to my graduate advisor, Cori Bargmann, for her guidance, support, and encouragement over the years. Her standards of excellence, encyclopedic knowledge, love of opera, and appreciation of Glenn Gould are just a few of the aspects that I most admire.

I would like to thank the members of my thesis committee, Ira Herskowitz and Lily Jan, for their insight into the multiple projects of my thesis. David Cox and Tris Parslow have done an outstanding job directing the Medical Scientist Training Program, and Sue Adams, Jana Toutolmin, Michelle Roberts, and Caroline Murphy have all eased the bureaucratic burdens of being part of UCSF.

I would like to acknowledge all the past and present members of the Bargmann Lab for creating an atmosphere that perfectly combined competence and insanity. A few individuals deserve special mention: Kayvan Roayaie for our “business lunches” at great restaurants and cafés, late-night hallway hockey, at the buzzer last ski runs, expertise in the fine art of slacking, and overall maintenance of sanity; Piali Sengupta for being an incredible role model in science; Erin Peckol for her unique outlook on lab, life, the world, and everything; Tim Yu for grueling mountain bike runs and for reminding me that graduate students don’t have to be jaded; and Villu Maricq for teaching me humility at the pool table. I am grateful to Kate Wesseling, Penny Mapa, Liqin Tong, Shannon Grantner, and Yongmei Zhang, for their expert technical assistance.

There are many people at UCSF whose friendship has enriched my time here. Hernan Espinoza, Louise (and Marc and Clara) Laurent, José de la Torre, and Luke Hoffman have all reminded me how much fun there is to be had in San Francisco. I’d like to thank Joyce Liao, Alfred Kuo, Sarah

Mutka, Tracy Ware, Sondra Vazirani, and Chris Leptak, for good company, commiseration, and companionship.

Because I am awful at keeping in touch with people, Liddy Olds, Aaron Lamport, and Rick Chang deserve special thanks for their perseverance in maintaining contact despite the miles and the years. In particular, I'd like to thank Tom Conlan, my hiking buddy, confidant, and friend: given the choice between scrambling up the stinging nettle and poison oak-infested cliff or wading around the point, I still think we could have made it without being swept off to sea.

Thinking back on my years in San Francisco, I have many fond memories of both people and places. For all the good times and good food, those who know me will understand my desire to pay tribute to the following establishments: Art's Cafe, Avenue 9, The Beanery, Brother's BBQ, Cafe Chez Panisse, Caffe Greco, Casa Aguila, Cha Cha Cha, Chevys, Crescent City Cafe, Des Alpes, Dottie's True Blue Cafe, Doug's BBQ, Golden Gate Bakery, Guaymas, Harbor Village, Helmand, House, House of Nanking, Kate's Kitchen, Kim's BBQ, La Taqueria, LuLu, M's Cafe, Mamaya, Marnee Thai, Maykadeh, McDonald's, Mescolanza, Minh Garden, Minh Tri, Plouf, San Tung Dumpling Restaurant, Thanh Long, Ti Couz, Ton Kiang, Vicolo, Vietnam II, Woodward's Garden, Yuet Lee, Zachary's, and all the others.

Most importantly, I'd like to thank my mother, father, and sister. Without their support, advice, understanding, and encouragement, I could not have reached this point. And finally, no words can adequately express my gratitude to Jean Chang, my wife, who has so enriched my life, lent me her strength, and reminded me what truly matters.

513 Parnassus Avenue, S-1471
Department of Anatomy
University of California
San Francisco, CA 94143-0452
(415) 476-3557

29 May 1998

Editorial Offices
Cell
1050 Massachusetts Avenue
Cambridge, MA 02138
FAX: (617) 661-7061

To whom it may concern:

I would like permission to include in my dissertation a copy of the following papers, which were published in Cell:

Sengupta, P., Chou, J. H., and Bargmann, C. I. (1996). odr-10 encodes a seven transmembrane domain olfactory receptor required for responses to the odorant diacetyl. *Cell* 84, 899-909.

Troemel, E. R., Chou, J. H., Dwyer, N. D., Colbert, H. A., and Bargmann, C. I. (1995). Divergent seven transmembrane receptors are candidate chemosensory receptors in *C. elegans*. *Cell* 83, 207-18.

The dissertation will be bound and placed in the University campus library and be microfilmed by University Microfilms International for distribution of single copies upon request.

Please respond by fax to (415) 476-3493. Thank you for your consideration.

Sincerely,

Joseph Chou

Joseph Chou
for Cell Press

SUN 09 1998

Permission granted subject to citation of the original manuscript, and notation that copyright is held by Cell Press. Our permission is contingent on permission of the author.

513 Parnassus Avenue, S-1471
Department of Anatomy
University of California
San Francisco, CA 94143-0452
(415) 476-3557

29 May 1998

Permissions Office of the Proceedings
2101 Constitution Avenue, NW
Washington, DC 20418
FAX: (202) 625-4749

To whom it may concern:

I would like permission to include in my dissertation a copy of the following paper, which was published in the Proceedings of the National Academy of Sciences, USA:

Zhang, Y., Chou, J. H., Bradley, J., Bargmann, C. I., and Zinn, K. (1997). The *Caenorhabditis elegans* seven-transmembrane protein ODR-10 functions as an odorant receptor in mammalian cells. *Proc Natl Acad Sci U S A* **94**, 12162-7.

The dissertation will be bound and placed in the University campus library and be microfilmed by University Microfilms International for distribution of single copies upon request.

Please respond by fax to (415) 476-3493. Thank you for your consideration.

Sincerely,

Joseph Chou

Permission granted. Please cite full
journal reference and "Copyright (year)
National Academy of Sciences, U.S.A."

Diane M. Sullenberger, Managing Editor
DAB for DMS 6/4/98

Abstract

Molecular genetic analysis of chemosensory behaviors in *C. elegans*

by Joseph H. Chou

The soil nematode *Caenorhabditis elegans* uses just two pairs of chemosensory neurons, AWA and AWC, to respond to a large number of volatile attractants. In this dissertation, behavioral and molecular genetic approaches were used to study the mechanisms of chemotaxis.

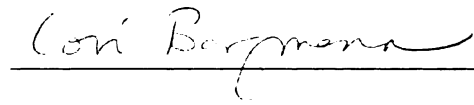
Genetic ablation of distinct sets of neurons demonstrated that a single class of chemosensory neuron can discriminate among multiple odorants, implying the existence of multiple ligand binding sites on each sensory neuron and suggesting the presence of odorant-specific downregulation pathways. However, some forms of olfactory discrimination require input from multiple sensory neurons.

A molecular basis for recognizing diverse ligands was suggested by identification of a large family of divergent candidate G protein-coupled receptors that are expressed in chemosensory neurons. Consistent with the discriminatory ability noted previously, single chemosensory neurons can express multiple receptors.

A genetic approach was used to identify a seven transmembrane receptor, ODR-10, required for responses to diacetyl. The specificity of its mutant phenotype and expression in the AWA chemosensory neurons strongly supported the identification of ODR-10 as the *C. elegans* diacetyl receptor. Heterologous expression and functional characterization of ODR-10 in mammalian cells provided proof that ODR-10 can act as an olfactory receptor for diacetyl. Comparison of ODR-10 function *in vivo* and *in vitro* suggests that additional factors contribute to ligand specificity.

G protein-coupled receptor phosphorylation is a well-characterized mechanism for desensitization. Site-directed mutagenesis of ODR-10 was employed to determine the role of phosphorylation in chemosensory behaviors. All carboxy terminal serine and threonine potential phosphorylation sites were dispensable for ODR-10-mediated chemotaxis, discrimination, and adaptation. In contrast, mutation of two potential phosphorylation sites in the third intracellular loop abolished chemotaxis without affecting discriminatory ability.

The *odr-2* gene is required for behaviors mediated by the AWC chemosensory neurons. To identify new molecules involved in olfaction, *odr-2* was cloned and characterized. *odr-2* encodes an alternatively spliced, neuronally-expressed protein with distant similarity to the Ly-6 superfamily of extracellular proteins.

A handwritten signature in cursive script, reading "Cori Bergman", is positioned above a horizontal line.

Graduate Advisor

Table of Contents

Introduction	1
Olfactory Receptors	2
G protein-coupled signal transduction during olfaction.....	6
Vomeronasal receptors and signal transduction	10
Regulation of G protein-coupled receptor signaling	11
<i>C. elegans</i> as a model system for studying behavior	20
Overview of this thesis	25
Chapter 1. Divergent seven transmembrane receptors are candidate chemosensory receptors in <i>C. elegans</i>	27
Chapter 2. <i>odr-10</i> encodes a seven transmembrane domain olfactory receptor required for responses to the odorant diacetyl.	40
Chapter 3a. The <i>Caenorhabditis elegans</i> seven-transmembrane protein ODR-10 functions as an odorant receptor in mammalian cells.	52
Chapter 3b. Ligand specificity of ODR-10 in <i>C. elegans</i>	59
<i>odr-10</i> is neither necessary nor sufficient to sense pyruvic acid.	59
Ectopic expression of ODR-10 does not alter pyruvic acid chemotaxis	60
Pyruvic acid and diacetyl do not compete effectively with each other for receptor binding or signaling.	60
Chapter 4. Mechanisms of olfactory discrimination: behavioral and mutational analysis.....	68
Genetic ablation of chemosensory neuron function.....	71
The AWA sensory neurons can discriminate between multiple odorants	71
The AWC sensory neurons can discriminate between multiple odorants.....	72

Animals possessing only AWC display some loss of discrimination	72
Molecular mechanisms of discrimination	73
Cassette mutagenesis of <i>odr-10</i>	73
Effect of ODR-10 alterations on chemotaxis to low concentrations of diacetyl.....	74
Discrimination between diacetyl and pyrazine is unaffected by the altered forms of ODR-10	75
Adaptation to diacetyl is unaffected by the altered forms of ODR-10	76
 Chapter 5. <i>odr-2</i> : a novel gene required for chemotaxis	 94
Molecular cloning of <i>odr-2</i>	98
Sequence analysis of <i>odr-2</i> cDNAs	99
Genomic organization of <i>odr-2</i>	100
<i>odr-2</i> is predicted to encode a novel extracellular protein linked to the plasma membrane via a glycosylphosphatidyl inositol anchor.	100
ODR-2 may share structural similarity with the Ly-6 superfamily of proteins	101
Identification of mutations	101
ODR-2 is widely expressed in neurons	102
ODR-2 isoforms can functionally substitute for one another	103
Complex regulation of <i>odr-2</i> expression	104
No neuroanatomical defects are observed in <i>odr-2</i> (<i>n2145</i>) mutants	106
A family of <i>odr-2</i> -related genes in <i>C. elegans</i>	106
 Perspectives and future directions	 145
 Bibliography	 150

List of Figures and Tables

Chapter 3.

Figure 3-1. Pyruvic acid chemotaxis does not depend on <i>odr-10</i> and is not affected by ectopic expression of ODR-10.	65
Figure 3-2. Pyruvic acid chemotaxis requires AWC chemosensory neuron function.	66
Figure 3-3. High concentrations of pyruvic acid do not interfere with diacetyl chemotaxis.	67

Chapter 4.

Figure 4-1. Odorant discrimination by animals possessing only AWA chemosensory neuron function.	86
Figure 4-2. Odorant discrimination by animals possessing only AWC chemosensory neuron function.	88
Figure 4-3. Putative topology of ODR-10 and summary of mutagenesis.	90
Figure 4-4. Diacetyl chemotaxis rescue mediated by ODR-10 altered by site-directed mutagenesis.	91
Figure 4-5. Discrimination between pyrazine and diacetyl is unaffected by ODR-10 mutation.	92
Figure 4-6. Diacetyl adaptation is unaffected by alterations of ODR-10.	93

Chapter 5.

Table 5-1. Cysteine spacing in the Ly-6 superfamily.	122
Figure 5-1. Rescue of the <i>odr-2</i> benzaldehyde chemotaxis defect.	124
Figure 5-2. Exon sequence of the <i>odr-2</i> isoforms.	126
Figure 5-3. Genomic organization of <i>odr-2</i> and summary of chemotaxis experiments.	128

Figure 5-4. Hydrophobicity plots of the ODR-2 isoforms.	129
Figure 5-5. The solution structure of soluble CD59.	130
Figure 5-6. Epitope-tagged ODR-2 rescues the isoamyl alcohol chemotaxis defect.	132
Figure 5-7. Expression of epitope-tagged ODR-2.	134
Figure 5-8. ODR-2 expressed in AWC does not rescue isoamyl alcohol chemotaxis.	135
Figure 5-9. Coding and regulatory regions required for <i>odr-2</i> rescue.	136
Figure 5-10. ODR-2 isoforms can functionally substitute for one another.	137
Figure 5-11. Expression of <i>odr-2</i> and <i>hot-1a</i> GFP fusion constructs.	139
Figure 5-12. The <i>n1939</i> mutation is sufficient to abolish <i>odr-2</i> function.	140
Figure 5-13. Sequence alignment of the ODR-2 family of proteins.	142
Figure 5-14. Hydrophobicity plots of the <i>odr-2</i> paralogs in <i>C. elegans</i>	144

Introduction

Fundamental to the survival of any living organism is the ability to sense relevant stimuli in its environment and to respond appropriately. Simple unicellular organisms such as *Escherichia coli* can detect a food source, chemotax towards it, and alter gene expression to make available pertinent metabolic enzymes. Billions of years of evolution have endowed animals with complex nervous systems that can detect, process, and respond to the sensory modalities of light, sound, touch, taste, and smell.

The mammalian olfactory system is remarkable in its ability to recognize thousands of structurally unrelated compounds while maintaining the ability to discriminate among many or most of them. How can these opposing requirements of wide sensitivity and precise specificity be explained in molecular terms? Research during the last decade has elucidated much about the initial events of olfactory signal transduction. Notably, certain aspects of signal transduction are conserved in species as divergent as worms, frogs, fish, and mice. At the same time, enormous diversity exists within and between different species at the level of the olfactory receptor proteins.

How is an extracellular stimulus converted into an intracellular signal? One mechanism, G protein-coupled receptor signal transduction, has been adapted to detect such divergent stimuli as peptides, hormones, neurotransmitters, and photons of light, and is conserved in organisms from yeast to humans. Studies in the last fifteen years indicate that this pathway is used for the detection of odorants as well.

The following section introduces the components of vertebrate olfactory signal transduction and reviews the mechanisms by which this signaling might be regulated. Subsequently, I review use of the free-living soil nematode *Caenorhabditis elegans* as a model system for studying not only the

initial events of chemosensation, but also as a means towards understanding the generation of behavior.

Olfactory Receptors

Molecular identification of odorant receptors

A major step forward in explaining the extraordinary range of sensed odorants came with the identification of a large family of genes that are likely to encode olfactory receptors (Buck and Axel, 1991). In a landmark study, 18 genes whose expression was limited to the rat olfactory epithelium were shown to encode seven-transmembrane proteins with short conserved motifs found in previously identified G protein-coupled receptors. Genomic hybridization using the initial set of cloned genes suggested that the gene family was likely to number in the hundreds. Subsequent identification of additional mammalian receptor subfamilies suggests that the total repertoire may be as many as a thousand (Levy et al., 1991; Parmentier et al., 1992). Similar receptor families have been identified in other vertebrate species, including catfish (Ngai et al., 1993b), frogs (Freitag et al., 1995), mice (Ressler et al., 1993), and humans (Parmentier et al., 1992; Ben-Arie et al., 1994). However, homologous receptors have not been identified to date in any invertebrate species.

The extraordinary sequence variability in this family of genes (Buck and Axel, 1991) may reflect the need for olfactory receptors to detect the large universe of structurally dissimilar odorants.

Organization of olfactory receptor expression and neuronal projections

How many types of receptors does each olfactory neuron express? Odorant receptor RNAs were localized in the olfactory epithelium of mice and catfish by *in situ* hybridization. In both cases, the fraction of neurons detected using subfamily-specific receptor probes corresponded with the reciprocal of the predicted receptor family size (Ngai et al., 1993a; Ressler et al., 1993). In addition, hybridization with four receptor subfamily probes indicated that each subfamily was expressed

in largely non-overlapping set of neurons (Ngai et al., 1993a). PCR amplification of limiting dilutions of isolated olfactory neurons confirmed that only 1 in 1,700 neurons expresses the I7 receptor gene (Chess et al., 1994; J.H.C., calculation not shown). Together, these experiments suggest that individual olfactory neurons express only a few, perhaps a single, olfactory receptor.

Since the identity of a perceived odorant is encoded by the set of olfactory receptors it activates, this tight control of receptor expression is likely to be necessary for maintaining specificity of olfactory discrimination. If each cell expresses only one type of receptor, the problem of identifying which receptors have responded to an odorant is simplified to identifying which neurons are activated.

Considering the predicted importance of identifying precisely which receptors are activated, it was surprising that the *in situ* hybridization experiments above also demonstrated that receptor expression was not highly organized in the olfactory epithelium. In mice and rats, expression of receptor subfamilies appeared to be limited to one of four circumscribed zones, but within these zones expression appeared to be randomly distributed (Ressler et al., 1993; Vassar et al., 1993). In catfish, expression of a given receptor may be randomly distributed throughout the entire olfactory epithelium (Ngai et al., 1993a). However, experiments in zebrafish that more precisely compensate for distortion of sections used for *in situ* hybridization suggest that fish olfactory receptors are expressed in broadly overlapping concentric zones (Weth et al., 1996).

The olfactory system possesses additional opportunities for spatial organization. Each olfactory sensory neuron in the olfactory epithelium projects a single unbranched axon to synapse on second-order neurons in the olfactory bulb. At the surface of the bulb, spherical neuropil called glomeruli represent collections of several thousand of these synapses.

Receptor subfamily probes hybridizing with mRNA in the sensory axon terminals at the olfactory bulb of rats and mice were used to map the projections of the population of sensory neurons expressing those receptors. This technique demonstrated that axons from neurons expressing the

same receptors organize to converge onto very few bilaterally symmetric glomeruli on the olfactory bulb (Ressler et al., 1994; Vassar et al., 1994). Additionally, the topographic map of olfactory receptor expression is constant between individuals within a species. Based on the number of glomeruli detected and the number of receptors in each receptor subfamily, it is possible that the axonal projections of all sensory neurons expressing a given olfactory receptor converge onto two glomeruli in each olfactory bulb, one lateral and one medial. Consistent with this hypothesis, transgenic mice that express LacZ bicistronically with a specific olfactory receptor gene reveal that all olfactory sensory neurons expressing that gene project axons that converge on two topographically fixed glomeruli in each bulb (Mombaerts et al., 1996). The olfactory receptors play an instructive role in the precise convergence of sensory axons to specific glomeruli, as transgenic mice with olfactory receptor swaps, deletions, or nonsense mutations exhibit altered glomerular targeting (Mombaerts et al., 1996; Wang et al., 1998).

Odorant specificity and information coding

Since the number of distinct odorants that can be detected by mammals exceeds the predicted number of olfactory receptors, individual receptors are likely to respond to multiple odorants. A number of studies have attempted to address the question of whether olfactory receptors are broadly tuned or highly specific.

A fundamental problem in assessing the specificity and sensitivity of olfactory receptors to odorants lies in a paradox of interpretation. In order to study receptor activation, one must see a response to odorants. If in physiological conditions, olfactory receptors are extremely sensitive and extremely specific, one is experimentally very unlikely to chance upon the particular odorant that activates a given receptor. Therefore, to generate a measurable response, higher concentrations of odorants are used which nonspecifically activate a larger proportion of receptors, and one erroneously concludes that olfactory receptors are broadly tuned and not highly sensitive. This dilemma must be kept in mind when interpreting the results of olfactory receptor activation experiments.

Initial experiments *in vivo* were consistent with the model of broadly tuned receptors.

Electrophysiological responses of 74 frog olfactory receptor neurons were evaluated in response to 20 different odorants at high concentrations (5–33% of saturated vapor at room temperature) for 2 seconds (Sicard and Holley, 1984). Cells were responsive to multiple compounds and displayed unique profiles of differential sensitivity. In another study, individual tiger salamander olfactory receptor cells were monitored electrophysiologically for response to three odorants at 500 μ M for durations varying from 0.5 to 1.5 seconds (Firestein et al., 1993). These cells responded to anywhere from none to all three of the applied odorants, with more than half responding to at least one odorant.

More recent experiments suggest that olfactory receptors can be significantly more selective. An adenovirus vector was used to deliver a specific olfactory receptor to rat olfactory epithelium *in vivo*, thereby causing over-representation of that receptor in olfactory neurons. Electro-olfactogram recordings demonstrated that from a panel of 74 odorants, increased response was observed to only four closely related odorants (straight chain *n*-heptaldehyde to *n*-decyl aldehyde) (Zhao et al., 1998). Other aldehydes tested, including *n*-hexaldehyde and *n*-undecylic aldehyde, did not elicit increased responses. Odorants were applied in the vapor phase as an 0.1 second pulse from the equilibrated airspace above a 1 to 10 mM liquid odorant source. It was not possible to determine the concentration of the stimulus at the olfactory epithelium. These results demonstrate that for at least one receptor in an experimental system that closely resembles physiological conditions, olfactory receptors can exhibit significant odorant specificity.

Thus, a model for olfactory information coding emerges. Odorants differentially activate subsets of the receptor repertoire. Although expression of each type of activated receptor is broadly distributed throughout the olfactory epithelium, all axons of sensory neurons expressing a given receptor project to a pair of topographically fixed glomeruli. In this way, the identity of a perceived odorant is encoded by discrete patterns of activity at the olfactory bulb.

Direct evidence supporting this model now exists from experiments done in zebrafish (Friedrich and Korsching, 1997). Presynaptic odor-evoked activity of the entire zebrafish olfactory bulb was simultaneously monitored by calcium-sensitive dye labeling of olfactory neurons. Administration of any of 18 amino acids induced a unique activity pattern at the olfactory bulb that was reproducible between different animals. However, all responses to amino acids were limited to a subregion comprising less than 2% of the olfactory bulb; in this region glomeruli are not anatomically well-delineated, and are described as “glomerular modules.” It is unclear whether the rest of the olfactory bulb was not responsive to amino acids or if responses were not detectable using their experimental system. However, individual glomerular modules responded to multiple odorants and exhibited complex response profiles dependent not only on the amino acid applied, but also on the concentration tested, ranging from 10 nM to 100 μ M. Thus, both identity and concentration can be encoded on the olfactory bulb’s topographic map.

Many of these experiments have not addressed the issue of sensitivity. Psychophysical experiments demonstrate a threshold of sensitivity at concentrations many orders of magnitude lower (in the picomolar range) than those used in the above experiments. It remains possible that at high concentrations, olfactory receptors are not as selective, but that at lower, and more physiologically relevant, concentrations, specific receptors may be exquisitely sensitive to individual odorants.

G protein-coupled signal transduction during olfaction

Overview

Odorant recognition by olfactory receptors initiates a transduction cascade that ultimately induces sensory neuron depolarization and generation of action potentials. An extensive literature has conclusively demonstrated that G protein-coupled pathways, which are used for detecting peptides, hormones, neurotransmitters, and photons of light, also transduce vertebrate olfactory signaling.

The key components of this conserved pathway include an integral membrane receptor that spans the plasma membrane seven times and an intracellular guanine nucleotide-binding protein (G protein), composed of a heterotrimer of α , β , and γ subunits (Probst et al., 1992; Strader et al., 1994; Bourne, 1997). In its inactive state, the $G\alpha$ subunit binds GDP. To initiate signaling, extracellular ligand binds the receptor, inducing exchange of GDP for GTP. This nucleotide exchange causes dissociation of the GTP-bound α subunit from the $\beta\gamma$ subunits, and either α or $\beta\gamma$ subunits can activate downstream effects, including enzyme activation or direct gating of ion channels. Effector enzyme activation can produce compounds such as cAMP, IP3, and DAG, which act as second messengers that induce further effects. Signaling ceases when the intrinsic GTPase activity of $G\alpha$ subunits hydrolyzes the bound GTP to GDP, causing reassociation of $G\alpha$ with $G\beta\gamma$.

In the proposed model for vertebrate olfactory transduction, which will be detailed below, odorant binding to seven-transmembrane receptors triggers G protein-mediated activation of adenylyl cyclase. The cAMP produced gates cation channels to initiate membrane depolarization. Many aspects of this model have been confirmed by biochemical analysis of olfactory sensory neurons and many of the components have now been molecularly identified.

$G\alpha_{olf}$, a G protein α subunit required for olfactory transduction.

The seven-transmembrane olfactory receptors mediate detection of odorant molecules, but this interaction is transduced to the cell interior via a G protein heterotrimer. $G\alpha_{olf}$ is a G protein α subunit identified by low stringency screening of a rat olfactory cDNA library (Jones and Reed, 1989). It is highly expressed in sensory neurons of the olfactory epithelium. Like $G\alpha_s$, with which it shares the greatest sequence identity, $G\alpha_{olf}$ activates adenylyl cyclase when expressed in a heterologous system. Its presumed olfactory role in the intact organism was confirmed recently with the generation of transgenic mice deficient in $G\alpha_{olf}$ (Belluscio et al., 1998). These animals exhibit a profound decrease in response to seven structurally distinct odorants, as determined by electro-olfactogram, and are likely functionally anosmic. The mutant mice also display various

behavioral abnormalities that may result both from the olfactory defect as well as defects in $G\alpha_{olf}$ -mediated signal transduction elsewhere in the central nervous system.

Adenylyl cyclase and second messenger production.

One of the earliest indications that olfactory transduction occurs via a G protein-coupled signaling pathway came with the detection of high levels of adenylyl cyclase activity in isolated sensory cilia of frog and rat olfactory epithelium (Pace et al., 1985; Sklar et al., 1986). Notably, odorant application (2.5 to 250 μ M) increased adenylyl cyclase activity, dependent on the presence of GTP.

Experiments using a rapid mix/quench device demonstrated subsecond kinetics of odorant-induced cAMP generation by isolated olfactory cilia from rats (Boekhoff et al., 1990; Breer et al., 1990). This time course is sufficiently rapid to mediate odorant-evoked membrane depolarization, which electrophysiological studies had shown to occur after a latency of several hundred milliseconds (Firestein et al., 1990).

A candidate adenylyl cyclase that mediates olfactory transduction has been cloned by low stringency screening of a rat olfactory cDNA library (Bakalyar and Reed, 1990). This novel adenylyl cyclase (type III) appears to be expressed specifically in olfactory epithelium but not in six other tissues tested. Specific antibodies localize its expression to the olfactory sensory cilia, consistent with a role in transduction.

Cyclic nucleotide-gated ion channels and membrane depolarization

Patch-clamp recordings of frog olfactory sensory cilia revealed a cyclic-nucleotide gated conductance and suggested a direct mechanism by which cAMP could initiate olfactory neuron depolarization (Nakamura and Gold, 1987). Within the olfactory neuron, these cyclic nucleotide-gated channels are 400-fold more concentrated at the sensory cilia than in the dendrite and cell body, as determined by variance analysis of channel activity (Kurahashi and Kaneko, 1991).

Further confirming the role of this conductance in olfactory signaling, cAMP-induced and odorant-evoked whole-cell currents in sensory neurons from the newt and salamander were indistinguishable (Kurahashi, 1990; Firestein et al., 1991).

Two distinct subunits of olfactory cyclic nucleotide-gated channel, α and β , have been cloned from the rat by low stringency olfactory library screens and by degenerate PCR amplification (Dhallan et al., 1990; Bradley et al., 1994; Liman and Buck, 1994). Both subunits are co-expressed primarily in olfactory receptor neurons. Heterologous expression of the α subunit alone yielded channel activity but exhibited functional differences from native olfactory channels. Co-expression of the two subunits, however, yields channel activity more closely resembling the native conductance (Bradley et al., 1994; Liman and Buck, 1994). A second β subunit has been identified from a rat olfactory cDNA library that represents a splice variant of the rod photoreceptor channel that is expressed in olfactory neurons but not in the retina (Sautter et al., 1998). When this β subunit is co-expressed with the previously identified α and β subunits, the resulting channel activity even more closely resembles the native conductance, suggesting that the native olfactory cyclic nucleotide-gated channels exists as a hetero-oligomer that includes these three subunits.

Transgenic mice lacking the α subunit of the olfactory cyclic nucleotide-gated channels display a profound defect in response to all odorants tested, as determined by electro-olfactogram (Brunet et al., 1996). Expression of odorant receptors, type III adenylyl cyclase, $G\alpha_{olf}/G\alpha_s$, and other olfactory markers were normal in these mice. This study provides direct evidence for a physiological role of cyclic nucleotide-gated channels in olfactory signal transduction.

In addition to the non-selective cation current conducted by the cyclic nucleotide-gated channel, a concomitant chloride influx, triggered by calcium entry, also contributes significantly to the total odorant-evoked current in both amphibians and mammals (Kleene and Gesteland, 1991; Kleene, 1993; Kurahashi and Yau, 1993; Lowe and Gold, 1993). This chloride current displays a highly sigmoidal dependence on cAMP concentration and may act to amplify suprathreshold olfactory

signals relative to basal transduction noise, improving response to weak stimuli (Lowe and Gold, 1993; Kleene, 1997).

Inositol trisphosphate as an alternative second messenger

Distinct from cAMP-mediated olfactory transduction, a less well-characterized pathway involving inositol trisphosphates has been described in vertebrates (Boekhoff et al., 1990; Restrepo et al., 1990; Restrepo et al., 1993). Although IP₃-pathways are likely involved in invertebrate chemosensation (Breer et al., 1990; Newell et al., 1990; Fadool and Ache, 1992; Boekhoff et al., 1994b; Riesgo-Escovar et al., 1995), their physiologic relevance in vertebrates is unclear given the complete anosmic phenotype of mice lacking cyclic nucleotide-gated channels (Brunet et al., 1996). Further study may reveal, for example, a modulatory role for IP₃ in olfactory signaling.

Vomer nasal receptors and signal transduction

Pheromone detection in mammals is mediated by the vomeronasal organ, an anatomically **d**istinct structure from the olfactory epithelium. The receptors that sense pheromones and the **s**ignal transduction components that mediate pheromone perception have not been as well **c**haracterized as the olfactory pathways. Evidence is accumulating, however, for many **s**imilarities between the two sensory systems. Genes encoding two families of receptors have **b**een isolated from rat and mouse vomeronasal organs by differential expression library screening (**D**ulac and Axel, 1995; Herrada and Dulac, 1997; Matsunami and Buck, 1997; Ryba and Tirindelli, **1997**). Neither are significantly homologous to one another or to the previously identified **o**lfactory receptors, but both bear similarities to the seven-transmembrane domain G protein-**c**oupled receptor superfamily.

Vomer nasal organ signal transduction appears to utilize signaling machinery distinct from that **u**sed in olfactory transduction. Vomer nasal neurons do not express high levels of G α_{olf} , type III **a**denylyl cyclase, or rOCN1, the α subunit of the olfactory cyclic nucleotide-gated channel, all of **w**hich are highly expressed in olfactory sensory neurons (Berghard et al., 1996). Rather,

vomeronal neurons express type II adenylyl cyclase, and within the vomeronasal organ, distinct subregions of neurons express either $G\alpha_o$ or $G\alpha_{i2}$ (Berghard and Buck, 1996).

Interestingly, expression of the two families of vomeronasal organ receptors may be restricted to either the $G\alpha_o^+$ or $G\alpha_{i2}^+$ classes of neurons (Dulac and Axel, 1995; Herrada and Dulac, 1997; Matsunami and Buck, 1997; Ryba and Tirindelli, 1997). *In situ* hybridizations with probes specific for subfamilies of vomeronasal receptors has suggested that each family consists of ~100 members; however, up to two thirds of these may be pseudogenes for the $G\alpha_o$ receptors. Thus, the olfactory and vomeronasal sensory structures use similar yet distinct strategies of signal transduction.

Regulation of G protein-coupled receptor signaling

Thus far, we have focused on how odorant binding activates an intracellular signal. However, it is equally important to terminate the signal appropriately. The intrinsic GTPase activity of G protein α subunits provides one mechanism for ending signaling. Another is provided in the olfactory mucus layer, where odorant binding proteins and metabolizing enzymes may remove or deactivate olfactory receptor ligands (Carr et al., 1990; Pelosi, 1996).

Organisms also require mechanisms to downregulate olfactory signaling after continuous or repeated stimulation. Desensitization is important for detecting novel stimuli, sensing concentration changes, and ignoring non-informative signals. Conversely, in the absence of stimulation, sensory transduction pathways are often upregulated to increase sensitivity.

Mechanisms by which olfactory transduction is regulated have been proposed in a number of studies, many inspired by work in the more thoroughly characterized G protein-coupled transduction systems of phototransduction and adrenergic receptor signaling.

Downregulation mediated by phosphorylation of G protein-coupled receptors

Seven-transmembrane receptor phosphorylation on serine and threonine residues is a well-characterized mechanism of desensitization, mediated by second messenger-dependent and G protein-coupled receptor kinases (Freedman and Lefkowitz, 1996; Bohm et al., 1997).

Heterologous and homologous desensitization describe two distinct mechanisms of phosphorylation-mediated downregulation.

During heterologous desensitization, second messengers produced during G protein-coupled signaling activate protein kinases. cAMP activates protein kinase A, whereas lipid-derived second messengers, at times in conjunction with calcium, activate protein kinase C (Bohm et al., 1997). These serine/threonine kinases have broad substrate specificity and phosphorylate a number of proteins, including receptors. This pathway is termed heterologous desensitization because signaling through one receptor can downregulate other receptors, including those not previously activated. Receptor phosphorylation by second messenger-dependent kinases is thought to directly uncouple receptors from G proteins (Benovic et al., 1985; Pitcher et al., 1992a).

In contrast, homologous desensitization is mediated by G protein-coupled receptor kinases (GRKs) that specifically phosphorylate activated, or ligand-bound, receptors (Premont et al., 1995; Freedman and Lefkowitz, 1996; Bohm et al., 1997). GRKs frequently require regulated localization to the plasma membrane to exert their effects. Receptor phosphorylation alone is insufficient for maximal downregulation: cofactors called arrestins bind phosphorylated receptors to effect uncoupling from G proteins. At least six GRKs, including rhodopsin kinase and β -adrenergic receptor kinase-1 and -2 (β ARK-1 and β ARK-2), and four arrestins have been identified, with varying tissue distributions and substrate specificities.

Although phosphorylation-dependent regulation has been studied primarily using rhodopsin and adrenergic receptors as substrates, evidence is accumulating that the same mechanisms regulate desensitization of vertebrate olfactory signal transduction.

Fast kinetics mix/quench experiments have shown that isolated rat olfactory cilia treated with micromolar concentrations of some odorants produce a transient increase in cAMP that peaks within 50 milliseconds and returns to near baseline within several hundred milliseconds (Breer et al., 1990). The rapid decrease of cAMP in the continued presence of odorant is indicative of rapid desensitization of the odorant response. Studies, which will be summarized below, now support a role for both second messenger-dependent kinases and G protein-coupled receptor kinases in rapid olfactory desensitization.

Phosphorylation of proteins in olfactory cilia was observed after 1 μ M odorant treatment for 1 second (Boekhoff et al., 1992). For odorants that induced cAMP generation, phosphate incorporation was prevented by Walsh reagent, which inhibits protein kinase A. The functional significance of phosphorylation was assessed by observing the effect of pharmacologic agents on the kinetics of second messenger formation. Pretreatment of olfactory cilia with Walsh inhibitor prevented the rapid decrease of cAMP levels following odorant treatment, such that elevated levels persisted for seconds (Boekhoff and Breer, 1992). These experiments support a role for phosphorylation during rapid signal termination.

In parallel with second messenger-dependent kinases, G protein-coupled receptor kinases are also required for desensitization. β -adrenergic receptor kinase-2 (β ARK-2) is highly expressed in olfactory cilia, while β ARK-1 is not, as determined by ELISA using subtype-specific antibodies (Schleicher et al., 1993). Similarly, *in situ* immunohistochemistry revealed that β ARK-2 and β -arrestin-2 are expressed in the cilia and dendritic knobs of olfactory neurons (Dawson et al., 1993).

Pretreatment of isolated olfactory cilia with anti- β ARK-2 antibodies or heparin, which blocks receptor-specific kinases, abolished rapid decreases of cAMP following 1 μ M odorant stimulation, similar to the effects of Walsh inhibitor. However, phosphate incorporation in ciliary proteins was decreased more by protein kinase A inhibition than by heparin or anti- β ARK-2 antibody treatment (Schleicher et al., 1993). Another study showed that anti- β ARK-2 as well as anti- β -

arrestin-2 antibodies not only decreased the rapid attenuation of cAMP, but also greatly increased the peak levels of cAMP achieved; these experiments were performed using odorant at 100 μ M (Dawson et al., 1993). Thus, it appears that both protein kinase A as well as β ARK-2 / β -arrestin-2 are required for rapid desensitization of olfactory signaling, suggesting that the two kinase pathways may act sequentially.

A possible mechanism integrating the two kinase pathways during downregulation has been proposed, via PKA-regulated translocation of β ARK-2 to the plasma membrane. Prenylated G protein $\beta\gamma$ subunits target β ARK-1 and β ARK-2 to the plasma membrane via interaction with carboxy terminal regions of the kinases, thereby enhancing phosphorylation of the β -adrenergic receptor (Pitcher et al., 1992b; Koch et al., 1993; Pei et al., 1994).

Phosducin competes with β ARK binding to $G\beta\gamma$, thereby inhibiting β ARK-mediated receptor phosphorylation (Hawes et al., 1994; Hekman et al., 1994). Upon phosphorylation on a specific serine residue by PKA, phosducin releases $G\beta\gamma$, which is then available for β ARK-mediated desensitization. Phosducin has been detected in rat olfactory cilia preparations using anti-phosducin antibodies (Boekhoff et al., 1997).

Experiments using isolated olfactory cilia are consistent with the proposed role for PKA, phosducin, $G\beta\gamma$, and β ARK-2 during rapid desensitization. Odorant stimulation of olfactory cilia preparations for less than 1 second induces a dose-dependent (from 1 nM to 1 μ M) translocation of β ARK-2 from cytosolic to membrane fractions. Pretreatment of the isolated cilia with β ARK-2 regions analogous to the β ARK-1 $G\beta\gamma$ -binding segments abolishes membrane translocation, reduces ciliary protein phosphorylation, and eliminates the rapid decrease of cAMP levels following odorant stimulation (Boekhoff et al., 1994a).

Recombinant phosducin added to isolated cilia results in a similar effect, preventing membrane translocation of β ARK-2 and inhibiting rapid termination of the cAMP signal (Boekhoff et al., 1997). Phosducin with an S73D mutation that might mimic the phosphorylated state exhibits

decreased G $\beta\gamma$ binding, and addition of recombinant S73D phosducin decreases the peak cAMP level achieved following odorant stimulation and slightly accelerated the kinetics of decay.

Together, these experiments in isolated olfactory cilia support the following model for rapid termination of olfactory signaling: odorant binding to receptors induces G α_{olf} activation of adenylyl cyclase and increased cAMP levels; cAMP-activated protein kinase A phosphorylates phosducin, releasing G $\beta\gamma$; liberated G $\beta\gamma$ is free to mediate translocation of β ARK-2 to the plasma membrane, where phosphorylation of activated receptors occurs; finally, β -arrestin-2 binding to phosphorylated receptors effects uncoupling from G proteins.

Resensitization of receptors, or maintenance of the proper equilibrium between active and inactive receptors, may require the action of protein phosphatases. Protein phosphatase 2A is expressed in cilia of the olfactory epithelium, as visualized by immunohistochemical staining with subtype-specific antibodies (Kroner et al., 1996). Treatment of isolated cilia with the phosphatase inhibitor okadaic acid or anti-phosphatase 2A antibodies resulted in a decreased amplitude of cAMP production, without significantly altering the kinetics of the response or desensitization (Boekhoff and Breer, 1992; Kroner et al., 1996). Conversely, protamine, which activates phosphatase 2A, caused an increase in the cAMP response. These results in isolated olfactory cilia suggest that phosphatases may modulate the odorant-induced response. A role for phosphatases in resensitization has not yet been demonstrated. However, in a non-olfactory receptor, the G protein-coupled vasopressin receptor, dephosphorylation may be required for recycling internalized receptors to the plasma membrane (Innamorati et al., 1998); this type of mechanism in olfactory signaling might not be evident when using isolated cilia.

Phosphorylation of signaling components

Signal transduction molecules other than the receptor and phosducin may also be targets for phosphorylation. For example, in experiments using purified components, protein kinase A phosphorylates and decreases the catalytic activity of adenylyl cyclase *in vitro* (Iwami et al., 1995).

Likewise, in *S. cerevisiae*, G β is phosphorylated at several sites following pheromone exposure. Mutations in G β that prevent phosphorylation lead to increased sensitivity to pheromone and impaired recovery from pheromone adaptation (Cole and Reed, 1991).

Receptor downregulation, sequestration, and degradation

Receptor phosphorylation and arrestin binding mediate rapid desensitization to stimuli. Over longer time courses, receptor expression at the cell surface can be decreased, either by diminished synthesis or increased removal (Bohm et al., 1997). Endocytosed receptors can be sequestered within inactive intracellular pools until future recycling to the surface or degraded in lysosomes.

The yeast pheromone signaling pathway demonstrates the principle of complex and overlapping regulation during G protein-coupled signal transduction. In addition to regulation of G β by phosphorylation mentioned above, the α -factor pheromone receptor undergoes increased rates of internalization after pheromone stimulation. This increase is dependent on both phosphorylation and ubiquitination, as demonstrated by mutants lacking casein kinase I and ubiquitin-conjugating enzymes. Mutation of potential phosphorylation and ubiquitination sites in wild-type and truncated α -factor receptors suggests that hyperphosphorylation of carboxy terminal serines allows ubiquitination of neighboring lysines and that ubiquitination acts as an internalization and degradation signal (Hicke and Riezman, 1996; Hicke et al., 1998). It is not known whether vertebrate G protein-coupled receptors also undergo ubiquitin-dependent downregulation.

Regulators of G protein signaling: RGS proteins

In recent years, a convergence of genetic and biochemical approaches has led to the identification of a large family of proteins, conserved from yeast to mammals, that negatively regulates G protein signaling.

In yeast, the *SST2* gene encodes the first identified RGS protein. *sst2* loss of function mutants are hypersensitive to pheromone and defective in pheromone adaptation. Conversely, *SST2* gain-of-function mutants inhibit responses to pheromone. Epistasis experiments and the finding that *SST2* mutant phenotypes can be suppressed by mutations in the G protein α subunit in an allele-specific manner suggested that Sst2p acts directly on Gpa1p to negatively regulate signaling (Dohlman et al., 1995; Dohlman et al., 1996). Similarly, in *C. elegans*, alterations in activity of the RGS protein EGL-10 and a G protein α subunit GOA-1 produce opposite phenotypes, shown by mutation or by modifying gene dosage. Epistasis experiments between *egl-10* and *goa-1* were consistent with *egl-10* functioning upstream of, or directly on *goa-1*, to inhibit signaling (Koelle and Horvitz, 1996).

The molecular mechanism by which RGS proteins inhibit G protein signaling has since been elucidated. RGS proteins act as GTPase activating proteins (GAPs) for G protein α subunits, thereby increasing the rate of $G\alpha$ inactivation (Berman et al., 1996; Hunt et al., 1996; Watson et al., 1996). Initially, GAP activity was demonstrated using mammalian RGS proteins acting on G protein subunits in the $G\alpha_i$ family. Subsequent work has confirmed that yeast Sst2p also acts as a GAP (Apanovitch et al., 1998) and demonstrated that other RGS proteins can act on $G\alpha_q$ (Hepler et al., 1997; Heximer et al., 1997; Yan et al., 1997). In addition to GAP activity, one RGS protein appears to occlude association of $G\alpha_q$ with its effector enzyme, phospholipase C β , suggesting that RGS proteins may have multiple mechanisms of inhibiting G protein signaling (Hepler et al., 1997).

The identification of GAP proteins for heterotrimeric G proteins can explain the puzzle of how G protein deactivation *in vivo* can occur orders of magnitude faster than *in vitro*. It is not known whether RGS proteins are required for the rapid termination of olfactory signaling observed in isolated olfactory cilia. However, an RGS mRNA has been identified in isolated catfish olfactory neurons by RT-PCR (Bruch and Medler, 1996).

Role of calcium in modulating olfactory signaling

During initiation of vertebrate olfactory signaling, calcium has been called a third messenger because of its role in gating chloride channels (Kleene, 1993; Kurahashi and Yau, 1993; Lowe and Gold, 1993). In addition to its role in signal generation, calcium acts subsequently to downregulate signaling at multiple levels of the signaling cascade.

Signal termination by calmodulin-dependent phosphodiesterase

In fast kinetic analysis of isolated rat olfactory cilia, second messenger levels induced by odorants decay rapidly within several hundred milliseconds (Breer et al., 1990). The rapid decrease in cAMP levels observed suggests that phosphodiesterase activity is important for signal termination. Consistent with this hypothesis, pharmacological inhibition of phosphodiesterase activity prolonged the odor-induced current in salamander olfactory neurons (Firestein et al., 1991).

Rat olfactory neurons express high levels of calmodulin-dependent phosphodiesterase (CaM-PDE) localized to the cilia, as determined by immunohistochemistry. Its activity is stimulated by submicromolar concentrations of calcium (Borisov et al., 1992). A calmodulin-dependent phosphodiesterase isozyme was subsequently cloned and demonstrated to be highly expressed in olfactory epithelium. When expressed in COS cells, the olfactory CaM-PDE demonstrated a much lower K_m for cAMP than previously described in other neuronal CaM-PDEs, consistent with a role in efficiently terminating olfactory signaling (Yan et al., 1995). Regulation by calcium may allow olfactory CaM-PDE to modulate signaling in response to prior stimulation.

Calcium has also been reported to reduce odorant-induced cAMP generation by a mechanism not affected by phosphodiesterase inhibitors (Boekhoff et al., 1996). These rapid mix/quench experiments suggest that low micromolar concentrations of calcium act by decreasing cAMP generation, rather than by increasing its removal. It is not clear, however, whether the method of isolating rat olfactory cilia, by high concentration calcium shock, might confound the analysis.

Modulation of cAMP-gated channel activity by calcium

Recordings from macro patches of catfish olfactory neurons revealed strong inhibition of the cAMP-elicited current by micromolar concentrations of intracellular calcium. Calcium does not appear to act directly on the channel but is proposed to interact with a labile protein that washes out from the membrane patches (Kramer and Siegelbaum, 1992). This regulatory protein is likely to be calmodulin. Micromolar calcium in the presence of calmodulin strongly inhibits the cyclic nucleotide-generated current in patches of rat olfactory receptor neurons as well as in heterologously expressed α subunits of the rat olfactory cyclic nucleotide-gated channel (Chen and Yau, 1994). Calcium-calmodulin acts directly on the heterologously expressed channel by binding a specific domain on the amino terminus (Liu et al., 1994). The mechanism of inhibition is presumably similar in the heterologously expressed homo-oligomeric and the native hetero-oligomeric channels. However, an additional calmodulin-independent pathway, also dependent on calcium, has been proposed to inhibit cyclic nucleotide-gated channel activity, based on differential susceptibility to exogenous antagonists (Balasubramanian et al., 1996).

Role of calcium in olfactory adaptation

The previously described mechanisms of calcium-mediated inhibition of olfactory signaling *in vitro* may manifest *in vivo* as olfactory adaptation. In whole-cell recordings of newt olfactory neurons, inactivation of currents induced by prolonged application of high concentrations of odorants (10 mM) was seen only in the presence of calcium (Kurahashi and Shibuya, 1990).

In one experimental setup, the primary mechanism of olfactory adaptation appears to be calcium-mediated modulation of the cyclic nucleotide-gated channel. As a paradigm for adaptation, a conditioning pulse of odorant at millimolar concentrations reduced the response to a subsequent stimulus, as monitored by whole-cell recordings of dissociated newt olfactory neurons.

Adaptation was calcium dependent. Interestingly, after an odorant-induced conditioning pulse, similar adaptation was seen in response to photolysis of caged cAMP, demonstrating that the mechanism of adaptation acted downstream of the receptor, G protein, and adenylyl cyclase.

Kinetic analysis was consistent with adaptation via calcium-mediated modulation of the cAMP-

gated channel activity rather than increased phosphodiesterase activity (Kurahashi and Menini, 1997). In summary, mechanisms entirely downstream of cAMP production account for adaptation in this system, raising questions about the importance of receptor-based regulation, for example, by receptor kinases and arrestins. Because these studies were performed at high odorant concentrations, it is possible that other mechanisms might contribute to olfactory adaptation at lower concentrations.

***C. elegans* as a model system for studying behavior**

The soil nematode *C. elegans* is an attractive model organism for studying behavior because of its genetic tractability and simple structure (Brenner, 1974). Genetic manipulations are aided by its size (~ 1 mm), rapid life cycle (4 days at 20°C), and ability to reproduce both hermaphroditically and sexually.

A cellular understanding of behavior in *C. elegans* is made possible by its stereotyped nervous system, consisting of only 302 neurons in the adult hermaphrodite (White et al., 1986). Serial section electron microscopy has generated a nearly complete neuronal connectivity diagram, which should provide much of the basis for behavior. Cellular morphology provides clues to neuronal function, which can then be confirmed by analysis of defects that result from laser ablation of individual neurons.

Olfactory behaviors in *C. elegans*

Despite its simplicity, *C. elegans* possesses a wealth of behaviors and responds to many environmental cues, spanning physical, chemical, and thermal modalities. *C. elegans* senses both volatile and water-soluble chemicals in the environment in processes analogous to smell and taste (Ward, 1973; Bargmann et al., 1993). Both attractive and repellent compounds have been identified by chemotaxis assays.

Many volatile compounds are sensed by *C. elegans* (Bargmann et al., 1993). Fifty of 121 volatile chemicals tested were strong attractants, and included alcohols, ketones, esters, pyrazines, thiazoles, aldehydes, and aromatic compounds. For most attractive odorants, a ~100 nanomole point source is sufficient for chemotaxis on a 10 cm assay plate; a few compounds are efficient attractants at 100-fold lower concentrations. Experiments using tethered worms and computer tracking suggest that the threshold of chemosensitivity in *C. elegans* approaches 10^{-10} M (Terrill and Dusenbery, 1996).

Olfactory chemotaxis exhibits structural specificity, as wild-type *C. elegans* can discriminate among several different attractive odorants in saturation assays (Bargmann et al., 1993). In these assays, high uniform concentrations of an odorant abolish response to that odorant without interfering with chemotaxis to other odorants. At least seven classes of odorants can be discriminated from one another.

Behavioral responses can be altered by prior experience. In olfactory adaptation, prolonged exposure to an odorant selectively diminishes subsequent response to that odorant without affecting responses to other attractants (Colbert and Bargmann, 1995). Additional environmental signals, such as starvation, can modulate both adaptation and recovery from adaptation, and increase odorant discrimination (Colbert and Bargmann, 1997).

Neuroanatomy of chemosensation in *C. elegans*

Candidate chemosensory neurons were initially identified ultrastructurally (Ward et al., 1975; Ware et al., 1975; Perkins et al., 1986; White et al., 1986). In three classes of *C. elegans* sensilla, a non-neuronal socket cell forms a pore in the cuticle, while a sheath cell envelops the terminal cilia of associated neurons. Together, these cells form the amphid and inner labial sensilla in the head of the animal and the phasmid sensilla of the tail. The neurons in these sensilla have been proposed to be chemosensory based on the exposure of their cilia to the external environment.

Twelve classes of bilaterally symmetric neurons contribute to the amphid sensilla. The ciliated endings of eight types of neurons are directly exposed to the environment through the amphid pore. Laser ablation of these neurons has shown that they primarily direct responses to water-soluble compounds (Bargmann et al., 1990; Bargmann and Horvitz, 1991; Kaplan and Horvitz, 1993). The cilia of one class of neuron (AFD) is part of the amphid sensilla but is not associated with the pore. This neuron is required for thermosensation (Mori and Ohshima, 1995).

The cilia of three types of neurons, including AWA and AWC, are enveloped by the amphid sheath cell and not directly exposed, but are continuous with the external environment via matrix material secreted by the sheath cell. The AWA and AWC neurons are the only neurons required for chemotaxis to all tested volatile attractants. Each neuron directs chemotaxis to a subset of sensed odorants (Bargmann et al., 1993; Piali Sengupta, personal communication). AWA is necessary for response to pyrazine and diacetyl, whereas AWC is required for chemotaxis to benzaldehyde, isoamyl alcohol, 2,3-pentanedione, and butanone. Either neuron can direct chemotaxis to 2,4,5-trimethylthiazole.

Olfactory signal transduction

When work on this thesis was begun, little was known about the molecular components of olfactory signal transduction in *C. elegans*. During the following years, genetic analysis of mutants defective in chemosensory behaviors has identified signal transduction components potentially involved in the initial events of sensory perception. These studies have revealed striking parallels with the signaling pathways used during vertebrate olfaction.

The identification of candidate seven-transmembrane G protein-coupled chemosensory receptors and the functional characterization of one of them are described in this thesis (Chapters 1, 2, and 3).

A G protein α subunit encoded by *odr-3* is required for normal chemotaxis to odorants sensed by the AWA and AWC chemosensory neurons (Roayaie et al., 1998). Consistent with a role in signal

transduction, *odr-3* antibodies and an *odr-3* translational fusion reveal expression localized to the sensory cilia.

Two guanylyl cyclases, *odr-1* and *daf-11*, are required for AWA chemosensory function (Bargmann et al., 1993; Vowels and Thomas, 1994; N. L'Etoile, personal communication; D. Birnby, submitted). In addition, ~30 receptor guanylyl cyclases have been identified in the sequenced regions of the *C. elegans* genome (Yu et al., 1997). All eight analyzed cyclases are expressed in distinct sensory neurons, including AWC, and at least one is localized to sensory cilia. Expression of three of the guanylyl cyclases in ASE demonstrates absolute right- or left-sidedness, suggesting that chemosensory receptors previously thought to be bilaterally symmetric and equivalent may be functionally distinct. It is unclear whether these guanylyl cyclases are effector enzymes for G protein-coupled signaling, additional chemosensory receptor molecules, or both.

tax-2 and *tax-4* encode two subunits of cyclic nucleotide-gated channels and may represent downstream targets of the guanylyl cyclases. *tax-2* and *tax-4* are required for both chemotaxis mediated by AWC and for thermotaxis (Coburn and Bargmann, 1996; Komatsu et al., 1996). Both are expressed in the AWC chemosensory and AFD thermosensory neurons and are localized to the cilia, consistent with a role in sensory transduction.

In contrast, *osm-9*, which encodes a putative ion channel similar to the capsaicin receptor and Trp ion channels in *Drosophila* phototransduction, is required for AWA-mediated chemosensation (Colbert et al., 1997). These findings suggest that the AWA and AWC chemosensory neurons use distinct signaling mechanisms, as AWA chemotaxis requires the OSM-9 putative ion channel whereas AWC function is dependent on the TAX-2/TAX-4 cyclic nucleotide-gated channel. Although *osm-9* is not required for AWC-mediated chemotaxis, *osm-9* mutants possess an AWC olfactory adaptation defect, suggesting that OSM-9 may play a modulatory role in AWC.

Genetic analysis has also revealed genes required for neuronal development and cell biology. *odr-7* encodes a transcription factor required for AWA sensory function (Sengupta et al., 1994), while *odr-4* is required for proper localization of some seven-transmembrane receptors to AWA and AWC sensory cilia (Dwyer et al., 1998).

Neuronal networks and the generation of behavior

Less is known about how the initial perception mediated by a chemosensory neuron is converted through a network of interneurons, motoneurons, and muscle cells into chemotactic behavior. Worms chemotax directly up a concentration gradient to a point source of attractant (Ward, 1973; Bargmann et al., 1990; Bargmann and Horvitz, 1991). Based on the location of chemosensory cilia at the tip of animal's nose and their orthogonal orientation to the plane of movement, chemotaxis probably does not involve the simultaneous comparison of attractant concentration at two points in space. Instead, attractant perception is temporally integrated into a molecular memory of odorant concentrations. Furthermore, a worm appears to orient to the attractant by positioning its head directly up the concentration gradient — worms with a kinked neck spiral inwards towards a point source of attractant, rather than chemotaxing directly to the odorant (Ward, 1973). The neuronal circuitry that mediates this complex behavior is not understood.

In other behavioral responses, more is known about the neuronal networks that generate behavior. For example, in the light touch aversive response, laser ablations and the known ultrastructural connectivity of neurons have suggested a simple reflex circuit of mechanosensory neuron to interneuron to motor neuron (Herman, 1996). Within the mechanosensory neuron, ion channels proposed to be directly gated by mechanical stress have been genetically implicated as critical for touch response. The simple forward or backward movement response suggests that relatively uncomplicated neural processing is required for generating this behavior.

Thermotaxis is a more complicated behavior in which worms exhibit a memory and preference for their prior cultivation temperature. Upon transfer to a plate with a radial temperature

gradient, wild-type animals migrate to and move within an isothermal track corresponding to their cultivation temperature (Hedgecock and Russell, 1975). Laser ablation experiments have identified thermosensory receptor neurons (AFD) and several pairs of interneurons required for thermotaxis (AIY, AIZ, and RIA) (Mori and Ohshima, 1995). Interestingly, antagonistic output from two classes of these interneurons is required for proper thermotaxis. Animals lacking AIY due to laser ablations or mutations are cryophilic, while AIZ-deficient animals are thermophilic (Mori and Ohshima, 1995; Hobert et al., 1997; Hobert et al., 1998). The RIA interneuron may play a role in signal integration, as defined by laser ablation experiments and known neural connectivity. The molecular mechanisms by which these competing signals are integrated with one another and with a memory of cultivation temperature is unknown. Thermotaxis is particularly relevant to the study of chemotaxis because the two behaviors share some of the same signal transduction components and interneurons downstream of the sensory receptors (Coburn and Bargmann, 1996; Komatsu et al., 1996).

Overview of this thesis

Chapter 1 describes the identification of a large family of candidate chemosensory receptors from the sequenced regions of the *C. elegans* genome. Their similarity to seven-transmembrane G protein-coupled receptors, large number, high diversity, and expression in chemosensory neurons suggest that they might mediate chemosensation.

In **Chapter 2**, a genetic approach was used to identify a seven-transmembrane receptor, ODR-10, specifically required for responses to diacetyl. The specificity of its mutant phenotype and expression in the chemosensory neurons that sense diacetyl support the identification of ODR-10 as an olfactory receptor.

Chapter 3 details the functional characterization of ODR-10 heterologously expressed in mammalian cells. This analysis provided proof that ODR-10 acts as an olfactory receptor for

diacetyl. The second part of the chapter explores the ligand specificity of ODR-10 expressed *in vitro* and *in vivo*.

Chapter 4 explores possible neuronal and molecular mechanisms of olfactory discrimination and downregulation. These studies demonstrate that isolated chemosensory neurons are capable of discriminating between multiple odorants. Site-directed mutagenesis of ODR-10 was employed to determine the role of phosphorylation and ubiquitination in chemosensory behaviors.

Chapter 5 describes the cloning and characterization of *odr-2*, a gene required for behaviors mediated by the AWC chemosensory neurons. *odr-2* is shown to encode an alternatively spliced, neuronally-expressed protein with distant similarity to the Ly-6 superfamily of extracellular proteins.

Chapter 1. Divergent seven transmembrane receptors are candidate chemosensory receptors in *C. elegans*.

Published in: (1995) Cell 83: 207-218. Copyright © 1995 by Cell Press.

Statement of contributions

In this paper, 41 potential chemosensory receptors, grouped into six families, were identified from the sequenced regions of the *C. elegans* genome, and expression patterns were determined for 14 of the receptors.

I identified three of six families (16 of 41 candidate receptors) and carried out multiple sequence alignment and phylogenetic analysis of all the receptors. I designed, cloned, and injected seven of the 14 green fluorescent protein constructs that yielded expression patterns. My work contributed substantially to all figures and tables in the published paper except Table 2.

Divergent Seven Transmembrane Receptors Are Candidate Chemosensory Receptors in *C. elegans*

Emily R. Troemel,* Joseph H. Chou,* Noelle D. Dwyer,*
Heather A. Colbert,* and Cornelia I. Bargmann
Howard Hughes Medical Institute
Programs in Developmental Biology, Neuroscience,
and Genetics
Department of Anatomy
University of California, San Francisco
San Francisco, California 94143-0452

Summary

Using their senses of taste and smell, animals recognize a wide variety of chemicals. The nematode *C. elegans* has only fourteen types of chemosensory neurons, but it responds to dozens of chemicals, because each chemosensory neuron detects several stimuli. Here we describe over 40 highly divergent members of the G protein-coupled receptor family that could contribute to this functional diversity. Most of these candidate receptor genes are in clusters of two to nine similar genes. Eleven of fourteen tested genes appear to be expressed in small subsets of chemosensory neurons. A single type of chemosensory neuron can potentially express at least four different receptor genes. Some of these genes might encode receptors for water-soluble attractants, repellents, and pheromones.

Introduction

The olfactory and gustatory systems detect a variety of structurally unrelated molecules, from ions to complex organic compounds. These heterogeneous chemical signals are recognized by specialized sensory receptors and sensory neurons. Unlike the visual system, which detects many wavelengths of light but uses only a few types of receptor neurons, the olfactory system contains many types of sensory neurons that each detect particular chemical cues.

To analyze the mechanisms of sensory recognition and discrimination by the nervous system, we are studying chemosensation in the nematode *Caenorhabditis elegans*. *C. elegans* can detect touch, temperature, and light, but its responses to chemicals are the most diverse responses in its behavioral repertoire. *C. elegans* eats bacteria; chemicals produced by bacteria stimulate chemotaxis, egg laying, feeding, and defecation (Ward, 1973; Dusenbery, 1974; Horvitz et al., 1982; Avery and Horvitz, 1990; Thomas, 1990; Bargmann et al., 1993), while toxic or aversive compounds are avoided (Culotti and Russell, 1978). Pheromones contribute to mating between males and hermaphrodites (Liu and Sternberg, 1995). A pheromone also controls the development of an alternative larval stage called a dauer larva (Golden and Riddle, 1984).

The neurons involved in these chemosensory re-

*These authors made similar contributions to this work.

sponses can be precisely defined within the nervous system of *C. elegans*. An adult hermaphrodite has exactly 302 neurons, whose positions, morphology, and synaptic connections are reproducible from animal to animal (White et al., 1986). Among these neurons are 32 neurons that appear to be chemosensory, since they have ciliated endings that are exposed to the environment through specialized sensory structures (Ward et al., 1975; Ware et al., 1975). These neurons can be divided into fourteen types, where one neuron type typically consists of two bilaterally symmetric neurons. For ten types of neurons, chemosensory function has been directly demonstrated by observing behavioral deficits after laser killing of defined cell types. For example, the two ASE chemosensory neurons respond to water-soluble attractants including salts, cAMP, and biotin; the two AWC olfactory neurons respond to volatile aldehydes, ketones, alcohols, and thiazoles; and the two ASH neurons respond to both chemical and mechanical stimuli (Bargmann and Horvitz, 1991a; Bargmann et al., 1993; Kaplan and Horvitz, 1993). The neurons that sense attractants (seven types) and repellents (two types) do not overlap, and they synapse onto distinct synaptic targets that mediate chemotaxis and avoidance behaviors (White et al., 1986).

Interestingly, different kinds of sensory information can be sorted out within a single type of sensory neuron. For example, three pairs of neurons regulate both chemotaxis and dauer larva formation, while two pairs of neurons regulate both chemotaxis and egg laying (Bargmann and Horvitz, 1991b; E. Sawin and H. R. Horvitz, personal communication). Thus, two distinct responses can be generated by a single sensory cell type. In addition, animals can adapt independently to two different chemicals that are detected by the same chemosensory neuron (Colbert and Bargmann, 1995), and the response to one chemical detected by a chemosensory neuron can be saturated without blocking the response to a second chemical detected by that neuron (Ward, 1973; Bargmann et al., 1993).

How can a small number of chemosensory neurons generate responses to a much larger number of chemicals? One possibility is that each chemosensory neuron possesses multiple receptor proteins or binding sites for different compounds. In that case, some aspects of discrimination between sensory stimuli could occur within a single sensory neuron. Alternatively, each sensory neuron might express only one type of receptor that binds to many chemicals; in this case, downstream integration of information from several types of sensory neurons could be used to generate diverse responses. Unfortunately, it has not been possible to examine chemosensory receptor expression directly. A family of G protein-coupled vertebrate olfactory receptors has been identified (Buck and Axel, 1991), but homologs of these receptors have not been identified in *C. elegans*. G protein-mediated second messengers have been implicated in insect chemoreception (Breer et al., 1990), but the receptors that mediate chemosensation in invertebrates are unknown.

We describe here a family of seven transmembrane receptor genes whose products might mediate chemosensation in *C. elegans*. These genes were sequenced by the *C. elegans* genome sequencing consortium, which has sequenced about 15% of the genome (Sulston et al., 1992; J. Sulston, A. Coulson, R. Waterston, et al., personal communication). The genes are highly divergent from known genes and from one another. However, they have secondary structures and key residues that define them as members of the G protein-coupled receptor superfamily. The receptor genes are clustered in the genome, with up to nine genes present in a single cluster. Most of these genes are expressed in sensory neurons, and multiple receptors can be expressed by a single sensory neuron.

Results

A Large Family of Potential Seven Transmembrane Receptors

In *C. elegans*, genes with related functions are often found clustered in the genome in operons: a primary transcript encoding several genes is cleaved to produce multiple mature mRNAs (Zorio et al., 1994). Therefore, we examined regions around potential olfactory signaling molecules in the sequenced DNA of *C. elegans* for genes that might be chemosensory receptors. Immediately adjacent to a transmembrane guanylyl cyclase on chromosome II, we found nine novel genes that were related to one another. Although these genes were not homologous to any known genes, they encoded proteins with multiple predicted transmembrane domains, as would be expected of receptors. These sequences were used to search databases for related genes, which were then used in further sequence searches (Altschul et al., 1990). From this analysis, we identified 41 potential *C. elegans* receptor genes that fell into six families based on sequence similarity with one another. The gene families were named *sra*, *srb*, *srg*, *srd*, *sre*, and *sro* (for serpentine receptor classes a, b, g, d, e, and o). The chromosomal locations of these genes are shown on Figure 1A; their sequences are presented in Figure 2.

The *sra*, *srb*, *srg*, *srd*, and *sre* genes were not significantly similar to any known gene in homology searches. However, when their sequences were manually aligned with consensus sequences for seven transmembrane receptors, they were found to contain features that are characteristic of that family. Each gene displayed approximately seven hydrophobic peaks that could be transmembrane domains (Figure 1B) (Kyte and Doolittle, 1982) as well as some key residues that are usually present in G protein-coupled receptors (Probst et al., 1992). The regions of conservation in each subfamily were most pronounced in predicted transmembrane domains 3 and 7 and in linker regions between transmembrane domains. These regions tend to be most conserved among related seven transmembrane receptors, supporting the hypothesis that the *sra*, *srb*, *srg*, *srd*, *sre*, and *sro* genes encode G protein-coupled receptors from this superfamily (Probst et al., 1992).

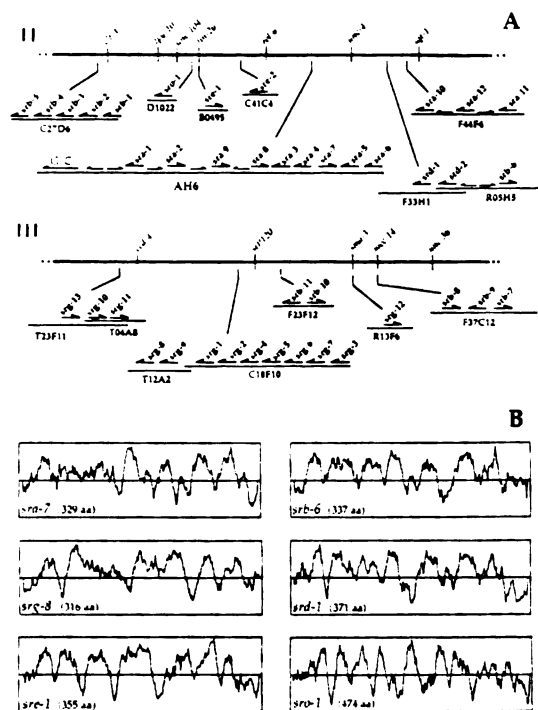


Figure 1. Genomic Organization and Structure of Predicted Receptor Genes

(A) Genomic organization of predicted receptor genes (not to scale). Approximately two thirds of chromosome III and one third of chromosome II were available through GenBank when these genes were discovered. At the top is shown the approximate genetic map position of each set of genes. In insets are shown the cosmids from which each gene was derived. Predicted receptor genes are indicated by the thicker lines; interspersed genes that did not belong in these receptor families are indicated by the thinner lines. In the *sra-1*-*sra-9* cluster, the interspersed genes were *AH6.5*, a zinc finger-containing protein, *AH6.15*, a transposon, and *AH6.13*, a fragment of an *sra*-like gene. *G. C.* is the guanylyl cyclase *AH6.1*. In the *sra-10*-*sra-12* cluster, the interspersed genes were *F44F4.6*, a β -1,6-N-acetylglucosaminyltransferase, and *F44F4.8*, a transposase. In the *srd-1*-*srd-2*-*srb-8* cluster, the interspersed genes were *R05H5.2*, a phosphatase, and *R05H5.7*, a novel protein.

(B) Hydrophobicity plots of representative genes. Six of the genes whose expression patterns are presented in Figures 3-6 are shown. Hydrophobic peaks predicted by Kyte-Doolittle analysis (Kyte and Doolittle, 1982) appear above the center line in each graph. Similar plots were obtained for all family members shown in Figure 2.

The three largest families of genes were the *sra*, *srb*, and *srg* genes. The *sra* family included the nine genes that initiated the search, *sra-1* through *sra-9*, which shared about 35% amino acid identity overall, and three other genes, *sra-10* through *sra-12*, which were about 20%-25% identical with *sra-1* through *sra-9*. The eleven *srb* genes were distantly related to the *sra* genes (about 10%-15% amino acid identity) but significantly more closely related to one another (about 30% identity). The thirteen *srg* genes were essentially unrelated to the *sra* and *srb* genes by sequence, but between 10%-30% identical to one another. The *srg* genes were independently predicted to be G protein-coupled receptors by E. Sonnhammer of the Sanger Center (personal communication).

Fewer members of the *srd*, *sre*, and *sro* families of genes were detected. *srd-1* and *srd-2* were 48% identical to one another at the amino acid level. *sre-1* and *sre-2* were 28% identical to one another at the amino acid level, and marginally similar to members of the *srb* gene family. While the *sra-sre* genes were unrelated in sequence to known sensory receptors, the single *sro-1* gene displayed distant similarity to opsin genes (Figure 2). *sro-1* is highly diverged from known opsins; it lacks the lysine that forms a Schiff base with retinal, so its sequence similarity with opsins might not reflect functional similarity (Thomas and Stryer, 1982).

Most of the *sra*, *srb*, *srg*, and *srd* genes were found in clusters of two to nine related genes (see Figure 1A). Contrary to the initial rationale of the search, the nine original *sra* genes were not organized into a single operon with the guanylyl cyclase gene or each other. Although they were all found within a 30 kb region, different members were transcribed from different DNA strands and presumably had different promoters (see Figure 1A). The three additional *sra* genes *sra-10*, *sra-11*, and *sra-12* were also closely linked to one another, but they were far from *sra-1-sra-9* on chromosome II. In both cases, the *sra* genes were not strictly clustered: unrelated genes were interspersed among the *sra* genes. By contrast, many of the *srb*, *srg*, and *srd* clusters were uninterrupted and might encode polycistronic transcripts, since the genes were transcribed in the same orientation within 1 kb of each other (see Figure 1A) (Zorio et al., 1994). The five genes *srb-1-srb-5* and the nine genes *srg-1-srg-9* might each arise from a single transcript. With the exception of the *srd-1-srd-2-srb-6* cluster, closely linked genes fell within one sequence family (e.g., all *sra* or all *srb* genes), and with the further exception of two *srb* clusters (*srb-7-srb-9* and *srb-10-srb-11*), the linked genes were always the most closely related genes within a family.

The candidate vertebrate olfactory receptors are encoded by genes that are similar enough to cross-hybridize with one another at high stringency (Buck and Axel, 1991), but their level of sequence similarity is higher than that of the families of genes described here. To determine whether many other genes might belong to the *sra*, *srb*, and *srg* gene families, we used the coding regions of *sra-6*, *sra-7*, *srb-1*, *srb-8*, *srb-10*, and *srg-8* to probe genomic Southern blots of *C. elegans* DNA at high (65°C) or reduced (55°C) stringency. Each gene appeared to detect only its own sequence at both high and lowered stringency (data not shown).

Expression of Seven Transmembrane Receptors in Sensory Neurons

The large number of related sequences in the *sra*, *srb*, and *srg* gene families, their relatively small size (311–371 amino acids), and their clustering in the genome (Ben-Arie et al., 1994) were reminiscent of vertebrate olfactory receptors. To ask whether these genes might be expressed by chemosensory neurons, upstream regions of 22 genes were fused to the reporter gene *GFP* (green fluorescent protein) and introduced into the germline of *C. elegans* to

produce transgenic animals (see Experimental Procedures) (Chalfie et al., 1994). Interestingly, many of these reporter gene constructs yielded highly specific expression patterns (see Figures 3–6; Table 1). By aligning *GFP* fluorescence with differential interference Nomarski images, expression could be localized to single cell types (Figure 4).

Of thirteen genes whose expression was observed in hermaphrodites, seven were expressed only in small subsets of chemosensory neurons. Fusion genes derived from the two linked *srg* genes *srg-2* and *srg-8* and the two linked *sra* genes *sra-7* and *sra-9* were expressed exclusively in the two ASK sensory neurons (Figure 3A). The ASK neurons, which are implicated in chemotaxis to the amino acid lysine and in sensory regulation of egg laying, are easily recognized by their positions in a trio of cell bodies at the dorsal midline (Figure 4A).

Three other fusion genes were also localized strictly to sensory neurons. *srd-1::GFP* was expressed in the sensory neuron ASI, which detects water-soluble attractants and the dauer pheromone that regulates nematode development (Figures 3B and 4C). *sre-1::GFP* was expressed in the ADL neuron, which is required for the response to some repellents (Figures 3C and 4B; Table 2; B. E. Kimmel, C. I. B., and J. H. Thomas, unpublished data). In addition, a lower level of *sre-1::GFP* expression was detected in the sensory neuron ASJ, which is implicated in pheromone detection. *srg-13::GFP* was expressed in the PHA neurons in the tail (Figure 5D). The function of these neurons is unknown, but their morphology is characteristic of chemosensory neurons.

In addition to the seven genes that were expressed exclusively in chemosensory neurons, three additional fusion genes were expressed predominantly in chemosensory neurons. *srb-6::GFP* was expressed in five types of sensory neurons, three in the head and two in the tail (see Table 1; Figures 5A and 5B). In addition to this neuronal expression, a low level of expression of the reporter gene was observed in the egg laying structures in the mid-body region. *sra-8::GFP* also showed both sensory and nonsensory expression. The ASH and ASI sensory neurons expressed the fusion gene (Figures 5C and 5E), as did the PVQ interneurons (Figure 5E). *sro-1::GFP* was expressed mainly in the ADL sensory neurons (see Figure 3C), but lower expression was observed in the SIA neurons, which have unknown functions.

Three gene fusions were expressed predominantly outside the chemosensory system (see Table 1; data not shown). The linked genes *sra-10* and *sra-11* were expressed in some sensory neurons, interneurons, and pharyngeal neurons and muscle. *srg-12*, the most divergent *srg* gene, was expressed in the excretory cell and the gut.

Expression of the gene fusions was examined in animals of all developmental stages. In all cases, *GFP* expression was observed in animals from the first larval stage through the adult, though some variability was apparent (for example, *srg-8* was consistently expressed more strongly in young larvae than in adults). A total of 22 predicted genes were tested by this approach (see Experimental Proce-

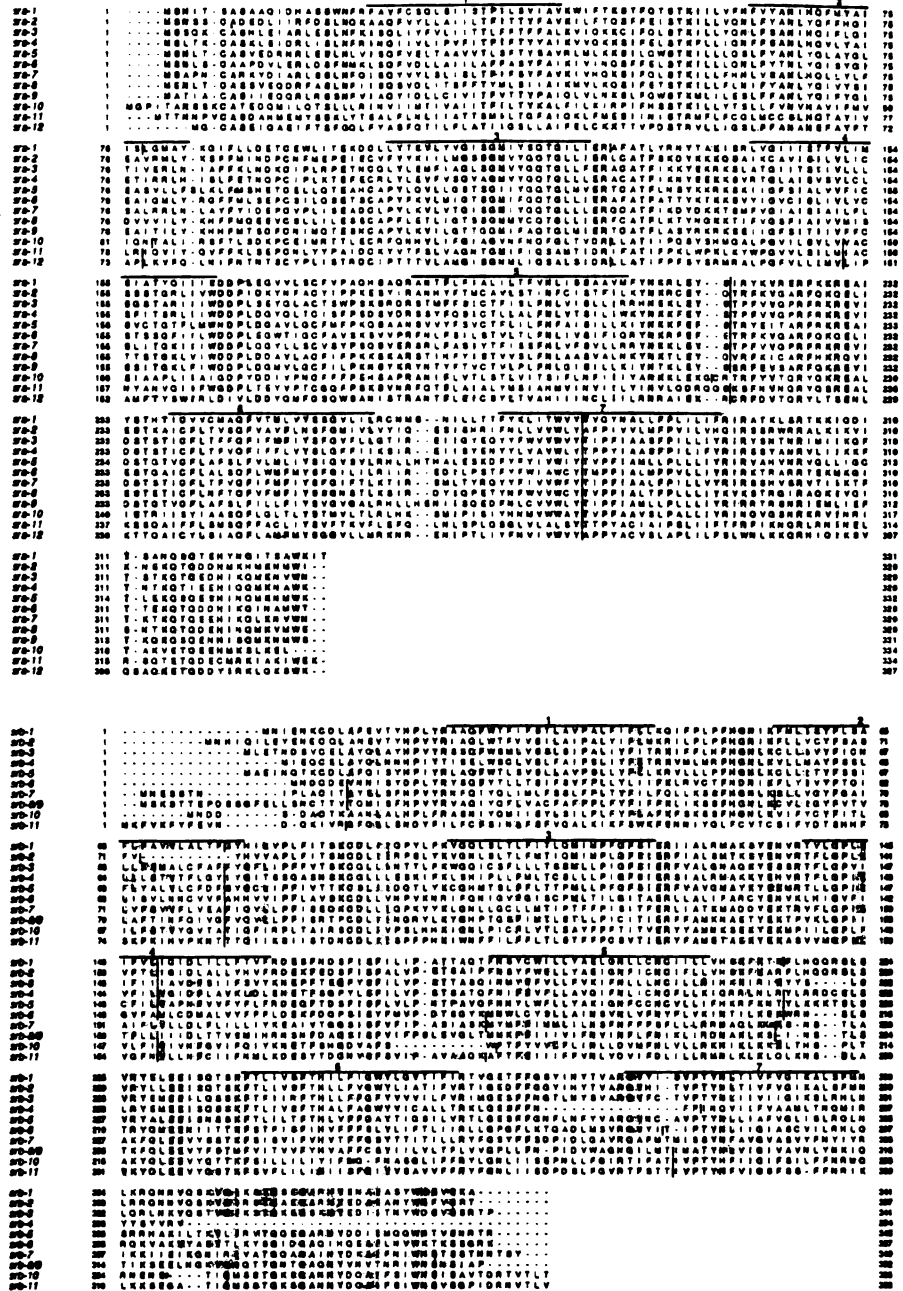


Figure 2. Sequence Alignments of Predicted Seven Transmembrane Receptors

Unless otherwise noted, all genes were as predicted by the *C. elegans* sequencing consortium. Residues conserved in $\geq 50\%$ of the clones are shaded in grey. The approximate locations of predicted transmembrane domains 1 through 7 are noted. Exon/intron boundaries are denoted by slash marks.

The *sra* family: *sra-5* contained a single frameshift, which was introduced at the position marked with the number symbol in its sequence to align it with the other genes (see Experimental Procedures). *sra-11* and *sra-12* were modified from the previously predicted genes (see Experimental Procedures).

The *srb* family: *srb-1*, *srb-2*, *srb-3*, *srb-4*, and *srb-5* were all different from the previously predicted genes. *srb-8* and *srb-9* were also different from the previously predicted genes; these two genes are identical at the amino acid level. *srb-4*, *srb-7*, and *srb-10* could only be aligned with these sequences by introducing frameshifts, denoted by a number symbol.

The *srg* family: *srg-1*, *srg-2*, *srg-3*, and *srg-9* were all modified from previously predicted genes. *srg-4*, *srg-5*, *srg-6*, and *srg-7* were identified on the basis of searches of genomic regions in the C18F10 cosmid.

The *srd* family: *srd-2* was modified from the previously predicted gene.

The *sre* family: *sre-2* was modified from the previously predicted gene.

sro-1: alignment of *sro-1* with the rh2 ocular opsin from *Drosophila pseudoobscura* (Carulli and Hart, 1992) and the rh1 photoreceptor opsin from *Calliphora vicina* (Huber et al., 1990). The lysine that forms a Schiff base with retinal is denoted with an asterisk.

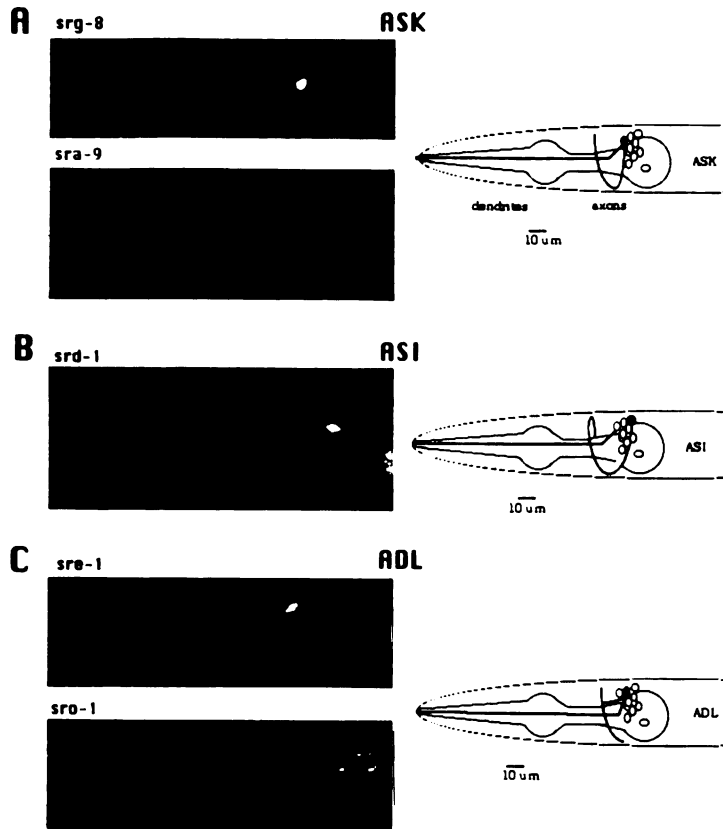


Figure 3. Expression of Reporter Gene Constructs in the ASK, ADL, and ASI Neurons

Fusions of the upstream regions of various genes were made to *GFP* and visualized in transgenic animals.

(A) Expression of *srg-8::GFP* and *sra-9::GFP* in ASK. Note the staining of axons and dendrites of the ASK neurons in the transgenic animals. Staining with *sra-7::GFP* and *srg-2::GFP* constructs was similar, but weaker.

(B) Expression of *srd-1::GFP* in the ASI neurons.

(C) Expression of *sre-1::GFP* and *sro-1::GFP* in the ADL neurons. Faint ASJ staining is also visible at lower right in *sre-1::GFP*. At right, morphology of the ASK, ASI, and ADL sensory neurons. Note the different axon morphologies, which were used to confirm the cell identifications made on the basis of position. The positions of the pharynx and other chemosensory neurons of the head are included for reference. Anterior is at left and dorsal up in all cases.

Table 1. Summary of *GFP* Expression Data

Gene	Cell	Function
Expression in chemosensory neurons		
<i>sra-7, sra-9, src-2, src-8</i>	ASK	Lysine chemotaxis; egg laying
<i>srb-6, sre-1, sro-1</i>	ADL	Octanol avoidance; water-soluble avoidance
<i>srd-1, sra-6</i> (faint)	ASI	Dauer pheromone; Na ⁺ , Cl ⁻ , cAMP, biotin, lysine chemotaxis
<i>srb-6</i> (faint), <i>srd-1</i> (males only)	ADF	Dauer pheromone; Na ⁺ , Cl ⁻ , cAMP, biotin chemotaxis
<i>sra-6, srb-6</i>	ASH	Osmotic avoidance, nose touch avoidance
<i>sre-1</i> (faint)	ASJ	Dauer pheromone (recovery)
<i>srg-13, srb-6</i>	PHA	Unknown, chemosensory
<i>srb-6</i>	PHB	Unknown, chemosensory
<i>sra-1</i> and <i>sra-6</i> (males only)	SPD/SPV	Sex pheromones/mating
<i>srd-1</i> (males only)	R8/R9?	Sex pheromones/mating
Expression in other cells		
<i>sra-8</i>	PVQ	Interneuron (chemosensory)
<i>sra-11</i>	AIY	Interneuron (chemosensory)
	AVB	Interneuron, locomotion
		One pharyngeal neuron
<i>sra-10</i>	URX	Sensory neuron
	ALA	Interneuron
		Additional interneurons, pharyngeal neurons, and muscle
<i>srb-6</i>		Vulval region
<i>srg-12</i>		Gut, excretory cell
<i>sro-1</i>	SIA	Neuron, unknown function

The cellular pattern of expression of each gene is given, along with the predicted function of those cells.

References are as follows. ASK, Bargmann and Horvitz, 1991a; E. Sawin and H. R. Horvitz, personal communication. ADL, Table 2; J. H. Thomas, personal communication. ASI and ADF, Bargmann and Horvitz, 1991a, 1991b. ASH, Bargmann et al., 1990; Kaplan and Horvitz, 1993; Table 2. ASJ, Bargmann and Horvitz, 1991b. SPD, SPV, and ray neurons, Liu and Sternberg, 1995.

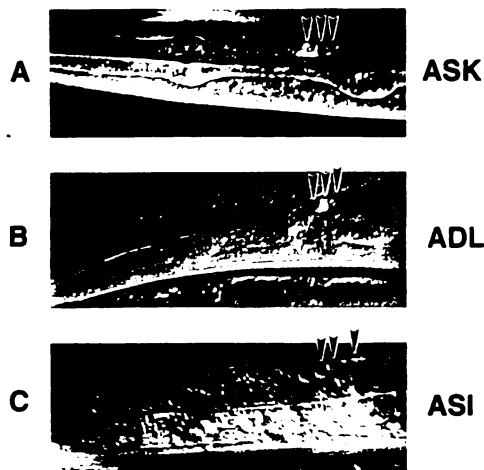


Figure 4. Alignment of Fluorescence and Nomarski Images (A), *srg-8::GFP* staining ASK; (B), *sre-1::GFP* staining ADL; (C), *srd-1::GFP* staining ASI. In all cases, the positions of the three dorsal neurons ASK, ADL, and ASI are noted on the Nomarski image with arrowheads (compare relative positions of these three neurons in Figure 3). Slides of fluorescence and Nomarski images of the same animal were aligned with Adobe Photoshop.

dures), but reporter gene expression was only observed in 14. This success rate is typical for promoter fusions with *C. elegans* genes (Lynch et al., 1995). The absence of expression in some cases might occur because the fusions lacked control sequences within the body of the gene, because of errors in predicting gene structure from genomic sequence, or because these genes are actually not expressed under our culture conditions (e.g., they might be expressed in alternative larval stages, or they might be pseudogenes).

Some Receptor Genes Are Expressed in Sex-Specific Patterns

During mating, the *C. elegans* male exhibits a stereotyped series of behaviors whose progress is regulated by sensory feedback (Hodgkin, 1983; Liu and Sternberg, 1995). The mating structures in the male tail contain 75 male-specific neurons, out of a total of 79 extra neurons in the male adult (Sulston et al., 1980). Cell ablation experiments have revealed functions for many male-specific neurons in different steps of male mating (Liu and Sternberg, 1995). Over 20 of the male-specific neurons have exposed sensory endings and therefore are candidate chemoreceptor neurons that might detect pheromones during mating (Sulston et al., 1980). To investigate whether some of the *sra-sro* genes might function as mating pheromone receptors, each gene fusion was examined in adult male animals.

Most of the gene fusions had identical patterns of expression in males and hermaphrodites, but three genes showed interesting patterns of male-specific expression. The most striking difference was observed with the fusion gene *sra-1::GFP*, for which no staining was observed in hermaphrodites. In males, sensory neurons associated

Table 2. ADL and ASH Function in Avoidance of Volatile Repellents

Animals	Time to Reversal (seconds)			Number of Assays (number of animals)
	Median	Mean	SEM	
Octanol avoidance				
Intact animals	4	6.07	0.56	60 (12)
ASH killed	19.5	14.03	0.88	66 (10)
ADL killed	8	10.47	0.93	47 (11)
AWB killed	5	6.75	1.0	20 (4)
Benzaldehyde avoidance				
Intact animals	4	4.97	0.63	33 (8)
ASH killed	20	15.45	1.23	22 (5)
ADL killed	3	4.96	0.90	28 (7)
AWB killed	5	6.3	1.13	16 (4)

Median and mean time to reversal for intact, ASH-killed, ADL-killed, and AWB-killed animals in the presence of the repellents 1-octanol and benzaldehyde are given. If animals did not reverse within 20 s, their time to reversal was scored as 20 s. Avoidance of octanol was significantly impaired in both ADL and ASH-killed animals (Mann-Whitney rank sum test, $p < 0.001$), but not in AWB-killed animals, while avoidance of benzaldehyde was impaired only in ASH-killed animals ($p < 0.001$).

with the spicules stained brightly with this fusion gene (Figures 6B and 6C). The spicules are spikelike mating structures that probe the ventral surface of the hermaphrodite during mating. They contain the putative chemosensory neurons SPD and SPV, which coordinate sperm release into the vulva and have been proposed to sense vulval pheromones (Liu and Sternberg, 1995). The neuroanatomy of the male tail is not as well described as the neuroanatomy of the hermaphrodite, but the cells that stained with *sra-1::GFP* were probably the spicule neurons SPD and SPV. One of these neurons was unambiguously a spicule-associated sensory neuron, since its dendrite invaded the spicule shaft (Figure 6B).

The gene *sra-6::GFP* was also expressed in one neuron pair associated with the spicules (Figure 6D). In addition, *sra-6::GFP* males showed staining in the PVQ interneurons and the ASH and ASI head chemosensory neurons, as did hermaphrodites that contained the *sra-6::GFP* transgene.

srd-1::GFP also had a different staining pattern in males and hermaphrodites, but it was found in a sex-specific pattern in nonsex-specific neurons. Both males and hermaphrodites expressed this gene fusion in the ASI sensory neurons; in addition, in males the fusion was expressed in the ADF sensory neurons (Figure 6E). While the ADF neurons are present in both sexes, the promoter fusion reveals a potential sex-specific regulation of gene expression in these neurons. The ADF and ASI neurons detect pheromones in hermaphrodites (Bargmann and Horvitz, 1991b); these cells might participate in sex-specific pheromone detection in males. *srd-1::GFP* was also expressed in some male-specific neurons in the tail (Figure 6F). Their morphology and position did not permit unambiguous identification of the neurons, but they might be chemosensory neurons associated with the sensory rays.

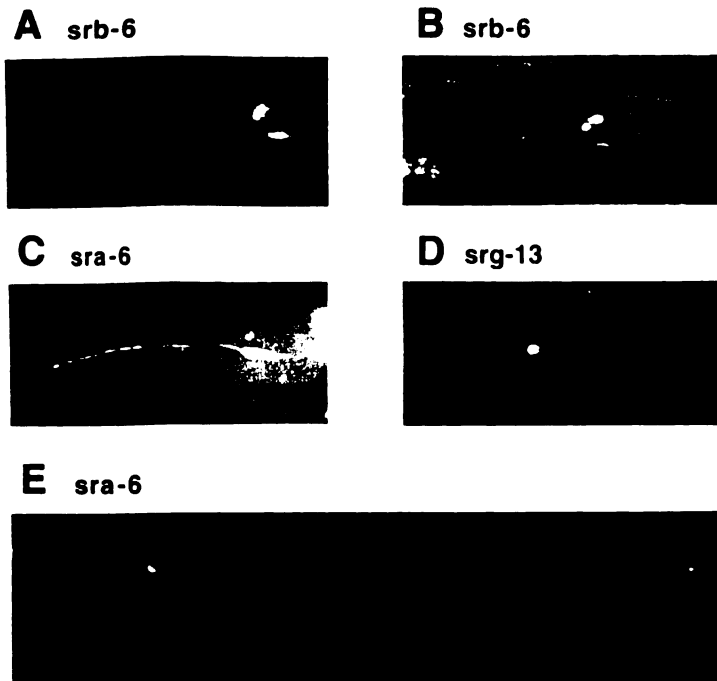


Figure 5. Expression of Additional Reporter Gene Constructs in Sensory and Nonsensory Cell Types

(A and B) Expression of *srb-6* in the ASH and ADL (A) and PHA and PHB (B) sensory neurons. ADF expression was weaker and is not obvious in this plane of focus. ASH and ADF morphologies are similar to that of ASK (Figure 3); PHA and PHB are bipolar sensory neurons in the tail with posterior dendrites and anterior axons. Gut autofluorescence is visible at the anterior edge of this photograph.

(C) Expression of *sra-6* in the ASH sensory neurons. Faint expression in the ASI neuron is visible just dorsal to the ASH neuron.

(D) Expression of *srg-13::GFP* in the PHA sensory neurons of the tail.

(E) Expression of *sra-6* in the ASH sensory neurons (anterior) and in the PVQ interneurons (posterior). Each PVQ neuron sends a single axon to the head. Anterior is at left and dorsal up in all cases.

Discussion

Novel Receptor-like Proteins from *C. elegans*

The *sra*, *srb*, *srg*, *srd*, *sre*, and *sro* genes have many properties reminiscent of the candidate olfactory receptor genes of vertebrates. First, they encode seven transmembrane receptors that could potentially be coupled to G proteins. The preponderance of evidence from both invertebrate and vertebrate systems supports the notion that such receptors are utilized in chemosensation (Breer et al., 1990; Buck and Axel, 1991; Boekhoff et al., 1994). Recent data implicate G protein-coupled receptors in *C. elegans* chemosensation as well. Animals mutant for the G proteins *gpa-2* and *gpa-3* are defective in pheromone detection (R. Zwaal and R. Plasterk, personal communication), and animals triply mutant for the G proteins *gpa-1*, *gpa-2*, and *gpa-3* are defective in chemotaxis to water-soluble attractants (E. R. T. and C. I. B., unpublished data). *gpa-1*, *gpa-2*, and *gpa-3* are expressed in sensory neurons, including those that express the *sra-sro* genes (J. Mendel and P. Sternberg, personal communication).

Second, at least eleven of these genes appear to be expressed in small numbers of chemosensory neurons. Eight genes were expressed only in sensory neurons, and six were expressed only in a single type of sensory neuron. Our results are based on expression of reporter gene constructs and therefore may not fully reflect the endogenous expression patterns of the receptor genes. Nonetheless, the highly reproducible patterns of sensory-specific expression are likely to reflect at least some aspects of the regulation of these genes in their natural context.

Third, a substantial number of these genes are present in the genome. Hermaphrodites have 14 classes of che-

mosensory neurons, and males probably have more; at a minimum, one receptor gene per type of chemosensory neuron would be expected to exist. Only a subset of these genes has been examined, but expression is already suggested for eight types of hermaphrodite chemosensory neurons and three types of male-specific chemosensory neurons.

Most of these genes are found in small clusters, like the vertebrate olfactory receptors, which are found in clusters of 10–100 genes (Ben-Arie et al., 1994). The largest *sra* and *srg* clusters are particularly striking, with nine genes each included within a region of about 30 kb. Unlike the immunoglobulin or T cell receptor genes, the vertebrate olfactory gene clusters do not seem to be rearranged or precisely coexpressed, so the reason for this clustering is unknown. Perhaps this arrangement helps coordinate receptor expression so that only one or a small number of receptors are expressed per sensory neuron (Chess et al., 1994). Although the *C. elegans* genes are clustered, all genes within a cluster did not share identical regulatory elements; for example, three different expression patterns were observed with fusion genes to four *sra* genes from one cluster.

Several other functions could be proposed for these receptor-like proteins. Some might be neurotransmitter receptors, but relatively few synaptic connections are made onto chemosensory neurons, so they are not expected to express many neurotransmitter receptors (White et al., 1986). Alternatively, they might be receptor molecules used for axon guidance or for the selection of synaptic targets by the chemosensory neurons. Each chemosensory neuron synapses onto several classes of target neurons, and no two types of neurons share the identical

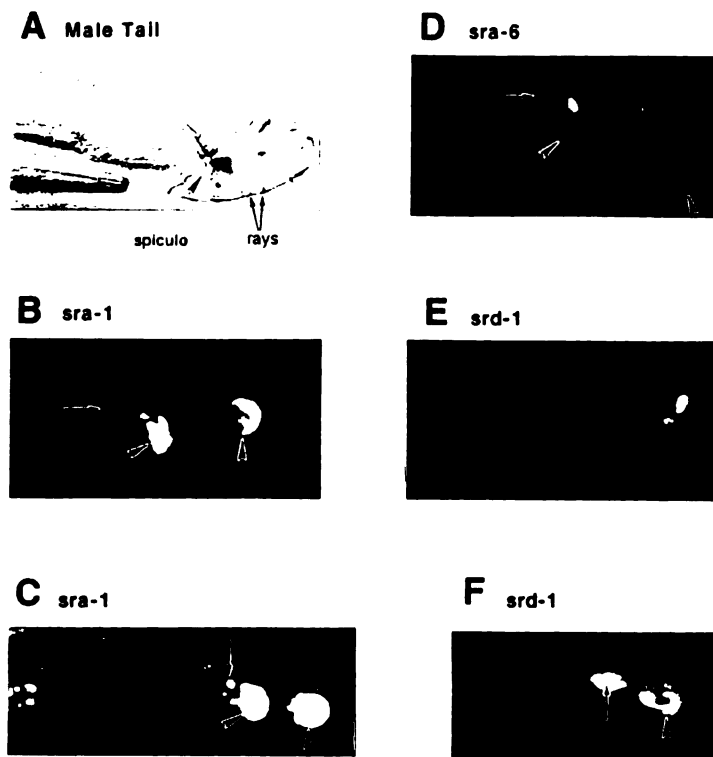


Figure 6. Male-Specific Expression of Fusion Genes

(A) Nomarski image of the male tail, with spicules and rays (compare hermaphrodite tail morphology in Figure 5). The male spicules and posterior male tail structures have an intense yellow autofluorescence (arrowheads here and in remainder of figure). Rays are located around the circumference of the male tail; only two are indicated.

(B) Expression of *sra-1::GFP* in the male tail. The *sra-1::GFP* fluorescence in SPD is green (arrow), while spicule and other autofluorescence is yellow (arrowheads). The dendrite of the spicule neuron SPD can be seen invading the shaft of the spicule.

(C) Axons of the SPD spicule neurons in the ventral nerve cord, as visualized in *sra-1::GFP* animals. An SPD cell body is denoted by an arrow.

(D) Expression of *sra-6::GFP*. One pair of male spicule neurons (arrow) and the PVQ neurons (unmarked; these neurons also stain in hermaphrodites) are visible.

(E and F) Expression of *srd-1::GFP* in males (compare Figure 3C). Two pairs of neurons, the ASI and ADF neurons, are visible in the head (e). Two additional neurons in the tail are visible, one denoted with an arrow in (F); they are bipolar neurons with one apparent sensory dendrite and one axon. These cells may be the R8 or R9 ray neurons.

downstream targets (White et al., 1986). The mechanism by which these connections are made is unknown, but it might involve specific receptors like those described here. Since there are multiple gene families, these models are not mutually exclusive; it is possible that some of the genes described here encode sensory receptors, and some of the genes have developmental or synaptic functions.

The *sra-sro* Receptors Might Sense Attractants, Repellents, or Pheromones

Since each of the sensory neurons appears to sense multiple chemicals, it is not obvious which chemical might be detected by a particular receptor gene. However, various fusion genes were expressed in chemosensory neurons that sense attractants, repellents, and pheromones.

A role in pheromone detection is suggested for the three genes for which sex-specific expression patterns were observed. Males demonstrate multiple responses to hermaphrodites that might involve chemosensation, including long-range chemotaxis to hermaphrodite pheromones, short-range behavioral changes in response to proximal hermaphrodites, and responses to vulval cues during mating (Liu and Sternberg, 1995; J. Hodgkin, E. Jorgensen, and J. H. Thomas, personal communication). Specific neurons mediate each successive step in male mating, suggesting that several sensory cues are detected during this process. Two fusion genes (to *sra-1* and *sra-6*) were expressed in sensory neurons that recognize the vulva during mating, suggesting that a mating pheromone might be detected by these receptors. Interestingly, there are

indications that some of the vertebrate olfactory receptor genes are expressed in sperm (Vanderhaeghen et al., 1993). In addition, the *srd-1::GFP* fusion gene was expressed in neurons implicated in both pheromone detection and chemotaxis, suggesting that these receptors might direct male responses to hermaphrodite pheromones.

All of the neurons that express the *sra-sro* genes are thought to detect water-soluble compounds, although the ASH and ADL neurons can also detect some volatile compounds. At this point it is unclear whether the receptors used for volatile chemotaxis in *C. elegans* will belong to this gene family. The *C. elegans* genes have no primary sequence similarity to the candidate vertebrate olfactory receptors (Buck and Axel, 1991), nor are they similar to a novel family of genes from the rat vomeronasal organ that might encode vertebrate pheromone receptors (Dulac and Axel, 1995 [this issue of *Cell*]). Water-soluble molecules might be recognized by a different type of receptor than volatile molecules; alternatively, the chemosensory systems of nematodes and mammals may have evolved independent, though related, receptor systems. One gene, *sro-1*, was distantly related to opsin genes, but on the basis of its sequence it is unlikely to be covalently linked to a retinal chromophore (Thomas and Stryer, 1982). One possibility is that this receptor might transiently interact with a hydrophobic retinal-like chemical and act as a chemoreceptor rather than a photoreceptor.

Despite the sensory enrichment of expression observed, some of these genes were expressed predominantly in

nonsensory cell types. These genes might encode receptors for other molecules used in communication between cells. For example, the receptors for attractive amino acids in chemosensory neurons might be similar to receptors for peptide or amino acid neurotransmitters in other cells.

C. elegans Sensory Neurons Are Likely to Express Multiple Receptors

The *GFP* expression patterns predict that several receptor genes, from different gene families, will be expressed in one chemosensory cell type. Four different fusion genes were expressed in the two ASK neurons, three genes in the ADL neurons, and two genes each in the ASI neurons, the ASH neurons, and the PHA neurons. Since only fourteen genes have been examined, it is likely that the total number of genes expressed per neuron will increase.

Even considering possible problems with expression of fusion genes, it is likely that more than one of these receptor genes is expressed per sensory neuron. Over 40 candidate receptor genes were found in the sequenced DNA of *C. elegans*, which encompasses about 15% of the genome. Even if only half of these genes are sensory receptors, the approximate number of receptors expected in the genome would be about 100, suggesting that many receptors could be found in one cell type.

These results contrast with observations in the vertebrate olfactory epithelium, where single neurons express a very small number of receptor genes, probably one per cell (Ressler et al., 1993; Vassar et al., 1993; Chess et al., 1994). Mammalian neurons expressing a single receptor gene appear to project to common targets in the olfactory bulb, where sensory information is integrated (Ressler et al., 1994; Vassar et al., 1994). By contrast, in *C. elegans* much of this integration may occur within the peripheral sensory neurons. The neurons detect multiple chemically dissimilar compounds; we propose that this occurs because each neuron expresses multiple receptors with different specificities. This prediction is also consistent with the behavioral data that indicate that responses to different attractants sensed by one neuron saturate and adapt independently (Ward, 1973; Colbert and Bargmann, 1995).

In addition, the possibility that multiple cells might express one receptor gene could explain other features of the *C. elegans* sensory system. In cell ablation studies, it was often found that a particular molecule was sensed, not by one cell type, but by a small group of neurons (Bargmann and Horvitz, 1991a, 1991b). The expression of *sra-6*, *srb-6*, and *sre-1* in two, five, and two sensory cell types, respectively, suggest that this cellular redundancy might derive from less specific expression of some receptor genes.

One open question raised by these results is the extent to which multiple receptors expressed on a single cell type contribute to perceptual discrimination, as opposed to recognition of various compounds. Behavioral discrimination in *C. elegans* was demonstrated by distinct patterns of cross-saturation and adaptation between different compounds sensed by one neuron. However, cross-saturation and adaptation experiments in humans suggest that different bitter compounds are recognized by different recep-

tors, even though the perception of all bitter compounds is the same to a human subject (McBurney et al., 1972; Lawless, 1987). Thus, the existence of several independently adapting receptors might not generate a true discrimination on the part of the animal. However, discrimination is strongly indicated in cases where one neuron mediates qualitatively different responses to different chemical stimuli. For example, the ADF and ASI sensory neurons affect both development, probably by detecting a pheromone, and chemotaxis, probably by detecting chemoattractants (Bargmann and Horvitz, 1991a, 1991b). It should be possible to ask whether this functional discrimination between chemicals arises at the level of receptors, signal transduction mechanisms, or assemblies of activated neuronal types.

Experimental Procedures

Sequence Analysis

The sequence of the cosmid AH6, which contains homology to a predicted guanylyl cyclase, was obtained from the Sanger Center Network site maintained by the *C. elegans* sequencing consortium (Sulston et al., 1992). AH6 was first analyzed by use of the BLASTX program, which translates sequences in all six frames before searching protein databases. All BLASTP (protein sequence) and BLASTX (DNA sequence) searches were performed with the NCBI (National Center for Biotechnology Information) BLAST network service to search databases including GenBank, SwissProt, PIR, and the Brookhaven Protein Data Bank (Altschul et al., 1990). BLASTX searches revealed at least ten different regions of AH6 that detected the previously sequenced *C. elegans* gene F44F4.5 (now *sra-10*). These regions were subsequently found to correspond to ten genes predicted by the *C. elegans* sequencing consortium, *sra-1-sra-9* and AH6.13, which appears to be a gene fragment. Each gene contained multiple potential transmembrane domains predicted by hydropathy analysis using the Kyte-Doolittle algorithm in Geneworks (Kyte and Doolittle, 1982).

The sequences of other *C. elegans* cosmids and coding regions predicted by the sequencing consortium were obtained through GenBank. BLASTP searches with *sra-1-sra-10* revealed more distant similarities to genes in the *srb* family. Continued searches with *sra* and *srb* genes led to the identification of the *arg*, *srf*, *sre*, and *sro* genes. In general, even weak sequence similarities were pursued if several members of a gene family recognized a new gene, and if that new gene encoded multiple predicted transmembrane domains.

Sequence alignments were produced by using the CLUSTAL W program (Thompson et al., 1994). In the initial alignments of the receptor clusters, many genes appeared to be gene fragments rather than full-length coding regions, on the basis of a smaller number of transmembrane domains. Unlike the vertebrate olfactory and vomeronasal receptors, all of the genes contain predicted introns. Analysis of the genomic organization of the receptors revealed that genes within one receptor family often shared conserved splice junctions (see, for example, *sra-2-sra-9*, all of which are generated from three similar exons [Figure 2]). Where the *C. elegans* sequencing project had predicted gene fragments rather than full-length gene products, we searched the genomic DNA for possible splice sites that corresponded precisely to those splice sites that were conserved in other family members. In several cases, changing the predicted genes to incorporate these conserved splice sites generated the full-length gene products shown in Figure 2.

In addition, for all genes with incomplete sequences, genomic DNA was examined for alternative exons or splice patterns. Genomic DNA was used to search the GenBank databases by using the BLASTX program as described above. This analysis revealed that many cosmids contained additional regions of homology to the receptor gene families. This information was used to predict full-length coding regions for those genes in which frameshifts or poor splice junctions were included (see below and Figure 2).

Genes that correspond exactly to genes predicted by the *C. elegans* sequencing project were as follows (the names for these genes given

by the sequencing project are shown in parentheses): *sra-1* (AH6.4), *sra-2* (AH6.6), *sra-3* (AH6.7), *sra-4* (AH6.8), *sra-6* (AH6.10), *sra-7* (AH6.11), *sra-8* (AH6.12), *sra-9* (AH6.14), *sra-10* (F44F4.5), *srb-6* (R05H5.6), *srb-11* (F23F12.10), *srg-8* (T12A2.9), *srg-10* (T04A8.1), *srg-12* (R13F6.3), *srg-13* (T23F11.5), *srd-1* (F33H1.5), *sre-1* (B0495.1), and *sro-1* (D1022.6).

Genes that differ in their splicing pattern from previously predicted genes include *srb-8* (modified from F37C12.6), *srb-9* (F37C12.8), *srg-1* (C18F10.4), *srg-2* (C18F10.5), *srg-3* (C18F10.6), *srg-9* (T12A2.10), *srd-2* (R05H5.1), and *sre-2* (C41C4.2). Similar analysis of a single predicted gene, C27D6.2, revealed five internal regions that could each encode a full-length receptor protein (renamed *srb-1*–*srb-5*). Analysis of the predicted gene F44F4.7 on the advice of S. Jones from the Sanger Center (personal communication) revealed that it most likely consisted of a false fusion of two genes, which were renamed *sra-11* and *sra-12*.

A few of the genes could only be aligned well to the other sequences if unfavorable splices or frameshifts were incorporated into their sequences. These genes might be pseudogenes or they might have sequencing errors; their alignments are shown in Figure 2 with incorporated frameshifts denoted by number symbols. They include *sra-5* (AH6.9, one frameshift), *srb-4* (one frameshift), *srb-7* (F37C12.5, one unfavorable splice, one frameshift), *srb-10* (F23F12.5, four frameshifts), and *srg-11* (T04A8.2, one unfavorable splice). BLASTP searches also revealed several predicted gene fragments that could not be aligned with complete coding regions of these genes; these genes have not been included here.

If a putative receptor gene was found near a region of 2 kb or more with no predicted coding regions, those regions were scanned for additional receptor genes with the BLASTX program. From this analysis, we found four additional genes in the C18F10 cluster (*srg-4*, *srg-5*, *srg-6*, and *srg-7*). Genes were predicted on the basis of a combination of amino acid similarity to other family members and conserved splice junctions.

Expression Constructs

Promoter fusions for the genes *sra-7* and *sra-11* were generated by using standard molecular biology methods to subclone these genes from cosmid clones (Sambrook et al., 1989). Four kilobases upstream of *sra-7* were included in a fusion to the reporter gene *GFP* (Chalfie et al., 1994); the fusion site was a HindIII site 31 amino acids into the predicted coding region of *sra-7*. Six kilobases upstream of *sra-11* and approximately two thirds of its coding region were included in an XhoI–XbaI fragment for a translational fusion to *GFP*.

All other promoter fusions were generated by using the polymerase chain reaction (PCR) to join *GFP* to the first 7–20 predicted amino acids of a given gene product. These fusions included 3–4 kb upstream of the predicted translational start site (2 kb of upstream region were used for *srg-8*). The downstream PCR primer was engineered to end in a BamHI site and the upstream primer in an SphI or PstI site, and the fragment was inserted into the *C. elegans GFP* expression vectors TU#61 and TU#62 (Chalfie et al., 1994). Promoters were amplified from purified cosmid DNA or *C. elegans* genomic DNA and checked for predicted restriction sites, and junctions were confirmed by DNA sequencing.

Most primers were amplified with Taq polymerase by PCR in 50 mM KCl, 10 mM Tris (pH 8.0), 2.5 mM MgCl₂, 200 μM each dNTP, and 50 ng of total genomic DNA or 10 ng of cosmid DNA. Cycling conditions were 94°C for 30 s, 55°C for 60 s, 72°C for 3–4 minutes for 30 cycles on an MJ Research thermal cycler. For some primer sets, this protocol did not give good amplification; in these cases, the amplifications were conducted with the Expand long template PCR kit (Boehringer) and conditions recommended by the manufacturer.

Microinjection and Analysis of Transgenic Animals

Expression constructs (10–50 ng/μl) were injected into the germline of *lin-15* (*n765ts*) animals together with the *lin-15* plasmid pJM23 (30–50 ng/μl), which was used as a coinjection marker to facilitate identification of transgenic animals (Mello et al., 1991; Huang et al., 1994). *lin-15* mutants have a multivulval phenotype; after injection, transgenic F1 animals were recognized by their normal vulval morphology at 20°C. These animals were used to establish transmitting lines of transgenic animals that expressed both plasmids from unstable arrays.

Typically, 40%–90% of the F2 or F3 animals in these lines would be rescued for the *lin-15* phenotype and therefore presumed to be transgenic. At least four independent lines were established for each expression construct, and *GFP*-expressing cells were identified in at least ten independent animals (in most cases, 20–30 animals were examined for each fusion gene). For the genes *sra-6*, *sra-7*, *sra-9*, *sra-10*, *sra-11*, *srb-6*, *srg-12*, *srg-13*, *srd-1*, *sre-1*, and *sro-1*, all examined lines showed comparable expression patterns. Promoter fusions to *srg-2* and *srg-8* did not give reproducible expression in all lines; we observed staining in only 3 of 8 tested lines for both of these constructs. For both *srg-2* and *srg-8*, all of those lines showed identical expression patterns (i.e., only ASK expressed the fusion gene). Promoter fusions to the genes *sra-2*, *sra-3*, *sra-8*, *srb-1*, *srb-8*, *srb-9*, *srb-10*, and *srb-11* showed no detectable *GFP* expression in at least four independently derived lines. *sra-1* was expressed only in males (see below).

Cell identifications were made by comparing the fluorescence image with Nomarski images of the same animal. Particular neurons were identified by using a combination of their position and their morphology, as previously described (Bargmann and Horvitz, 1991a). In all cases, cells were observed in well-fed animals that had been grown on standard nematode culture plates under sparse conditions (Brenner, 1974).

To identify staining cells in males, wild-type males were crossed to adult transgenic hermaphrodites and the resulting cross-progeny viewed by fluorescence optics. Only a fraction of the male cross-progeny carried the transgenic array, but since *lin-15* is on the X chromosome, all males that did not carry the array were multivulval at high temperature.

Behavioral Assays

Avoidance assays for volatile odorants were conducted by presenting concentrated odorant in front of the animal's nose in a 20 μl microcapillary pipette, or dipping an eyebrow hair into the odorant and presenting it in front of the animal's nose. Animals were scored for the time until their next reversal. Typically, wild-type animals reversed less than once per minute in the absence of odorant, while they reversed in approximately 4 s when presented with octanol or benzaldehyde. Wild-type and laser-operated animals were presented with odorants for four to ten trials per animal, with at least 5 min of rest between trials, and scored for reversal responses. If animals did not reverse within 20 s, the odorant was removed and the animal scored as negative. Results were compared by use of a Mann-Whitney rank sum test in the Statview II program. Cell ablations were conducted with a nitrogen-pumped dye laser and standard methods (Avery and Horvitz, 1987).

Acknowledgments

We thank Piali Sengupta and Kayvan Roayale for their advice and assistance; Liqin Tong for technical assistance; Erik Sonhammer, Steve Jones, Richard Zwaal, Ronald Plasterk, Jane Mendel, Paul Sternberg, Beth Sawin, Catherine Dulac, Richard Axel, and especially the *C. elegans* genome sequencing consortium for sharing unpublished data; and Piali Sengupta, Marc Tessier-Lavigne, and Richard Axel for their comments on this manuscript. This work was supported by Public Health Service grant DC01393. C. I. B. is a Markey Scholar and a Searle Scholar, and this work was supported in part by grants from these foundations. C. I. B. is an Assistant Investigator of the Howard Hughes Medical Institute.

Received July 21, 1995; revised August 21, 1995.

References

- Altschul, S.F., Gish, W., Miller, W., Myers, E.W., and Lipman, D.J. (1990). Basic local alignment search tool. *J. Mol. Biol.* 215, 403–410.
- Avery, L., and Horvitz, H.R. (1987). A cell that dies during wild-type *C. elegans* development can function as a neuron in a *ced-3* mutant. *Cell* 51, 1071–1078.
- Avery, L., and Horvitz, H.R. (1990). Effects of starvation and neuroactive drugs on feeding in *Caenorhabditis elegans*. *J. Exp. Zool.* 253, 263–270.
- Bargmann, C.I., Hartwig, E., and Horvitz, H.R. (1993). Odorant-

- selective genes and neurons mediate olfaction in *C. elegans*. *Cell* 74, 515–527.
- Bargmann, C.I., and Horvitz, H.R. (1991a). Chemosensory neurons with overlapping functions direct chemotaxis to multiple chemicals in *C. elegans*. *Neuron* 7, 729–742.
- Bargmann, C.I., and Horvitz, H.R. (1991b). Control of larval development by chemosensory neurons in *Caenorhabditis elegans*. *Science* 251, 1243–1248.
- Bargmann, C.I., Thomas, J.H., and Horvitz, H.R. (1990). Chemosensory cell function in the behavior and development of *Caenorhabditis elegans*. *Cold Spring Harbor Symp. Quant. Biol.* 55, 529–538.
- Ben-Arie, N., Lancet, D., Taylor, C., Khen, M., Walker, N., Ledbetter, D., Carozzo, R., Patel, K., Sheer, D., Lehrach, H., and North, M.A. (1994). Olfactory receptor gene cluster on human chromosome 17: possible duplication of an ancestral receptor repertoire. *Hum. Mol. Genet.* 3, 229–235.
- Boekhoff, I., Michel, W., Breer, H., and Ache, B. (1994). Single odors differentially stimulate dual second messenger pathways in lobster olfactory receptor cells. *J. Neurosci.* 14, 3304–3309.
- Breer, H., Boekhoff, I., and Tareilus, E. (1990). Rapid kinetics of second messenger formation in olfactory transduction. *Nature* 345, 65–68.
- Brenner, S. (1974). The genetics of *Caenorhabditis elegans*. *Genetics* 77, 71–94.
- Buck, L., and Axel, R. (1991). A novel multigene family may encode odorant receptors: a molecular basis for odor recognition. *Cell* 65, 175–187.
- Carulli, J.P., and Hartl, D.L. (1992). Variable rates of evolution among *Drosophila* opsin genes. *Genetics* 132, 193–204.
- Chalfie, M., Tu, Y., Euskirchen, G., Ward, W.W., and Prasher, D.C. (1994). Green fluorescent protein as a marker for gene expression. *Science* 263, 802–805.
- Chess, A., Simon, I., Cedar, H., and Axel, R. (1994). Allelic inactivation regulates olfactory receptor gene expression. *Cell* 78, 823–834.
- Colbert, H.A., and Bargmann, C.I. (1995). Odorant-specific adaptation pathways generate olfactory plasticity in *C. elegans*. *Neuron* 14, 803–812.
- Culotti, J.G., and Russell, R.L. (1978). Osmotic avoidance defective mutants of the nematode *Caenorhabditis elegans*. *Genetics* 90, 243–256.
- Dulac, C., and Axel, R. (1995). A novel family of genes encoding putative pheromone receptors in mammals. *Cell* 83, this issue.
- Dusenbery, D.B. (1974). Analysis of chemotaxis in the nematode *Caenorhabditis elegans* by countercurrent separation. *J. Exp. Zool.* 188, 41–47.
- Golden, J.W., and Riddle, D.L. (1984). A *Caenorhabditis elegans* dauer-inducing pheromone and an antagonistic component of the food supply. *J. Chem. Ecol.* 10, 1265–1280.
- Hodgkin, J. (1983). Male phenotypes and mating efficiency in *Caenorhabditis elegans*. *Genetics* 103, 43–64.
- Horvitz, H.R., Chalfie, M., Trent, C., Sulston, J.E., and Evans, P.D. (1982). Serotonin and octopamine in the nematode *Caenorhabditis elegans*. *Science* 216, 1012–1014.
- Huang, L.S., Tzou, P., and Sternberg, P.W. (1994). The *lin-15* locus encodes two negative regulators of *Caenorhabditis elegans* vulval development. *Mol. Biol. Cell* 5, 395–412.
- Huber, A., Smith, D.P., Zuker, C.S., and Paulsen, R. (1990). Opsin of *Calliphora* peripheral photoreceptors R1–8: homology with *Drosophila* Rh1 and posttranslational processing. *J. Biol. Chem.* 265, 17906–17910.
- Kaplan, J., and Horvitz, H. (1993). A dual mechanosensory and chemosensory neuron in *Caenorhabditis elegans*. *Proc. Natl. Acad. Sci. USA* 90, 2227–2231.
- Kyte, J., and Doolittle, R.F. (1982). A simple method for displaying the hydropathic character of a protein. *J. Mol. Biol.* 157, 105–132.
- Lawless, H.T. (1987). Gustatory psychophysics. In *Neurobiology of Taste and Smell*, T.E. Finger and W.L. Silver, eds. (New York: John Wiley and Sons), pp. 401–420.
- Liu, K.S., and Sternberg, P.W. (1995). Sensory regulation of male mating behavior in *Caenorhabditis elegans*. *Neuron* 14, 79–89.
- Lynch, A.S., Briggs, D., and Hope, I.A. (1995). A screen of developmental expression patterns for genes predicted in the *C. elegans* genome sequencing project. *Nature Genet.*, in press.
- McBurney, D.H., Smith, D.V., and Shick, T.R. (1972). Gustatory cross adaptation: sourness and bitterness. *Percept. Psychophys.* 11, 228–232.
- Mello, C.C., Kramer, J.M., Stinchcomb, D., and Ambros, V. (1991). Efficient gene transfer in *C. elegans*: extrachromosomal maintenance and integration of transforming sequences. *EMBO J.* 10, 3959–3970.
- Probst, W.C., Snyder, L.A., Schuster, D.I., Brosius, J., and Sealfon, S.C. (1992). Sequence alignment of the G-protein coupled receptor superfamily. *DNA Cell Biol.* 11, 1–20.
- Ressler, K., Sullivan, S., and Buck, L. (1993). A zonal organization of odorant receptor gene expression in the olfactory epithelium. *Cell* 73, 597–609.
- Ressler, K.J., Sullivan, S.L., and Buck, L.B. (1994). Information coding in the olfactory system: evidence for a stereotyped and highly organized epitope map in the olfactory bulb. *Cell* 79, 1245–1256.
- Sambrook, J., Fritsch, E.F., and Maniatis, T. (1989). *Molecular Cloning: A Laboratory Manual, Second Edition* (Cold Spring Harbor, New York: Cold Spring Harbor Laboratory Press).
- Sulston, J., Du, Z., Thomas, K., Wilson, R., Hillier, L., Staden, R., Halloran, N., Green, P., Thierry-Mieg, J., Qiu, L., Dear, S., Coulson, A., Craxton, M., Durbin, R., Berks, M., Metzstein, M., Hawkins, T., Ainscough, R., and Waterston, R. (1992). The *C. elegans* genome sequencing project: a beginning. *Nature* 356, 37–41.
- Sulston, J.E., Albertson, D.G., and Thomson, J.N. (1980). The *Caenorhabditis elegans* male: postembryonic development of nongonadal structures. *Dev. Biol.* 78, 542–576.
- Thomas, D.D., and Stryer, L. (1982). Transverse location of the retinal chromophore in rod outer segment disc membranes. *J. Mol. Biol.* 154, 145–157.
- Thomas, J.H. (1990). Genetic analysis of defecation in *Caenorhabditis elegans*. *Genetics* 124, 855–872.
- Thompson, J.D., Higgins, D.G., and Gibson, T.J. (1994). CLUSTAL W: improving the sensitivity of progressive multiple sequence alignment through sequence weighting, position-specific gap penalties and weight matrix choice. *Nucl. Acids Res.* 22, 4673–4680.
- Vanderhaeghen, P., Schurmans, S., Vassart, G., and Parentier, M. (1993). Olfactory receptors are displayed on dog mature sperm cells. *J. Cell Biol.* 123, 1441–1452.
- Vassar, R., Ngai, J., and Axel, R. (1993). Spatial segregation of odorant receptor expression in the mammalian olfactory epithelium. *Cell* 74, 309–318.
- Vassar, R., Chao, S.K., Sitcheran, R., Nufiez, J.M., Vooshall, L.B., and Axel, R. (1994). Topographic organization of sensory projections to the olfactory bulb. *Cell* 79, 981–992.
- Ward, S. (1973). Chemotaxis by the nematode *Caenorhabditis elegans*: identification of attractants and analysis of the response by use of mutants. *Proc. Natl. Acad. Sci. USA* 70, 817–821.
- Ward, S., Thomson, N., White, J.G., and Brenner, S. (1975). Electron microscopical reconstruction of the anterior sensory anatomy of the nematode *Caenorhabditis elegans*. *J. Comp. Neurol.* 160, 313–337.
- Ware, R.W., Clark, D., Crossland, K., and Russell, R.L. (1975). The nerve ring of the nematode *Caenorhabditis elegans*: sensory input and motor output. *J. Comp. Neurol.* 162, 71–110.
- White, J.G., Southgate, E., Thomson, J.N., and Brenner, S. (1986). The structure of the nervous system of the nematode *Caenorhabditis elegans*. *Phil. Trans. Roy. Soc. (Lond.) B* 314, 1–340.
- Zorio, D., Cheng, N., Blumenthal, T., and Spieth, J. (1994). Operons as a common form of chromosomal organization in *C. elegans*. *Nature* 372, 270–272.

Chapter 2. *odr-10* encodes a seven transmembrane domain olfactory receptor required for responses to the odorant diacetyl.

Published in: (1996) Cell 84: 899-909. Copyright © 1996 by Cell Press.

Statement of contributions

My contributions to this paper involved isolating and characterizing the *odr-10* null mutation.

Analysis of this mutant demonstrated that *odr-10* was necessary only for the response to diacetyl and not to pyrazine.

***odr-10* Encodes a Seven Transmembrane Domain Olfactory Receptor Required for Responses to the Odorant Diacetyl**

Piali Sengupta,* Joseph H. Chou,
and Cornelia I. Bargmann
Howard Hughes Medical Institute
Programs in Developmental Biology, Neuroscience,
and Genetics
Department of Anatomy
University of California
San Francisco, California 94143-0452

Summary

Olfactory signaling is initiated by interactions between odorants and olfactory receptors. We show that the *C. elegans odr-10* gene is likely to encode a receptor for the odorant diacetyl. *odr-10* mutants have a specific defect in chemotaxis to diacetyl, one of several odorants detected by the AWA olfactory neurons. *odr-10* encodes a predicted seven transmembrane domain receptor; a green fluorescent protein-tagged Odr-10 protein is localized to the AWA sensory cilia. *odr-10* expression is regulated by *odr-7*, a transcription factor implicated in AWA sensory specification. Expression of *odr-10* from a heterologous promoter directs behavioral responses to diacetyl, but not to another odorant detected by the AWA neurons. These results provide functional evidence for a specific interaction between an olfactory receptor protein and its odorant ligand.

Introduction

The remarkable discriminatory power of the olfactory system allows animals to generate diverse behavioral responses to odorants. Subtle alterations in chemical structures between two odorants can result in substantial differences in perceived olfactory quality. For example, two enantiomers of carvone produce the distinct sensations of spearmint and caraway. This perceptual difference suggests that distinct neuronal pathways are preferentially activated by each enantiomer, probably owing to selective binding of the odorants to different olfactory receptor proteins.

The receptors that interact with odorants are likely to be G protein-coupled seven transmembrane domain proteins. Vertebrate olfactory neurons produce cAMP in response to odorants (Pace et al., 1985; Sklar et al., 1986), which activates a cyclic nucleotide-gated channel in the olfactory cilia (Nakamura and Gold, 1987; Firestein et al., 1991). The cAMP pathway is thought to be the major vertebrate olfactory transduction pathway, but odorants also stimulate IP₃ production in invertebrate and vertebrate olfactory neurons (Boekhoff et al., 1990, 1994; Breer et al., 1990). Candidate receptor molecules have been identified in several sensory systems. In mammals, putative olfactory receptors are encoded by a large family consisting of ~1000 receptor genes (Buck and Axel, 1991) that may interact with odorants (Raming et al., 1993). An additional family of genes might encode

mammalian pheromone receptors (Dulac and Axel, 1995). These genes are expressed in the neurons of the olfactory epithelium and the vomeronasal organ, respectively. In the nematode *Caenorhabditis elegans*, several different families of candidate chemosensory receptor genes have been identified (the *sr* genes, which consist of *sra*, *srb*, *srd*, *sre*, *srg*, and *sro* families) (Troemel et al., 1995). These gene families encode potential chemosensory receptors based on their similarity to known G protein-coupled receptors and their preferential expression in chemosensory neurons.

It is not known how any of these sensory receptors interacts with its ligands. It is possible that each receptor interacts with only a small number of odorants, so that specific olfactory stimuli activate only a few receptors. Alternatively, the receptors might be able to recognize many different odorant molecules, with discrimination arising through later processing and integration of information by the nervous system. To address these issues, it is necessary to identify the odorant ligands that activate a given olfactory receptor protein under physiological conditions.

In the nematode *C. elegans*, molecular and functional properties of individual chemosensory neurons can be analyzed in the whole animal. An adult *C. elegans* hermaphrodite has 302 neurons in its nervous system, including 14 types of chemosensory neurons (White et al., 1986). In most cases, one type of neuron consists of a bilaterally symmetric pair of neurons with similar functions. The functions of 10 types of chemosensory neurons have been defined through behavioral analysis of animals in which particular cells have been killed. Two types of chemosensory neurons, called AWA and AWC neurons, are similar to vertebrate olfactory neurons in that they detect volatile (airborne) attractants (Bargmann et al., 1993). Each pair of neurons detects several different odorants: the AWA olfactory neurons detect diacetyl, pyrazine, and thiazoles, whereas the AWC olfactory neurons detect benzaldehyde, butanone, isoamyl alcohol, and thiazoles. In the presence of saturating levels of one odorant, animals can still respond to other odorants that are sensed by the same olfactory neuron (Bargmann et al., 1993; Colbert and Bargmann, 1995). These behavioral experiments suggest that one olfactory neuron has several distinct odorant-binding sites.

The expression patterns of the candidate *sr* receptor genes in *C. elegans* provide a possible explanation for the diverse functions mediated by single sensory cell types (Troemel et al., 1995). Multiple candidate receptor genes are expressed in a single chemosensory neuron, suggesting that the ability of these neurons to recognize many chemicals arises through the expression of several different receptors. However, the ligands for the *sr* receptors have not been defined.

A genetic approach to chemosensation provides a way to relate the functions of individual genes to particular behavioral responses. To identify the functions of genes involved in olfaction in *C. elegans*, we have conducted behavioral screens for mutants with specific olfactory defects (*odr*, or odorant-response mutants). Mutations in some *odr* genes affect many or all olfactory

*Present address: Department of Biology, Brandeis University, Waltham, Massachusetts 02254.

responses, whereas others have more selective effects on olfaction (Bargmann et al., 1993). Here we describe the genetic and molecular characterization of the *odr-10* gene, which functions in the response to a specific odorant, diacetyl. *odr-10* encodes a predicted seven transmembrane receptor that might interact directly with diacetyl in olfactory transduction.

Results

odr-10 Mutants Are Defective in Chemotaxis to Diacetyl

When placed in a gradient of an attractive odorant, *C. elegans* moves toward the peak of the gradient (Bargmann et al., 1993). Over 90% of wild-type animals accumulate at a point source of a strong attractant such as diacetyl in chemotaxis assays. A modified version of this assay was used to identify mutants with defects in their diacetyl responses. Mutagenized animals were given a choice between the attractants diacetyl and pyrazine, which are both recognized by the AWA olfactory neurons (Bargmann et al., 1993). Under the conditions used, wild-type animals preferentially accumulated at the diacetyl, animals that did not sense either odorant distributed randomly across the plate, and animals that did not sense diacetyl accumulated at the pyrazine. After two rounds of this behavioral enrichment and subsequent retesting, a single strain with a mutation in the *odr-10* gene was isolated.

odr-10(ky32) mutants were tested for chemotaxis to a panel of volatile odorants. The mutants were defective in their response to diacetyl, but exhibited wild-type behavior in their responses to all other tested odorants (Figure 1A). They also displayed normal responses to water-soluble attractants such as NaCl and lysine, to water-soluble repellents, and to mechanical stimuli (data not shown). Their development, locomotion, and fertility appeared to be normal.

Diacetyl is very similar in its chemical structure to two other attractants, butanone and 2,3-pentanedione, which are sensed primarily by the AWC olfactory neurons (Bargmann et al., 1993; P. S. and C. I. B., unpublished data) (Figure 1B). To determine whether *odr-10* mutants were subtly affected in their responses to any of these odorants, they were tested for chemotaxis to a range of different odorant concentrations (Figure 1C). *odr-10* mutants responded to high but not low concentrations of diacetyl (Figure 1C). However, their responses to all other odorants were normal for the entire range of tested concentrations.

odr-10 was mapped to the X chromosome, close to the gene *unc-6* (see Experimental Procedures). A deletion that spans the *odr-10* locus was used to determine whether the *odr-10* mutant defect was enhanced by lowering levels of *odr-10* activity. When *odr-10(ky32)* was placed in *trans* to the genetic deficiency *uDf1*, which deletes the *odr-10* region, the heterozygous animals did not exhibit additional defects (data not shown). In particular, *odr-10(ky32)/uDf1* animals displayed normal chemotaxis to pyrazine, and their chemotaxis to diacetyl was similar to that of *odr-10(ky32)* animals. No other behavioral or developmental defects were apparent in

this strain. These results are consistent with the *odr-10(ky32)* mutation causing a loss of *odr-10* function.

odr-10 Encodes a Predicted Seven Transmembrane Domain Receptor

The *odr-10* gene was cloned using the *C. elegans* physical map and rescue of the *odr-10* behavioral phenotype (Coulson et al., 1986, 1988). In brief, genetic map data placed *odr-10* between the *unc-6* gene, which is cloned (Ishii et al., 1992), and the DNA polymorphism *stP33* (Williams et al., 1992) (Figure 2A). Cosmids from this interval were injected into *odr-10* mutants together with the *lin-15* gene as a marker to identify transgenic animals (Mello et al., 1991; Clark et al., 1994; Huang et al., 1994). The resulting transgenic strains were tested for chemotaxis to diacetyl. The cosmid C41B5 was able to complement the *odr-10* defect, as was a 3.3 kb *Scal*-*EcoRV* subclone of the cosmid (Figure 2B).

The *Scal*-*EcoRV* subclone was used to probe a mixed-stage *C. elegans* cDNA library (Barstead and Waterston, 1989), and three cDNA clones were isolated. Two cDNAs appeared to be full length, based on the fact that they began with sequences from the *C. elegans* splice leader SL1 (Krause and Hirsh, 1987) and ended with a polyA stretch. The full-length cDNAs were 1118 bp long, and encoded a predicted protein of 339 amino acids (Figure 3A). The corresponding genomic region has been sequenced by the *C. elegans* sequencing consortium (Sulston et al., 1992; Wilson et al., 1994; R. Waterston, A. Coulson, J. Sulston, et al., personal communication). The *odr-10* gene is entirely contained within the 3.3 kb rescuing fragment and includes eight exons and seven introns (Figure 3B).

Hydrophobicity analysis of *odr-10* revealed seven hydrophobic peaks that could correspond to membrane-spanning domains (Figure 3C). This structure is reminiscent of G protein-coupled receptors (Probst et al., 1992). BLAST (basic local alignment search technique) searches of GenBank and EST (expressed sequence tag) databases did not reveal a high degree of similarity between *odr-10* and any known gene (Altschul et al., 1990). However, the highest similarity that was detected in these searches was to one of the candidate vertebrate olfactory receptors, I14 (Buck and Axel, 1991), with which *odr-10* showed 12% amino acid identity over its entire length. Weak similarity was also observed between *odr-10* and *srd-1* and *srd-2*, two of the candidate chemosensory receptor genes that have recently been identified in *C. elegans* (Troemel et al., 1995).

To confirm that this coding region corresponded to *odr-10*, a frameshift mutation was generated within the cloned gene at an *XhoI* site just before transmembrane domain VI. This frameshifted clone could no longer complement the *odr-10* mutant phenotype (Figure 2B).

A Null Mutation in *odr-10* Causes a Diacetyl-Specific Chemotaxis Defect

The coding region of the *odr-10* gene was sequenced in *odr-10(ky32)* to identify the mutation responsible for its defect. The *odr-10(ky32)* mutation is a G to A transition on the noncoding strand that results in the substitution of a tyrosine for a histidine in the third predicted

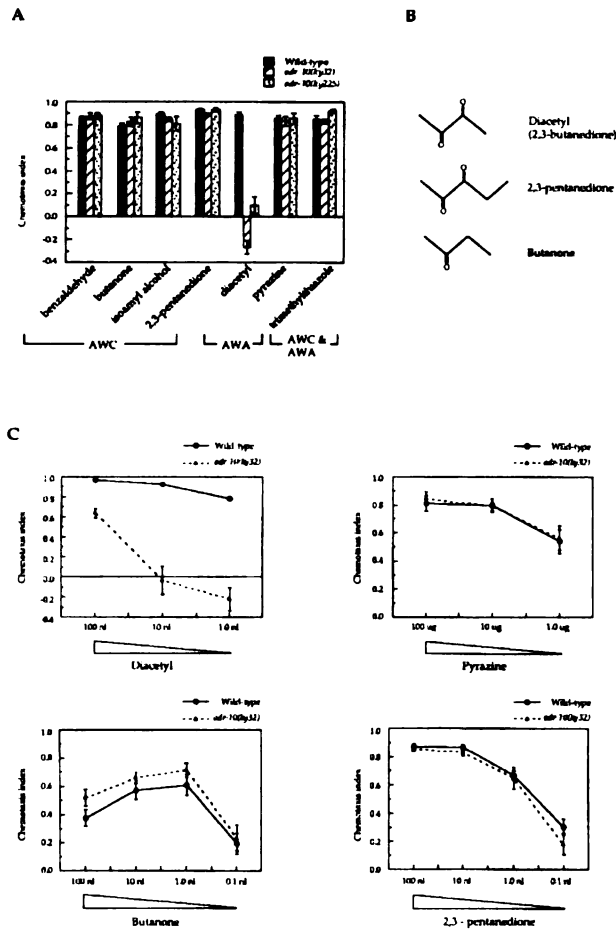


Figure 1. *odr-10* Mutants Do Not Respond to Diacetyl

(A) Chemotaxis responses of wild-type and *odr-10* mutants to volatile odorants. Responses of wild-type animals are indicated by closed bars, responses of *odr-10(ky32)* mutants by hatched bars, and responses of *odr-10(ky225)* animals by stippled bars. Chemotaxis index = (animals at the odorant - animals at the control)/total animals on the plate. A chemotaxis index of 1.0 indicates complete attraction; a chemotaxis index of -1.0 indicates complete repulsion. Each data point represents the average of six independent chemotaxis assays, using ~100 animals in each assay. Error bars equal the SEM. One microliter of diluted odorant was used per assay. Dilutions of odorants (in ethanol) were the following: 1:200 benzaldehyde, 1:1000 butanone, 1:200 isoamyl alcohol, 1:1000 2,3-pentanedione, 1:1000 diacetyl, 10 mg/ml pyrazine, and 1:1000 2,4,5-trimethylthiazole. Neurons required for the responses to these dilutions of odorants are indicated.

(B) Chemical structures of diacetyl (2,3-butanedione), 2,3-pentanedione and butanone. (C) Chemotaxis responses of wild-type and *odr-10(ky32)* mutants to different dilutions of diacetyl, pyrazine, butanone, and 2,3-pentanedione. Responses of wild-type animals are shown by open circles and those of *odr-10(ky32)* mutants by closed triangles; *odr-10(ky225)* mutants were similar to *odr-10(ky32)* mutants (data not shown). Each data point represents the average of six independent assays. Error bars equal the SEM. The indicated amount of each odorant was diluted in 1 µl of ethanol.

membrane-spanning domain of the protein (Figures 3A and 3B). This missense mutation might cause a partial defect in *odr-10* function, or it might eliminate all *odr-10* activity.

To determine the consequences of a complete loss of *odr-10* function, we generated a mutation that deleted most of the *odr-10* coding region. The mutation *odr-10(ky225)* was generated by insertion of the transposon Tc1 into the endogenous *odr-10* gene followed by imprecise Tc1 excision (Zwaal et al., 1993). This deletion eliminated all *odr-10* coding sequences beyond the end of the third predicted transmembrane domain of the protein (Figures 3A and 3B). *odr-10(ky225)* animals were tested for chemotaxis and found to be indistinguishable from *odr-10(ky32)* animals (Figure 1A and data not shown). Like *odr-10(ky32)* mutants, they showed a strong defect in chemotaxis to diacetyl, but normal chemotaxis to other ketones and to other odorants sensed by AWA. Since this deletion allele is likely to eliminate

all *odr-10* function, these results indicate that *odr-10* is uniquely important for the diacetyl response.

odr-7 Is Expressed in the Cilia of the AWA Olfactory Neurons

The Specific phenotype of *odr-10* mutants and the similarity between *odr-10* and other receptors suggested that *odr-10* might encode an olfactory receptor for diacetyl. To determine where the *odr-10* gene was expressed, the *odr-10* promoter was used to drive expression of the reporter gene GFP (green fluorescent protein) in transgenic worms (Chalfie et al., 1994; A. Fire, S. Xu, J. Ahnn, and G. Seydoux, personal communication). This fusion gene was strongly expressed in the two AWA neurons, which are the only neurons that sense low concentrations of diacetyl (Figure 4). The AWA neurons have sensory cilia that are exposed to the environment in specialized sensory organs at the tip of the

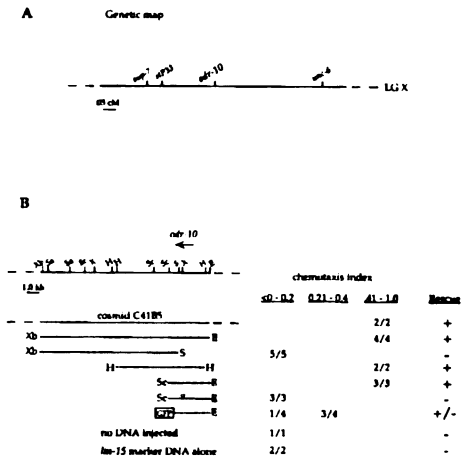


Figure 2. Genetic Map Position and Cloning of *odr-10*
(A) Genetic map position of *odr-10* on linkage group X.
(B) Localization of the *odr-10* gene. At top is a restriction map of the *odr-10* genomic region. The arrow indicates the direction of *odr-10* transcription. Below are shown the subclones that were tested for rescue of the *odr-10* mutant phenotype. The number of independent transgenic lines with an average chemotaxis index in the indicated intervals is shown as a fraction of the total lines tested; a minimum of 3 independent chemotaxis assays were conducted per line. An inverted triangle indicates the insertion of a frameshift mutation (see Experimental Procedures). The coding region of GFP was fused to *odr-10* to create a GFP-tagged Odr-10 protein (see text and Experimental Procedures). Xb = XbaI, Sa = SacI, Sc = Scal, X = XhoI, H = HpaI, S = SmaI, E = EcoRV.

animal's nose (Ward et al., 1975; Ware et al., 1975). From these cilia, the AWA dendrites project back to cell bodies near the posterior pharynx (Figure 4A). Since GFP diffuses freely through the cytoplasm of the cells, the characteristic axon and dendrite morphology of the cells, together with the position of the cell bodies, was used to assign their identity as AWA neurons. A lower level of GFP expression was observed in the four mechanosensory neurons called CEP (e.g., see Figure 6B); this weak staining may not reflect expression of the endogenous *odr-10* gene (see Experimental Procedures).

If *odr-10* is directly involved in odorant recognition, its protein product should be localized to the sensory cilia, the site at which odorants interact with their receptors. To examine the subcellular localization of Odr-10, the GFP reporter was fused to the extreme C terminus of *odr-10* to produce a fluorescently tagged Odr-10 protein. This fusion gene partially complemented the diacetyl chemotaxis defect of *odr-10* mutants (see Figure 2B). Expression of the GFP-tagged Odr-10 protein was limited to the extreme anterior region of the AWA olfactory

and the extent of the *ky225* deletion are indicated, along with the nucleotide and predicted amino acid alterations in *ky32*.
(C) Hydrophobicity plot of Odr-10. The plot was derived by Kyte-Doolittle hydrophobicity analysis of the predicted amino acid sequence of Odr-10 (Kyte and Doolittle, 1982).

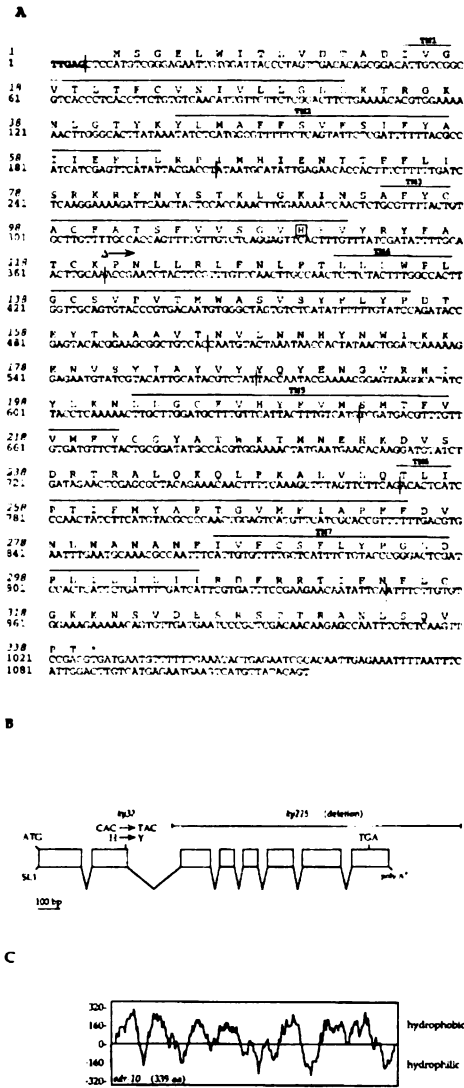


Figure 3. Sequence Analysis of *odr-10*
(A) Nucleotide and predicted amino acid sequences of the *odr-10* cDNA. Nucleotides are numbered beginning at the first nucleotide of the cDNA. Amino acids are numbered (in italics) starting at the first methionine. The STOP codon is marked by an asterisk. Splice junctions are marked by vertical lines and were determined by comparison of the sequences of the cDNA and corresponding genomic region. Nucleotides in bold at the 5' end are predicted to be derived from the *trans*-splice leader SL1 (Krause and Hirsh, 1987). The histidine residue that is altered to a tyrosine in the *ky32* mutation is boxed. The open triangle denotes the beginning of the *ky225* deletion. Residues predicted to form transmembrane domains 1 through 7 are indicated. The GenBank accession number for *odr-10* is U49449.
(B) Structure of the *odr-10* gene. The location of the *ky32* mutation

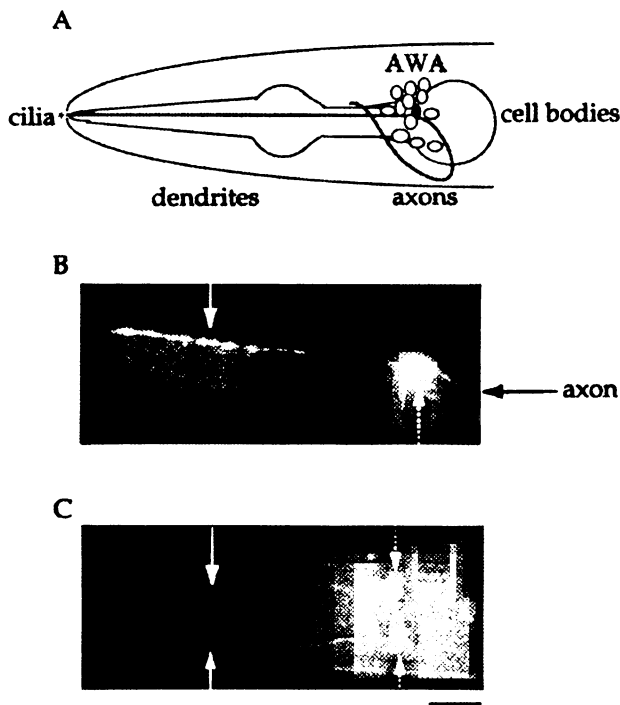


Figure 4. An *odr-10::GFP* Fusion Gene Is Expressed in the AWA Neurons

(A) Schematic diagram of cell bodies in the anterior sensory ganglion (lateral view). The cell body and processes of the AWA neuron are indicated in green. Anterior is at left and dorsal is up.

(B) Lateral view of a transgenic animal expressing the integrated *odr-10::GFP* fusion gene (see Experimental Procedures). The solid arrow indicates the dendrite and the dashed arrow indicates the cell body of the AWA neuron.

(C) Dorsal view of a transgenic animal expressing the integrated *odr-10::GFP* fusion gene. The solid arrows indicate the dendrites and the dashed arrows indicate the cell bodies of the AWA neurons. Scale bar = 10 μ m.

neurons, within the stereotypic branched AWA sensory cilia (Figure 5). Thus, the Odr-10 gene product appears to be localized to the sensory structures that mediate olfaction.

***odr-10* Expression Is Controlled by the *odr-7* Gene, Which Regulates Olfactory Specificity**

The *odr-7* gene is specifically required for olfactory function of the AWA neurons (Sengupta et al., 1994). Although their AWA neurons appear normal, *odr-7* null mutants are unable to respond to any of the odorants that are recognized by the AWA neurons. *odr-7* encodes a predicted transcription factor with similarity to the DNA-binding domains of the nuclear receptor superfamily; it has been proposed to regulate AWA sensory specificity by controlling the expression of AWA olfactory signaling molecules (Sengupta et al., 1994). If this explanation is correct, and if *odr-10* encodes the receptor for diacetyl, *odr-10* expression should be regulated by *odr-7*.

The expression of endogenous *odr-10* mRNA was examined in wild-type and *odr-7* mutant animals by reverse transcription-polymerase chain reaction. The *odr-10* message was present in wild-type animals but barely detectable in *odr-7(ky4)* null mutants (Figure 6A). The expression of the *odr-10::GFP* fusion gene was also examined in *odr-7* mutant animals. An integrated *odr-10::GFP* fusion gene was expressed in AWA in 100% of wild-type adults ($n = 36$). By contrast, the same integrated fusion gene was expressed in AWA in only 20%

of *odr-7(ky4)* animals ($n = 40$), and its expression in those animals was much weaker than observed in wild-type animals (Figure 6B). This *odr-10::GFP* fusion gene included 1 kb upstream of the predicted start site of *odr-10*, indicating that sequences sufficient to confer regulation by *odr-7* are included within this region.

***odr-10* Rescues Diacetyl but Not Pyrazine Responses in an *odr-7* Mutant**

The loss-of-function alleles of *odr-10* indicate that this gene is necessary for chemotaxis to diacetyl, but not necessary for chemotaxis to pyrazine. Two general models could explain these results. Odr-10 protein might specifically interact with diacetyl and not pyrazine. Alternatively, Odr-10 protein might interact with both odorants but be partly redundant with a second receptor in the AWA neurons that senses pyrazine, but not diacetyl. To distinguish between these models, we asked whether *odr-10* could rescue specific odorant responses in animals that lacked all AWA functions due to a mutation in the *odr-7* gene (Sengupta et al., 1994).

The wild-type *odr-10* cDNA was introduced into *odr-7* mutants under control of the *odr-3* promoter, which drives expression in both the AWA and the AWC sensory neurons (K. Roayaie and C. I. B., unpublished data). *odr-7* mutants did not chemotax to diacetyl or pyrazine, but transgenic *odr-7* animals expressing the *odr-3::odr-10* fusion gene were able to chemotax to diacetyl, but not pyrazine (Table 1). Thus, the *odr-10* gene product was sufficient to restore the diacetyl response in an

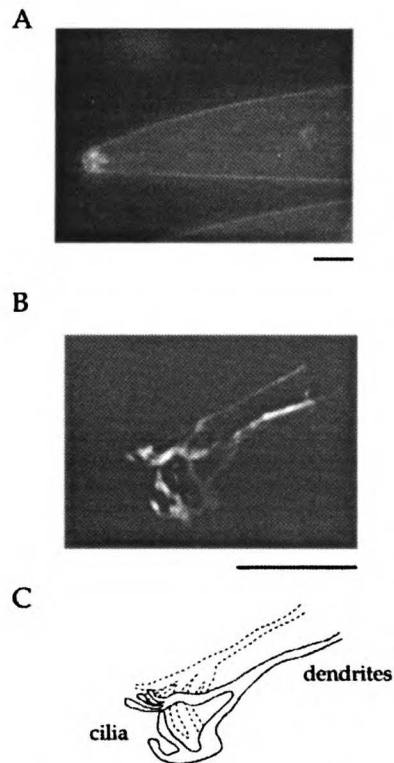


Figure 5. The Odr-10 Protein is Localized to the Sensory Cilia of the AWA Neurons

(A) Expression of the Odr-10 protein tagged with GFP (see Experimental Procedures). Strong GFP expression is seen at the tip of the nose, and faint expression is seen in the dendrites and cell bodies of the AWA neurons. Scale bar = 10 μ m.

(B) Higher magnification view of the cilia of a transgenic animal expressing the Odr-10 protein tagged with GFP. The AWA cilia are identified by their characteristic branched pattern. Three dimensional images were acquired using wide-field fluorescence microscopy and constrained iterative deconvolution (Hiraoka et al., 1990). Scale bar = 10 μ m.

(C) Schematic diagram of the sensory cilia of the AWA neurons. The image of the sensory cilia in (B) is shown. The solid and dashed lines represent the cilia of the two bilaterally symmetrical AWA neurons on the near and far sides of the animal, respectively.

odr-7 mutant, but not sufficient to restore the pyrazine response. These results indicate that expression of Odr-10 can confer a specific responsiveness to diacetyl on either the AWA or the AWC olfactory neurons.

Discussion

odr-10 Encodes a Candidate Receptor for Diacetyl

Based on their sequences and expression patterns, several families of vertebrate and invertebrate seven transmembrane domain proteins have been proposed to encode olfactory receptors (Buck and Axel, 1991; Ngai et

al., 1993b; Dulac and Axel, 1995; Troemel et al., 1995). The data presented here provide direct evidence that a single *C. elegans* receptor is required for the physiological response to an odorant, and indicate that the *odr-10* gene product is likely to be a receptor for the odorant diacetyl.

Two genetic results implicate *odr-10* as a critical component of the olfactory response to diacetyl. First, mutations in *odr-10* lead to a selective loss in the animal's ability to sense diacetyl. The mutants exhibit normal responses to other odorants recognized by the AWA olfactory neurons, and thus are not completely defective in AWA function. Second, expression of a wild-type *odr-10* cDNA specifically restores diacetyl sensitivity to a mutant (*odr-7*) that has lost its response to several odorants.

The pattern of *odr-10* expression suggests that *odr-10* is directly involved in sensory transduction. *odr-10::GFP* gene fusions are expressed at high levels in the AWA neurons, the single type of olfactory neuron that senses low concentrations of diacetyl. In addition, a tagged protein that contains the entire *odr-10* coding region is localized to the AWA sensory cilia. These cilia are probably used mainly for sensory transduction, and expression here suggests sensory function for *odr-10*. Because all AWA synapses are located on the AWA axons, which are distant from the cilia, *odr-10* is unlikely to participate in synaptic transmission (White et al., 1986).

Sequence analysis predicts that *odr-10* encodes a seven transmembrane domain receptor of the G protein-coupled superfamily, with distant similarity to the candidate mammalian olfactory receptors. At least 10 additional *C. elegans* genes that are similar to *odr-10* have been found in the sequenced regions of the *C. elegans* genome (Wilson et al., 1994; J. H. C., E. Troemel, and C. I. B., unpublished data; J. Sulston, A. Coulson, R. Waterston et al., personal communication). The predicted *odr-10* sequence includes several residues that are conserved in the G protein-coupled receptor superfamily, particularly residues around the third and seventh transmembrane domains (Probst et al., 1992). As yet there is no direct evidence for G protein involvement in *C. elegans* olfaction, but G proteins have been shown to function in pheromone detection and in other forms of chemosensation in worms (R. Zwaal and R. Plasterk, personal communication; E. Troemel and C. I. B., unpublished data). Since G protein signaling pathways are used in olfaction in vertebrates and other invertebrates (Jones and Reed, 1989; Breer et al., 1990), it is likely that they also function in the *C. elegans* olfactory system.

In mammals, it has been suggested that olfactory receptors may be part of an axon guidance system for olfactory neurons (Singer et al., 1995; Sullivan et al., 1995); neurons that express a single olfactory receptor project to common target glomeruli in the olfactory bulb (Ressler et al., 1994; Vassar et al., 1994). Two observations make it unlikely that *odr-10* plays a direct role in axon guidance of *C. elegans* olfactory neurons. First, *odr-10* mutants have morphologically normal AWA axons, so this receptor is not required for normal axon outgrowth and guidance. Second, the Odr-10 gene product appears to be localized to the sensory cilia of the AWA neurons, while axon outgrowth occurs from a distant part of the cell.

NOT LOAN

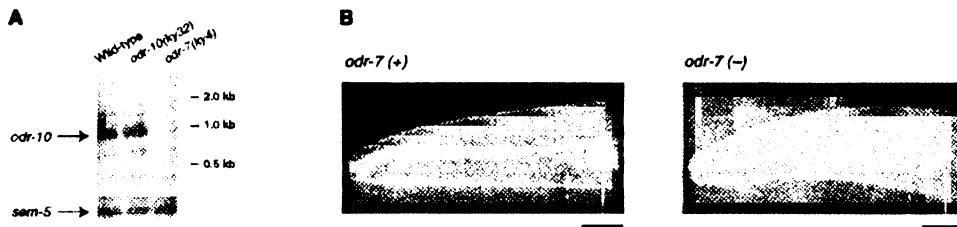


Figure 6. Expression of *odr-10* is Regulated by *odr-7*
(A) Expression of *odr-10* in wild-type, *odr-10(ky32)*, and *odr-7(ky4)* mutant animals. *odr-10* message was amplified by nested reverse transcription-polymerase chain reaction and detected by hybridization to an *odr-10* cDNA probe (see Experimental Procedures). *sem-5* message was amplified in parallel as a positive control.
(B) Expression of an *odr-10::GFP* integrated fusion gene in wild-type and *odr-7(ky4)* animals (lateral views). (Left) Expression of the fusion gene in an *odr-7(+)* background. The solid arrow indicates the position of the AWA cell body showing bright expression. The dashed arrow indicates the position of the CEP neurons. (Right) Expression of the integrated fusion gene in *odr-7(ky4)* mutants. The solid arrow indicates the expected position of the cell body of the AWA neuron. The dashed arrow indicates faint expression in one of four CEP neurons (see text and Experimental Procedures). This is the same fusion gene that is shown in Figure 4. Scale bar = 10 μ m.

Odorant Specificity of the *odr-10* Gene Product

Individual olfactory neurons in *C. elegans* can sense several different odorants, including odorants that can be distinguished by the animal in behavioral assays (Bargmann et al., 1993; Colbert and Bargmann, 1995). In principle, each neuron could express one olfactory receptor that detects many odorants, or several more specific olfactory receptors. The expression patterns of the putative chemosensory receptors encoded by the *sra*, *srb*, *srd*, *sre*, *srg*, and *sro* genes indicate that one sensory neuron can express many different candidate receptors (Troemel et al., 1995). Similarly, the genetic properties of *odr-10* favor the model that several olfactory receptors are expressed per neuron. The AWA olfactory neurons sense several structurally dissimilar odorants that are discriminated by the animal, including diacetyl and pyrazine. *odr-10* null mutants have defective responses to diacetyl but not pyrazine, suggesting the existence of at least one additional receptor on the AWA neurons.

Diacetyl specificity of Odr-10 was also indicated by

Table 1. *odr-10* Expression Driven by the *odr-3* Promoter Rescues Diacetyl but Not Pyrazine Responses in *odr-7(ky4)* Mutants

Strain	Fusion Gene Injected	Chemotaxis	
		Diacetyl	Pyrazine
<i>odr-7(ky4)</i>	none	-	-
<i>odr-7(ky4)</i>	<i>odr-10</i> cDNA (no promoter)	-	-
<i>odr-7(ky4)</i>	<i>odr-3::odr-10</i>	+	-
<i>odr-10(ky32)</i>	none	-	+
<i>odr-10(ky32)</i>	<i>odr-3::odr-10</i>	+	+

Fusion genes were microinjected into an *odr-7(ky4) lin-15(n765ts)* X strain or an *odr-10(ky32) lin-15(n765ts)* X strain together with *lin-15* marker DNA. At least four independent transgenic lines carrying each fusion gene were tested. Chemotaxis indices of 0–0.3 were scored as negative; indices of 0.3–1.0 were scored as positive. A minimum of three chemotaxis assays were conducted per transgenic line.

the observation that the *odr-10* cDNA rescues the diacetyl but not the pyrazine defect of *odr-7* mutants. Presumably, at least one additional gene controlled by the candidate transcriptional regulator *odr-7* is required for a normal pyrazine response.

The AWA neurons sense diacetyl at low concentrations, probably in the nanomolar range. However, they detect 2,3-pentanedione 10- to 100-fold less efficiently, and they do not detect 2-butanone at all (Bargmann et al., 1993; P. S. and C. I. B., unpublished data). Therefore, the diacetyl-sensing pathway of the AWA neurons selects among molecules with similar structures. If *odr-10* encodes the diacetyl receptor, this selectivity might be an intrinsic property of Odr-10, and the biochemical sensitivity of the Odr-10 protein to odorant agonists or antagonists could generate behavioral specificity.

Although many other tested odorant responses are normal in *odr-10* mutants, Odr-10 might sense odorants other than diacetyl. The AWA neurons are redundant with the AWC neurons for a number of olfactory responses, and a defect in the AWA component of those responses might not be apparent in behavioral assays.

Parallels between Vertebrate and Invertebrate Olfaction

The sequence similarity between *odr-10* and the vertebrate olfactory receptors is limited to a few residues in the predicted proteins (~10% overall amino acid identity). *odr-10* is more similar to these receptors than to other G protein-coupled receptors, but it is unclear whether the vertebrate and invertebrate olfactory receptors are derived from a common ancestor.

Vertebrate olfactory neurons have been reported to respond to many different odorants. For example, as many as 25% of all salamander olfactory neurons generate an electrical response to cineole (Firestein et al., 1993). If these salamander neurons are like mammalian olfactory neurons and express only one olfactory receptor gene per neuron, then that one receptor might recognize a broad variety of odorants. One rat olfactory receptor clone, OR5, has been shown to generate an

IP₃ response to many different odorants when expressed in SF9 cells (Raming et al., 1993). These studies suggest that vertebrate odorant-receptor interactions are relatively promiscuous. However, they were conducted at micromolar odorant concentrations, whereas physiological levels are in the nanomolar or picomolar range. At lower odorant concentrations, vertebrate receptors might also show the striking specificity observed with Odr-10.

Whereas individual *C. elegans* neurons probably express several receptor genes, mammalian olfactory neurons probably express only one receptor gene per neuron (Ressler et al., 1993; Vassar et al., 1993; Chess et al., 1994). Why should this difference exist? *C. elegans* has only 32 chemosensory neurons, but chemosensation is its most complex sensory modality and the main mechanism by which the animal makes qualitative judgments of its environment. Given the apparent chemical specificity of Odr-10 and the small number of sensory neurons, each cell might need to express many receptors for the animal to recognize the full spectrum of salient odorants. It will be interesting to determine whether olfactory systems of intermediate complexity, such as those of insects (Siddiqi, 1987), lobsters (Boekhoff et al., 1994), and fish (Ivanova and Caprio, 1993; Ngai et al., 1993a; Kang and Caprio, 1995), follow the mammalian pattern or the nematode pattern of receptor expression.

Experimental Procedures

Strains and Genetics

Wild-type worms were *C. elegans* variety Bristol, strain N2. Worms were grown using standard methods (Brenner, 1974).

Strains used in this work were: CX2111 *unc-58(e665dm)* X, MT1079 *egl-15(n484)* X, PS1032 *syDf1/unc-2(e55) lon-2(e678)* X, TY1093 *unc-42(e270)* V; *szT1/uDf1* X, CX2641 *dpy-8(e130) stDf1/lon-2(e678) egl-15(n484)* X; CB678 *lon-2(e678)* X, TY0367 *unc-18(e81) dpy-6(e14)* X, CX2629 *lon-2(e678) odr-10(ky32) unc-6(n102)* X, CX2818 *lin-15(n765ts)* X, CX2366 *odr-7(ky4) lin-15(n765ts)* X, CX2275 *odr-7(ky4) unc-9(e101)* X, CB101 *unc-9(e101)* X, MT3126 *mut-2(r459) I; dpy-19(n1347) III* and *C. elegans* variety Bergerac, strain RW7000.

Isolation of *odr-10(ky32)* and *odr-10(ky225)*

odr-10(ky32) was identified in a behavioral screen for animals that could not chemotax to diacetyl. The mutagenesis and mutant screens were performed as described previously (Bargmann et al., 1993). In brief, wild-type animals were mutagenized using the mutagen ethyl methanesulfonate (EMS). The F₂ progeny of ~3600 mutagenized F₁ animals were screened by giving them a choice between point sources of 1:10 dilution of diacetyl and 1 mg/ml pyrazine. After two rounds of choosing animals at the pyrazine, individual animals were placed on 6 cm plates, allowed to self-fertilize, and their progeny retested for chemotaxis defects.

odr-10(ky225) was generated by insertion and imprecise excision of the transposon Tc1 (Zwaal et al., 1993). Tc1 and *odr-10*-specific primers were used to screen 1000 frozen stocks of the mutator strain MT3126 by PCR, identifying one strain with a Tc1 insertion within the second intron of *odr-10*. The *odr-10::Tc1* strain was subjected to 68.7 mJ/cm² irradiation in a Stratagene UV Stratallinker to produce DNA breaks, and the progeny screened via PCR for imprecise excision of Tc1. An animal with a 1351 bp deletion that extended from the Tc1 insertion site to 428 bp past the *odr-10* stop codon was identified. The predicted product from this deletion (*odr-10(ky225)*) lacks all coding sequences past the N-terminal 120 amino acids of *odr-10*.

Both mutations were backcrossed four times before behavioral testing.

Mapping of *odr-10*

The initial isolate of *odr-10* carried two mutations: *odr-10(ky32)* and *odr(ky47)*. Both mutations were linked to *unc-58(e665dm)* X. *odr(ky47)* was mapped near *egl-15(n484)* X. *odr-10(ky32)* was covered by the genetic deficiency *syDf1* X but uncovered by the genetic deficiencies *uDf1* X and *stDf1* X. These data placed *odr-10(ky32)* between *mec-2* and *unc-6* on LG X.

odr-10(ky32) was separated from *odr(ky47)* by the following strategy: a strain carrying the two linked mutations *odr-10(ky32)* and *dpy-6(e14)* X was generated by isolating Dpy non-Unc recombinants in *odr-10(ky32) odr(ky47)/unc-18(e81) dpy-6(e14)* X animals. 8/8 Dpy non-Unc recombinants segregated *odr-10(ky32)*. Males carrying the *lon-2(e678)* X mutation were mated with *odr-10(ky32) dpy-6(e14)* X animals, and recombinants carrying only the *odr-10(ky32)* mutation were isolated on the basis of their behavioral phenotype in chemotaxis assays.

Restriction fragment length polymorphisms between the Bristol strain N2 and the Bergerac strain RW7000 were used to further localize *odr-10*. The polymorphism *stP33* is a 260 bp fragment detected in RW7000 using PCR (Williams et al., 1992). RW7000 males were mated with hermaphrodites carrying the three linked mutations *lon-2(e678) odr-10(ky32) unc-6(n102)* X. 3/13 Lon non-Unc recombinants lost the *stP33* Bergerac polymorphism. Of these three, two recombinants segregated *odr-10(ky32)*. This analysis placed *odr-10* between *stP33* and the gene *unc-6* on the physical map.

Molecular Biology Methods

All general molecular biology manipulations were performed using standard methods (Sambrook et al., 1989). Sequencing was performed using the fmol sequencing system (Promega). Sequence analysis was carried out using GeneWorks (Intelligenetics). Sequence comparisons were performed using the BLAST network service (Altschul et al., 1990) and the CLUSTAL W program (Thompson et al., 1994). Preliminary sequence of the *odr-10* genomic region was obtained courtesy of the *C. elegans* sequencing consortium at Washington University (St. Louis) (Wilson et al., 1994).

Germline Transformation

Germline transformation was carried out as described (Mello et al., 1991; Sengupta et al., 1994). Marker *lin-15* DNA (Huang et al., 1994) was used at a concentration of 50 µg/ml and test DNA at a concentration of 30 µg/ml. Transgenic animals were identified by rescue of the *lin-15(n765ts)* multivulval phenotype at 20°C.

Isolation and Characterization of cDNAs

The 3.3 kb Scal-EcoRV rescuing genomic fragment was used to screen approximately 1X 10⁶ plaques of a mixed stage *C. elegans* cDNA library (Barstead and Waterston, 1989). Three positive clones were identified and partial sequences were obtained from both ends of the clones. One clone was a hybrid cDNA obtained from fusion of a partial *odr-10* cDNA with an unidentified cDNA. The remaining two cDNAs were identical and encoded *odr-10*. One of these cDNAs was sequenced completely on both strands using ³²P-end-labeled oligonucleotides.

Sequencing of the *odr-10(ky32)* Mutant Allele

Genomic DNA was isolated from N2 and *odr-10(ky32)* animals as described (Klein and Meyer, 1993). The genomic region containing the *odr-10* gene was amplified using the primers PS-37 (5'-CCT CGT GAA ATC AGA TTT CAG-3') and PS-38 (5'-ACA TTC ATC ACG TCG GAA CTT-3') flanking the open reading frame. At least one strand of the open reading frames of all eight exons, the splice junctions, and ~50 bp beyond the initiator methionine and the termination codon were sequenced. The exon containing the *ky32* mutation was sequenced on both strands.

Generation of the Frameshift Mutation

A frameshift mutation was created at the XhoI site in the sixth exon of the *odr-10* gene using the following strategy: the Scal-EcoRV rescuing genomic fragment was cloned into the EcoRV site of the

pBluescript plasmid. The XhoI site in the polylinker was destroyed by digesting this plasmid with Apal and Sall, blunting the overhanging ends, and religating. A frameshift was then created at the remaining XhoI site in the *odr-10* gene by digesting with XhoI, filling in the protruding ends, and religating. This results in a frameshift after Arg-241 of Odr-10. The mutation was confirmed by DNA sequencing.

Generation of *odr-10* Expression Constructs

A translational *odr-10::GFP* fusion gene was made by ligating ~1 kb of upstream promoter sequences and sequences encoding the first four amino acids of *odr-10* in-frame into the GFP expression vector pPD95.77 (Chalfie et al., 1994; A. Fire, S. Xu, J. Ahnn, and G. Seydoux, personal communication). The GFP gene used in all experiments contains five engineered introns and the mutation S65C (Heim et al., 1995). *odr-10* sequences were amplified from a subclone of the genomic region in pBluescript. PCR was performed using the T3 primer and an *odr-10*-specific primer engineered to contain a BamHI site at one end (PS-44; 5'-TAG GGT AAT GGA TCC TTC CGA CAT GGA GCT GTA-3'). The resulting product was subcloned into the Sall and BamHI sites of pPD95.77. This strategy resulted in the addition of 20 amino acids between the fourth residue of the Odr-10 protein and the first methionine of GFP.

The Odr-10 protein tagged with GFP was constructed by amplifying ~1 kb of *odr-10* promoter sequences together with sequences encoding residues 1-337 of the Odr-10 protein, and ligating the PCR product in-frame into pPD95.77. Amplification was performed from a subclone of the *odr-10* genomic region in pBluescript using the primers T3 and PS-59 (5'-CAT TCA TCA GGA TCC AAC TTG AGA CAA ATT GGC-3'). PS-59 was designed to contain a BamHI site at the end. The amplified fragment was cloned into the Sall and BamHI sites of the pPD95.77 vector. This tagged protein includes 20 additional amino acids between Val-337 of Odr-10 and the initiator methionine of GFP. The sequence of the PCR product was confirmed by DNA sequencing.

The *odr-3::odr-10* expression construct was made in several steps. First, *odr-10* sequences encoding residues 1-337 of Odr-10 were amplified and inserted into pBluescript to remove the 3' untranslated region and polyA tail. Amplification was carried out on a plasmid containing the *odr-10* cDNA using the T3 and PS-59 primers. Second, a STOP codon was inserted by ligating an NheI linker (New England Biolabs) containing Stops in all three frames at the 3' end of the modified *odr-10* cDNA. Sequence analysis of this cDNA revealed three PCR-induced point mutations, which were removed by replacing an NsiI-BsmI fragment of the cDNA with a fragment from the original *odr-10* cDNA. Third, the GFP gene in the Tu#62 expression vector was replaced with the *odr-10* cDNA. This essentially creates a promoterless *odr-10* "expression" vector. Finally, a HindIII fragment containing approximately 3 kb of upstream sequences and sequences encoding the first 36 amino acids of *odr-3* was inserted into the SphI site in the polylinker of the *odr-10* "expression" vector by blunt-ended ligation. All junctions were verified by sequencing.

Most amplification reactions were carried out using 50-100 ng of plasmid DNA and 100 ng of each primer in 50 mM KCl, 10 mM Tris (pH 8.0), 1.5 mM MgCl₂, and 200 μM of each dNTP. Reaction conditions were 94°C for 30 s, 52°C for 1 min, 72°C for 1 min for 15 cycles on an MJ Research thermal cycler.

Detection of *odr-10* Transcripts by Reverse Transcription-Polymerase Chain Reaction

Total RNA was prepared from mixed stage N2, *odr-10(ky32)* and *odr-7(ky4)* animals by LiCl precipitations (Michael Finney, personal communication). First strand cDNAs for *odr-10* and *sem-5* (Clark et al., 1992) were prepared in the same reaction using the primers PS-38 and *sem-5* (5'-TGG AGA TTA AGT AAG AGA GGG C-3') and 10 μg of total RNA, essentially as described (Aatsinki et al., 1994). The cDNAs were used as templates for PCR amplification, using the primers SL1, PS-38, and *sem-5* to detect *odr-10* (test) and *sem-5* (positive control) messages. The first amplification of *odr-10* and *sem-5* cDNAs was performed in the same reaction. Reactions were subjected to additional rounds of amplification using SL1 and the nested primer PS-43 (5'-TGA AAT TGG CGT TTG CAT TCA-3')

for *odr-10* and SL1 and *sem-5* (5'-GTT GAA TTT GAC AGC C-3') for *sem-5*. Nested reactions for *odr-10* and *sem-5* were performed separately. The conditions for PCR were as described above except that 30 cycles of amplification were carried out in each round. The reaction products were resolved by electrophoresis, transferred to a nylon membrane, and probed with ³²P-labeled *odr-10* cDNA or a *sem-5* genomic fragment.

Expression of *odr-10::GFP* Fusion Genes

Transgenic *C. elegans* lines generated by microinjection bear extrachromosomal arrays of the injected DNA that are occasionally lost during meiosis and mitosis. To confirm the expression pattern of the *odr-10::GFP* fusion gene, a strain was generated where the fusion gene (and marker *lin-15* DNA) were integrated into the genome (Mello et al., 1991). Approximately 40 L4 larvae of a transgenic line carrying the extrachromosomal array of *odr-10::GFP* and *lin-15* were irradiated with gamma rays from a ¹³⁷Cs source (6000 rads). Six hundred transgenic F2 progeny of the mutagenized animals (recognized by their *lin-15*⁺ phenotype) were cloned onto individual plates. Potential integrants were identified by the absence of *lin-15* mutant progeny. A single strain CX3260 (*lin-15(n765ts); kytln37*) resulted from integration of the extrachromosomal array into LG II, near *rad-6*. This strain showed bright GFP expression in both AWA neurons in all animals. Although somewhat masked by this bright fluorescence, faint but consistent expression was also observed in the CEP neurons. Rarely, expression was also observed in other neurons, including ASI.

The expression pattern of the *odr-10::GFP* fusion gene was unaltered in *odr-10(ky32)* animals (data not shown). Additionally, the localization of the Odr-10 protein tagged with GFP was unaltered, and the AWA neurons had normal morphology of their sensory cilia, axons, and dendrites in *odr-10* mutants. An *odr-7::GFP* fusion gene is expressed only in the AWA neurons. Expression of this fusion gene was unaltered in *odr-10(ky32)* animals, indicating that the *odr-10(ky32)* mutation did not alter AWA cell fate (data not shown).

To visualize *odr-10::GFP* expression in *odr-7* mutants, the following strategy was used: N2 males were mated with *lin-15(n765ts); kytln37* hermaphrodites to obtain *lin-15(n765ts); kytln37/+* males. Heterozygous males were mated with *unc-9(e101) X* and *odr-7(ky4) unc-9(e101) X* hermaphrodites, and cross-progeny heterozygous for both *kytln37* and *unc-9* were cloned out. *Unc* animals in the F2 generation were again cloned out and homozygosed for *kytln37* by examination under fluorescence. The presence of the *odr-7(ky4)* mutation was confirmed by complementation analysis. GFP expression was observed faintly but consistently in the CEP neurons in both wild-type and *odr-7(ky4)* animals. Since the endogenous *odr-10* message was greatly reduced or absent in *odr-7(ky4)* mutants (Figure 6A), the expression of the reporter gene fusion in CEP may not be characteristic of the endogenous *odr-10* gene.

Acknowledgments

We thank Wallace Marshall for generating the high magnification image of the AWA cilia. We are grateful to Liqin Tong and Penny Mapa for excellent technical support; Kate Wesseling for the Tc1 insertion library; Kayvan Roayaie for the *odr-3* clone; Scott Clark for *sem-5* sequences; Bob Barstead for the cDNA library; Alan Coulson and John Sulston for cosmids; Andy Fire and Marty Chalfie for the GFP expression vectors; the Caenorhabditis Genetics Center and the Meyer lab for strains; and the *C. elegans* sequencing consortium at Washington University, St. Louis, for preliminary sequence data. We would also like to thank Caroline Murphy for assistance with software and Andrew Murray, Ira Herskowitz, Cynthia Kenyon, Noelle Dwyer, and Villu Maricq for critical comments on the manuscript.

P. S. was supported by a fellowship from the American Cancer Society, California Division. C. I. B. is an Assistant Investigator of the Howard Hughes Medical Institute, a Searle Scholar, and a Markey Scholar. This work was supported by Public Health Service grant DC01393 from the National Institute on Deafness and Other Communication Disorders at the National Institutes of Health.

Received December 21, 1995; revised January 29, 1996.

References

- Aatsinki, J.T., Lakkakorpi, J.T., Pietila, E.M., and Rajanemi, H.J. (1994). A coupled one-step reverse transcription PCR procedure for generation of full-length open reading frames. *BioTechniques* 16, 282-288.
- Altschul, S.F., Gish, W., Miller, W., Myers, E.W., and Lipman, D.J. (1990). Basic local alignment search tool. *J. Mol. Biol.* 215, 403-410.
- Bargmann, C.I., Hartwig, E., and Horvitz, H.R. (1993). Odorant-selective genes and neurons mediate olfaction in *C. elegans*. *Cell* 74, 515-527.
- Barstead, R.J., and Waterston, R.H. (1989). The basal component of the nematode dense-body is vinculin. *J. Biol. Chem.* 264, 10177-10185.
- Boekhoff, I., Tareilus, E., Strotmann, J., and Breer, H. (1990). Rapid activation of alternative second messenger pathways in olfactory cilia from rats by different odorants. *EMBO J.* 9, 2453-2458.
- Boekhoff, I., Michel, W., Breer, H., and Ache, B. (1994). Single odors differentially stimulate dual second messenger pathways in lobster olfactory receptor cells. *J. Neurosci.* 14, 3304-3309.
- Breer, H., Boekhoff, I., and Tareilus, E. (1990). Rapid kinetics of second messenger formation in olfactory transduction. *Nature* 345, 65-68.
- Brenner, S. (1974). The genetics of *Caenorhabditis elegans*. *Genetics* 77, 71-94.
- Buck, L., and Axel, R. (1991). A novel multigene family may encode odorant receptors: a molecular basis for odor recognition. *Cell* 65, 175-187.
- Chalfie, M., Tu, Y., Euskirchen, G., Ward, W.W., and Prasher, D.C. (1994). Green fluorescent protein as a marker for gene expression. *Science* 263, 802-805.
- Chess, A., Simon, I., Cedar, H., and Axel, R. (1994). Allelic inactivation regulates olfactory receptor gene expression. *Cell* 78, 823-834.
- Clark, S.G., Stern, M.J., and Horvitz, H.R. (1992). *C. elegans* cell-signaling gene *sem-5* encodes a protein with SH2 and SH3 domains. *Nature* 356, 340-344.
- Clark, S.G., Lu, X., and Horvitz, H.R. (1994). The *Caenorhabditis elegans* locus *lin-15*, a negative regulator of a tyrosine kinase signaling pathway, encodes two different proteins. *Genetics* 137, 987-997.
- Colbert, H.A., and Bargmann, C.I. (1995). Odorant-specific adaptation pathways generate olfactory plasticity in *C. elegans*. *Neuron* 14, 803-812.
- Coulson, A.R., Sulston, J., Brenner, S., and Karn, J. (1986). Towards a physical map of the genome of the nematode *Caenorhabditis elegans*. *Proc. Natl. Acad. Sci. USA* 83, 7821-7825.
- Coulson, A., Waterston, R., Kiff, J., Sulston, J., and Kohara, Y. (1988). Genome linking with yeast artificial chromosomes. *Nature* 335, 184-186.
- Dulac, C., and Axel, R. (1995). A novel family of genes encoding putative pheromone receptors in mammals. *Cell* 83, 195-206.
- Firestein, S., Zufall, F., and Shepherd, G.M. (1991). Single odor-sensitive channels in olfactory receptor neurons are also gated by cyclic nucleotides. *J. Neurosci.* 11, 3565-3572.
- Firestein, S., Picco, C., and Menini, A. (1993). The relation between stimulus and response in olfactory receptor cells of the tiger salamander. *J. Physiol.* 468, 1-10.
- Heim, R., Cubitt, A.B., and Tsien, R.Y. (1995). Improved green fluorescence. *Nature* 373, 663-664.
- Hiraoka, Y., Sedat, J.W., and Agard, D.A. (1990). Determination of three-dimensional imaging properties of a light microscope system. Partial confocal behavior in epifluorescence microscopy. *Biophys. J.* 57, 325-333.
- Huang, L.S., Tzou, P., and Sternberg, P.W. (1994). The *lin-15* locus encodes two negative regulators of *Caenorhabditis elegans* vulval development. *Mol. Biol. Cell* 5, 395-412.
- Ishii, N., Wadsworth, W.G., Stern, B.D., Culotti, J.G., and Hedgecock, E.M. (1992). UNC-6, a laminin-related protein, guides cell and pioneer axon migrations in *C. elegans*. *Neuron* 9, 873-881.
- Ivanova, T.T., and Caprio, J. (1993). Odorant receptors activated by amino acids in sensory neurons of the channel catfish *Ictalurus punctatus*. *J. Gen. Physiol.* 102, 1085-1105.
- Jones, D.T., and Reed, R.R. (1989). Golf: an olfactory neuron specific-G protein involved in odorant signal transduction. *Science* 244, 790-795.
- Kang, J., and Caprio, J. (1995). In vivo responses of single olfactory receptor neurons in the channel catfish, *Ictalurus punctatus*. *J. Neurophys.* 73, 172-177.
- Klein, R.D., and Meyer, B.J. (1993). Independent domains of the Sdc-3 protein control sex determination and dosage compensation in *C. elegans*. *Cell* 72, 349-364.
- Krause, M., and Hirsch, D. (1987). A trans-spliced leader sequence on actin mRNA in *C. elegans*. *Cell* 49, 753-761.
- Kyte, J., and Doolittle, R.F. (1982). A simple method for displaying the hydrophobic character of a protein. *J. Mol. Biol.* 157, 105-132.
- Mello, C.C., Kramer, J.M., Stinchcomb, D., and Ambros, V. (1991). Efficient gene transfer in *C. elegans*: Extrachromosomal maintenance and integration of transforming sequences. *EMBO J.* 10, 3959-3970.
- Nakamura, T., and Gold, G.H. (1987). A cyclic-nucleotide gated conductance in olfactory receptor cilia. *Nature* 325, 442-444.
- Ngai, J., Chess, A., Dowling, M., Nicles, N., Macagno, E., and Axel, R. (1993a). Coding of olfactory information: topography of odorant receptor expression in the catfish olfactory epithelium. *Cell* 72, 667-680.
- Ngai, J., Dowling, M., Buck, L., Axel, R., and Chess, A. (1993b). The family of genes encoding odorant receptors in the channel catfish. *Cell* 72, 657-666.
- Pace, U., Hanski, E., Salomon, Y., and Lancet, D. (1985). Odorant-sensitive adenylate cyclase may mediate olfactory reception. *Nature* 316, 255-258.
- Probst, W.C., Snyder, L.A., Schuster, D.I., Brosius, J., and Sealfon, S.C. (1992). Sequence alignment of the G-protein coupled receptor superfamily. *DNA Cell Biol.* 11, 1-20.
- Raming, K., Krieger, J., Strotmann, J., Boekhoff, I., Kubick, S., Baumstark, C., and Breer, H. (1993). Cloning and expression of odorant receptors. *Nature* 361, 353-356.
- Ressler, K.J., Sullivan, S.L., and Buck, L.B. (1993). A zonal organization of odorant receptor gene expression in the olfactory epithelium. *Cell* 73, 597-609.
- Ressler, K.J., Sullivan, S.L., and Buck, L.B. (1994). Information coding in the olfactory system: evidence for a stereotyped and highly organized epitope map in the olfactory bulb. *Cell* 79, 1245-1256.
- Sambrook, J., Fritsch, E.F., and Maniatis, T. (1989). *Molecular Cloning: A Laboratory Manual* (Cold Spring Harbor, NY: Cold Spring Harbor Press).
- Sengupta, P., Colbert, H.A., and Bargmann, C.I. (1994). The *C. elegans* gene *odr-7* encodes an olfactory-specific member of the nuclear receptor superfamily. *Cell* 79, 971-980.
- Siddiqi, O. (1987). Neurogenetics of olfaction in *Drosophila melanogaster*. *Trends Genet.* 3, 137-142.
- Singer, M.S., Shepherd, G.M., and Greer, C.A. (1995). Olfactory receptors guide axons. *Nature* 376, 19-20.
- Skilar, P.B., Anholt, R.R.H., and Snyder, S.H. (1986). The odorant-sensitive adenylate cyclase of olfactory receptor cells: differential stimulation by distinct classes of odorants. *J. Biol. Chem.* 261, 25538-25543.
- Sullivan, S.L., Bohm, S., Ressler, K.J., Horowitz, L.F., and Buck, L.B. (1995). Target-independent pattern specification in the olfactory epithelium. *Neuron* 15, 779-789.
- Sulston, J., Du, Z., Thomas, K., Wilson, R., Hillier, L., Staden, R., Halloran, N., Green, P., Thierry-Mieg, J., Qiu, L., et al. (1992). The *C. elegans* genome sequencing project: a beginning. *Nature* 356, 37-41.
- Thompson, J.D., Higgins, D.G., and Gibson, T.J. (1994). CLUSTAL

- W: Improving the sensitivity of progressive multiple sequence alignment through sequence weighting, position-specific gap penalties and weight matrix choice. *Nucl. Acids Res.* **22**, 4673–4680.
- Troemel, E.R., Chou, J.H., Dwyer, N.D., Colbert, H.A., and Bargmann, C.I. (1995). Divergent seven transmembrane receptors are candidate chemosensory receptors in *C. elegans*. *Cell* **83**, 207–218.
- Vassar, R., Ngai, J., and Axel, R. (1993). Spatial segregation of odorant receptor expression in the mammalian olfactory epithelium. *Cell* **74**, 309–318.
- Vassar, R., Chao, S.K., Sitcheran, R., Nunez, J.M., Vosshall, L.B., and Axel, R. (1994). Topographic organization of sensory projections to the olfactory bulb. *Cell* **79**, 981–992.
- Ward, S., Thomson, N., White, J.G., and Brenner, S. (1975). Electron microscopical reconstruction of the anterior sensory anatomy of the nematode *Caenorhabditis elegans*. *J. Comp. Neurol.* **160**, 313–337.
- Ware, R.W., Clark, D., Crossland, K., and Russell, R.L. (1975). The nerve ring of the nematode *Caenorhabditis elegans*: sensory input and motor output. *J. Comp. Neurol.* **162**, 71–110.
- White, J.G., Southgate, E., Thomson, J.N., and Brenner, S. (1986). The structure of the nervous system of the nematode *Caenorhabditis elegans*. *Phil. Transact. R. Soc. Lond. B* **314**, 1–340.
- Williams, B.D., Schrank, B., Huynh, C., Shownkeen, R., and Waterston, R.H. (1992). A genetic mapping system in *Caenorhabditis elegans* based on polymorphic sequence-tagged sites. *Genetics* **137**, 609–624.
- Wilson, R., Alnscough, R., Anderson, K., Baynes, C., Barks, M., Bonfield, J., et al. (1994). 2.2 Mb of contiguous nucleotide sequence from chromosome III of *C. elegans*. *Nature* **368**, 32–38.
- Zwaal, R.R., Broeks, A., van Meurs, J., Groenen, J.T., and Plasterk, R.H. (1993). Target-selected gene inactivation in *Caenorhabditis elegans* by using a frozen transposon insertion mutant bank. *Proc. Natl. Acad. Sci. USA* **90**, 7431–7435.

Chapter 3a. The *Caenorhabditis elegans* seven-transmembrane protein ODR-10 functions as an odorant receptor in mammalian cells.

Published in: (1997) Proc Natl Acad Sci USA 94: 12162-7. Copyright © 1997, National Academy of Sciences, U.S.A.

Statement of contributions

Chapter 2 presented genetic evidence that the seven-transmembrane protein ODR-10 was likely to act as the diacetyl receptor in *C. elegans*. However, this work did not confirm biochemically that ODR-10 is sufficient to mediate signaling in response to diacetyl. To address this issue, I entered into a collaboration with Kai Zinn's lab at the California Institute of Technology to show that ODR-10, expressed in a heterologous system, could function as a diacetyl receptor. This work represents the first definitive identification of an olfactory receptor with a known ligand.

The first part of this chapter is the publication that resulted from the collaboration with the Zinn group. In this paper, ODR-10 is shown to be capable of mediating a response to diacetyl when expressed in mammalian cells. Confirming the genetic findings, ODR-10 was highly specific, responding to diacetyl but not to the structurally related compounds butanone and 2,3-pentanedione. Surprisingly, however, transfected cells also exhibited responsiveness to the unrelated compounds pyruvic acid and citric acid.

My contribution to the publication included generation of all *odr-10* mammalian expression constructs and conducting the *C. elegans* experiments referred to in the paper. These experiments, which address the ability of ODR-10 to respond to pyruvic acid and citrate in *C. elegans in vivo*, are described in the second part of this chapter.

The *Caenorhabditis elegans* seven-transmembrane protein ODR-10 functions as an odorant receptor in mammalian cells

(olfaction/G protein-coupled receptor/signal transduction/chemotaxis)

YINONG ZHANG*, JOSEPH H. CHOU†, JONATHAN BRADLEY*§, CORNELIA I. BARGMANN†, AND KAI ZINN*¶

*Division of Biology, California Institute of Technology, Pasadena, CA 91125; and †Howard Hughes Medical Institute, Programs in Developmental Biology, Neuroscience, and Genetics, Department of Anatomy, University of California, San Francisco, CA 94143-0452

Communicated by Norman Davidson, California Institute of Technology, Pasadena, CA, August 26, 1997 (received for review July 20, 1997)

ABSTRACT The nematode *Caenorhabditis elegans* exhibits behavioral responses to many volatile odorants. Chemotaxis toward one such odorant, diacetyl (butanedione), requires the function of a seven-transmembrane receptor protein encoded by the *odr-10* gene. To determine directly whether ODR-10 protein is an odorant receptor, it is necessary to express the protein in a heterologous system and show that it responds to diacetyl by activation of a G protein signaling pathway. Here we demonstrate that human cells expressing ODR-10 on their surfaces exhibit a transient elevation in intracellular Ca^{2+} levels after diacetyl application. Volatile compounds that differ from diacetyl only by the addition of a methyl group (2,3-pentanedione) or the absence of a keto group (butanone) are not ODR-10 agonists. Behavioral responses to these compounds are not dependent on *odr-10* function, so ODR-10 specificity in human cells resembles *in vivo* specificity. The apparent affinity of ODR-10 for diacetyl observed in human cells is consistent with the diacetyl concentration ranges that allow efficient nematode chemotaxis. ODR-10 expressed in human cells also responds to two anionic compounds, pyruvate and citrate, which are metabolic precursors used for diacetyl production by certain bacterial species. Ca^{2+} elevation in response to ODR-10 activation is due to release from intracellular stores.

In both vertebrates and invertebrates, the olfactory system can detect hundreds or thousands of volatile odorants, yet is capable of discriminating between compounds that differ only slightly in chemical structure. Binding of odorants to receptors in the vertebrate olfactory epithelium is thought to activate adenylyl cyclase (AC) via a G_{α} -like G protein (reviewed in ref. 1). The cAMP thus produced opens a cyclic nucleotide-gated cation channel that is required for all odorant responses in mice (2). The best candidates for mammalian odorant receptors are the members of a very large family (>500 genes) of olfactory-specific seven-transmembrane receptors (1, 3). These receptors have not been demonstrated to bind to odorants or to activate AC when expressed in heterologous cells, however.

Because it has only 32 chemosensory neurons and is accessible to genetic analysis, the soil nematode *Caenorhabditis elegans* provides a valuable system in which to define genes and proteins that control olfactory behavior. Chemotaxis to volatile attractants is mediated by two pairs of ciliated neurons, AWA and AWC (4). A cyclic nucleotide-gated channel is required for volatile odorant responses mediated by AWC but not for those controlled by AWA (5, 6). Like vertebrates, *C. elegans* has a large repertoire (>100 genes) of seven-

transmembrane receptors expressed in chemosensory neurons (7).

Mutations in the nematode *odr-10* gene affect chemotaxis toward only one volatile odorant, diacetyl (butanedione) (8). Diacetyl is produced as an end product of fermentation by bacteria that can serve as a food source for the nematode. The ability to respond to diacetyl and other volatile metabolites provides a mechanism for long-range detection of bacterial populations. Attractive responses to diacetyl are mediated by the AWA neuron, whereas the responses to two closely related odorants, butanone and 2,3-pentanedione, require AWC function and are unaffected by ablation of AWA (8) (P. Sengupta and C.I.B., unpublished results).

The *odr-10* gene encodes a seven-transmembrane domain protein that is distantly related to the G protein-coupled receptor superfamily. *odr-10* is expressed only in the AWA neurons, and an ODR-10 fusion protein localizes to the distal cilia of the AWA dendrites where odorant detection is thought to occur (8). These results suggest that ODR-10 could selectively interact with diacetyl from the external environment and activate a G protein in response to diacetyl binding. Because AWA function is not dependent on the cyclic nucleotide-gated channel, ODR-10 might be expected to couple to a different signaling pathway than that used by vertebrate odorant receptors.

Alternative models could also explain these genetic data. For example, ODR-10 could bind to a number of structurally related odorants, but behavioral responses to compounds other than diacetyl might be suppressed by mechanisms downstream of the receptor. To distinguish between these models requires a functional assay in which ODR-10 specificity can be directly evaluated. Here we show that ODR-10 expressed in human cells can activate a G protein signaling pathway leading to release of Ca^{2+} from intracellular stores. Our results indicate that ODR-10 is indeed a diacetyl-specific odorant receptor.

MATERIALS AND METHODS

Molecular Biology. A full-length *odr-10* cDNA was inserted into pCS2 cytomegalovirus (CMV) promoter expression vectors. In the Myc-ODR-10 plasmid, the ODR-10 coding sequence was inserted immediately 3' to a sequence encoding six copies of a 13-residue c-myc epitope in the vector pCS2+MT (9). The epitope-tagged β_2 -adrenergic receptor (HA- β_2 AdR) sequence is in pcDNA1/amp (Invitrogen), and the plasmid

Abbreviations: HA, hemagglutinin; HEK293, human embryonic kidney 293; β_2 AdR, β_2 -adrenergic receptor; ACh, acetylcholine; M_1 AChR, muscarinic M_1 ACh receptor; EC_{50} , half-maximal effective concentration.

¶To whom reprint requests should be addressed. e-mail: zinnk@ccat.caltech.edu.

§Present address: Laboratoire de Neurobiologie, Ecole Normale Supérieure, 46 rue d'Ulm, 75005 Paris, France.

The publication costs of this article were defrayed in part by page charge payment. This article must therefore be hereby marked "advertisement" in accordance with 18 U.S.C. §1734 solely to indicate this fact.

© 1997 by The National Academy of Sciences 027-8424/97/9412162-6\$2.00/0 PNAS is available online at <http://www.pnas.org>.

contains one copy of the 12CA5 influenza hemagglutinin (HA) epitope at the N terminus of β 2AdR.

Cell Culture and Immunofluorescence. HEK293 cells were maintained in a high glucose medium (GIBCO) with 10% fetal calf serum and lacking pyruvate. Cells were plated onto poly-D-lysine-coated 15-mm glass coverslips in 35-mm tissue culture dishes 24 hr before transfection. Lipofectamine (GIBCO) was used as the DNA carrier. Two micrograms of plasmid DNA (ODR-10 plasmids or control plasmid vectors) was added to each culture dish. The cells were incubated with the mixture for 10 hr at 37°C. Two days after transfection, cells were fixed and permeabilized with methanol at -20°C for 20 min. Anti-c-myc (Oncogene Sciences; 9E10) and anti-HA (Boehringer Mannheim; 12CA5) mAbs were used at 1:1,000 and 1:200 dilutions, respectively. Fluorescein isothiocyanate (FITC)-conjugated secondary antibody (Jackson ImmunoResearch) was used at a 1:200 dilution. Staining and visualization were carried out according to standard procedures.

Flow Cytometry. For flow cytometry, cells were grown on 10-cm tissue culture plates and transfected as described above. For each plate, 16 μ g of plasmid DNA was used. The control vector in the experiment of Fig. 1 was pCS2-CMV-lacZ. The transfected cells were gently washed off the plate after incubation in divalent-free Hanks' balanced salt solution (HBSS; GIBCO). The solution was supplemented with 2.5 mg/ml BSA, 5 mM NaN₃, 250 μ g/ml DNase, and 0.5 mM EDTA. The cells were counted, spun down, and resuspended in the above HBSS buffer with divalents to allow DNase digestion. The

secondary antibody was a phycoerythrin-conjugated goat anti-mouse IgG (Caltag, South San Francisco, CA). After staining, the cell suspensions were washed and filtered through a fine nylon mesh and incubated in HBSS at 2×10^6 cells per ml. Cells were analyzed on a Coulter Epics Elite flow cytometer with an argon laser exciting at 488 nm (15 mW).

Fura-2 Ca²⁺ Imaging. Approximately 48 hr after transfection, cells were incubated for 45 min at 37°C in a loading buffer (pH 7.4) containing 140 mM NaCl, 3 mM KCl, 10 mM Hepes, 10 mM glucose, 2 mM CaCl₂, 0.005 mM Fura-2-AM (Molecular Probes), and 0.1% Pluronic F-127. The cells were then incubated for another 1.5 hr at room temperature before washing. The loaded coverslips were mounted onto a micro-imaging chamber (RC21A, Warner Instruments, Hamden, CT). The bath volume of the chamber was 150 μ l. Bath perfusion and drug delivery were controlled by an automated solenoid valve controller (AutoMate Science, Oakland, CA). The solution exchanging time was about 5 sec. Diacetyl, butanone, 2,3-pentanedione, acetoin, pyrazine, and the anionic compounds were all dissolved in water and diluted into loading buffer. Hydrophobic odorants were dissolved in dimethyl sulfoxide, mixed into pools, and sonicated into loading buffer (final concentration = 5 μ M each; names of tested odorants are available from the authors on request).

The imaging chamber was mounted on top of a Zeiss Axiovert-10 inverted microscope, and a Zeiss Plan-Neofluar 40 \times oil immersion objective lens was used. Samples were illuminated by a 75-W xenon bulb, and a computer-controlled

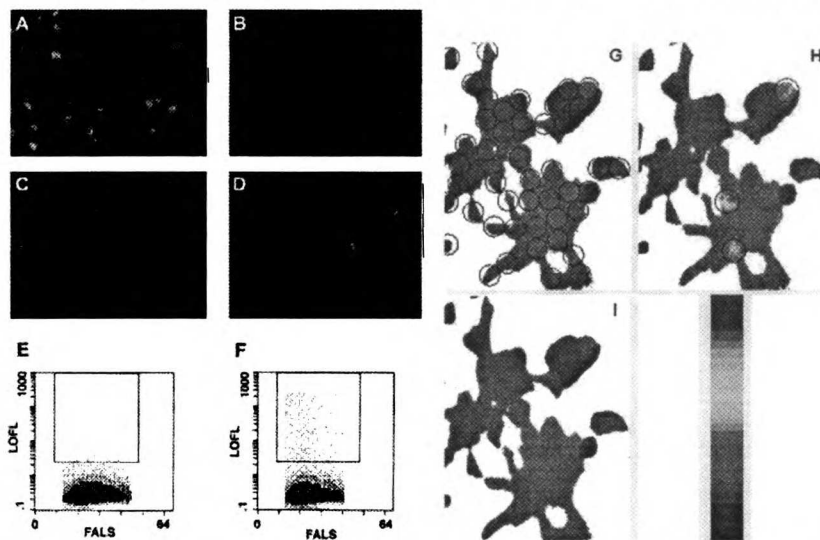


FIG. 1. ODR-10 expression and function in human cells. For immunofluorescence, the primary antibodies were mAbs against the Myc and HA epitopes, and the secondary antibody was a FITC-conjugated goat anti-mouse IgG (green). The yellow color is due to exposure saturation. (A) Myc-ODR-10-transfected HEK293 cells, 630 \times ; cytoplasmic fluorescence. (B) Myc-ODR-10-transfected cells, 630 \times ; perimeter fluorescence. (C) Myc-ODR-10-transfected cells, 630 \times ; cytoplasmic fluorescence. (D) HA- β 2AdR-transfected cells, 630 \times ; perimeter fluorescence. (E and F) Two-dimensional dot plots of flow cytometry measurements. The rectangular boxes enclose dots representing cell populations that display surface Myc epitope expression at levels above an arbitrarily defined threshold. Each cytogram compiled data from 100,000 cells identified as viable by forward and 90° light scatter. The different texture levels (from lightest to darkest) indicate threefold increases in frequency. LOFL, log orange fluorescence level; FALS, forward angle light scatter. (E) Control vector-transfected cells (<0.01% of cell population was Myc-positive above threshold). (F) Myc-ODR-10-transfected cells (0.3% of cell population was Myc-positive above threshold in this experiment). The graded color bar is a calibration of the imaging system. The red color in the calibration bar indicates the highest Ca²⁺ level measured by the imaging system. (G-I) Images of Ca²⁺ measurements for a group of cells that were transiently transfected with wt ODR-10 plasmid. The graded color bar is a calibration of the imaging system. The red color in the calibration bar indicates the highest Ca²⁺ level measured by the imaging system. (G) Prior to diacetyl perfusion. (H) Three minutes after onset of a 1-min application of 10 μ M diacetyl. (I) Seven min after the onset of diacetyl application.

filter changer (Lambda-10; Sutter Instruments, Novato, CA) was used to switch the excitation wavelength. An intensified CCD camera (Hamamatsu, Ichinocho, Japan) was used in detecting fluorescence. Images were acquired at 5- or 10-sec intervals and analyzed with VideoProbe system (ETM Systems, Irvine, CA) hardware and software. All cells within a field were selected (circled) and analyzed (see Fig. 1G for examples), and up to 20% of circled cells might exhibit odorant responses. Instrument calibration was carried out with standard Ca^{2+} solutions (Molecular Probes) in custom-made microglass chambers that were 150 μm deep and 3 mm^2 in area.

RESULTS

Expression of ODR-10 on the Surfaces of Transfected Human Cells. To evaluate ODR-10 expression, we transfected mammalian cells with a plasmid encoding an ODR-10 protein with a Myc epitope tag at its N terminus, which should be exposed at the external face of the plasma membrane. Myc-ODR-10 was expressed at high levels in about 30% of transiently transfected human HEK293 cells (Fig. 1A). In the majority of expressing cells, the protein appeared to be cytoplasmic, although staining extended to the cell perimeters (Fig. 1B). Some cells, however, exhibited bright fluorescence around their perimeters with little cytoplasmic staining (Fig. 1C). This localization pattern is similar to that observed for HA- β 2AdR expressed in transfected HEK293 cells (Fig. 1D).

To determine whether Myc-ODR-10 could reach the surface of transiently transfected human cells, we used flow cytometry to measure Myc epitope expression on live cells. About 0.3–1.0% of total cells assayed displayed Myc-ODR-10 on their surfaces at levels that were well above the fluorescence background observed with vector-transfected cells (Figs. 1E and F). Expression of Myc-ODR-10 at the cell surface is inefficient by comparison to HA- β 2AdR, for which >8% of total cells assayed exhibited high-level surface expression (data not shown). Unhealthy or otherwise antibody-permeable cells do not account for the apparent surface Myc expression seen in Fig. 1F, because HEK293 cells expressing several different Myc-tagged vertebrate olfactory receptors did not stain for surface Myc when assayed by flow cytometry (data not shown). These and other data indicate that expression of Myc-tagged receptors does not induce permeability to antibodies.

Our results also indicate that immunofluorescent staining of cell perimeters cannot be used as a criterion for surface expression, because the percentage of cells that actually express surface Myc as measured by flow cytometry is much lower than the percentage showing staining extending out to the perimeter. This is true even if only cells with weak cytoplasmic staining (as in Fig. 1C) are considered.

ODR-10 Mediates Ca^{2+} Elevation in Response to Diacetyl Application. To assay ODR-10 function, we measured intracellular Ca^{2+} levels in ODR-10-expressing cells using fura-2-based Ca^{2+} imaging. Upon perfusion of diacetyl (10 μM) onto HEK293 cells transfected with plasmids encoding wild-type (wt) ODR-10 or Myc-ODR-10, a transient increase in intracellular Ca^{2+} was observed in a fraction of the cells (Fig. 1G–I). Such responses were never seen in vector-transfected or untransfected cells. They were also not observed in cells expressing the muscarinic M_1 acetylcholine receptor (M_1AChR), which couples efficiently to release of Ca^{2+} from intracellular stores.

Fig. 2 shows graphs of time-dependent changes in intracellular Ca^{2+} , each averaged over 10 or more responding cells. The Ca^{2+} elevation response was maximal about 3 min after the onset of diacetyl application and decayed within 4 min (Fig. 2A). These kinetics are considerably slower than those observed for the M_1AChR response to acetylcholine (ACh; Fig. 4D). Basal Ca^{2+} levels in populations of ODR-10 plasmid or vector-transfected cells varied between 50 and 150 nM. A 10%

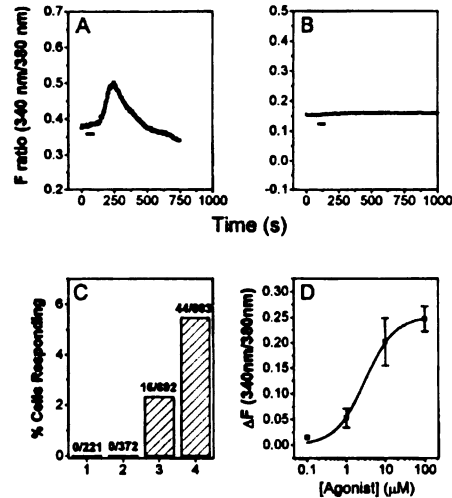


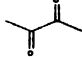
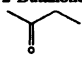
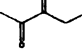
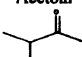
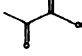
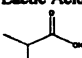
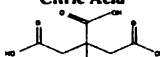
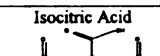
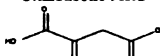
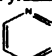
FIG. 2. Characterization of diacetyl responses in ODR-10-expressing HEK293 cells. *A* and *B* are plots of changes in fluorescence intensity ratios (340 nm/380 nm). Each plot represents an average of measurements from more than 10 individual cells. The images were collected at 5-sec intervals (represented by individual points). The duration of odorant perfusion (1 min) is marked by a horizontal bar. (*A*) Ten micromolar diacetyl, wt ODR-10-transfected cells. (*B*) Ten micromolar diacetyl, control vector-transfected cells. (*C*) Bar graph of numbers and percentages of cells responding to 10 μM diacetyl. (*D*) Diacetyl dose-response relation. Each symbol represents the average of measurements from >10 single cells from the same transfection. Error bars (SD) are also indicated. The line is a fit to the Hill equation. The calculated EC_{50} value from the Hill equation is $2.25 \pm 0.53 \mu\text{M}$, and the Hill coefficient is 1.12.

change in fluorescence intensity ratio corresponds to an increase of about 100 nM in Ca^{2+} concentration, and the highest Ca^{2+} concentration attained during the diacetyl response in a typical experiment was about 300 nM. Due to the inaccuracy inherent in calibrating the Ca^{2+} imaging system between different populations of transfected cells, we report here fluorescence ratios rather than estimated Ca^{2+} concentrations.

Ten micromolar diacetyl elicited transient increases in intracellular Ca^{2+} in ODR-10-transfected cells (Fig. 2A and C) but never in vector-transfected, untransfected, or M_1AChR -transfected cells (Figs. 2B and C and 4D). The percentage of responding cells and the magnitude of the Ca^{2+} increases were higher in cells expressing wt ODR-10 (5.5%, $n = 803$; Fig. 2C) than in those expressing Myc-ODR-10 (2.3%, $n = 692$). Comparison of the percentage of Myc-ODR-10-transfected cells responding to diacetyl with the percentage expressing the Myc epitope on their surfaces suggests that cells that express Myc-ODR-10 at levels below the threshold required for separation from the untransfected population in a flow cytometric assay can still exhibit diacetyl responses in the fura-2 assay.

Dose-dependent responses to diacetyl were observed at concentrations of 0.1–100 μM (71/1394 wt ODR-10-transfected cells analyzed exhibited responses; Table 1). When the dose-response relationship was fitted to the Hill equation, it yielded an EC_{50} value of $2.3 \pm 0.5 \mu\text{M}$ (Fig. 2D). The increase in Ca^{2+} saturates at about 100 μM diacetyl. *odr-10* mutant worms respond normally to butanone and 2,3-pentanedione, which are sensed by AWC. They also respond to pyrazine, a

Table 1. Summary of odorant screening using Fura-2 Ca^{2+} imaging

Compound	Odorant concentrations tested (μM)	Cells responding/cells tested
2,3-Butanedione (Diacetyl) 	0.1, 1, 10, 50, 100, 500	71/1394 (5.1%)
2-Butanone 	1, 10	0/189
2,3-Pentanedione 	1, 10, 100	0/149
Acetoin 	1, 10, 100	0/108
Pyruvic Acid 	1, 5, 10, 50, 100	35/476 (7.4%)
Lactic Acid 	10, 100	0/244
Citric Acid 	0.1, 1, 10, 100, 500	52/759 (6.9%)
Isocitric Acid 	10, 100	0/189
Oxaloacetic Acid 	1, 10, 100	0/147
Pyrazine 	10, 100	0/171

*Bold type identifies compounds that are agonists for ODR-10.

structurally unrelated compound detected by AWA (8). None of these compounds produced a Ca^{2+} elevation response in ODR-10-expressing cells, even at 100 μM (Table 1). 3-Hydroxybutanone (acetoin) also did not elicit responses. We tested 44 other volatile odorants representing a variety of different chemical groups on ODR-10-expressing cell populations and found that none produced any receptor-dependent elevation in Ca^{2+} levels (data not shown).

ODR-10 Responds to the Nonvolatile Compounds Pyruvate and Citrate. We have been unable thus far to identify any

volatile compound other than diacetyl that produces a Ca^{2+} elevation response in ODR-10-expressing HEK293 cells. In an effort to define another ODR-10 agonist, we also tested anionic compounds that are structurally related to diacetyl. We found that one such compound, pyruvate, produced Ca^{2+} elevation in ODR-10-expressing cells (35/476 cells analyzed; Table 1 and Fig. 3A) but never in vector-transfected cells (Fig. 3C). Pyruvate has a similar EC_{50} to diacetyl ($3.2 \pm 0.9 \mu\text{M}$; Fig. 3D). Interestingly, diacetyl, which is an end product of fermentation in some species of bacteria, can be synthesized in two steps directly from pyruvate, using the enzyme diacetyl synthase. Diacetyl production is a specific signature for certain bacterial species, whereas acetoin is produced by almost all bacteria.

That ODR-10 responded to diacetyl and pyruvate, but not to the structurally related fermentation end products acetoin and lactate (Table 1), suggested that ODR-10 activation might be indicative of the presence of bacterial species that generate diacetyl via the diacetyl synthase pathway. The preferred substrate for pyruvate and diacetyl formation in some of these bacteria is citrate. Bacteria convert citrate to oxaloacetate and then to pyruvate under anaerobic conditions. In the presence of oxygen, citrate is preferentially isomerized to isocitrate by aconitase and enters the tricarboxylic acid cycle (10).

We tested whether other compounds in the diacetyl synthesis pathway might elicit ODR-10 responses and found that citrate is an agonist for ODR-10 (Fig. 3B; 52/759 cells analyzed). Again, citrate never induced Ca^{2+} elevation responses in vector-transfected cells (Fig. 3C). The EC_{50} for citrate ($0.34 \pm 0.08 \mu\text{M}$) was lower than that for diacetyl itself (Fig. 3D). The citrate response is surprising, because citrate does not have a close structural relationship to diacetyl or pyruvate, and most citrate molecules bear three negative

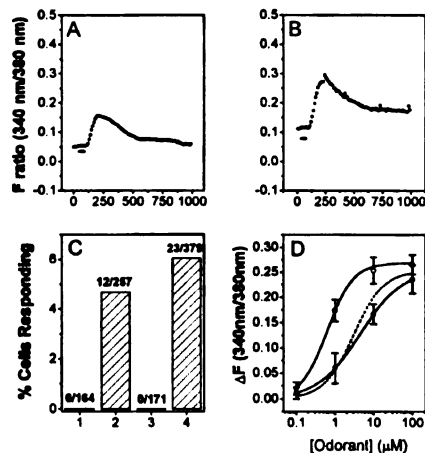


FIG. 3. ODR-10 responds to pyruvate and citrate. Symbols and markers have the same meaning as in Fig. 2. Images were collected at 10-sec intervals. (A) Ten micromolar pyruvate, wt ODR-10-transfected cells. (B) Ten micromolar citrate, wt ODR-10-transfected cells. (C) Bar graph of numbers and percentages of cells responding to pyruvate and citrate (10 μM). (D) Dose-response relations for pyruvate and citrate. The closed squares and open circles are data points for pyruvate and citrate, respectively. The calculated EC_{50} values from the Hill equation are $3.23 \pm 0.9 \mu\text{M}$ for pyruvate and $0.34 \pm 0.08 \mu\text{M}$ for citrate. The Hill coefficients are 0.9 and 1.28 for pyruvate and citrate, respectively. The dotted line shows the diacetyl dose-response relationship for comparison.

charges at neutral pH. It is specific, however, because isocitrate, which has the same negative charge distribution and differs only in the positioning of an -OH group, did not produce ODR-10 responses (Table 1).

ODR-10 Signaling and Desensitization in Human Cells. To investigate the signaling pathway used by ODR-10 in human cells, we examined the origin of the Ca^{2+} signal detected in the imaging experiments. Eliminating extracellular Ca^{2+} had little effect on ODR-10-mediated increases in Ca^{2+} (Fig. 4A), suggesting that Ca^{2+} elevation is primarily due to release from intracellular stores. Internal Ca^{2+} stores whose release is mediated by G protein-coupled receptors are depleted by caffeine, which produces a slow increase in cytoplasmic Ca^{2+} as the stores are emptied. After caffeine treatment of transfected HEK293 cells, diacetyl, citrate, and pyruvate failed to elicit a further Ca^{2+} increase (Fig. 4B), suggesting that ODR-10 and caffeine affect similar calcium stores. Preincubation of transfected cells with pertussis toxin (PTX; 100 nM) had no effect on odorant-induced Ca^{2+} elevation (data not shown), indicating that ODR-10 is likely to couple to a PTX-resistant G protein. Although the activation of a human G protein by ODR-10 shows that the receptor is promiscuous in its coupling ability, the overall signaling mechanism used by ODR-10 may be similar in human cells and in *C. elegans*, because behavioral responses to diacetyl require a protein related to *Drosophila* Trp (11). Trp is required for rapid refilling of intracellular Ca^{2+} stores in fly photoreceptors (reviewed in ref. 12).

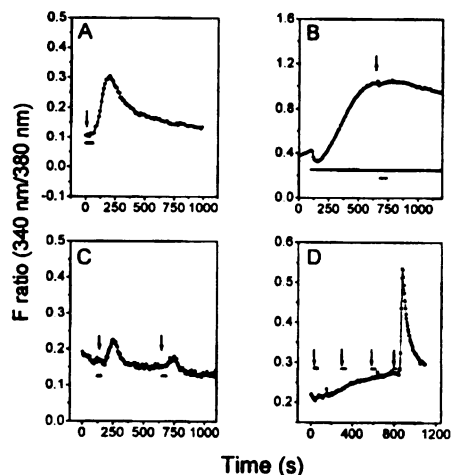


Fig. 4. ODR-10 signaling and desensitization. Symbols and markers have the same meaning as in Fig. 2. The starting point of agonist application is indicated by arrows. Images were collected at 10-sec intervals. (A) Ten micromolar citrate, wt ODR-10-transfected cells in Ca^{2+} -free extracellular solution. (B) Ten micromolar citrate, wt ODR-10-transfected cells treated with 10 mM caffeine. Caffeine was present before and after odorant application (long horizontal bar). Identical results were observed for diacetyl and pyruvate (10 μM ; data not shown). (C) ODR-10 desensitization by low concentrations of diacetyl. Diacetyl (1 μM) was applied at 120 and 620 sec. The cells were continuously washed between diacetyl applications. (D) Effects of odorants on M_1AChR -mediated Ca^{2+} elevation. Each arrow indicates application of a different odorant or agonist. The sequence of application was: butanone, 2,3-pentanedione, pyrazine (all at 10 μM), followed by ACh (20 μM). Diacetyl (10 μM) also had no effect on the ACh response (data not shown).

ODR-10 undergoes desensitization upon activation in HEK293 cells. When ODR-10 expressing cells were exposed to 1 μM diacetyl, a second application of diacetyl at the same concentration elicited a much smaller response (Fig. 4C). Higher concentrations of diacetyl, citrate, or pyruvate produced complete and long-lasting desensitization (data not shown). Diacetyl and other volatile odorants had no effect on subsequent ACh-induced release of Ca^{2+} from intracellular stores in cells expressing M_1AChR (Fig. 4D).

DISCUSSION

In this paper, we have shown that the nematode seven-transmembrane domain protein ODR-10 functions as a receptor for the volatile odorant diacetyl (butanedione) when expressed in human HEK293 cells. ODR-10 responds to volatile odorants with high selectivity in human cells, and this selectivity resembles that observed for the behavioral response *in vivo* (8). In both systems, the receptor distinguishes between diacetyl and compounds that differ from it only by the presence of an extra methyl group (2,3-pentanedione) or by the absence of a keto group (butanone; Table 1).

The apparent affinity of ODR-10 for diacetyl observed in human cells ($\text{EC}_{50} = 2.3 \mu\text{M}$; Fig. 3D) is consistent with the diacetyl concentration ranges that allow efficient nematode chemotaxis. In volatile chemotaxis assays, odorant is spotted either on the surface of an agar plate or on the underside of the lid, and nematodes move across the agar and accumulate at or directly under the odorant source (4). The mean concentration of diacetyl in air in a typical assay is about 0.1 μM (J.H.C. and C.I.B., unpublished results). At this concentration of diacetyl in liquid, the ODR-10 response in 293 cells is about 5% of maximum (Fig. 2D; data not shown). The saturating concentration of diacetyl above which nematodes cannot follow a diacetyl gradient is about 100 μM , which corresponds approximately to the concentration required to saturate the response in 293 cells.

ODR-10 is very specific in its recognition of diacetyl as a ligand, and we were unable to identify any other volatile odorant that could serve as an ODR-10 agonist. We found that two anionic compounds, pyruvate and citrate, can function as ODR-10 agonists in human cells and that citrate has a lower EC_{50} (0.34 μM) than diacetyl (2.3 μM). Analyses of Ca^{2+} elevation responses in sections of olfactory epithelium show that a single mammalian olfactory receptor neuron can respond to volatile alcohols and to fatty acids, which are non-volatile (anionic) at neutral pH (13). Thus, mammalian and invertebrate olfactory receptors can apparently interact with both volatile and nonvolatile compounds.

Although the pyruvate and citrate results are intriguing, there is no evidence at present indicating that a behavioral response to these compounds can be mediated by ODR-10. *C. elegans* exhibits chemotaxis to volatile pyruvic acid and soluble citrate, but these responses are also observed in *odr-10* mutant worms. Moreover, the pyruvic acid response is dependent on AWC and not on AWA, so ODR-10 is unlikely to be one of several redundant receptors for this odorant (J.H.C. and C.I.B., unpublished results).

Pyruvic acid is an unusual odorant, because it exists in both neutral and anionic forms. In a volatile chemoattraction assay, pyruvic acid evaporating into the air would quickly set up two types of gradients: a pyruvic acid gradient in the air and a pyruvate gradient in the buffered agar. In principle, the worm might follow either of these gradients to reach the pyruvic acid source. That pyruvic acid chemotaxis is dependent on the volatile odorant receptor neuron AWC suggests that pyruvic acid is the species recognized by the worm during chemotaxis. In the 293 cell system, however, pyruvate is dissolved in a pH 7.4 buffer, in which the concentration of pyruvic acid is about 10^5 -fold lower than that of pyruvate anion. This indicates that

the ligand for ODR-10 in 293 cells is likely to be pyruvate rather than pyruvic acid.

Pyruvate and citrate cannot compete effectively with diacetyl for access to ODR-10 on AWA cilia, because diacetyl chemotaxis, which is completely blocked by 100 μ M diacetyl in the agar, was unaffected when the agar contained 1.4 mM pyruvate or 5 mM citrate (J.H.C. and C.I.B., unpublished results). Thus, pyruvate and citrate are apparently less accessible to ODR-10 on AWA cilia than in human cells. Cilia that detect volatile odorants are encased within the amphid sheath cell, whereas neurons that sense water-soluble molecules are exposed at the tip of the nose (4, 14). One possibility is that AWA and AWC may not be able to interact efficiently with membrane-impermeable compounds such as the pyruvate and citrate anions. Alternatively, an accessory protein, posttranslational modification, or receptor conformation that affects the ability to respond to pyruvate and citrate could differ between ODR-10 expressed in HEK293 cells and ODR-10 *C. elegans* neurons.

Interestingly, pyruvate and citrate are direct biosynthetic precursors to diacetyl in bacteria, and citrate is the preferred carbon source used for diacetyl formation. Lactic acid bacteria generate diacetyl, which is the characteristic flavor of butter, from citrate in milk. Fungi such as *Aspergillus*, which produce very high levels of citrate and are used for its industrial production, provide a potential citrate source for soil bacteria. Under anaerobic conditions, citrate is broken down to pyruvate in two enzymatic steps, and pyruvate is in turn converted to diacetyl (10). These results suggest that ODR-10 activation could be a signature for the presence of bacterial species that use this metabolic pathway. ODR-10 on AWA cilia apparently cannot be activated by pyruvate and citrate. If expression of the receptor were induced in an exposed chemosensory neuron under some conditions in the natural environment, however, it is likely that ODR-10 could mediate a behavioral response to these compounds.

We thank Henry A. Lester, Norman Davidson, David J. Anderson, Barbara Imperiali, Chand Desai, Yasuhito Uezono, and the members of the Zinn and Bargmann groups for helpful discussions; Rochelle Diamond for flow cytometry; Gary Belford for advice on calcium imaging; Marc Caron for the HA- β 2AdR plasmid; and Bo Yu for the M₁AChR plasmid. We also thank the Caltech Cell Sorting facility for access to flow cytometry equipment and the Beckman Imaging Center for use of the imaging facility. This work was supported by grants from the National Institute of Mental Health to K.Z. and from the American Cancer Society to C.I.B. C.I.B. is an Assistant Investigator of the Howard Hughes Medical Institute. Y.Z. was supported by a National Research Service Award postdoctoral fellowship from the National Institutes of Health (National Institute on Deafness and Other Communication Disorders).

1. Buck, L. B. (1996) *Annu. Rev. Neurosci.* **19**, 517-544.
2. Brunet, L. J., Gold, G. H. & Ngai, J. (1996) *Neuron* **17**, 681-693.
3. Buck, L. & Axel, R. (1991) *Cell* **65**, 175-187.
4. Bargmann, C. I., Hartweig, E. & Horvitz, H. R. (1993) *Cell* **74**, 515-527.
5. Coburn, C. M. & Bargmann, C. I. (1996) *Neuron* **17**, 695-706.
6. Komatsu, H., Mori, I., Rhee, J. S., Akaike, N. & Ohshima, Y. (1996) *Neuron* **17**, 707-718.
7. Troemel, E. R., Chou, J. H., Dwyer, N. D., Colbert, H. A. & Bargmann, C. I. (1995) *Cell* **83**, 207-218.
8. Sengupta, P., Chou, J. H. & Bargmann, C. I. (1996) *Cell* **84**, 899-909.
9. Rupp, R. A. W., Snider, L. & Weintraub, H. (1994) *Genes Dev.* **8**, 1311-1323.
10. Gottschalk, G. (1986) *Bacterial Metabolism* (Springer, New York), 2nd Ed.
11. Colbert, H. A., Smith, T. L. & Bargmann, C. I. (1997) *J. Neurosci.*, in press.
12. Ranganathan, R., Malicki, D. M. & Zuker, C. S. (1995) *Annu. Rev. Neurosci.* **18**, 283-317.
13. Sato, T., Hirono, J., Tonoike, M. & Takebayashi, M. (1994) *J. Neurophysiol.* **72**, 2980-2989.
14. Ward, S., Thomson, N., White, J. G. & Brenner, S. (1975) *J. Comp. Neurol.* **160**, 313-337.

Chapter 3b. Ligand specificity of ODR-10 in *C. elegans*

Rationale

Chapter 3a demonstrated that ODR-10 expressed in human HEK293 cells can mediate a response to diacetyl ($EC_{50} = 2.3 \pm 0.5 \mu\text{M}$). The unexpected finding in this heterologous system that ODR-10 could also respond to pyruvic acid ($EC_{50} = 3.2 \pm 0.9 \mu\text{M}$) and citric acid ($EC_{50} = 0.34 \pm 0.08 \mu\text{M}$) raised the possibility that these two compounds, not previously tested in chemotaxis assays, may also be sensed by ODR-10 in worms.

In fact, *C. elegans* find both citrate and pyruvic acid attractive. Sodium citrate, adjusted to neutral pH, acts as a very weak water-soluble attractant (data not shown), while pyruvic acid is a robust attractant (this chapter). Pyruvic acid acts as a volatile attractant, because a point source spotted on the lid above the assay plate was as effective an attractant as a spot on the assay plate agar (data not shown). The following experiments focus primarily on the ability of ODR-10 to detect pyruvic acid rather than citrate because of the greater likelihood of a volatile attractive response being mediated by the AWA olfactory neurons that express ODR-10.

Results

***odr-10* is neither necessary nor sufficient to sense pyruvic acid.**

An *odr-10* null mutant was fully capable of pyruvic acid chemotaxis, demonstrating that *odr-10* is not required to sense pyruvic acid (Figure 3-1). Although this result shows that a receptor other than ODR-10 can mediate the pyruvic acid response, it does not rule out the possibility that ODR-10 may contribute to this response.

To determine which chemosensory neurons mediate the pyruvic acid response, strains bearing mutations that disrupted the function of specific chemosensory neurons were tested for pyruvic acid chemotaxis. *odr-1* and *odr-2* disrupt AWC function; *odr-7* disrupts AWA function; and *osm-3* disrupts the function of AWB and all chemosensory neurons with exposed ciliated endings (Perkins et al., 1986; Bargmann et al., 1993; Sengupta et al., 1994).

Figure 3-2 demonstrates that AWC function is required for pyruvic acid chemotaxis, whereas AWA and ciliated neurons are not. Since *odr-1* and *odr-2* mutants retain *odr-10* function in AWA but lose the ability to respond effectively to pyruvic acid, the conclusion is that *odr-10* in AWA is not sufficient to mediate an attractive response to pyruvic acid.

Ectopic expression of ODR-10 does not alter pyruvic acid chemotaxis

Expression of ODR-10 in chemosensory neurons that mediate repulsion has been shown to alter the normal attractive response to diacetyl to a repulsive response (Troemel et al., 1997; Emily Troemel and Liqin Tong, personal communication). To test whether ODR-10 expressed in other chemosensory neurons could direct a response to pyruvic acid, *odr-10* null mutants containing transgenes that directed *odr-10* cDNA expression in neurons that mediate repulsion were tested for pyruvic acid response. ODR-10 expressed in the AWB, ADL, and ASH neurons did not interfere with pyruvic acid chemotaxis (Figure 3-1).

It may be that ODR-10 in chemorepulsive neurons can sense pyruvic acid, but that AWC-mediated signaling for attraction was more effective than signaling by the chemorepulsive neurons. To increase the sensitivity of detecting a response, this experiment could be better executed in a background lacking an attractive pyruvic acid response, for example in *odr-1 odr-10* double mutants.

Pyruvic acid and diacetyl do not compete effectively with each other for receptor binding or signaling.

Finally, it was possible that ODR-10 was capable of initiating signaling in response to pyruvic acid, but that the signaling was not productive for mediating chemotaxis. If diacetyl and pyruvic acid shared an overlapping recognition site on ODR-10, these compounds might display competition for ligand binding, manifested as interference in cross-saturation assays.

To test the ability of pyruvic acid to compete with diacetyl at the ODR-10 ligand binding site, wild-type animals were tested for chemotaxis to a point source of diacetyl in the presence of 1.4 mM pyruvic acid. This experiment showed that pyruvic acid was unable to cross-saturate the diacetyl response (Figure 3-3). Likewise, similar experiments using 5 mM sodium citrate as a saturant did not interfere with diacetyl chemotaxis; in contrast, diacetyl at 0.9 mM is sufficient to abolish the diacetyl response (Chapter 4 and data not shown).

Because ODR-10, expressed in AWA, is the only receptor capable of mediating diacetyl chemotaxis under these conditions, these experiments show that neither pyruvic acid nor sodium citrate are capable of competing effectively with diacetyl recognition by ODR-10. Therefore, either the AWA cilia are inaccessible to pyruvic acid and sodium citrate or the diacetyl recognition site of ODR-10 does not bind pyruvic acid or citrate.

Discussion

In this chapter, evidence is presented that ODR-10 expressed in mammalian cells can function as a specific receptor for diacetyl. However, a puzzling discrepancy emerged in which ODR-10 expressed in HEK293 cells also mediated a response to pyruvate and citrate, even though ODR-10 seems unable to direct a similar response in *C. elegans*.

For land vertebrates, atmospheric odorants must traverse an aqueous layer formed by the olfactory mucus layer before initiating signaling by binding olfactory receptors. The effect of the gaseous–aqueous interface has been alternately proposed to prevent or promote the passage of

odorants. Most odorants are small hydrophobic molecules, which might be expected to be poorly soluble in an aqueous environment; however, the partition coefficients of many common odorants suggest that many would actually be concentrated by an order of magnitude into the aqueous phase because of the much higher molar density of liquids (Pelosi, 1996).

The situation is further complicated within the mucus layer, which contains water, electrolytes, and a number of proteins secreted by olfactory support cells (Carr et al., 1990; Pelosi, 1996). The proteins include nonspecific odorant-binding proteins and enzymes with powerful redox and conjugating activities, similar to the detoxifying enzymes of the liver. These proteins are likely to modify both the accessibility and structure of odorants, either before or after signal transduction.

Likewise, the olfactory neurons of insects are surrounded by an aqueous layer of sensillar lymph, and in *C. elegans*, the AWA and AWC sensory cilia lie embedded within an electron-dense matrix material secreted by amphid sheath cells (Perkins et al., 1986). The physiological role of the matrix during odorant sensation is not known.

C. elegans dose-response experiments spanning a 1,000-fold concentration range indicate that pyruvic acid gradients formed in the air are as effective or more effective than those originating on the surface of the agar (data not shown). Pyruvic acid is volatile, while pyruvate anion is not. Thus un-ionized pyruvic acid generates the odorant gradient sensed by *C. elegans* and may act as the species that is detected in the amphid environment. In the mammalian expression system, the experiments were performed in buffered medium in which the concentration of pyruvate anion is predicted to be 10^5 -fold higher than un-ionized pyruvic acid. Perhaps ODR-10 *in vitro* responds to the anion, whereas the amphid matrix context *in vivo* favors un-ionized pyruvic acid which may not be detected by ODR-10 but is instead sensed by a distinct receptor on AWC.

The lack of effect by ODR-10 misexpression in the ASH chemorepulsive neuron, whose cilia are more directly exposed to the environment, could argue against a role for modification of pyruvic

acid presentation by the matrix. One possibility is that ASH responses were masked by more efficient attractive signaling mediated by AWC.

Other explanations for the difference in ODR-10 specificity in HEK293 cells and *C. elegans* include the existence of accessory coreceptors or ODR-10 post-translational modifications or conformational changes that further restrict the specificity of ODR-10 *in vivo*.

For example, recent work has identified the single-transmembrane domain RAMP family of receptor-activity modifying proteins, which modulates seven-transmembrane receptor glycosylation, surface expression, and ligand specificity (McLatchie et al., 1998). When transfected into mammalian HEK293T cells, the seven-transmembrane domain calcitonin-receptor-like receptor is unable to mediate a response to two related peptides, calcitonin-gene related peptide (CGRP) and adrenomedullin (ADM). Likewise, transfection of either RAMP-1 or RAMP-2 alone does not impart peptide responsivity. In contrast, co-transfection of receptor and RAMP-1 yields sensitivity to CGRP, while receptor and RAMP-2 together allows response to ADM. The authors also demonstrate that RAMP/receptor interactions are necessary for efficient cell surface expression and are responsible for differential glycosylation of the calcitonin-receptor-like receptor.

Although RAMP proteins have not been identified in invertebrates, a similar mechanism may explain the differences between ODR-10 activity *in vivo* and *in vitro*. These studies of seven-transmembrane receptor function underscore the importance of combining both physiological and biochemical approaches in defining the activities of signal transduction components.

Methods

Strains and genetics

Wild-type worms were *C. elegans* variety Bristol, strain N2. Worms were grown at 20°C with abundant food using standard methods (Brenner, 1974).

Strains used in this work included CX2378 *odr-1* (*ky29*) X, CX3030 *odr-7* (*ky4*) X, CX2304 *odr-2* (*n2145*) V, CX3411 *odr-10* (*ky225*) X, PR802 *osm-3* (*p802*) IV, and CX3548 *kyIs103* [*str-1* promoter driving *odr-10* cDNA expression in AWB] V; *odr-10* (*ky225*) *lin-15* (*n765ts*) X. CX3574 *kyIs107* [*sre-1* driving *odr-10* cDNA expression in ADL] *odr-10* (*ky225*) *lin-15* (*n765ts*) X and CX3575 *kyIs108* [*sra-6* promoter driving *odr-10* cDNA expression in ASH] *odr-10* (*ky225*) *lin-15* (*n765ts*) X are unpublished reagents, courtesy of Liqin Tong.

Behavioral assays

All behavioral assays were conducted on well-fed adults. Standard chemotaxis assays were performed as previously described (Bargmann et al., 1993). Assay plates were used 1–3 days after pouring. Cross-saturation assays were performed similarly to standard chemotaxis assays, except that an amount of saturating odorant was well mixed into the assay agar, and plates were used within one day after pouring.

Acknowledgments

I would like to thank Liqin Tong for the ADL::*odr-10* and ASH::*odr-10* strains.

Ectopic expression of ODR-10 does not affect pyruvic acid chemotaxis

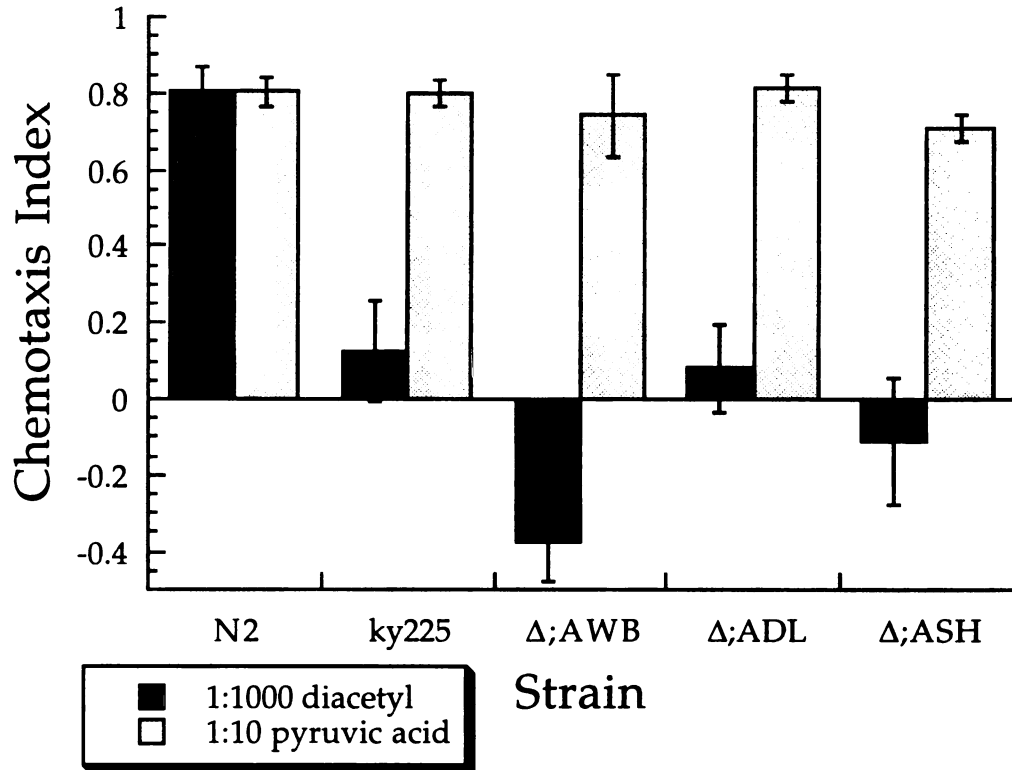


Figure 3-1. Pyruvic acid chemotaxis does not depend on *odr-10* and is not affected by ectopic expression of ODR-10. Wild-type, *odr-10* (*ky225*) null mutant animals, and *odr-10* (*ky225*) mutant animals ectopically expressing ODR-10 in chemosensory neurons that direct repulsion were tested for chemotaxis to diacetyl and pyruvate at the concentrations listed. Relevant genotypes: Δ;AWB: *kyIs103* [*str-1* promoter driving *odr-10* cDNA expression in AWB] V; *odr-10* (*ky225*) X, Δ;ADL: *kyIs107* [*sre-1* driving *odr-10* cDNA expression in ADL] *odr-10* (*ky225*) X, and Δ;ASH: *kyIs108* [*sra-6* promoter driving *odr-10* cDNA expression in ASH] *odr-10* (*ky225*) X.

Pyruvic acid chemotaxis requires AWC chemosensory neuron function

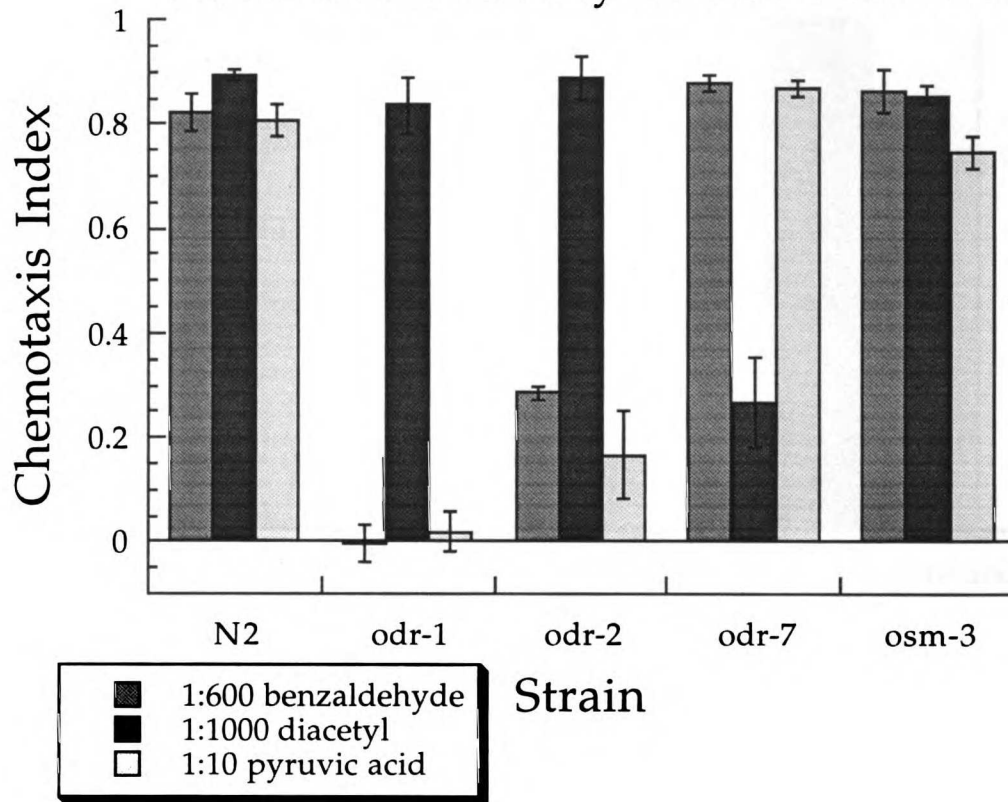


Figure 3-2. Pyruvic acid chemotaxis requires AWC chemosensory neuron function. Wild-type and mutant animals were tested for chemotaxis to the listed attractants. *odr-1* and *odr-2* are required for AWC function, *odr-7* is required for AWA function, and *osm-3* is required for function all other amphid and phasmid chemosensory neurons.

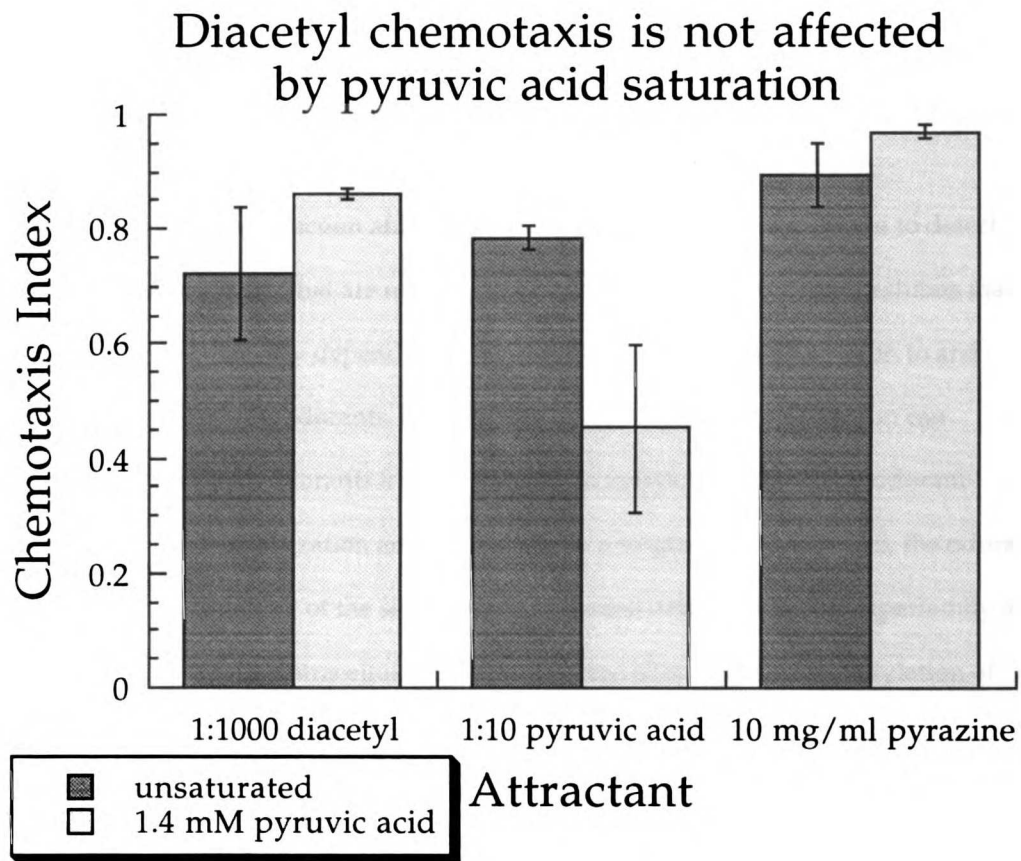


Figure 3-3. High concentrations of pyruvic acid do not interfere with diacetyl chemotaxis. Wild-type N2 animals were tested for chemotaxis to diacetyl, pyruvic acid, and pyrazine in the presence or absence 1.4 mM of pyruvic acid in the assay plate.

Chapter 4. Mechanisms of olfactory discrimination: behavioral and mutational analysis.

Abstract

Downregulation of signal transduction after prolonged stimulation allows a system to detect novel stimuli and ignore signals that are no longer relevant. *Caenorhabditis elegans* exhibits many chemosensory behaviors that may depend on downregulation, including adaptation to and discrimination between distinct odorants. Here I show that a single olfactory neuron can differentiate between multiple odorants in cross-saturation assays, indicating that odorant-specific mechanisms for desensitization are present within a single neuron. ODR-10, the odorant receptor for diacetyl, is a member of the seven-transmembrane domain receptor superfamily and has a large number of potential intracellular phosphorylation sites. Since phosphorylation of seven-transmembrane domain receptors is a well-characterized paradigm for desensitization, ODR-10 phosphorylation seemed likely to play a role in chemosensory behaviors. I found, however, that replacement of all eight intracellular C-terminal serine and threonine residues with alanine had no effect on chemotaxis, adaptation, or discrimination. On the other hand, specific residues in the third intracellular loop that might be phosphorylated were essential for chemotaxis. Alteration of either a serine or threonine in this loop resulted in loss of the ability of ODR-10 to mediate chemotaxis to diacetyl, without an accompanying change in discriminatory ability.

Introduction

C. elegans can discriminate between several different attractive odorants in cross-saturation assays (Bargmann et al., 1993). In these assays, high uniform concentrations of one odorant abolish

response to that odorant without interfering with chemotaxis to a point source of a different odorant. Saturation assays have defined at least seven classes of odorants that can be discriminated from each other, demonstrating structural specificity in the chemosensory response and delimiting a minimum number of independent ligand binding sites. Compounds that exhibit cross-saturation with each other presumably share some component of sensory transduction such as a common sensory neuron, signal transduction component, or receptor molecule.

How does *C. elegans* discriminate among multiple compounds? Ultrastructural studies of *C. elegans* identified 14 classes of neurons that may be chemosensory based on their exposure to the outside environment and the presence of ciliated dendrites (Ward et al., 1975; Ware et al., 1975). Laser ablation experiments demonstrate that just two pairs of chemosensory neurons, AWA and AWC, mediate attraction to all tested volatile compounds. The AWA chemosensory neuron is necessary for response to pyrazine and diacetyl, while AWC is necessary for chemotaxis to benzaldehyde, isoamyl alcohol, 2,3-pentanedione, and butanone (Bargmann et al., 1993; Piali Sengupta, personal communication). Cross-saturation assays have shown that these compounds can be discriminated from each other.

These results demonstrate that a single olfactory neuron in *C. elegans*, either AWA or AWC, is required to mediate chemotaxis but do not rule out the possibility that integration of information from additional chemosensory neurons is required for discrimination. In such a model, a broadly tuned receptor on one neuron would be required for chemotaxis, while a specific receptor on another neuron would be required for discrimination yet be insufficient for chemotaxis. In another model, single chemosensory neurons would possess distinct ligand binding sites coupled to signal transduction processes that could be independently saturable. To distinguish between these models, I tested animals with only a single functional type of chemosensory neuron for their ability to distinguish between odorants sensed by that neuron.

What is the molecular mechanism of chemosensory discrimination in *C. elegans*? The ability of two odorants to avoid cross-saturation, despite the ability of each odorant to self-saturate, implies

odorant-specific downregulation at some step of the signal transduction pathway, with downregulation occurring before the pathways downstream of each odorant converge. As in vertebrates, olfactory transduction in *C. elegans* is mediated by a G protein-coupled pathway. A number of signal transduction components have now been identified, including an odorant receptor, ODR-10, specifically required for diacetyl response, and a G protein α subunit, ODR-3, required for both AWA and AWC function (Sengupta et al., 1996; Roayaie et al., 1998).

One of the best characterized mechanisms of G protein-coupled receptor downregulation involves phosphorylation of the receptor by G protein-coupled receptor kinases (GRKs) such as rhodopsin kinase and β -adrenergic receptor kinase, followed by arrestin-mediated uncoupling of the receptor from G protein signaling (Premont et al., 1995; Freedman and Lefkowitz, 1996). These same components have been found localized to the sensory cilia of vertebrate olfactory neurons, and *in vitro* experiments have demonstrated a role for them in olfactory signal termination (Dawson et al., 1993; Schleicher et al., 1993; Boekhoff et al., 1994a). A worm GRK and arrestin homologue are each expressed in chemosensory neurons, as assessed by fusion to green fluorescent protein, suggesting that a similar mechanism may regulate olfactory receptors in *C. elegans* (Gage Crump, personal communication).

In a related mechanism, phosphorylation of the cytoplasmic tail of the α -factor pheromone receptor in yeast is required for its ubiquitin-mediated internalization and degradation (Hicke and Riezman, 1996; Hicke et al., 1998). Site-directed mutagenesis of either the C-terminal serines, which are phosphorylated, or a single lysine, which is ubiquitinated, abolishes both constitutive and ligand-stimulated internalization of a truncated receptor.

To determine whether either of these mechanisms might be important for normal chemosensory behaviors in *C. elegans*, I undertook site-directed mutagenesis of the diacetyl receptor, ODR-10. In this work, I demonstrate that worms possessing only a single functional chemosensory neuron are still capable of discriminating between multiple odorants. This ability likely occurs by some type of transduction desensitization within the neuron that prevents interference by saturating

odorants. In the case of diacetyl, I show that genetic ablation of multiple potential phosphorylation and ubiquitination sites in its seven-transmembrane domain receptor does not affect odorant discrimination. Moreover, other behaviors that have been proposed to depend on receptor desensitization, including chemotaxis and adaptation, are similarly unaffected by removal of potential phosphorylation or ubiquitination sites.

Results

Genetic ablation of chemosensory neuron function

To determine whether a single chemosensory neuron could discriminate between multiple odorants, several strains, genetically ablated for the function of all chemosensory neurons except one, were tested in cross-saturation assays.

The amphid and phasmid chemosensory organs encompass thirteen classes of chemosensory neurons. Ten classes have simple exposed ciliated endings, while three classes, AWA, AWB, and AWC, have elaborate branched cilia (Ward et al., 1975; Ware et al., 1975). Mutations in *osm-3* appear to abolish the function of all chemosensory neurons with exposed ciliated endings, including those that mediate responses to water-soluble compounds (Perkins et al., 1986). The AWB neurons are also somewhat defective in *osm-3* mutants, as evidenced by their failure to take up the vital dye DiO (C.I.B., unpublished results). Olfactory neurons such as AWA and AWC, whose dendrites are enveloped by the amphid sheath, are not affected in *osm-3* mutants. However, *odr-1* mutants are defective for all known AWC functions, while *odr-7* is required for all known AWA functions (Bargmann et al., 1993; Sengupta et al., 1994). Thus, AWA is the only functioning chemosensory neuron in *osm-3 odr-1* double mutant animals, while only AWC function remains in *osm-3 odr-7* animals.

The AWA sensory neurons can discriminate between multiple odorants

Animals that possess only AWA function are able to respond to the volatile attractants diacetyl, pyrazine, and 2,4,5-trimethylthiazole. Assay plates with uniform high concentrations of each of these odorants were used to determine whether *osm-3 odr-1* animals were still capable of discriminating between the odorants.

In the presence of saturating concentrations of each of these odorants, chemotaxis to a point source of the saturating odorant was abolished before chemotaxis to either of the other odorants was significantly affected (Figure 4-1). This result shows that in the absence of all other chemosensory neurons, the AWA neurons are still capable of discriminating between at least three different classes of odorants, implying the existence of at least three independently saturable, odorant-specific components of olfactory signal transduction.

The AWC sensory neurons can discriminate between multiple odorants

Animals limited to AWC chemosensory function are capable of sensing benzaldehyde, isoamyl alcohol, butanone, 2,3-pentanedione, and 2,4,5-trimethylthiazole.

The *osm-3 odr-7* animals display a more complex pattern of discrimination between odorants (Figure 4-2). Most odorants sensed by AWC can still be discriminated from each other. However, several odorant pairs display some degree of cross-saturation: trimethylthiazole partially cross-saturates butanone, isoamyl alcohol cross-saturates benzaldehyde, and benzaldehyde partially cross-saturates all odorants except butanone. For all of these odorants, the cross-saturation is not due to loss of input from the AWA, AWB, or the ciliated chemosensory neurons because wild-type animals behave similarly (data not shown). In wild-type animals, benzaldehyde and isoamyl alcohol are known to cross-adapt and cross-saturate (Bargmann et al., 1993; Colbert and Bargmann, 1995; Colbert and Bargmann, 1997).

Animals possessing only AWC display some loss of discrimination

The loss of AWA function abolishes response to low concentrations of diacetyl. However, the AWC neurons still direct chemotaxis towards very high concentrations of diacetyl (Sengupta et al., 1994; P. Sengupta, unpublished data). For example, *osm-3 odr-7* animals still chemotax efficiently to a 1:10 dilution of diacetyl.

Interestingly, the residual ability of *osm-3 odr-7* animals to sense high concentrations of diacetyl is exquisitely sensitive to cross-saturation by 2,3-pentanedione (Figure 4-2). In wild-type animals, chemotaxis to diacetyl is unaffected by pentanedione (saturated:unsaturated ratio = 0.92 ± 0.03 ; unsaturated chemotaxis index = 0.82). The results in *osm-3 odr-7* mutants was very different: pentanedione is more than 100 times more effective at abolishing the diacetyl response than diacetyl itself (data not shown). Thus, worms that possess only the AWC chemosensory neurons have lost the ability to discriminate between diacetyl and 2,3-pentanedione.

Molecular mechanisms of discrimination

The previous experiments show that individual olfactory neurons contain several distinct ligand binding sites whose signal transduction is independently saturable. Because the chemosensory receptors are believed to couple to common G proteins, a likely target for downregulation of odorant-specific transduction was the receptor itself.

G protein-coupled serpentine receptors are downregulated in many ways, including decreased expression, sequestration, degradation, and phosphorylation (Bohm et al., 1997). Saturation and adaptation of chemotaxis responses occurs over a time course of minutes, consistent with a role for phosphorylation. ODR-10 also possesses two C-terminal lysine residues that might be ubiquitinated in a manner analogous to the residues that play a role in yeast α -factor receptor internalization (Hicke and Riezman, 1996; Hicke et al., 1998). To test the contribution of these mechanisms on chemosensory behavior, I undertook site-directed mutagenesis of potential phosphorylation and ubiquitination sites of ODR-10, the putative diacetyl receptor.

Cassette mutagenesis of *odr-10*

The intracellular C-terminal tail of *odr-10* consists of 34 amino acids after the predicted seventh transmembrane domain, of which eight are potentially phosphorylatable serines and threonines. Four of the 33 amino acids in the third intracellular loop are serines or threonines. The first two intracellular loops of *odr-10* contain fewer serines and threonines, with a total of four (Figure 4-3) (Sengupta et al., 1996).

A set of minigenes was constructed in which the *odr-10* promoter was used to drive expression of wild-type and mutated *odr-10* cDNAs. To test the role of phosphorylation, the mutations replaced serines and threonines of the third intracellular loop and C-terminal tail with alanine. The last three of the four serines and threonines in the third intracellular loop were accessible to cassette mutagenesis — all three were replaced (IC3 3/4), or each was replaced individually (IC3 #2, IC3 #3, and IC3 #4). All eight serines and threonines in the C-terminal tail region were replaced with alanine — the first two (C 2/8), the last six (C 6/8), or all eight simultaneously (C 8/8). Two lysines in the C-terminus were replaced with arginines (C-KK), to test the possibility that ubiquitination on lysines might play a role in ODR-10 regulation (Figure 4-3).

These constructs were each introduced into a *C. elegans odr-10 (ky225)* null mutant to determine whether the mutated *odr-10* could direct chemotaxis, discrimination, and adaptation.

Effect of ODR-10 alterations on chemotaxis to low concentrations of diacetyl

All mutant minigenes were tested in an *odr-10* null mutant background for their ability to rescue chemotaxis to low concentrations of diacetyl. The C-terminal tail of ODR-10 was surprisingly permissive for alteration. Replacement of all eight serine and threonine residues with alanine (C 8/8) had no effect on diacetyl chemotaxis rescue, as compared to wild-type animals or animals rescued with a wild-type minigene construct (Figure 4-4). Alteration of subsets of the C-terminal serine and threonine residues, via the C 2/8 and C6/8 constructs, was similarly without effect (Figure 4-4). These results suggest that not only is C-terminal phosphorylation unnecessary for mediating chemotaxis, but that none of these residues are critical for transducing a signal to

downstream G proteins. Likewise, replacement of both C-terminal lysines to arginine (C-KK) had no effect on chemotaxis rescue.

The C-terminus is, however, necessary for ODR-10 function. An *odr-10* rescuing genomic fragment (ScaI–EcoRV) was altered to introduce a frameshift mutation that truncated the entire C-terminus (ScaI–EcoRVΔC). Deletion of the C-terminus abolished diacetyl chemotaxis rescue of *odr-10(ky225)* (chemotaxis index = 0.90 ± 0.03 for ScaI–EcoRV, versus 0.26 ± 0.06 for ScaI–EcoRVΔC).

The third intracellular loop, which contains a total of four serines and threonines, was more sensitive to alteration. The first threonine, T226, was inaccessible to cassette mutagenesis and was not mutated. When the second, third, and fourth serines and threonines were simultaneously replaced with alanine, the resulting *odr-10* minigene construct (IC3 3/4) was completely unable to mediate a chemotaxis response to diacetyl (Figure 4-4). To determine which of these mutated residues was responsible for the loss of activity, each serine and threonine was individually replaced with alanine. The IC3#2 minigene, which causes a T229A replacement, was fully competent for mediating diacetyl chemotaxis, while IC3#3 and IC3#4 each abolished chemotaxis rescue. Thus, the third and fourth serine and threonine residues of the third intracellular loop, S237 and T240, are critical for ODR-10 function in directing chemotaxis to low concentrations of diacetyl.

Discrimination between diacetyl and pyrazine is unaffected by the altered forms of ODR-10

The wild-type AWA chemosensory neuron is capable of discriminating between pyrazine and diacetyl — animals are capable of sensing and chemotaxing towards a point source of either odorant in the context of high uniform concentrations of the other odorant (Bargmann et al., 1993; this thesis). This discrimination might require downregulation of the receptor that responds to the saturating odorant, in order to prevent cross-saturation of downstream shared signal transduction components.

Since phosphorylation and ubiquitination are possible mechanisms for receptor downregulation, all mutagenized minigenes were tested in an *odr-10* null mutant background for ability to mediate discrimination between diacetyl and pyrazine. Chemotaxis assays were performed on assay plates containing high uniform concentrations of diacetyl. The amounts of diacetyl used were capable of preventing wild-type animals from responding to a point source of diacetyl but did not affect chemotaxis to pyrazine. Conversely, we reasoned that ODR-10 mutations that prevented receptor downregulation would lead to aberrant signaling under these conditions and therefore block pyrazine chemotaxis.

None of the mutant ODR-10 constructs affected discrimination between pyrazine and diacetyl, demonstrating that discrimination between diacetyl and pyrazine does not require phosphorylation of any of the C-terminal serines or threonines or T229 in the third intracellular loop, nor does it require ubiquitination on lysine in the C-terminal tail (Figure 4-5). The deletion of the entire C-terminal tail (ScaI-EcoRV Δ C) also did not alter pyrazine chemotaxis under conditions of diacetyl saturation (data not shown).

The lack of effect on pyrazine discrimination by mutation of the third and fourth serines and threonines in the third intracellular loop indicates that these mutant receptors are not constitutively activated in the presence of diacetyl such that pyrazine chemotaxis is impaired. Whether the lack of cross-saturation is due to complete absence of signaling by these mutant forms of ODR-10 or because other mechanisms serve to prevent cross-saturation is not known.

Adaptation to diacetyl is unaffected by the altered forms of ODR-10

Worms experiencing prolonged treatment to high concentrations of an odorant subsequently exhibit decreased attraction to that odorant without significant loss of response to other odorants, a process termed olfactory adaptation (Colbert and Bargmann, 1995). To test whether receptor phosphorylation or ubiquitination was required for diacetyl adaptation, mutant minigenes

capable of rescuing diacetyl chemotaxis were tested in an *odr-10* null mutant background for their ability to direct adaptation to diacetyl.

As shown above, mutant ODR-10 with replacements of third intracellular loop T229 (IC3#2) or all serine and threonine residues in the C-terminal tail (C 8/8), or of the two lysines in the C-terminal tail (C-KK), are all capable of rescuing diacetyl chemotaxis. *odr-10* null mutant animals rescued with these constructs were treated with high concentrations of diacetyl. All of these strains exhibited diacetyl adaptation similar to that seen in wild-type, demonstrating that phosphorylation or ubiquitination of these residues was not required for adaptation (Figure 4-6). We also tested these strains for responses to pyrazine following diacetyl adaptation. Nonspecific cross-adaptation with pyrazine was not seen, indicating that the decreased diacetyl chemotaxis in adapted animals was due to specific adaptation and not due to non-specific odorant toxicity.

Discussion

The experiments described here demonstrate that the AWA and AWC chemosensory neurons are each individually capable of discriminating between multiple odorants in *C. elegans*. Most odorants were discriminated equally well by wild-type animals and by animals in which only a single sensory neuron could function. However, discrimination between high concentrations of diacetyl and pentanedione does require multiple chemosensory neurons. Considering the structural similarity between these two compounds, a simple explanation for the loss of discrimination would be competition for a ligand binding site on a high affinity pentanedione receptor that was also capable of acting as a low affinity diacetyl receptor.

These results show that each chemosensory neuron expresses multiple ligand binding sites whose signal transduction can be independently desensitized and rule out the alternative model that integration of information from multiple chemosensory receptors is invariably required for olfactory discrimination. An obvious potential target for ligand-specific desensitization is the

odorant receptor itself. However, inactivation of potential phosphorylation and ubiquitination sites of the AWA-expressed diacetyl receptor, *odr-10*, indicated that these residues are not required for many behaviors postulated to involve desensitization, including chemotaxis, discrimination, and adaptation.

Specifically, none of the C-terminal serine, threonine, or lysine residues, nor T229 (IC3#2) in the third intracellular loop, was required for diacetyl chemotaxis, diacetyl adaptation, or discrimination between pyrazine and diacetyl. However, replacement of S237 (IC3#3) and T240 (IC3#4) in the third intracellular loop abolished diacetyl chemotaxis. Without a means to evaluate the ligand-binding and G protein-coupling activity of these mutants, it is not possible to determine the cause of the chemotaxis defect. The serine residue mutated in IC3#3 (S237) is highly conserved in the *C. elegans odr-10* gene family (H. Robertson, in press). However, because IC3#3 and IC3#4 did not affect pyrazine chemotaxis in the presence of saturating concentrations of diacetyl, there is no evidence for a constitutive activation of ODR-10 that can interfere with pyrazine chemotaxis.

Additionally, these results rule out one proposed mechanism for chemotaxis. In *E. coli* chemotaxis, methylation and demethylation of the chemosensory receptor serves as a molecular memory of exposure to prior concentrations of attractants; this adaptation process is absolutely required for chemotaxis (Falke et al., 1997). Because *C. elegans* can not simultaneously compare two points of concentration on a gradient of odorant (the ciliated endings of pairs of chemosensory neurons are arranged one above the other during locomotion on an assay plate), chemotaxis must depend on integration of the memory of odorant concentrations over time, as in *E. coli*. My results rule out an essential role for phosphorylation of the C-terminal cytoplasmic domain as an analogous graded mechanism of olfactory memory in *C. elegans*. Another possibility was that phosphorylation might act to alter the sensitivity of ODR-10 to diacetyl. However, preliminary evidence suggests that ODR-10 lacking the six of eight C-terminal serines

and threonines (C 6/8) possesses a normal dose-response curve to diacetyl across three logs of odorant concentration (data not shown).

The lack of effect on ODR-10 function after ablation of serine and threonine residues is surprising since phosphorylation of G protein-coupled receptors has been widely documented as a mechanism of desensitization in other systems, including vertebrate phototransduction and adrenergic receptor signaling.

It is possible that the focus on *in vitro* biochemical approaches in these systems has overrated the physiological relevance *in vivo* of the processes being studied. However, genetic approaches have indicated a physiological role for receptor phosphorylation, for example by ablation of phosphorylation sites of pheromone receptors in yeast (Chen and Konopka, 1996; Hicke and Riezman, 1996; Hicke et al., 1998) and by generation of transgenic mice bearing a C-terminal truncation of rhodopsin (Chen et al., 1995). Still, the inherent bias of studying a defined mechanism in reconstituted systems using supraphysiological levels of agonists and signal transduction components may have overshadowed the role of other desensitization mechanisms. Additional genetic analysis will further clarify the physiological role of receptor phosphorylation and may suggest novel areas of study.

A recent study has demonstrated that desensitization of chemosensory receptors in other eukaryotic organisms is independent of phosphorylation (Kim et al., 1997). In the amoeba *Dictyostelium*, the G protein-coupled cAMP receptor cAR1 mediates several biological responses that exhibit adaptation including chemotaxis to cAMP. Adaptation of these responses is closely correlated with receptor phosphorylation. A mutant cAR1 in which all 18 serine residues in the C-terminal tail were changed to alanine fails to undergo phosphorylation, yet surprisingly these cAR1 mutants exhibited wild-type behavior for all tested responses, including chemotaxis, aggregation, differentiation, and adaptation of adenylyl and guanylyl cyclase activation. Only a defect in agonist-induced decreased affinity of the receptor for cAMP was noted. The phosphorylation-independent mechanism for adaptation has not been defined in this system.

My results show that C-terminal receptor phosphorylation or ubiquitination in *C. elegans* is not the sole mechanism for mediating desensitization of olfactory transduction. It may be that the other intracellular serine and threonine residues are involved in a phosphorylation-dependent regulatory process. Another possibility is that ODR-10 is desensitized by a phosphorylation- and arrestin-independent mechanism, perhaps by diacetyl-induced receptor endocytosis, decreased *odr-10* expression, or increased degradation of ODR-10. Prolonged exposure to diacetyl, however, does not significantly decrease the levels of a partially-rescuing ODR-10::GFP fusion at the AWA sensory cilia (Piali Sengupta, personal communication).

What might be the molecular mechanism for odorant-specific desensitization within a single chemosensory neuron? The recent elucidation of the function of a protein containing multivalent PDZ domains suggests one elegant solution. In the fruitfly *Drosophila*, the InaD protein acts as a scaffold for organized assembly of the G protein-coupled phototransduction machinery (Tsunoda et al., 1997). Three of its five PDZ domains have been demonstrated to specifically bind components of light-activated signal transduction or regulation, including the effector enzyme, phospholipase C β ; the principal ion channel, Trp; and the regulatory enzyme, eye-specific protein kinase C. The authors propose a highly organized signaling complex, or “transducisome,” that may provide for rapid response kinetics as well as response specificity within cells containing multiple signal transduction pathways.

Some PDZ domains appear to bind a consensus sequence of Ser/Thr-X-Val-COO⁻ at the carboxy terminus of proteins (Ranganathan and Ross, 1997), but there is no evidence that an InaD-like PDZ protein binds ODR-10, which lacks such a sequence. Still, the concept of a transducisome complex provides a simple mechanism for odorant-specific regulation downstream of the receptor, even when signal transduction components are shared by multiple receptors. I propose that specific signaling proteins within a transducisome-like complex are inactivated when the associated receptor protein undergoes prolonged stimulation. The same transduction

components would remain active if associated with an unstimulated receptor in a separate transduction complex, allowing odorant-specific regulation.

Many studies have now shown that essentially every step of G protein-coupled signal transduction can be regulated. For example, the intrinsic GTPase activity of G α subunits is increased by RGS proteins (Koelle, 1997), phosducin tightly binds and may modulate activity of G $\beta\gamma$ (Schroder and Lohse, 1996), cyclic nucleotides and calcium-calmodulin can increase cyclic nucleotide phosphodiesterase activity (Yan et al., 1995; Juilfs et al., 1997), and calcium-calmodulin downregulates cyclic nucleotide-gated channels (Liu et al., 1994). If any of these molecules are found in transducisome-like complexes, they could play a role in odorant-specific desensitization in *C. elegans*, despite participating in signal transduction for multiple odorants.

Consistent with this hypothesis, null mutations in a putative Trp-like ion channel, *osm-9*, cause an adaptation defect in the AWC-sensed odorants butanone and isoamyl alcohol, despite the ability of each of these odorants to independently adapt in wild-type animals (Colbert and Bargmann, 1995; Colbert et al., 1997). Furthermore, *osm-9* mutants display wild-type adaptation to benzaldehyde, which is also sensed by AWC. The initially puzzling separation of adaptation phenotypes even within AWC may be explained by the formation of distinct transduction complexes; i.e., the receptors that mediate response to isoamyl alcohol and butanone may recruit OSM-9 as a regulatory component into their transducisomes, while the receptor(s) that mediate benzaldehyde response may not, thereby allowing different types of regulation within a chemosensory neuron. Independent signaling complexes of this sort could provide great advantages in efficiency for animals such as *C. elegans*, which must utilize just two pairs of chemosensory neurons for directing chemotaxis to a wide spectrum of volatile attractants.

Methods

Strains used

Wild-type worms were *C. elegans* variety Bristol, strain N2. Worms were grown at 20°C with abundant food using standard methods (Brenner, 1974).

Strains used in this work included: CX2285 *osm-3* (*p802*) IV; *odr-1* (*n1936*) X, CX2307 *osm-3* (*p802*) IV; *odr-7* (*ky4*) X, CX3411 *odr-10* (*ky225*) X, and CX3425 *odr-10* (*ky225*) *lin-15* (*n765ts*) X.

Behavioral assays

All behavioral assays were conducted on well-fed adults. Standard chemotaxis assays were performed as previously described (Bargmann et al., 1993). Assay plates were used 1–3 days after pouring. Cross-saturation assays were performed similarly to standard chemotaxis assays, except that an amount of saturating odorant was well-mixed into the assay agar. Saturation assay plates were used 1 day after pouring. Adaptation assays were performed as previously described (Colbert and Bargmann, 1995).

Molecular biology methods

General manipulations were performed using standard methods (Sambrook et al., 1989). Sequencing was performed with the Promega *fmol* sequencing kit in an MJR thermal cycler. The GeneWorks v2.5.1 software package (Intelligenetics) and DNA Strider v1.2 (public domain, by Christian Marck) were used for sequence analysis. Sequence of the *odr-10* region was confirmed with data courtesy of the *C. elegans* genome sequencing consortium (Sulston et al., 1992).

Construction of the *odr-10* minigene cassette vector

The 1.3 kb *odr-10* promoter region was isolated from a 12 kb EcoRV to XbaI cosmid fragment in pBluescript® KS(-) by PCR amplification with a T3 primer and the *odr-10*Xho primer (5'– CTC GAG CTG TAA GGT ATC TTA ATG–3'), which replaces the *odr-10* start methionine with an XhoI site.

The promoter fragment PCR product was cloned into a TA cloning vector (pCR 2.1, Invitrogen), recovered as a Sall to XhoI fragment, and introduced into the Sall site of the promoterless *odr-10* cDNA vector, TU#62 1₁A-STOP, whose construction has been previously described (Sengupta et al., 1996). The resulting *odr-10* minigene construct contains the *odr-10* promoter followed by ~120 nucleotides of polylinker and a synthetic intron, followed by the *odr-10* cDNA. Due to the method of construction of TU#62 1₁A-STOP, the *odr-10* cDNA in this construct has a replacement of the terminal two residues from ProThr<stop> to GlySerSer<stop>; this alteration does not affect the rescuing properties of the construct (Sengupta et al., 1996). The *odr-10* minigene prior to cassette modification was fully capable of rescuing the diacetyl chemotaxis defect of *odr-10* (*ky225*) (data not shown).

A number of alterations were made to the *odr-10* minigene construct to allow cassette mutagenesis. The unique Sall site was destroyed by cutting with Sall, blunting with Klenow polymerase, and religation. The *odr-10* cDNA was removed from the *odr-10* minigene as a SacI to EcoRI fragment and cloned into the same sites of pALTER-1 of the Promega Altered Sites mutagenesis system. Within pALTER-1, three changes were made by oligonucleotide-directed mutagenesis: 1) the SacI site was destroyed and an A insertion was introduced to improve the Kozak translation initiation sequence, using the oligo JHC-15 (5'-CTC CCG ACA TGG TAG CTC GGT ACC-3'); 2) the first PmlI site in *odr-10* was ablated, using the oligo JHC-13 (5'-CAA GTT TTT TCC GCG TGT TTT CAG A-3'); and 3) a Sall site in the C-terminal tail of *odr-10* was generated using the oligo JHC-16 (5'-CGA GCG GGA TTC GTC GAC ACT GTT TTT CTT TCC-3'). The modified *odr-10* cDNA was recloned into the Sall-ablated *odr-10* minigene construct as a KpnI to EcoRI fragment. All induced mutations and cloning junctions were confirmed by sequence analysis.

The end result of these manipulations did not alter any amino acids in the *odr-10* coding region but served to generate and remove sites, allowing subsequent cassette mutagenesis. Specifically, 1) PmlI and XhoI became unique sites that would drop out the region of *odr-10* intracellular loop

3 that codes for the residues Trp-Lys-Thr-Met-Asn-Glu-His-Lys-Asp-Val-Ser-Arg-Thr-Arg-Ala; 2) BclI and Sall became unique sites that flanked the first portion of the C-terminal tail region, consisting of Ile-Arg-Asp-Phe-Arg-Arg-Thr-Ile-Phe-Asn-Phe-Leu-Cys-Gly-Lys-Lys-Asn-Ser-Val; 3) Sall and EcoRI became unique sites that flanked the remaining portion of the C-terminal tail, including Asp-Glu-Ser-Arg-Ser-Thr-Thr-Arg-Ala-Asn-Leu-Ser-Gln-Val-Gly-Ser-Ser-Stop. Note that the final Gly-Ser-Ser-Stop are not the terminal residues found in wild-type *odr-10*, which are Pro-Thr-Stop. In all cassette mutageneses involving the C-terminus (C 2/8, C 6/8, C 8/8, C-KK), the wild-type terminal residues were re-introduced, while the unmutagenized minigene cassette (mg cassette) and all third intracellular loop constructs (IC3 3/4, IC3#2, IC3#3, IC3#4) are altered for the terminal residues.

Cassette mutagenesis of *odr-10*

Mutagenesis cassettes were generated by annealing two overlapping oligonucleotides that contained the desired mutations. Annealing protocol: 200 pmol of each oligonucleotide in 100 μ l of 1x Boehringer Mannheim "M" restriction enzyme buffer was heated to 85°C in an MJR thermal cycler and brought to 45°C at a rate of 1°C per minute, then quickly cooled to 22°C for 10 minutes, followed by an indefinite 4°C step. The oligonucleotides were designed to have the proper overhangs after annealing to replace relevant regions of the *odr-10* minigene cassette vector. All mutagenized cassette regions were confirmed by sequence analysis. Note that all cassette mutagenesis involving the first part of the C-terminal tail required BclI digestion of plasmids isolated from DNA methylase-deficient bacteria.

The following summarizes the mutant constructs generated. Amino acid numbering is as previously described (Sengupta et al., 1996). Sequences of oligonucleotides used in cassette mutagenesis are available upon request. Third intracellular loop mutations: IC3 3/4: T229A S237A T240A; IC3 #2: T229A; IC3 #3: T237A; IC3 #4: T240A. C-terminal tail mutations: C 2/8: T311A S322A; C 6/8: S326A S328A T329A T330A S335A T339A; C 8/8: T311A S322A S326A S328A T329A T330A S335A T339A; C-KK: K319R K320R

Construction of C-terminal frameshift *odr-10*

A cosmid-derived *odr-10* ScaI-EcoRV fragment grown in DNA methylase-deficient *E. coli*, was cut with BclI, blunted with Klenow polymerase, and religated, to generate ScaI-EcoRV Δ C. The induced frameshift, which was confirmed by sequence analysis, results in deletion of all residues after the seventh predicted transmembrane domain: i.e., the C-terminal residues are truncated from ...LIIRDF... to ...LIDHS(Stop).

Generation of transgenic worms

Germline transformation was by standard methods as previously described (Mello et al., 1991). All transformations were done in lines also bearing the *lin-15* (*n765ts*) mutation by co-injecting wild-type *lin-15* DNA pJM23 (50 ng/ μ l) with the construct of interest (also 50 ng/ μ l). Lines were isolated from independent F1 progeny rescued for the *lin-15* multivulval phenotype at 20°C.

Acknowledgments

I would like to express gratitude to Liqin Tong, Shannon Grantner, and Yongmei Zhang for expert sequencing assistance.

The AWA chemosensory neurons discriminate between multiple odorants

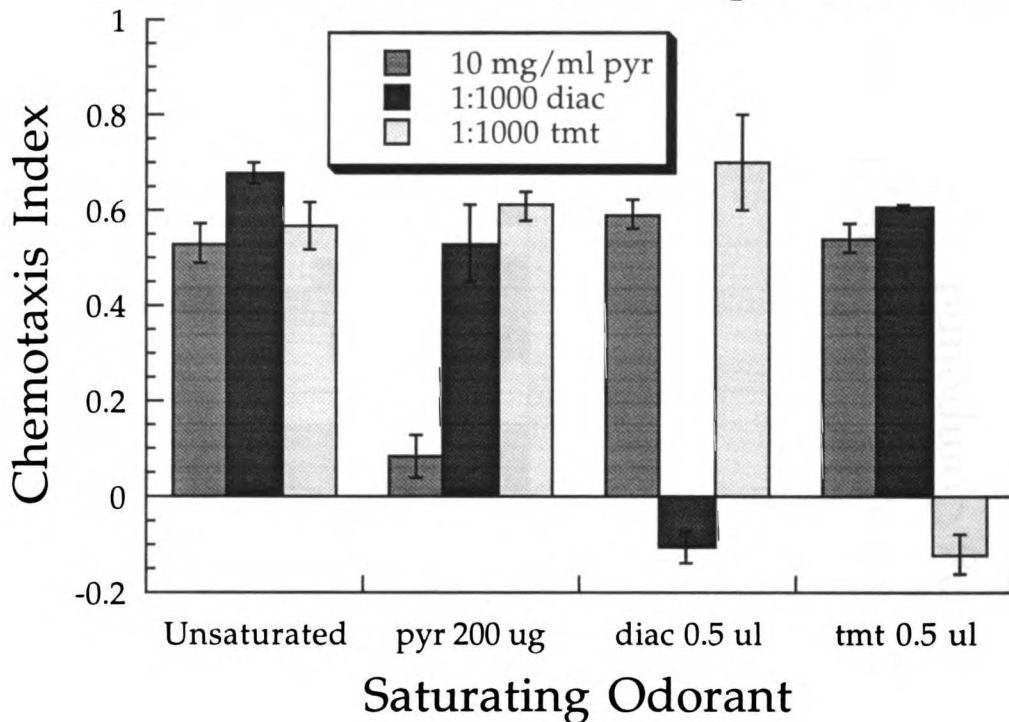


Figure 4-1. Odorant discrimination by animals possessing only AWA chemosensory neuron function. *osm-3 odr-1* animals were tested for ability to discriminate between odorants sensed by AWA. Abbreviations used: 2,4,5-trimethylthiazole (tmt); pyrazine (pyr); diacetyl (diac). The amounts of saturant used per assay plate and the concentrations of point sources of attractants are shown. Each bar represents a minimum of two independent chemotaxis assays; these results should be considered preliminary.

Odorant discrimination by
the AWC chemosensory neurons

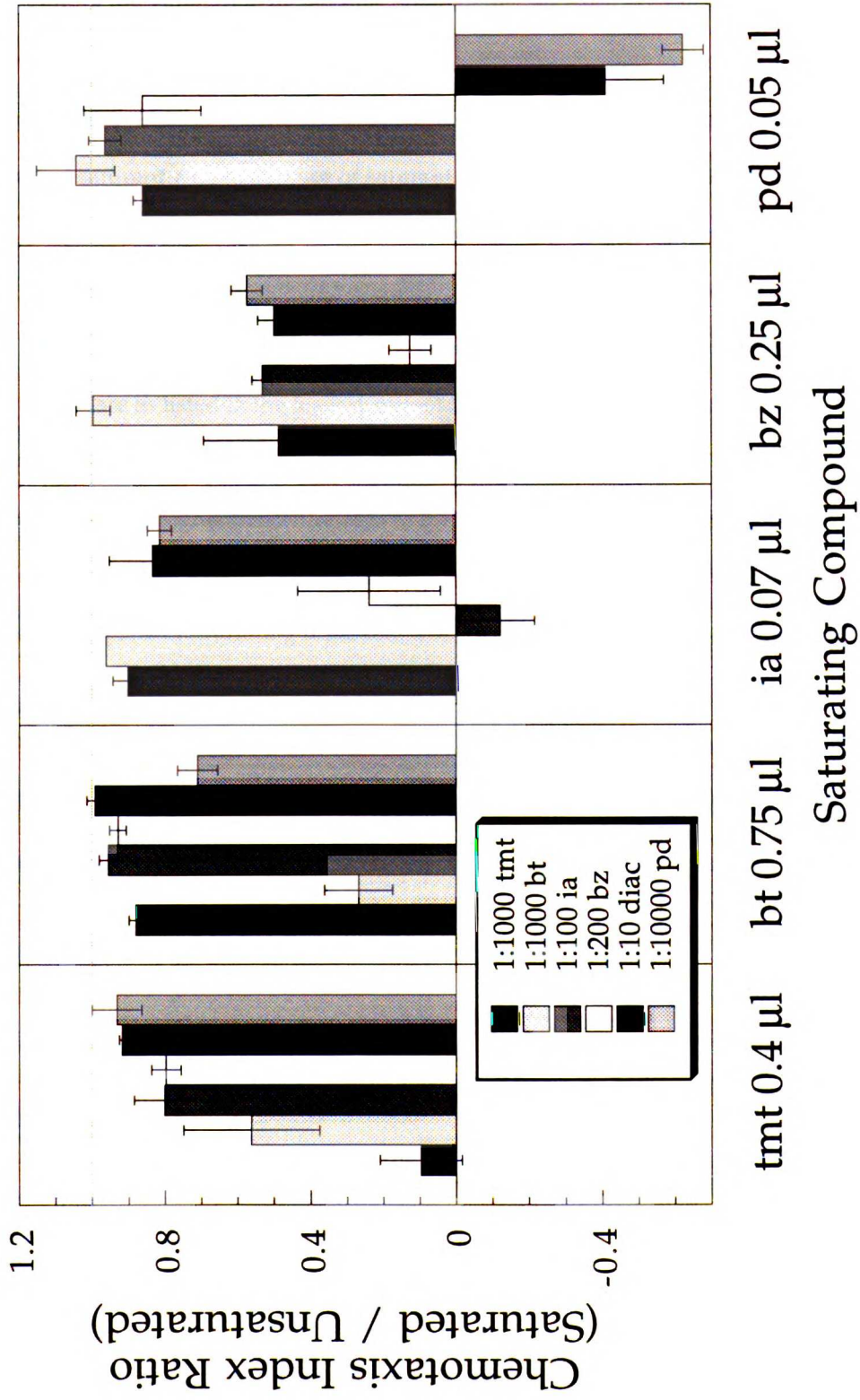
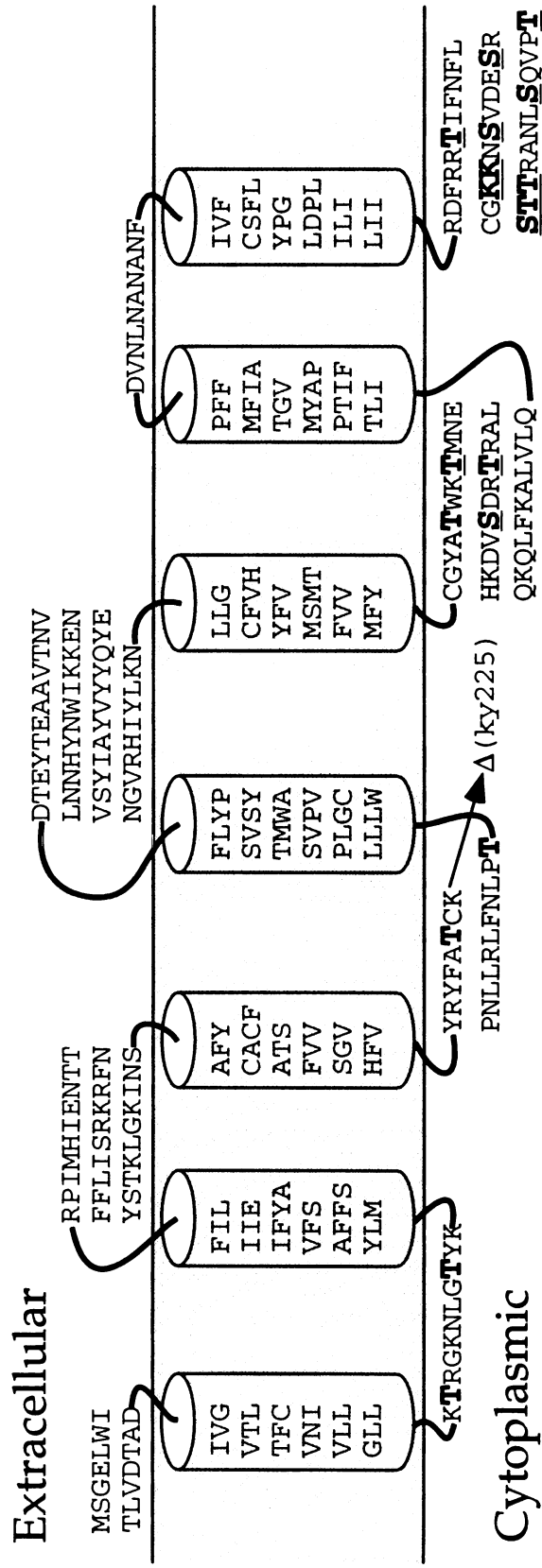


Figure 4-2. Odorant discrimination by animals possessing only AWC chemosensory neuron function. *osm-3 odr-7* animals were tested for ability to discriminate between odorants sensed by AWC. The results are presented as ratios of chemotaxis indices (CI) to a point source of odorant = CI in presence of saturant / CI in absence of saturant. Thus, if the saturant had no effect on chemotaxis, the ratio would be 1; likewise, if the saturant completely abolished chemotaxis, the ratio would be 0. Abbreviations used: 2,4,5-trimethyl thiazole (tmt), butanone (bt), isoamyl alcohol (ia), benzaldehyde (bz), diacetyl (diac), 2,3-pentanedione (pd). Concentrations of the point sources of odorant are as listed in the legend, except that 1:200 isoamyl alcohol and 1:1,000 pentanedione were used in isoamyl alcohol saturations. Amounts of saturant used per assay plate are listed. In some cases, higher concentrations of saturant were used: 0.5 μ l/plate of saturating trimethylthiazole was used against point sources of benzaldehyde, isoamyl alcohol, and butanone; and 1 μ l/plate of saturating butanone was used against point sources of isoamyl alcohol and pentanedione. Chemotaxis indices for unsaturated point sources of odorant were: 0.78 for 1:1,000 tmt; 0.75 for 1:1,000 bt; 0.89 for 1:100 ia; 0.82 for 1:200 ia; 0.87 for 1:200 bz; 0.68 for 1:10 diac; 0.81 for 1:10,000 pd; 0.89 for 1:1,000 pd. Each bar represents a minimum of two independent unsaturated and saturated chemotaxis assays; these results should be considered preliminary.

A. Putative topology of ODR-10



B. Summary of ODR-10 site-directed mutagenesis

Third intracellular loop mutations:

IC3 #3/4: T229A S237A T240A
IC3 #2: T229A
IC3 #3: T237A
IC3 #4: T240A

C-terminal tail mutations:

C 2/8: T311A S322A
C 6/8: S326A S328A T329A T330A S335A T339A
C 8/8: T311A S322A S326A S328A T329A T330A S335A T339A
C-KK: K319R K320R

ΔC: ...LIIRDF... becomes ...LIDHS (Stop)

Figure 4-3. Putative topology of ODR-10 and summary of mutagenesis. (A) ODR-10 is predicted to be a seven-transmembrane G protein-coupled receptor, with an extracellular amino terminus and intracellular carboxy terminus. Serine and threonine residues in the intracellular loops and the tail are in bold face, as are lysine residues in the carboxy terminal tail. Residues altered by site-directed mutation are underlined. As indicated, *odr-10* (*ky225*) is a mutation that deletes all *odr-10* coding region past the middle of the second intracellular loop; it is therefore predicted to be a null mutation (Sengupta et al., 1996). (B) Summary of ODR-10 mutations generated in this study. All point mutations were generated by cassette mutagenesis (see Methods). ΔC represents the *ScaI*-*EcoRV* ΔC frameshift mutation predicted to remove the entire carboxy terminal tail (see Methods).

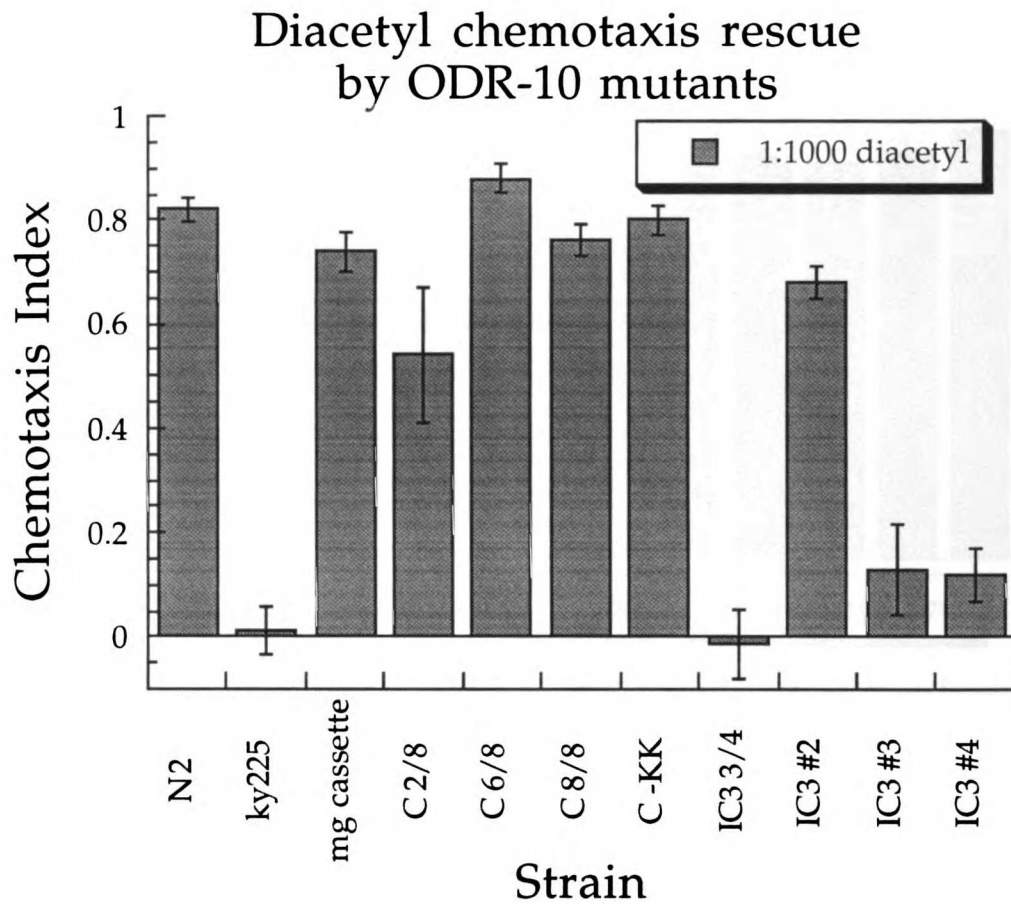


Figure 4-4. Diacetyl chemotaxis rescue mediated by ODR-10 altered by site-directed mutagenesis. *odr-10* (*ky225*) null animals expressing mutant ODR-10 were tested for chemotaxis to 1:1,000 diacetyl. Wild-type N2 and *odr-10* (*ky225*) animals expressing the unmutagenized *odr-10* minigene cassette construct (mg cassette) are included as positive controls.

ODR-10 mutants can discriminate pyrazine from diacetyl

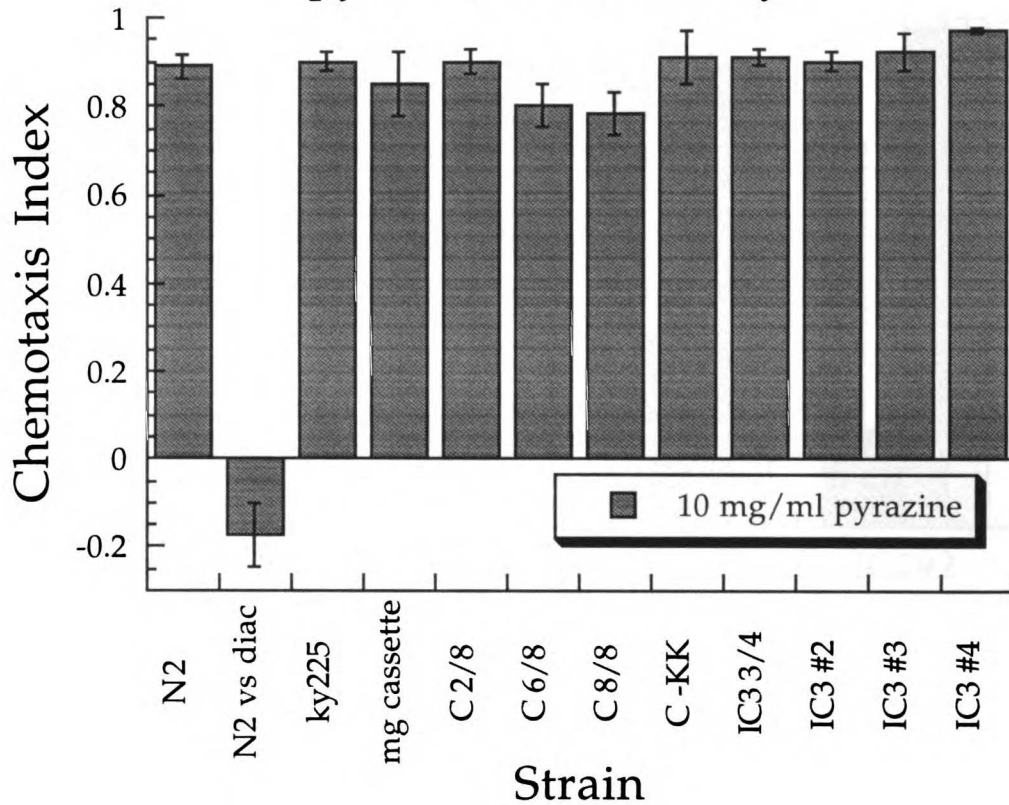


Figure 4-5. Discrimination between pyrazine and diacetyl is unaffected by ODR-10 mutation. *odr-10* (*ky225*) null animals expressing mutant ODR-10 were tested for chemotaxis to a point source of 10 mg/ml pyrazine in the presence of uniform high concentrations of diacetyl. The second bar, N2 vs. diacetyl, shows chemotaxis to a point source of 1:1,000 diacetyl, demonstrating that the diacetyl concentrations used were saturating. Wild-type N2 and *odr-10* (*ky225*) animals expressing the unmutagenized *odr-10* minigene cassette construct (mg cassette) are included as positive controls.

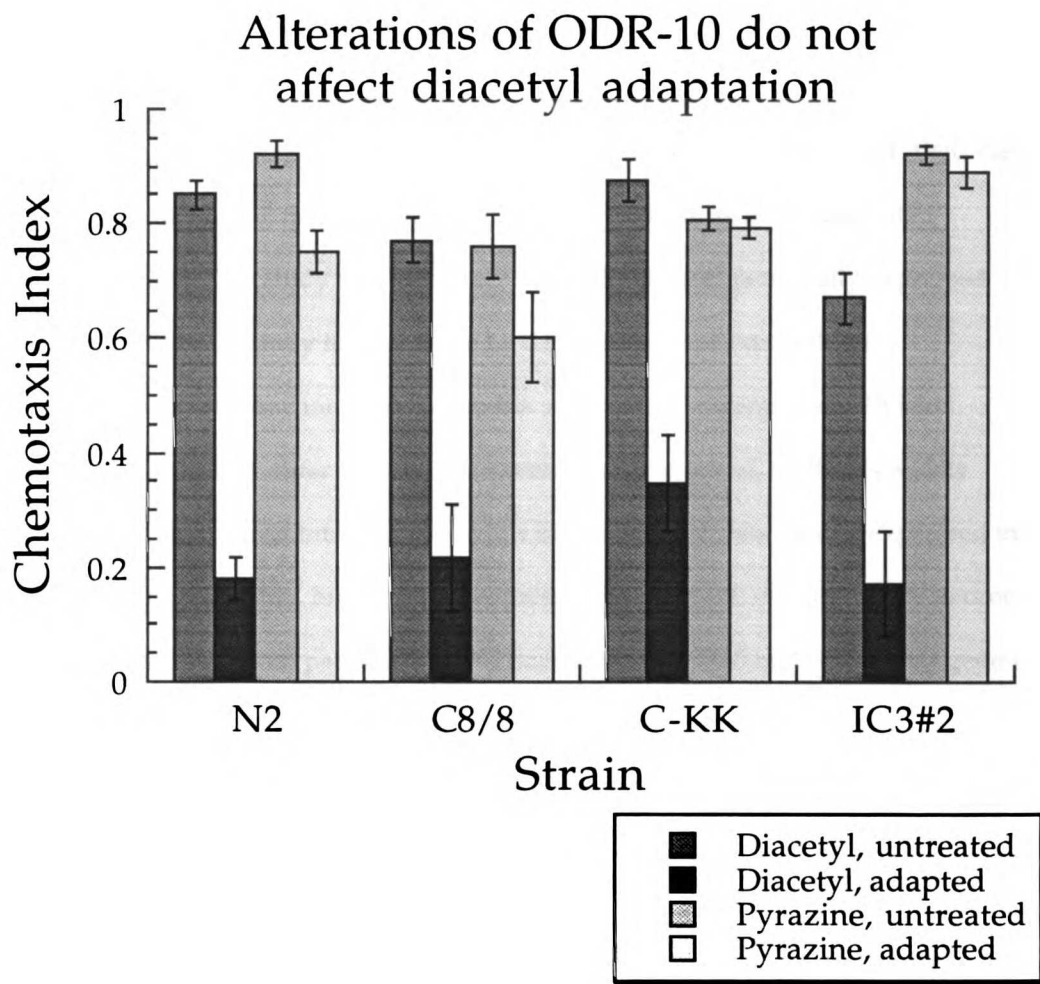


Figure 4-6. Diacetyl adaptation is unaffected by alterations of ODR-10. *odr-10* (*ky225*) null animals expressing mutant ODR-10 were adapted to 5 μ l of diacetyl for 1 hour and tested for chemotaxis to 1:1,000 diacetyl. Chemotaxis to 10 mg/ml pyrazine demonstrated lack of nonspecific pyrazine cross-adaptation.

Chapter 5. *odr-2*: a novel gene required for chemotaxis

Abstract

Caenorhabditis elegans chemotaxis to volatile attractants is mediated by the AWA and AWC classes of chemosensory neurons. *odr-2* mutants are specifically defective in all AWC-mediated chemosensory behaviors. This study shows that *odr-2* encodes a novel neuronally-expressed protein that appears to be distantly related to the Ly-6 superfamily of extracellular glycosylphosphatidylinositol-anchored glycoproteins. Alternative splicing of *odr-2* yields different protein isoforms that differ only at the extreme amino terminus. ODR-2 is widely expressed in sensory, motor, and interneurons, while individual isoforms may be expressed in different sets of neurons. Notably, high levels of expression in the AWC chemosensory neuron were not observed. At least seven paralogs of *odr-2* have been identified in the *C. elegans* genome, each of which may also undergo alternative splicing, and at least one of which also appears to be expressed exclusively in neurons. Thus, ODR-2 defines a new family of Ly-6 domain containing proteins in *C. elegans*. ODR-2 may modulate AWC-specific signaling within the neuronal network required for chemotaxis.

Introduction

Olfactory chemotaxis in *C. elegans*

C. elegans is an excellent model system for the study of behavior because of its simple structure and genetic tractability (Brenner, 1974). A nearly complete wiring diagram of its stereotyped nervous system has been elucidated by serial section electron microscopy and may permit the complete description of the generation of behavior at the neuronal level (White et al., 1986). The

contribution of specific neurons to various behaviors can be assessed by using a focused laser microbeam to ablate individual neurons, while the molecular components required can be revealed by molecular genetic analysis.

C. elegans sense volatile attractants using just two pairs of chemosensory neurons, AWA and AWC, as defined by laser ablation. Genetic screens for mutants unable to chemotax has been fruitful in identifying molecules required for olfactory behaviors. A number of signaling components likely to function in the chemosensory neuron itself have been identified, including odorant receptors, G proteins, guanylyl cyclases, and ion channels, as well as proteins important for receptor localization to the sensory cilia and transcription factors that determine the functional identity of chemosensory neurons (Sengupta et al., 1994; Coburn and Bargmann, 1996; Komatsu et al., 1996; Sengupta et al., 1996; Colbert et al., 1997; Dwyer et al., 1998; Roayaie et al., 1998; D. Birnby, submitted; Noelle L'Etoile, personal communication). These studies have defined a framework for the initial events of chemosensory perception and signaling. However, the mechanisms by which chemosensory neurons interact with interneurons and downstream motor neurons to generate chemotactic behavior is not understood.

The superfamily of Ly-6 domain proteins

The Ly-6 proteins were originally defined serologically as murine lymphocyte cell surface differentiation antigens (Gumley et al., 1995). Subsequent molecular cloning identified a superfamily of related proteins based on sequence similarity within a domain of ~75 amino acids, defined by the conservation of ten cysteine residues with a characteristic spacing pattern (Palfree, 1996). The Ly-6 domains of all members are extracellular and most are linked to the plasma membrane via a glycosylphosphatidyl inositol (GPI) moiety.

GPI-linked proteins are anchored to the external leaflet of the plasma membrane (Low, 1989). These proteins typically begin with an amino terminal signal sequence consisting of a positively charged amino end, a longer hydrophobic stretch, and a more polar carboxyl terminal segment

(von Heijne, 1994). The signal sequence is usually proteolytically removed during membrane translocation. At the extreme carboxyl terminus of a nascent GPI-anchored protein, a less well characterized hydrophobic signal directs attachment of the phosphoethanolamine of a preformed GPI anchor to the α -carboxyl group of an internal amino acid, thereby truncating the carboxyl terminus of the GPI-linked protein (Udenfriend and Kodukula, 1995). The site of GPI attachment can occur ~10–12 residues upstream of the C-terminal hydrophobic signal, although no strict consensus sequence defines the precise attachment site (Antony and Miller, 1994). No portion of the mature protein is inserted into the plasma membrane; membrane anchoring is mediated strictly by the phosphatidylinositol moiety. A common criterion for GPI-linkage is membrane release of proteins upon treatment with phosphatidylinositol-specific phospholipase C.

Most members of the Ly-6 superfamily contain a single Ly-6 domain, with an amino terminal membrane targeting signal sequence and carboxy terminal GPI membrane attachment signal. These include the family of rodent Ly-6 cell surface markers (Friedman et al., 1990; Palfree, 1996) and human complement-mediated lysis inhibitor CD59 (Davies and Lachmann, 1993), keratinocyte adhesion molecule E48 (Brakenhoff et al., 1995), and retinoic acid inducible protein RIG-E (Mao et al., 1996). The sole known invertebrate GPI-linked Ly-6 domain protein is Sgp-2, a squid neuronal glycoprotein (Williams et al., 1988). GPI-linkage for most of these proteins has been demonstrated by phosphatidylinositol-specific phospholipase C-mediated release from the plasma membrane.

Other single domain Ly-6 proteins that lack the C-terminal GPI anchor include a human sperm acrosomal protein SP-10 (Wright et al., 1990; Palfree, 1996) and trout protein DRTP-1 (Lee and Goetz, 1998). The secreted snake neurotoxins are unique among the Ly-6 superfamily in that they lack one conserved pair of Ly-6 cysteines and variably possess an additional pair of disulfide-bridged cysteines not found in other superfamily members (Betzel et al., 1991; Fleming et al., 1993; Ploug and Ellis, 1994). In addition, some proteins have two or more consecutive Ly-6 domains. These include the human GPI-linked urokinase plasminogen activator receptor (uPAR)

(Roldan et al., 1990; Ploug and Ellis, 1994), both subunits of the snake phospholipase A₂ inhibitor (PLA₂-I) (Ohkura et al., 1994), and the rodent bone and cartilage-expressed RoBo-1 (Noel et al., 1998). Recently, it has been recognized that the extracellular domain of the TGF β type I receptor kinase contain a Ly-6-like repeat (Jokiranta et al., 1995), as does its *C. elegans* homolog, *daf-1* (Georgi et al., 1990).

The Ly-6 domains exist as an autonomous structural unit as shown by limited proteolysis of uPAR (Behrendt et al., 1991; Behrendt et al., 1996). The crystal structure of cobratoxin and a 2-D NMR solution structure of CD59 demonstrated disulfide bridge pair conservation and overall structural similarity between these two proteins (Betzel et al., 1991; Fletcher et al., 1994; Kieffer et al., 1994). The main structural features of CD59 involve four pairs of cysteine disulfide bridges in a knot at the base of the molecule, from which emanate two fingers of antiparallel beta-sheets. A fifth disulfide bridge forms a loop at the tip of one of the beta-sheets.

Although the physiological function of many of these proteins remain undefined, some members have been implicated in modulation of extracellular matrix interactions (Wei et al., 1996) or cellular adhesion (Bamezai and Rock, 1995; Brakenhoff et al., 1995), signal transduction (Jokiranta et al., 1995), inhibition of postsynaptic ion channel function (Betzel et al., 1991), regulation of plasminogen activation (Plesner et al., 1997), and protection against complement-mediated lysis (Davies and Lachmann, 1993).

***odr-2* encodes a novel Ly-6 domain protein required for chemotaxis**

In this study, I describe the cloning of *odr-2*, a novel neuronally-expressed gene required for a AWC-mediated chemosensory behaviors in *C. elegans*. All three alleles of *odr-2* are similarly defective in chemotaxis to odorants sensed by AWC, including benzaldehyde, isoamyl alcohol, 2,3-pentanedione, and pyruvic acid (Bargmann et al., 1993; this chapter, chapter 3B). Chemotaxis to odorants sensed by AWA is not affected in *odr-2* mutants, indicating a degree of specificity to the chemosensory defects. The AWC sensory cilia in *odr-2* mutants appear grossly normal by

serial section electron micrographs, suggesting that their defect is not due to impaired odorant access (Bargmann et al., 1993).

odr-2 appears to be a distant member of the Ly-6 superfamily and includes the conserved cysteine motif and GPI-targeting sequences. Alternative splicing yields different protein isoforms that differ only at the extreme amino terminus. ODR-2 is widely expressed exclusively in neurons, and individual isoforms may be expressed in different sets of neurons; however, there is no indication that ODR-2 is expressed in the AWC chemosensory neurons. At least five paralogs of *odr-2* exist in *C. elegans*, each of which may also undergo alternative splicing, and at least one of which also appears to be expressed in neurons. ODR-2 may modulate AWC-specific signaling within the network of neurons required for generating chemotaxis.

Results

Molecular cloning of *odr-2*.

The initial characterization of *odr-2* mapped its position to between *nDf32* and *sDf30* on chromosome V (Bargmann et al., 1993). A former postdoctoral fellow in the lab, Piali Sengupta, further refined its map position and isolated a pool of rescuing cosmids that included NA2, F27A2, and F27B10.

I found that the overlapping cosmids NA2, VC5, and EB2 were each capable of rescuing the benzaldehyde chemotaxis defect of *odr-2(n2145)* mutants (data not shown). A 13.4 kb KpnI–SpeI EB2 subclone rescued nearly as well as the complete cosmid, but further subcloning drastically curtailed rescue (Figure 5-1). The 7.6 kb KpnI–StuI fragment showed very weak rescue, while the 5.8 kb StuI–SpeI fragment was completely incapable of directing chemotaxis rescue. The weakly rescuing 7.6 kb KpnI–StuI fragment was used to screen a mixed-stage *C. elegans* cDNA library. 1.1 x 10⁶ plaques were screened yielding 12 positives representing eight independent clones.

Sequence analysis of *odr-2* cDNAs

Sequence analysis revealed that all 6 cDNA messages shared identical 3' regions consisting of 453 nucleotides of open reading frame and 197 nucleotides of 3' untranslated region followed by polyadenylation (Figure 5-2). However, the 5' ends appear to be alternatively spliced. Thus, these clones represent a family of transcripts predicted to encode several related but distinct protein products.

Six of the cDNA classes are predicted to code for three proteins with alternatively spliced amino terminal segments, which will henceforth be referred to as ODR-2 isoforms 2b, 16, and 18.

Isolate 2b possessed 250 nucleotides of divergent 5' message spliced to the common region, with two potential in-frame start methionines which would result in 40 or 50 divergent amino termini residues respectively (1 clone). Isolate 16 had 185 nucleotides of divergent 5' sequence with a single in-frame start methionine resulting in 26 alternative residues (1 clone). Isolate 18 had 342 nucleotides of divergent 5' sequence with a single in-frame methionine resulting in 22 distinct residues (4 independent clones, see below).

One cDNA clone (isolate 2a) represents an incompletely processed message. Although introns within the common region were removed, no upstream exon was spliced to the common region, resulting in disruption of the open reading frame. This single clone suggests that processing of the common region in *odr-2* transcripts may precede selection of an alternative 5' exon.

A 22 nucleotide splice leader (SL1) is trans-spliced to the 5' end of some *C. elegans* mRNA (Krause and Hirsh, 1987). *odr-2* cDNA isolates 11, 22, and 21 were identical to isolate 18 except for 9, 7, and 1 nucleotides respectively of sequence matching the SL1 trans-spliced leader that replaced the first 131 nucleotides of isolate 18. Hemi-nested RT-PCR of *C. elegans* mRNA using an SL1 primer and two *odr-2* common region primers confirmed that isoform 18 is trans-spliced and demonstrated that isoform 2b can also be SL1 trans-spliced 5 nucleotides upstream of the 5' end of the original 2b cDNA isolate. This analysis did not reveal any additional *odr-2* isoforms.

Genomic organization of *odr-2*.

Standard molecular biological methods were used to determine the genomic organization of *odr-2* coding regions. The common region exons are clustered in a 1.6 kb region, while the three alternative N-termini were located 9.0 kb (2b), 5.7 kb (16), and 3.3 kb (18) upstream of the common region (Figure 5-3). Isoforms 16 and 18 are generated by a single alternative exon, while the isoform 2b possesses two alternative exons. The *odr-2* region was subsequently sequenced by the *C. elegans* genome sequencing project, confirming our analysis.

Deletion of the common region from the 13.4 kb genomic fragment abolished rescuing activity, indicating that the cDNAs isolated indeed represent *odr-2* message (Figure 5-1).

***odr-2* is predicted to encode a novel extracellular protein linked to the plasma membrane via a glycosylphosphatidyl inositol anchor.**

Basic local alignment sequence tool (BLAST) searches of the GenBank database using predicted ODR-2 protein sequences did not identify significant homology to any previously identified proteins. However, the predicted protein products have several notable features.

Each of the alternative N-termini contains a hydrophobic signal-like sequence for membrane targeting (Figure 5-4). The extreme C-terminus has a pronounced hydrophobic segment followed by a terminal arginine, consistent with a glycosylphosphatidylinositol membrane anchoring signal. Assuming that ODR-2 (2b) initiates translation at the first methionine, a good match for an N-terminal signal sequence is found with a predicted cleavage site after residue 27 (Figure 5-2; von Heijne, 1986). Isoforms 16 and 18 have less clear potential cleavage sites; however, GPI-modification in the absence of a cleavable N-terminal signal peptide has been described (Howell et al., 1994). The common region is relatively cysteine-rich, with 10 cysteines in the predicted mature protein. A speculative topology would represent ODR-2 protein as membrane-associated with an extracellular domain containing disulfide-linkages.

ODR-2 may share structural similarity with the Ly-6 superfamily of proteins

Extracellular proteins often retain a characteristic cysteine spacing to maintain disulfide bridges required for proper protein structure. The abundance of cysteines in the ODR-2 common region invited comparison of the relative spacing of these residues with those in other proteins.

This analysis revealed that ODR-2 shared a pattern of cysteine spacing with that found in the superfamily of Ly-6 domain-containing proteins (Table 5-1). The defining feature of these proteins is the presence of one or more domains of ten cysteine residues with a conserved spacing. Although very few non-cysteine residues are conserved between the more divergent members of the Ly-6 superfamily, one of them, an asparagine immediately following the tenth cysteine, is also found in ODR-2 (Figure 5-2).

ODR-2 is one of the most divergent members of the Ly-6 superfamily, based on the distance between its ten cysteines (Table 5-1). While the spacing between some ODR-2 cysteines are in good agreement with those found in the superfamily, others spacings fall outside the previously observed range. Interestingly, in two of the cases where the spacing in ODR-2 is dramatically divergent (between cysteines 3–4 and 6–7), the most similarly spaced Ly-6 relative is Sgp-2, the only previously identified invertebrate member of the Ly-6 superfamily. Similarly, ODR-2 and Sgp-2 are the only two members of the Ly-6 superfamily that have a single amino acid between cysteines 8 and 9, while all others have none. ODR-2 has 25 amino acids between cysteines 2 and 3, while those of all previously identified GPI-linked Ly-6 proteins have ranged from 4 to 8. However, these residues do not lie within the core of the Ly-6 domain structure and can be accommodated by increasing the loop formed by the disulfide bridge between cysteines 2 and 3 (Figure 5-5).

Identification of mutations

To further confirm the identity of *odr-2*, we characterized the mutations associated with each of the known alleles. Alternative and common region exons were amplified from genomic DNA

isolated from mutant strains carrying the *odr-2* alleles *n2145*, *n2148*, and *n1939*. All three mutations identified were G to A transitions, consistent with the known characteristics of ethyl methanesulfonate, the mutagen used to isolate the *odr-2* mutants (Bargmann et al., 1993).

The *n2145* allele represents a missense mutation in the common region converting the ninth cysteine to tyrosine, supporting an important structural role for the conserved cysteines in ODR-2. *n2148* is also a missense mutation in the common region, altering the glycine immediately before the sixth cysteine to aspartate. Because these mutations are in the common region, they would affect all ODR-2 isoforms.

n1939, however, was found to be associated with a nonsense mutation in the 2b isoform alternative region, possibly implicating this isoform as critical for mediating chemotaxis function (however, see below).

ODR-2 is widely expressed in neurons

To determine where ODR-2 might be required for mediating chemotaxis, an hemagglutinin (HA) epitope tag was inserted in-frame into five different locations of the common region in a rescuing fragment. Based on the known structure of CD59 and assuming that ODR-2 would fold similarly, the five locations were chosen to minimize interference with the core regions of the Ly-6 domain (Figure 5-5). The locations of the inserted epitope tags were: HA#1) at the beginning of the common region before the first cysteine residue; HA#2) in the loop formed by cysteines 2 and 3 (“A–B fingertip”); HA#3) in the loop between strands B and C, which link the two sets of antiparallel beta-sheets; HA#4) in the loop between strands D and E, before the seventh cysteine that precedes the helical region; and HA#5) immediately after the tenth cysteine, which incidentally displaces the conserved asparagine that follows it (Figure 5-2). Introduction of each of the first four constructs into *odr-2* (*n2145*) animals resulted in complete rescue of the isoamyl alcohol chemotaxis defect; the fifth construct rescued somewhat less well (Figure 5-6).

Whole mount antibody staining of the transgenic animals revealed widespread expression that was restricted to neurons (Figure 5-7). Staining was concentrated in axonal processes, was less prominent in dendritic processes, and was excluded from the nucleus. Because of the AWC chemosensory defects in *odr-2* mutant animals, it was significant that neither expression in AWC nor prominent staining in the amphid chemosensory cilium was noted.

It was possible that ODR-2 expression levels were too low in AWC to visualize, so an AWC-specific promoter was used to drive expression of cDNAs representing all three isoforms of ODR-2. These three clones were injected as a pool into *odr-2* (*n2145*) animals. No rescue of the isoamyl chemotaxis defect was observed (Figure 5-8). However, ODR-2 expression in AWC was not confirmed.

ODR-2 isoforms can functionally substitute for one another

The identification of a nonsense mutation in the 2b isoform suggested that this isoform might be essential for ODR-2's role in chemotaxis. To test the requirement of each of the alternative ODR-2 isoforms in AWC-mediated chemotaxis, internal deletions were made in a rescuing construct that specifically ablated the coding region of individual alternative isoforms.

Deletion of the 2b, 16, and 18 isoforms individually ($\Delta 2b$ or $\Delta 16$ or $\Delta 18$) did not affect the ability to rescue chemotaxis (Figure 5-9 and Figure 5-10). This result was surprising considering that the mutation responsible for the *odr-2* (*n1939*) phenotype was a nonsense mutation predicted to specifically affect the 2b isoform. Nonetheless, in rescue experiments none of the individual isoforms isolated thus far is required for AWC-mediated chemotaxis.

Furthermore, simultaneous deletion of the 2b and 16 alternative regions ($\Delta 2b\Delta 16$) also did not affect chemotaxis rescue (Figure 5-9 and Figure 5-10). However, simultaneous deletion of all three of the 2b, 16, and 18 isoforms ($\Delta 2b\Delta 16\Delta 18$) completely abolished chemotaxis rescue (Figure 5-10).

Taken together, these results indicate that expression of at least one of the 2b, 16, or 18 isoforms is required for AWC-mediated chemotaxis, and suggest that these isoforms can functionally substitute for one another. However, additional unidentified isoforms may contribute to, or be required for, ODR-2 function.

Complex regulation of *odr-2* expression

Multiple genomic regions required for ODR-2 function

The previously characterized isoform-specific deletions were extended to characterize their effect on chemotaxis rescue. As shown previously, the loss of the 18 isoform alone ($\Delta 18$) did not affect chemotaxis rescue (Figure 5-10). The Δ BstEII construct also ablated the alternative 18 isoform and further extended the deletion 1.8 kb upstream without impinging on isoform 16 alternative exons. This construct fails to rescue and suggests that some element within the 1.8 kb region is required for *odr-2*-mediated chemotaxis (Figure 5-9).

As shown previously, simultaneous deletion of the 2b and 16 alternative coding regions ($\Delta 2b\Delta 16$) did not affect chemotaxis rescue (Figure 5-9 and Figure 5-10). However, when the 2b deletion was extended to include a total of 4.1 kb (Δ Cla $\Delta 16$), ability to rescue chemotaxis was lost (Figure 5-9).

These experiments identify at least two regions in addition to the alternative coding exons found thus far that are required for *odr-2*-mediated chemotaxis. These regions might contain novel alternative isoforms required for *odr-2* function, or they might represent regulatory regions that are required to direct expression in the proper neurons.

ODR-2 isoforms may be expressed in distinct but overlapping sets of neurons

To begin to analyze the regulation of *odr-2* expression, several kilobases of genomic sequence upstream of the 2b, 16, and 18 isoform alternative start methionines were used to direct expression of the physiological marker green fluorescent protein (GFP). Each of these three constructs generated distinct but overlapping patterns of neuronal GFP expression (Figure 5-11).

No expression in non-neuronal cell types was seen. These results suggest that different neurons may express different complements of ODR-2 isoforms. The expression patterns overlapped with that seen using the rescuing epitope-tagged construct.

However, the individual regions upstream of each alternative start methionine appear to interact with other sequences to direct *odr-2::GFP* expression. A 10.8 kb SphI fragment translational fusion of the common region to GFP drove expression in a large number of neurons (Figure 5-11).

Although the SphI translational fusion contains all sequences used in the isoform 16 and isoform 18 transcriptional fusions, the expression pattern observed included additional neurons not seen in either isoform 16 or 18 GFP expression patterns, and did not include all neurons seen in the isoform 16 and 18 expression patterns. This result suggests that both positive and negative elements present within the SphI fragment, or interactions between the 16 and 18 upstream regions, regulate ODR-2 expression.

Although the significance of these GFP expression patterns is unclear, as relating to isoform- and neuron-specific ODR-2 expression, it is striking that all expression constructs specifically directed expression only in neurons. The finding that different genomic regions upstream of each alternative exon directed expression in different sets of neurons suggests that different ODR-2 isoforms may be expressed in different neurons.

Premature termination of the 2b isoform abolishes ODR-2 expression

ODR-2 isoform 2b is interesting in that a premature stop codon within its alternative coding region abolishes *odr-2*-mediated chemotaxis, whereas deletion of this alternative region does not appear to affect the ability to rescue chemotaxis. To confirm that the *odr-2 (n1939)* mutant phenotype resulted from the isoform 2b nonsense mutation, and not from an unidentified mutation in the common region, the mutation associated with *n1939* was introduced into a rescuing epitope-tagged construct. This nonsense mutation eliminated chemotaxis rescue (Figure 5-12).

Because the epitope tag was inserted in the common region, all ODR-2 isoforms should be visualized. However, whole mount antibody staining showed that the nonsense mutation in the alternative 2b coding region abolished all detectable ODR-2 expression (Figure 5-7).

No neuroanatomical defects are observed in *odr-2* (*n2145*) mutants

The enriched expression of functional epitope-tagged ODR-2 in the axons of neurons suggested it might play a role in axon outgrowth, guidance, or fasciculation. To visualize potential neuroanatomical defects, neuron-specific GFP constructs were each introduced into wild-type and *odr-2* (*n2145*) mutant animals. These constructs visualized the AWC chemosensory neurons (STR-2::GFP) (Dwyer et al., 1998), AIY interneurons (TTX-3::GFP) (Hobert et al., 1997), ASJ chemosensory neurons (*tax-2Δ*::GFP) (Coburn and Bargmann, 1996), PVQ interneurons (SRA-6::GFP) (Troemel et al., 1995), and the set of neurons labeled by ODR-2 (2b)::GFP (this study). In all cases, no obvious defects were observed in process trajectories (data not shown). To attempt to detect more subtle defects, strains expressing GFP in multiple neurons thought to synapse with one another were examined. No difference between wild-type and *odr-2* mutants were noted in strains expressing GFP in both AWC and AIY or in AWC and the ODR-2(2b) set of neurons (data not shown).

One mammalian GPI-anchored protein, Thy-1, has been detected in synaptic vesicles in addition to the plasma membrane (Jeng et al., 1998), suggesting a role for GPI-anchored proteins in synaptic function. To examine this possibility, a VAMP::GFP fusion protein that localizes to synaptic vesicles was expressed under an AWC-specific *str-2* promoter in wild-type and *odr-2* animals. No obvious defects were apparent in *odr-2* mutants (Gage Crump, personal communication).

This set of studies indicates that *odr-2* mutants do not have any obvious morphological defects in a number of neurons, although more subtle defects may have been overlooked.

A family of *odr-2*-related genes in *C. elegans*

The rodent Ly-6 genes exist as a family of related genes. To determine whether *odr-2* might also belong to a multigene family, the sequenced regions of the *C. elegans* genome were analyzed by TBLASTN searches using ODR-2 sequence. Thus far, a total of seven paralogs of *odr-2* have been identified, and Ly-6-like coding regions analogous to the *odr-2* common region for five of them deduced (Figure 5-13). I will refer to these as *hot* genes, for *homology to odr-2*.

Notable features of these genes include conservation of all ten cysteines and the spacing between them, the presence of an asparagine after the tenth cysteine, and a hydrophobic region at the extreme C-terminus, consistent with a GPI-anchorage signal (Figure 5-13, Figure 5-14). These features are strikingly similar to *odr-2* and the Ly-6 family of genes. The *hot* genes and *odr-2* have several conserved intron/exon boundaries, suggesting an evolutionary relationship with a common ancestral gene (Figure 5-13).

Another interesting feature is that most of the paralogs lack in-frame codons for potential start methionines upstream of the Ly-6-like domain, but instead possess consensus splice acceptor sequences. Thus, these genes might be alternatively spliced to yield protein isoforms with alternative amino termini, as in *odr-2*.

Consistent with this hypothesis, upstream exons that are spliced to the Ly-6 domain coding exons have been identified for *hot-1* and *hot-5*. The 5' exon of *hot-1a* was identified by hemi-nested RT-PCR using an SL1 splice leader primer and two primers in the *hot-1* predicted Ly-6-domain region, while the 5' *hot-5a* exon was defined by a *C. elegans* expressed sequence tag (EST yk162) identical to the predicted *hot-5a* sequence. As in *odr-2*, the *hot-1a* and *hot-5a* 5' exons are found far upstream of the Ly-6 domain coding region (6.5 kb and 2.6 kb upstream respectively, data not shown). Both amino termini contain hydrophobic regions that may correspond to signal sequences (Figure 5-14), consistent with GPI-attachment to the plasma membrane. Furthermore, these cDNAs demonstrate that at least two of the *odr-2* paralogs are expressed in *C. elegans*.

The most closely related paralog, *hot-1*, may be expressed in neurons. Sequence upstream of the identified mRNA message directed GFP expression in a set of neurons partially overlapping with the expression pattern observed with *odr-2* (data not shown). Because *hot-1* expression may also undergo complex regulation and alternative splicing, the physiological relevance of the observed expression pattern is unclear. However, it is striking that as with *odr-2*, no non-neuronal expression was observed. Although it has not yet been demonstrated, an intriguing possibility is that each of the *hot* genes may express multiple isoforms in distinct but overlapping sets of neurons.

Discussion

Mutations in *odr-2* result in impaired chemotaxis to volatile attractants sensed by the AWC chemosensory neurons, without affecting responses mediated by AWA. *odr-2* encodes a novel protein with at least three isoforms generated by alternative splicing. Despite the restricted *odr-2* mutant phenotype, *odr-2* isoforms appear to be expressed in a large number of motor, sensory, and interneurons. High expression of *odr-2* has not been detected in AWC. Thus, ODR-2 might act cell non-autonomously to modulate the activity of AWC or other neurons involved in generating AWC-mediated chemotactic behaviors.

odr-2 chemotaxis defects are variable and *odr-2* mutants usually exhibit some residual chemotaxis to AWC-sensed odorants (for example, *odr-1* vs. *odr-2* pyruvate chemotaxis in Chapter 3B; Figure 5-12; and data not shown). These results argue against an essential role for *odr-2* in sensory reception and signal transduction. We suggest that *odr-2* plays a modulatory role in AWC or in downstream interneurons.

Sequence analysis suggests that ODR-2 is an extracellular protein anchored to the plasma membrane by a GPI linkage. Spacing between ten cysteine residues in the ODR-2 common region resemble the spacing in a domain found in the Ly-6 superfamily of proteins, which are also

commonly GPI-linked. ODR-2 might be a distant relative of these proteins or share their structure.

Isoform-dependence of *odr-2* function

Deleting each of the three alternative first coding exons of *odr-2* individually did not affect the ability of *odr-2* to rescue chemotaxis. The physiological relevance of this functional redundancy is unknown. It is possible that deletion of one alternative coding region causes unphysiological expression of a different isoform in the cells that previously expressed only the first isoform. This may explain why deletion of the 2b isoform region did not affect *odr-2*-mediated chemotaxis, while a premature stop codon within the 2b isoform abolishes ODR-2 function.

The finding that a nonsense mutation in the alternative 2b region eliminated expression of all ODR-2 isoforms is harder to explain. Two models, neither particularly satisfactory, are suggested by this result. One possibility is that the ODR-2 (2b) is the primary isoform expressed, so that loss of this isoform in the context of a premature stop codon decreases all expression of the common region to below detectable levels. This model is inconsistent with the variety of isoform cDNAs isolated.

Alternatively, ODR-2 (2b) may be required for expression of the other isoforms, either within the same neuron or by interactions with neighboring neurons. ODR-2 (2b) might be permissive for expression of the other isoforms, or might stabilize the persistence of the other ODR-2 isoform proteins at the cell surface. This model is less consistent with the finding that deletion of the 2b alternative region does not affect chemotaxis rescue, and by the finding that regions upstream of the 16 and 18 coding exons are capable of driving expression in different neurons.

In either of these two models, one possibility is that the 2b deletion allows enhancer elements that normally act to promote isoform 2b expression to drive isoform 16 or 18 transcription. In contrast, the *odr-2* (*n1939*) nonsense mutation would not cause this hypothetical enhancer target switch,

resulting in expression of a truncated isoform 2b transcript. This scenario would also explain the finding that no single deletion of alternative isoform coding regions affected chemotaxis rescue.

It is unclear how the different isoform mRNAs arise, whether from transcriptional initiation from distinct sites upstream of each alternative exon, or as a result of a single long transcript that is subsequently modified by SL1 trans-splicing to the 5' ends of alternative exons. In either case, alternative splicing must occur, as the common region must be spliced to different alternative exons present in the longer transcripts. If a single site serves for transcription initiation for all ODR-2 isoforms, it is interesting to speculate that the *odr-2* (*n1939*) nonsense mutation, which should manifest during translation in the cytoplasm, could affect alternative splicing of the other isoforms, which should occur in the nucleus prior to translation. In a cell-free system, premature termination codons can inhibit RNA splicing by a mechanism independent of protein translation (Aoufouchi et al., 1996). Such a mechanism might resolve the confusing results observed with *odr-2*. Alternatively, the *odr-2* (*n1939*) point mutation may cause aberrant splicing that affects all isoforms, as the G to A transition found in *n1939* creates a potential new splice acceptor, albeit one that poorly matches the consensus acceptor sequence found in *C. elegans*.

Paradox of phenotype specificity vs. widespread expression

One of the most intriguing features of *odr-2* is the specificity of its mutant phenotype in the face of such widespread neuronal expression. Even AWA-mediated chemosensory behaviors are spared in *odr-2* mutants, despite the shared interneurons, including AIY, AIA, and possibly AIZ, downstream of the AWA and AWC chemosensory neurons (White et al., 1986; Bargmann et al., 1993; Cori Bargmann, personal communication).

A possible explanation is that genetic redundancy is provided by the family of *odr-2* paralogs. *odr-2* isoforms can functionally substitute for one another and may be expressed in overlapping sets of neurons. Likewise, the structure of the *hot* genes suggests that they may also possess multiple isoforms, and *hot-1a* may be expressed in a set of neurons partially overlapping with those that

express *odr-2*. In this model, the network of neurons that mediate chemotaxis to AWC-sensed odorants may be serendipitously sensitive to loss of *odr-2* function through lack of redundant paralog expression in the appropriate neurons. Alternatively, the incomplete loss of AWC function in *odr-2* mutants may reflect incomplete redundancy.

This genetic redundancy may extend to vertebrate Ly-6 domain proteins. Expression of the family of murine GPI-linked Ly-6 proteins is tightly regulated in overlapping cell types at specific stages of hematopoiesis and in different tissues (Gumley et al., 1995). Yet, despite the precise regulation of Ly-6A expression during thymocyte development, Ly-6A null knockout mice express normal fractions of all hematopoietic lineages and are only modestly affected in T cell activation (Stanford et al., 1997).

ODR-2, a novel member of the Ly-6 superfamily

Clearly there is not enough structural similarity between *odr-2* and any of the previously identified Ly-6 domain proteins to predict a homologous function. Rather, it is likely that the ten cysteine repeat is an extracellular structural unit that has been adapted to serve many purposes in different organisms and in different tissues. It is even possible that *odr-2* is evolutionarily unrelated to the remainder of the Ly-6 superfamily, and that its structure is a result of convergent evolution of a useful domain. This possibility is unlikely considering the shared GPI anchorage and closest similarity to Sgp-2, isolated from another invertebrate.

Additional evidence that ODR-2 may possess a similar structure to Ly-6 domain proteins is the finding that most of the epitope-tagged ODR-2 constructs were fully functional. The location of the tags were chosen to minimize interference with core structural regions based on the assumption that ODR-2 would fold similarly to the Ly-6 domain proteins CD59 and α cobratoxin. Although the epitope tagged regions are permissive for some alteration, larger insertions drastically curtailed ODR-2 function. When GFP was cloned in-frame into a unique site in each

HA epitope, all five of the resulting constructs rescued poorly or not at all, and none exhibited any detectable GFP fluorescence (data not shown).

Functions of Ly-6 superfamily members

The original mouse Ly-6 proteins were characterized as differentiation antigens on specific lymphocyte subpopulations. Further studies have shown that these and subsequently identified members of the GPI-anchored single Ly-6 domain family are much more widely expressed. Sgp-2 was purified from squid optic and central nervous system tissue (Williams et al., 1988).

Mammalian members have been found expressed in kidney, heart, liver, lung, muscle, testis, ovary, uterus, brain, microglia, osteoblasts, vascular endothelium, and keratinocytes (van de Rijn et al., 1989; Cray et al., 1990; Fleming et al., 1993; HogenEsch et al., 1993; MacNeil et al., 1993; Horowitz et al., 1994; Brakenhoff et al., 1995; Mao et al., 1996; Tanaka et al., 1997). Thus, the physiological roles of these molecules are unlikely to be confined to lymphocyte differentiation and activation.

It may be instructive to consider the functions that have been proposed for Ly-6 domain containing proteins for perspective on the role ODR-2 may play in mediating chemosensory behavior. Many functions have been attributed to Ly-6 proteins, including signal transduction, modulation of extracellular matrix binding, cell adhesion, and interference with postsynaptic ion channels.

Signal transduction by GPI-anchored proteins

Ly-6A/E and CD59, among many other GPI-anchored proteins, have been proposed to act as signal transduction molecules on lymphocytes and other cells. Antibody-mediated cross-linking of these proteins *in vitro* generates intracellular GPI-dependent signaling responses, including increased proliferation, intracellular calcium, inositol phosphate production, and expression of interleukin 2 (Korty et al., 1991; Su et al., 1991; van den Berg et al., 1995). In the case of Ly-6A/E, a

GPI anchor-independent inhibition of interleukin 2 expression has been demonstrated (Codias et al., 1992; Fleming and Malek, 1994).

A puzzling aspect of these studies has been how an extracellular GPI-anchored protein, which does not traverse the plasma membrane, can transduce a signal intracellularly. Recent work has demonstrated that signaling induced by glial cell line-derived neurotrophic factor and neurturin proceeds by a mechanism involving GPI proteins (Durbec et al., 1996; Jing et al., 1996; Treanor et al., 1996; Trupp et al., 1996; Baloh et al., 1997; Buj-Bello et al., 1997; Jing et al., 1997; Klein et al., 1997). These growth factor-like ligands are specifically recognized by distinct GPI-anchored proteins but transduce the signal intracellularly using a shared transmembrane receptor tyrosine kinase. Thus, the GPI-anchored proteins confer differential ligand specificity. The three GPI-anchored receptors identified thus far (GFR α -1-3) are expressed in overlapping but distinct sets of tissues, presumably conferring tissue-specific sensitivity to different ligands (Jing et al., 1997). Similarly, the ciliary neurotrophic factor receptor (CNTFR α) is a GPI-linked ligand specificity factor that shares signal transduction components with many cytokines. However, the ligand-binding components of the other cytokines are not GPI-linked, but transmembrane proteins (Davis et al., 1993; Stahl and Yancopoulos, 1994). Although the GFR α and CNTFR α GPI-anchored receptors are not similar to the Ly-6 proteins, they illustrate an elegant paradigm for GPI-mediated signaling.

Cellular adhesion and interactions with the extracellular matrix

A number of studies now suggest that Ly-6 domain proteins play a role in cell-cell and cell-extracellular matrix adhesive interactions. Three single domain GPI-linked Ly-6 proteins have been implicated in cell-cell adhesion. Transfection of the human keratinocyte gene E48 into fibroblasts induces aggregation, suggesting that E48 can mediate adhesion or activate adhesion pathways (Brakenhoff et al., 1995). Ly-6C monoclonal antibody treatment reduced lymphocyte binding to lymph nodes *in vitro* and decreased lymphocyte homing to lymph nodes *in vivo* (Hanninen et al., 1997). A third study found that thymocytes overexpressing Ly-6A aggregate in

culture. Phosphatidylinositol-specific phospholipase C and anti-Ly-6A antibodies both abolished reaggregation of paraformaldehyde-fixed thymocytes, supporting a direct role for Ly-6A.

Adhesion is not believed to occur by homotypic Ly-6A recognition, because normal T and B cells that do not overexpress Ly-6A co-aggregate with Ly-6A expressing thymocytes (Bamezai and Rock, 1995).

The urokinase-type plasminogen activator receptor (uPAR) contains three tandem Ly-6 domains and is GPI-anchored to the plasma membrane (Behrendt et al., 1991). In addition to its function in localizing and activating fibrinolytic proteases, uPAR can also modulate cellular adhesion to vitronectin and fibronectin, both independently and via interaction with integrins (Kanse et al., 1996; Wei et al., 1996; Plesner et al., 1997).

Other characterized roles of Ly-6 family proteins

Ly-6 family proteins have other characterized functions; in all cases these domains are associated with extracellular protein-protein interactions. CD59 prevents complement-mediated lysis of host tissues and blood cells (Davies and Lachmann, 1993). CD59 prevents final assembly of the membrane attack complex by binding to factor C8 within the nascent C5b-8 complex and interfering with C9 binding, polymerization, and membrane insertion. Alpha cobratoxin, which is secreted, inhibits the nicotinic acetylcholine receptor, a cation channel in the postsynaptic membrane of neuromuscular junctions (Betzel et al., 1991). TGF β type I and type II receptors are transmembrane serine/threonine kinases; the extracellular domain of type I receptors contains Ly-6-like sequences. Growth factor binding to the type II receptor results in recruitment of the type I receptor to the complex. Intracellularly, the type II receptor trans-phosphorylates and thereby activates the type I receptor, which in turn phosphorylates downstream components. In this system, the Ly-6 domain containing protein acts as a co-receptor that functions after initial ligand recognition (Wrana, 1998).

Possible roles for ODR-2

Given the wide variety of functions mediated by Ly-6 domain proteins, it is difficult to know how *odr-2* might function in the *C. elegans* nervous system to mediate chemosensory behaviors.

However, because distinct isoforms of ODR-2 and its paralogs may be expressed by overlapping sets of neurons, these proteins might act as cell surface markers that allow neurons to recognize each other. Distinct but overlapping expression patterns could provide an efficient code for neuronal identity; e.g., 10 isoforms expressed 3 at a time could uniquely identify more than 120 neurons.

In this role, the ODR-2 family of proteins could provide cues for axon guidance or synaptic target selection. *odr-2* family members might act as cellular adhesion molecules important for fasciculation or synaptic maintenance. Another possibility is that cell-cell contact might induce signaling that modulates neuronal function; in such a scenario, ODR-2 could act during signal transduction as a receptor, ligand, or both.

Expression of multiple isoforms of ODR-2 and its paralogs within the same neuron might provide genetic redundancy or increase fidelity of target selection via an increased number of combinatorial cues. Precedent for complementary and combinatorial cues in nervous system development is provided by the study of muscle innervation in *Drosophila*. Netrin A, netrin B, semaphorin II, fasciclin II, and other unidentified factors each contribute cues both independently and in combination to mediate accurate synaptic target selection (Winberg et al., 1998).

Further understanding *odr-2* function demands the identification of interacting proteins, which may be present in the same or different neurons that express *odr-2*. This might be approached biochemically by purification of proteins that bind ODR-2, or genetically by isolating suppresser mutations of the *odr-2* phenotype. Targeted disruption of *odr-2* paralogs would allow analysis of double mutants of *odr-2* and its family members, which may reveal more severe phenotypes currently masked by genetic redundancy. Any phenotypes identified in such a manner would render *odr-2* mutants a potentially sensitized background for identification of interacting genes

that cause similar phenotypes. There is much work to be done to understand the role of *odr-2* in *C. elegans*, which may in turn elucidate the function of the enigmatic Ly-6 superfamily of proteins.

Methods

Strains and genetics

Wild-type worms were *C. elegans* variety Bristol, strain N2. Worms were grown at 20°C with abundant food using standard methods (Brenner, 1974).

Strains used in this work included CX2304 *odr-2*(n2145) V; CX2058 *odr-2*(n1939) V; MT5304 *odr-2*(n2148) V; CX2818 *lin-15*(n765ts) X; and CX2188 *odr-2*(n2145) V; *lin-15*(n765ts) X.

Behavioral assays

All behavioral assays were conducted on well-fed adults. Standard chemotaxis assays were performed as previously described (Bargmann et al., 1993). Assay plates were used 1–3 days after pouring.

In my experience, all alleles of *odr-2* exhibited great variability in chemotaxis towards odorants previously described as being deficient in *odr-2* lines. The source of this variability did not appear to be age of animals assayed, age of assay plates (however, wet plates consistently minimized the *odr-2* chemotaxis defect), preparation of solutions, or source of odorant (data not shown).

Nonetheless, in dose-response assays, *odr-2* animals consistently underperformed wild-type animals when challenged with odorants sensed by AWC. Unfortunately, the threshold of odorant concentrations between normal wild-type response and deficient *odr-2* response typically varied from week to week. Thus, many different odorants and odorant concentrations have been used to follow the *odr-2* phenotype throughout this work. However, in all figures, only assays done

during a similar time period and using identical odorant concentrations are grouped for statistical analysis.

Molecular biology methods

General manipulations were performed using standard methods (Sambrook et al., 1989). Sequencing was performed with the Promega *fmol* sequencing kit in an MJR thermal cycler. The GeneWorks v2.5.1 software package (Intelligenetics) and DNA Strider v1.2 (public domain, by Christian Marck) was used for sequence analysis. BLAST (Altschul et al., 1990) and CLUSTAL-W (Thompson et al., 1994) were both used to generate sequence alignments; however, manual alignment of cysteine residues was frequently done prior to software-assisted alignment. Sequence of the *odr-2* region was confirmed with data courtesy of the *C. elegans* genome sequencing consortium (Sulston et al., 1992).

Generation of transgenic worms

Germline transformation was by standard microinjection methods as previously described (Mello et al., 1991). All injections were done in lines bearing the *lin-15* (*n765ts*) mutation using the transgene construct (50 ng/ μ l) with wild-type *lin-15* DNA pJM23 (50 ng/ μ l) as a co-injection marker. Rescued lines were isolated from independent rescued F1 progeny.

Generation of HA epitope-tagged *odr-2* constructs

PCR-directed insertional mutagenesis was used to insert the HA epitope tag in five different locations of the 1.9 kb KpnI–XhoI genomic fragment that contains the entire *odr-2* common region. Each fragment was inserted in-frame at the sites shown in Figure 5-2 and consisted of: 5'–GCC TAC CCA TAT GAT GTC CCA GAC TAC GCT GGA TCC–3', which codes for the amino acids Ala [Tyr Pro Tyr Asp Val Pro Asp Tyr Ala] Gly Ser; the bracketed residues represent the hemagglutinin HA epitope. Note that the last 6 nucleotides insert a BamHI restriction site. The

five PCR-derived KpnI-XhoI fragments containing the epitope insertions were used to replace the corresponding wild-type region in a rescuing KpnI-SpeI clone in pBluescript® II KS(-).

Oligonucleotide JHC-27, which is 5' to the XhoI site, and JHC-28, which is 3' to the KpnI site, were used for all epitope insertions. A 5' fragment was generated by PCR-amplification using JHC-27 and an "JHC-##b" oligo, while a partially overlapping 3' fragment was generated using JHC-28 and an "JHC-##a" oligo. These two fragments were gel purified and used as template to amplify the complete epitope-tagged KpnI-XhoI fragment using JHC-27 and JHC-28.

5' oligo: JHC-27: 5'-TTT ACG TAT CGA CAA TTG CGC GCA G-3'

3' oligo: JHC-28: 5'-CTA CTT ACT GTT CAG GAA GGT TAT G-3'

HA#1: JHC-29a) 5'-CCA TAT GAT GTC CCA GAC TAC GCT GGA TCC CGT CTA
CCA TGT TAC TCC TG-3'

JHC-29b) 5'-AGC GTA GTC TGG GAC ATC ATA TGG GTA GGC TAG TGC
TGA AAA AAT AAT AT-3'

HA#2: JHC-30a) 5'-CCA TAT GAT GTC CCA GAC TAC GCT GGA TCC TTC GAC
ACT CAT TGC GAT AA-3'

JHC-30b) 5'-AGC GTA GTC TGG GAC ATC ATA TGG GTA GGC AGA AAG
TGG TTT CCG GTA CA-3'

HA#3: JHC-31a) 5'-CCA TAT GAT GTC CCA GAC TAC GCT GGA TCC GAT ATG
TGT GTT ACT CTT AG-3'

JHC-31b) 5'-AGC GTA GTC TGG GAC ATC ATA TGG GTA GGC GGA ACA
GTT CTT TGA GTA GA-3'

HA#4: JHC-32a) 5'-CCA TAT GAT GTC CCA GAC TAC GCT GGA TCC CAG GGA
TGC TTG GGT GAG TT-3'

JHC-32b) 5'-AGC GTA GTC TGG GAC ATC ATA TGG GTA GGC CCT TTC
AGC CAA CGT TCG AA-3'

HA#5: JHC-33a) 5'-CCA TAT GAT GTC CCA GAC TAC GCT GGA TCC AAT TTC
TCC GTG TCG CCG CC-3'
JHC-33b) 5'-AGC GTA GTC TGG GAC ATC ATA TGG GTA GGC GCA CAG
ATT GTT ATG GCA TG-3'

Generation of epitope-tagged *n1939* construct

The *n1939* nonsense mutation was engineered into the rescuing pBlueScript® II KS(-) HA#3 construct. A 2.1 kb SphI–ClaI fragment containing the *n1939* mutation was isolated by PCR from genomic DNA isolated from *odr-2* (*n1939*) mutant animals. From the HA#3 rescuing construct, the 2.3 kb SpeI–SphI (containing *odr-2* genomic sequence) and 11.9 kb ClaI–SpeI fragment (containing 9 kb of *odr-2* genomic sequence and 2.9 kb of vector sequence) were isolated. These three fragments were ligated to yield the 16.3 kb HA#3 epitope-tagged *n1939* mutation clone. The presence of the *n1939* mutation was confirmed by sequence analysis.

Antibody staining

Glass microscope slides were treated with 0.1% w/v polylysine and allowed to air dry overnight. Worms were washed extensively in S Basal and H₂O, transferred to the coated slides, flattened slightly under a glass coverslip, and allowed to settle for 3 minutes at room temperature. Following freeze fracture on a slab of dry ice, the worms were fixed 5' in methanol and 5' in acetone and blocked for 1 hour at room temperature in PBS + 0.1% BSA + 0.2% Tween-20. The samples were then treated with primary anti-HA epitope monoclonal antibodies (BAbCo mouse monoclonal antibody HA.11, clone 16B12) at a 1:500 dilution into blocking solution for 1 hour at room temperature, washed with PBS + 0.2% Tween-20, incubated with secondary antibodies (Jackson ImmunoResearch Laboratories Cy3-conjugated AffiniPure goat anti-mouse IgG) at a 1:500 dilution in blocking solution, washed in PBS + 0.2% Tween-20, and visualized by fluorescence microscopy.

Generation of *odr-2* GFP constructs

Regions immediately upstream of the *odr-2* 2b, 16, and 18 isoforms and *hot-1a* predicted initiator methionines were isolated by PCR for use as transcriptional promoter fusions driving GFP. Cosmid EB2 subclones and genomic DNA isolated from wild-type animals were used as templates for *odr-2* and *hot-1a* promoters respectively. The PCR primers incorporated convenient restriction sites and were designed using sequence provided by the *C. elegans* genome sequencing consortium. GFP vectors were provided by Andy Fire. The *odr-2* 2b promoter (2.6 kb) was isolated as a SpeI fragment and cloned into the XbaI site of TU#62. *odr-2* 16 (3.2 kb), *odr-2* 18 (2.4 kb), and *hot-1a* (4.1 kb) promoters were isolated as PstI–BamHI fragments and cloned into wild-type GFP vector TU#62, except for the isoform 16 promoter, which was cloned into the pPD95.77 enhanced GFP vector. Oligonucleotide sequences are available upon request.

A 10.8 kb *odr-2* SphI fragment was cloned in-frame as a translational fusion into the TU#62 GFP vector modified to contain the synthetic transmembrane domain from pPD34.110 (Fire et al., 1990).

AWC promoter driving *odr-2* cDNA expression

3.7 kb of sequence immediately upstream of the *str-2* start methionine, which drives expression in the AWC chemosensory neurons (Dwyer et al., 1998), was PCR-amplified and cloned upstream of each of the *odr-2* 2b, 16, and 18 cDNAs in the pBlueScript® vector used by the Barstead cDNA library.

Generation of internal deletions of *odr-2*

Internal deletions were made in the KpnI–SpeI and KpnI–SpeI HA#3 *odr-2* rescuing constructs. Clones with multiple deletions were made by introducing individual deletions sequentially. The 2b alternative region was deleted by cutting with PmlI and religating; Δ 2b deletes a total 159 bp, including both in-frame methionines that could serve to initiate translation.

The 16 alternative region was ablated by cutting with AvrII and AflII, blunting the ends with Klenow polymerase, and religation; $\Delta 16$ deletes 652 bp, including the entire alternative amino terminal coding region, from 46 bp before the predicted initiation methionine and extending 529 bp into the following intron.

The 18 alternative region was deleted in the KpnI–SpeI HA#3 construct. First, the EagI site in the pBluescript® II KS(-) polylinker was destroyed by cutting with SpeI and NotI, blunting with Klenow polymerase, and religating. The 18 alternative region was then deleted by cutting with EagI and religating; $\Delta 18$ deletes 1553 bp, from 2 bp after the predicted initiator methionine and extending 1494 bp into the following intron.

The Δ BstEII construct was made by cutting with BstEII, blunting with Klenow polymerase, and religating; Δ BstEII deletes 2.6 kb, including the entire isoform 18 alternative exon. Δ ClaI was made by cutting with ClaI and religating; Δ ClaI deletes 4.1 kb, including both isoform 2b alternative exons.

Acknowledgments

I would like to thank Kate Wesseling, Penny Mapa, Liqin Tong, Shannon Grantner, and Yongmei Zhang for expert sequencing assistance; Tim Yu for generating the GFP confocal images; Alan Coulson and John Sulston for supplying cosmids; Y. Kohara for providing EST sequence; Bob Barstead for the cDNA library; Gary Ruvkun for *ttx-3::GFP*; Piali Sengupta for initiating the work; and the *C. elegans* genome sequencing project for providing an invaluable resource to the research community.

Table 5-1. Cysteine spacing in the Ly-6 superfamily.

Ly-6 domain protein	Number of residues between cysteines								
	1-2	2-3	3-4	4-5	5-6	6-7	7-8	8-9	9-10
Single-domain proteins									
CD59	2	6	5	6	12	5	17	0	4
vCD59	2	6	5	6	12	5	17	0	4
Ly-6A.2 / E.1 / Sca-1 / TAP	2	8	4	6	20	3	19	0	4
Ly-6C.2	2	8	4	6	20	3	16	0	4
Ly-6F.1	2	8	4	6	20	3	19	0	4
Ly-6G.1	2	8	4	6	20	3	19	0	4
Ly6-A (rat)	2	8	5	6	20	3	19	0	4
Ly6-B (rat)	2	8	5	6	20	3	19	0	4
Ly6-C (rat)	2	8	4	6	20	3	19	0	4
ThB	2	5	5	6	17	3	18	0	4
Sca-2 / TSA-1	2	8	5	6	21	3	17	0	4
Sgp-2	2	7	13	6	20	13	13	1	4
E48	2	5	5	6	17	3	18	0	4
RIG-E	2	8	5	6	22	3	16	0	4
DRTP-1	2	4	6	6	16	5	12	0	4
SP-10	2	8	6	7	17	3	15	0	5
alpha cobratoxin	NA	NA	NA	5	20	3	10	0	4
TGFβ-R, type I	1	2	6	5	16	14	13	0	4
DAF-1	1	5	25	5	14	19	13	0	5
Multi-domain proteins									
uPAR #1	2	5	4	6	20	NA	NA	NA	4
uPAR #2	2	6	9	6	24	5	16	0	4
uPAR #3	2	7	9	6	18	5	17	0	4
RoBo-1 #1	4	4	7	5	22	4	20	0	4
RoBo-1 #2	2	6	6	6	19	5	16	NA	NA
PLA2-I 25kD #1	2	6	6	6	20	5	20	0	4
PLA2-I 25kD #2	2	7	6	6	19	5	19	NA	NA
PLA2-I 31kD #1	2	6	6	6	20	5	20	0	4
PLA2-I 31kD #2	NA	NA	NA	6	21	3	21	NA	NA
Range	1-4	2-8	4-25	5-7	12-24	3-19	10-21	0-1	4-5
Median	2	6.5	5	6	20	3	17	0	4
ODR-2	2	25	14	3	20	20	25	1	4
HOT-1	2	25	14	3	20	24	23	1	4
HOT-2	2	25	13	3	21	24	25	1	4
HOT-3	2	26	13	3	22	22	21	1	4
HOT-4	ND	25	11	3	19	25	21	1	4
HOT-5	2	27	14	3	24	23	20	1	4

The 10 cysteines of Ly-6 domains form disulfide bridges as follow: 1–5, 2–3, 4–6, 7–8, 9–10. uPAR domain #1 lacks cysteines 7 and 8, RoBo-1 domain #2 lacks 9 and 10, PLA₂-I 25 kD domain #2 lacks 9 and 10, and PLA₂-I 31 kD domain #2 lacks 2 and 3 as well as 9 and 10. Snake venom long neurotoxins are unique in that they lack cysteines 2 and 3 and have an additional disulfide-linked cysteine pair between cysteines 5 and 6 that are not found in the rest of the Ly-6 domain superfamily (Ploug and Ellis, 1994). Missing cysteine pairs result in some spacings being not applicable (NA). The complete sequence is not known for HOT-4, so the spacing between its first two cysteines is not determined (ND).

Genes and their accession numbers. Human CD59 (JL0109) (Davies and Lachmann, 1993) and CD59 homolog from saimirine herpesvirus 1 (A43384) (Albrecht et al., 1992). Mouse Ly-6A.2 (M73552), Ly-6C.2 (M18466), Ly-6F.1 (X70922), and Ly-6G.1 (X70920) (LeClair et al., 1986; Palfree et al., 1988; Stanford et al., 1992; Fleming et al., 1993). Rat Ly6-A (M30692), Ly6-B (M30689), Ly6-C (M30691) (Friedman et al., 1990). Mouse thymocyte B cell antigen ThB (A46528) (Gumley et al., 1992). Mouse Sca-2 (U04268) (Classon and Coverdale, 1994). Human E48 antigen (X82693) (Brakenhoff et al., 1995). Human retinoic acid-induced RIG-E protein (U42376) (Mao et al., 1996). Differentially regulated trout protein 1, DRTP-1 (AF004739) (Lee and Goetz, 1998). Human intra-acrosomal sperm antigen SP-10 (M82967) (Wright et al., 1990). Mouse transforming growth factor-beta type I receptor precursor (543338) (Suzuki et al., 1994). *C. elegans* DAF-1 receptor protein kinase (118230) (Georgi et al., 1990). Human urokinase plasminogen activator receptor (uPAR) (X51675) (Roldan et al., 1990). Rat bone and growth plate cartilage-expressed protein RoBo-1 (AF041083) (Noel et al., 1998). The following were manually entered from the listed sources: Sgp-2 (Williams et al., 1988), cobra phospholipase A₂ inhibitor 31 and 25 kD subunits (Ohkura et al., 1994), and the long α -neurotoxin α -cobratoxin (Betz et al., 1991). The identification of *odr-2* and its paralogs are presented in the text.

Rescue of the *odr-2* benzaldehyde chemotaxis defect

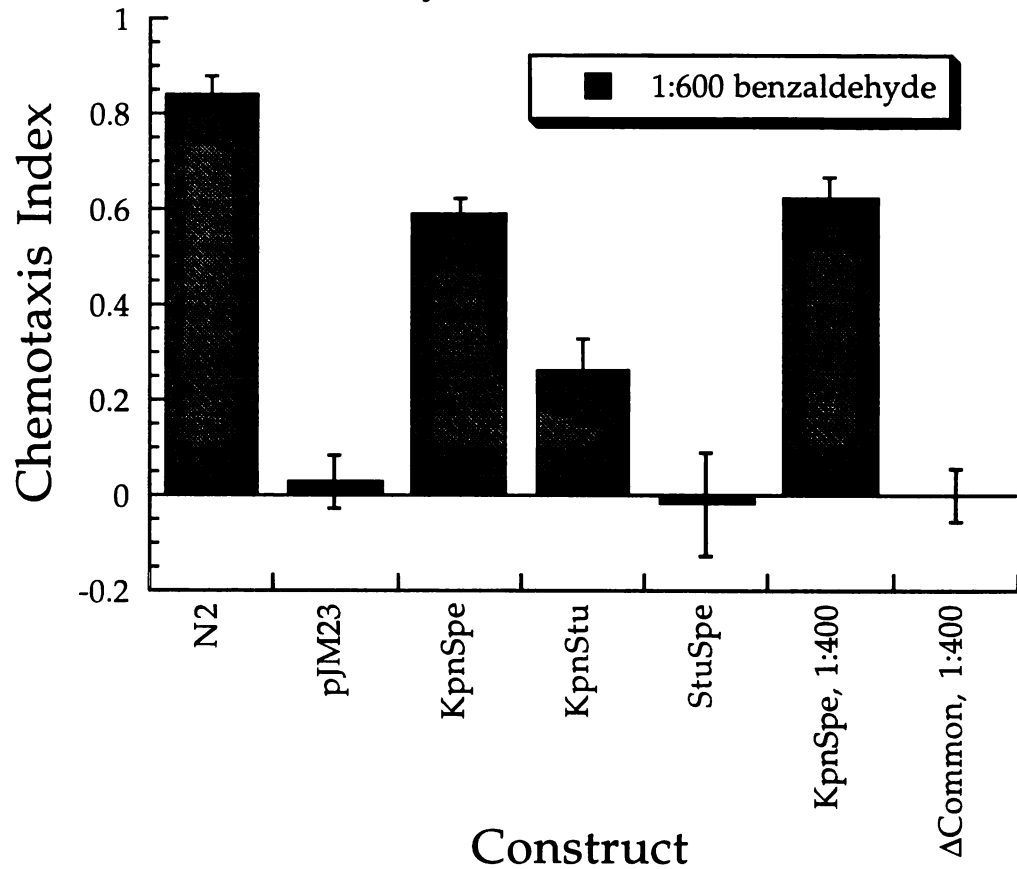


Figure 5-1. Rescue of the *odr-2* benzaldehyde chemotaxis defect. Genomic subclones from the *odr-2* region were introduced into *odr-2* (*n2145*) animals and tested for ability to rescue benzaldehyde chemotaxis. Co-injection marker alone was used as a negative control (pJM23). All assays were done using a 1:600 dilution of benzaldehyde, except the last two columns (1:400 dilution). KpnSpe represents a rescuing 13.4 kb construct. A *StuI* site within the KpnSpe fragment was used to generate the 7 kb KpnStu and 6 kb StuSpe fragments. ΔCommon represents a 1.9 kb truncation of KpnSpe which removes the common region of *odr-2*.

Figure 5-2. Exon sequence of the *odr-2* isoforms. The cDNAs encoding alternative isoforms were sequenced. Lowercase and uppercase nucleotides represent non-coding and coding regions respectively. Vertical lines in the sequence represent the positions of introns. G to A transitions found in *n1939*, *n2148*, and *n2145* are boxed. Filled arrowheads pointing downwards indicate sites where trans-splicing to SL1 leader RNA has been observed. Potential translation initiation methionines are in bold. Upward pointing hollow arrowheads indicate possible signal sequence cleavage sites (von Heijne, 1986); however the signal sequences predicted for the alternative 16 and 18 regions are quite poor matches to the consensus. (A) Sequence of the 2b alternative exons. The G to A transition found in *n1939* is boxed; this results in a premature stop codon. The area deleted in the $\Delta 2b$ construct is indicated; note that both potential start methionines are deleted as well as an intron in the 5' untranslated region. (B) Sequence of the 16 alternative exon. The $\Delta 16$ construct deletes all coding region of the alternative 16 exon downstream of the indicated site. (C) Sequence of the 18 alternative exon. The $\Delta 18$ construct deletes all coding region of the alternative 18 exon downstream of the indicated site. (D) Sequence of the common region found in all *odr-2* cDNAs. Cysteine residues are circled. In Sgp-2, the glycosylphosphatidylinositol attachment occurs on the conserved asparagine immediately following the tenth cysteine, as indicated. Thus, the eleventh cysteine of the common region may not be present in the mature forms of ODR-2. The locations of the five hemagglutinin (HA) epitope tag insertions are indicated.

Figure 5-3

odr-2 Genomic organization and Summary of chemotaxis rescue

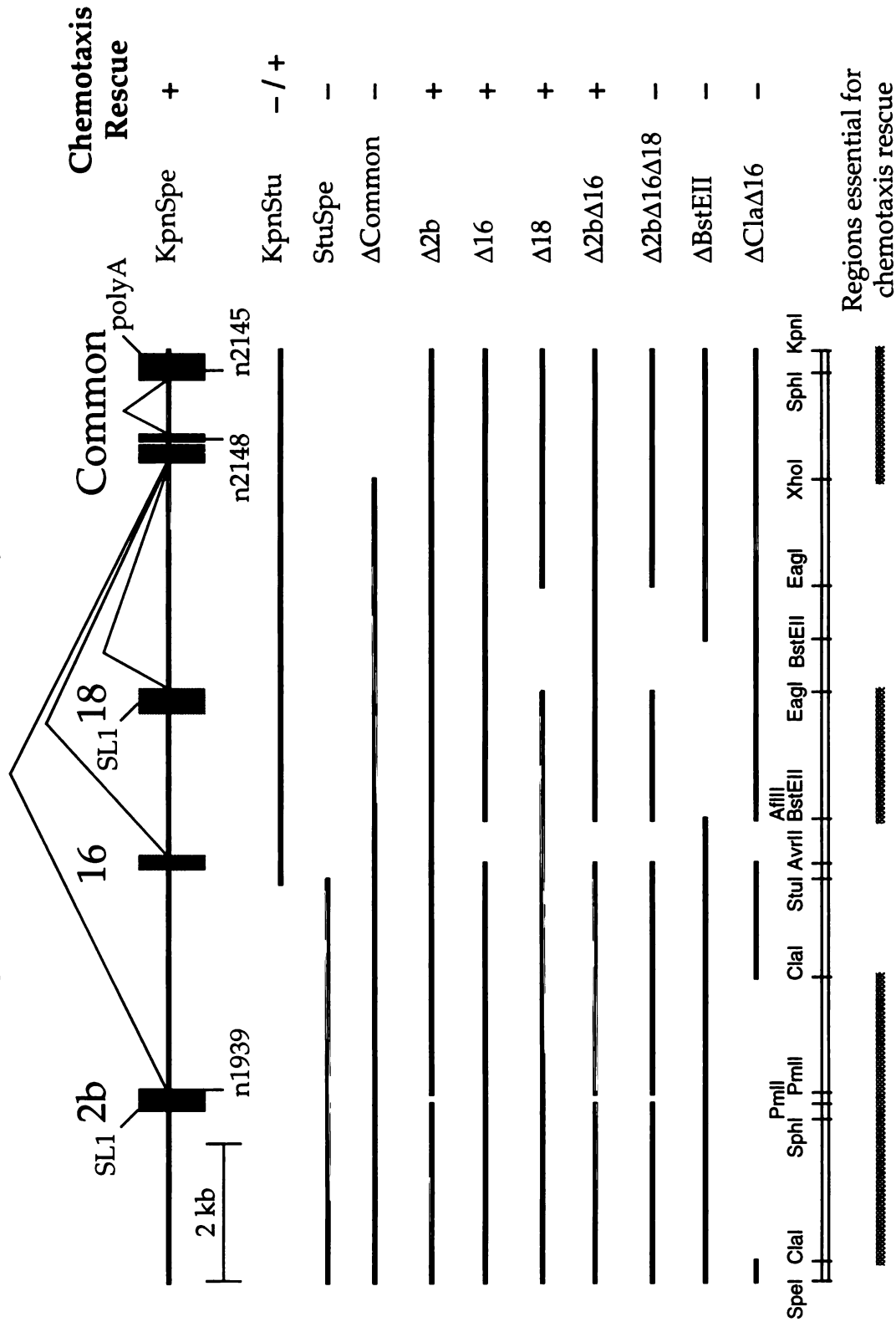


Figure 5-3. Genomic organization of *odr-2* and summary of chemotaxis experiments. The full-length horizontal line represents the rescuing 13.4 kb KpnI to SpeI genomic fragment (KpnSpe). Exons are represented by solid rectangles, and alternative splicing to the common exons is shown. The location of mutations found in the 3 alleles of *odr-2* are noted. The broken and shortened horizontal lines below the full-length KpnSpe fragment represent various genomic subclones and internal deletions used in this study: the gaps in the line represent regions deleted in a particular construct. Many of these deletions disrupt the common region (Δ Common) or particular alternative isoforms (Δ 2b, Δ 16, and Δ 18), while others represent larger deletions (Δ BstEII and Δ Cla). The results of these deletions on the ability to rescue the *odr-2* (*n2145*) chemotaxis defect are summarized on the right. Near the bottom, the locations of restriction sites used for generating the constructs are shown. At the bottom of the figure, regions deduced to be required for chemotaxis rescue, based on the Δ Common, Δ BstEII, and Δ Cla Δ 16 results, are represented by thick gray lines.

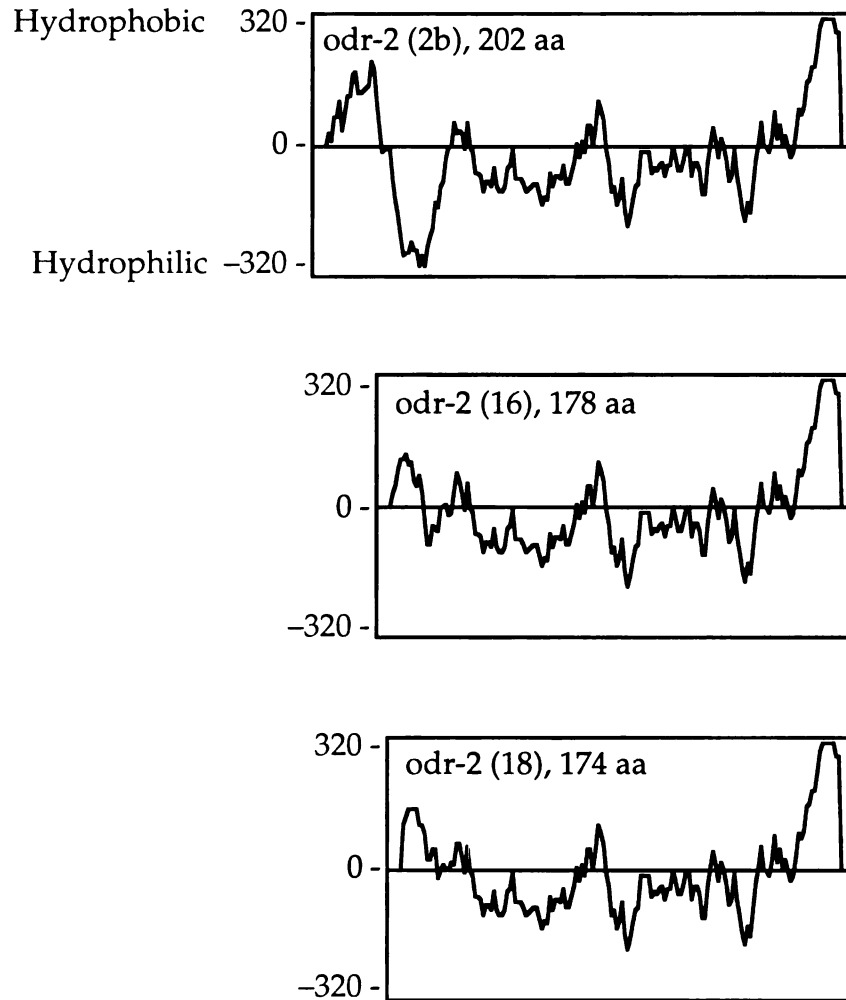


Figure 5-4. Hydrophobicity plots of the ODR-2 isoforms. Analysis was by the method of Kyte-Doolittle, such that positive and negative deflections reflect hydrophobic and hydrophilic character respectively (Kyte and Doolittle, 1982). Plots for the three isoforms of ODR-2 are derived from the predicted full-length precursor protein sequence from isolated cDNAs.

Structure of CD59 and analogous locations of ODR-2 epitope tag insertions

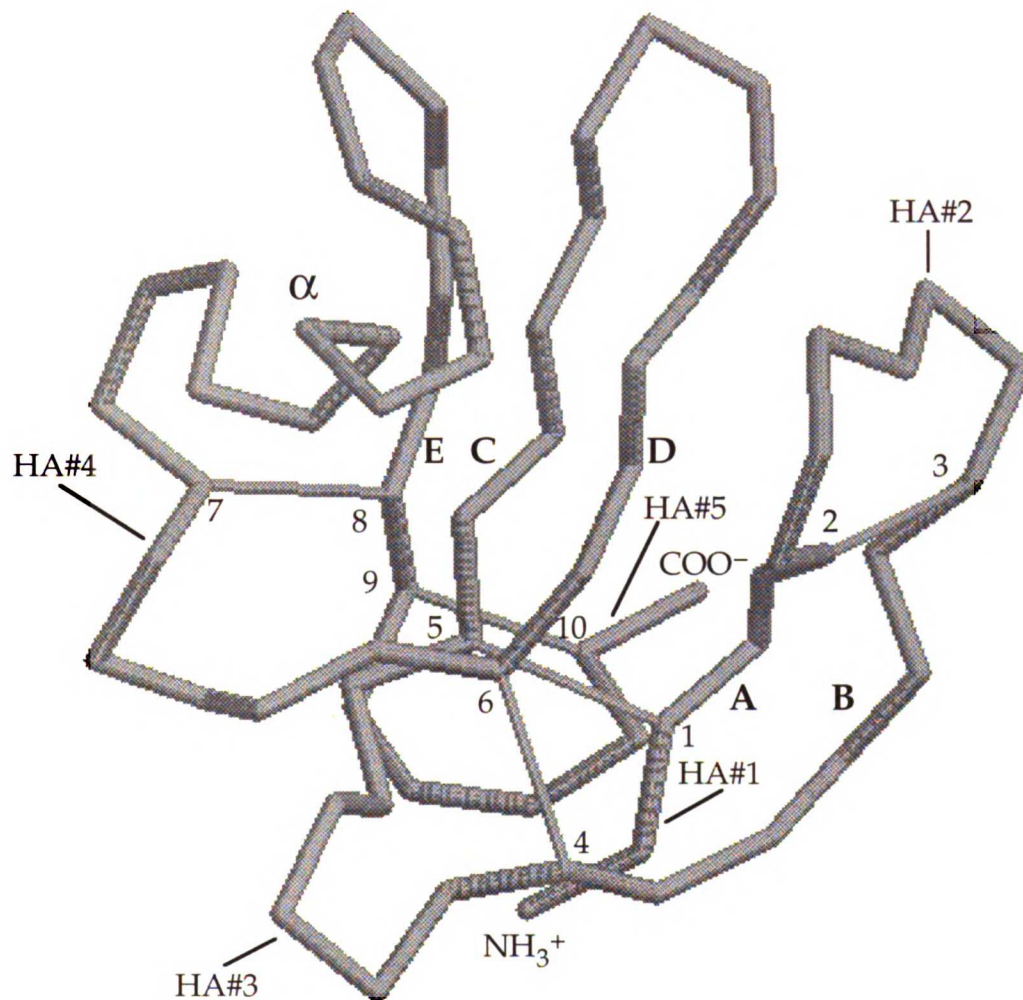


Figure 5-5. The solution structure of soluble CD59 (Kieffer et al., 1994). The α carbon backbone and disulfide bridges formed by the 10 cysteines, which are numbered consecutively, are shown. Strands A–B and strands C–D–E form two antiparallel beta-sheets. The short α helical segment that packs against one face of the C–D–E sheet is labeled. The predicted analogous regions of ODR-2 hemagglutinin epitope tag insertions are indicated. Coordinates of CD59 were obtained from the Brookhaven Protein Data Bank, accession 1ERH. The structure was displayed using

Epitope-tagged ODR-2 rescues isoamyl alcohol chemotaxis

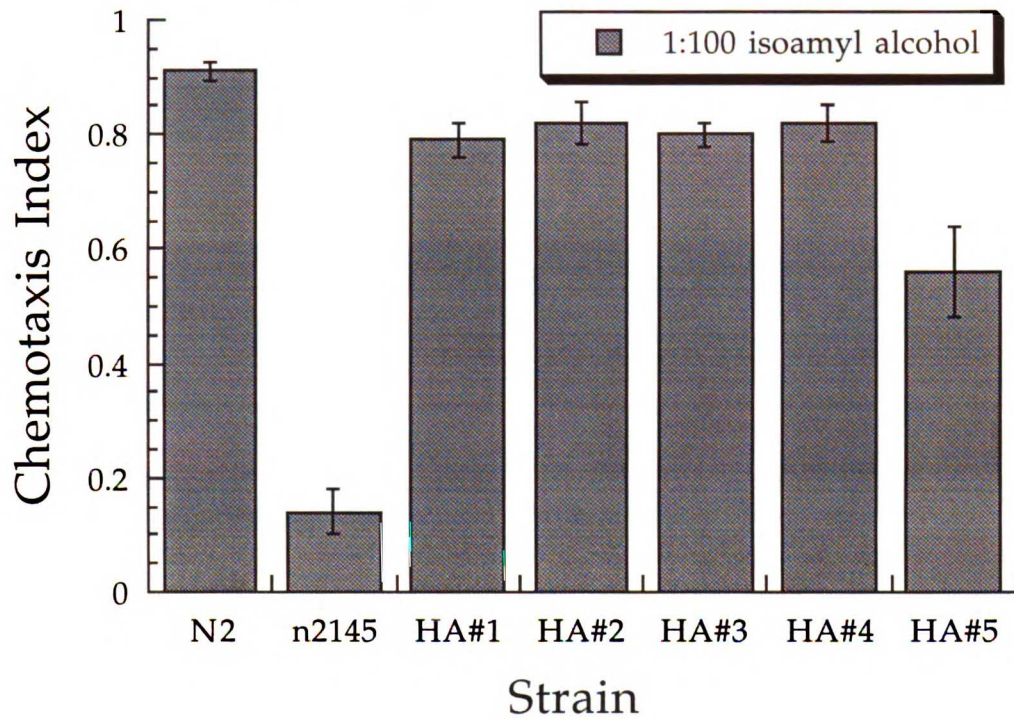


Figure 5-6. Epitope-tagged ODR-2 rescues the isoamyl alcohol chemotaxis defect. The hemagglutinin (HA) epitope tag was introduced into the *odr-2* KpnSpe rescuing construct at five different locations in the common region. Each of these constructs was tested for rescue of the *odr-2* (*n2145*) isoamyl alcohol chemotaxis defect. Based on the known structure of CD59 and assuming a similar conformation for ODR-2, HA epitope insertions were made at: HA#1, before the first cysteine; HA#2, AB loop; HA#3, BC loop; HA#4, DE loop; HA#5, after the tenth cysteine.

Figure 5-7.

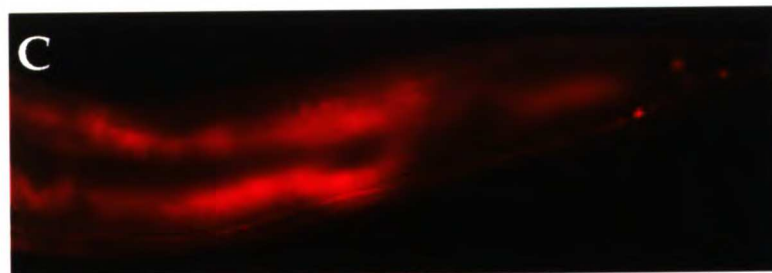
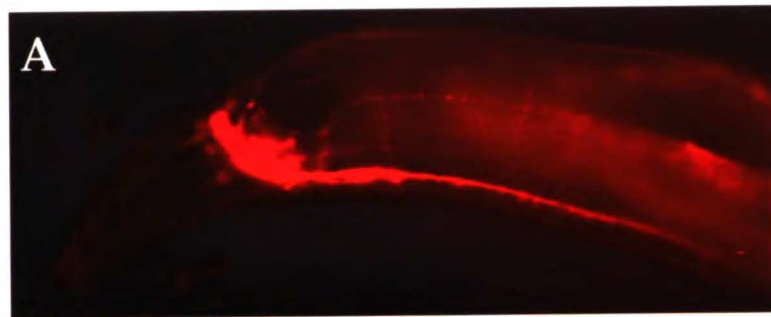


Figure 5-7. Expression of epitope-tagged ODR-2. The hemagglutinin epitope was introduced into the common region of ODR-2 and visualized by whole mount antibody staining of adult animals. Anterior is to the left and dorsal is up. (A), (B), and (C). Expression of a rescuing *odr-2* construct HA#3 in the head, mid-body, and tail regions respectively. (D) The *odr-2* (*n1939*) isoform 2b nonsense mutation abolishes HA#3 expression.

ODR-2 expressed in AWC does not rescue isoamyl alcohol chemotaxis

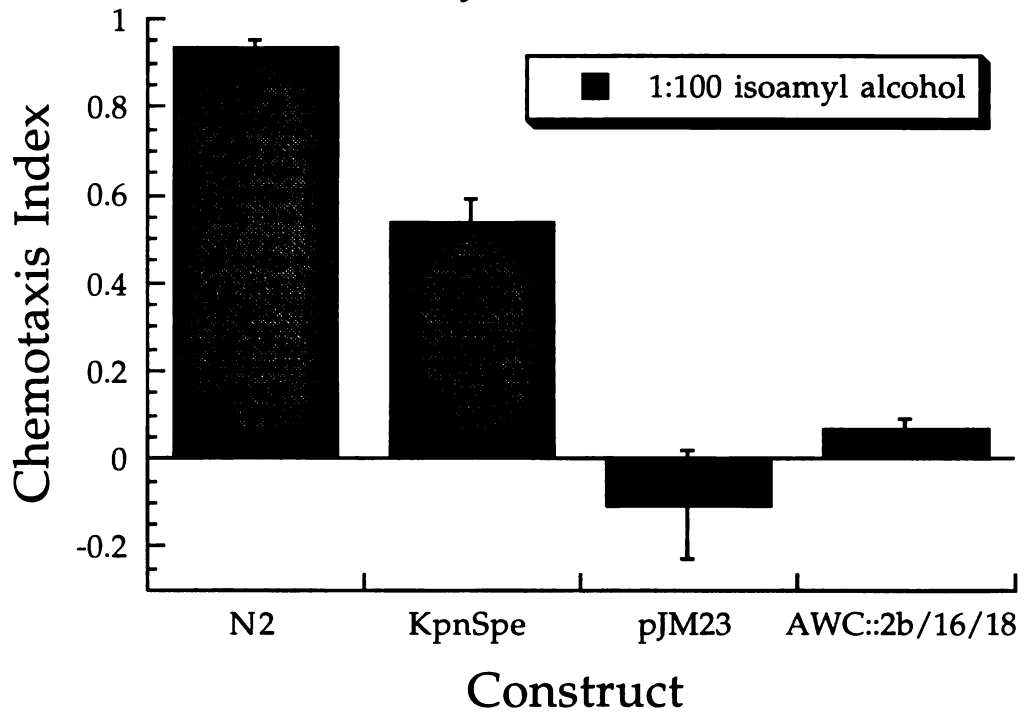


Figure 5-8. ODR-2 expressed in AWC does not rescue isoamyl alcohol chemotaxis. *odr-2* genomic and cDNA constructs were tested for ability to rescue chemotaxis to 1:100 isoamyl alcohol. Three constructs in which an AWC-specific promoter was used to drive *odr-2* 2b, 16, and 18 cDNA expression were pooled and injected into *odr-2* (*n2145*) animals. KpnSpe represents a rescuing 13.4 kb construct. Co-injection marker alone was used as a negative control (pJM23).

Coding and regulatory regions required for *odr-2* rescue

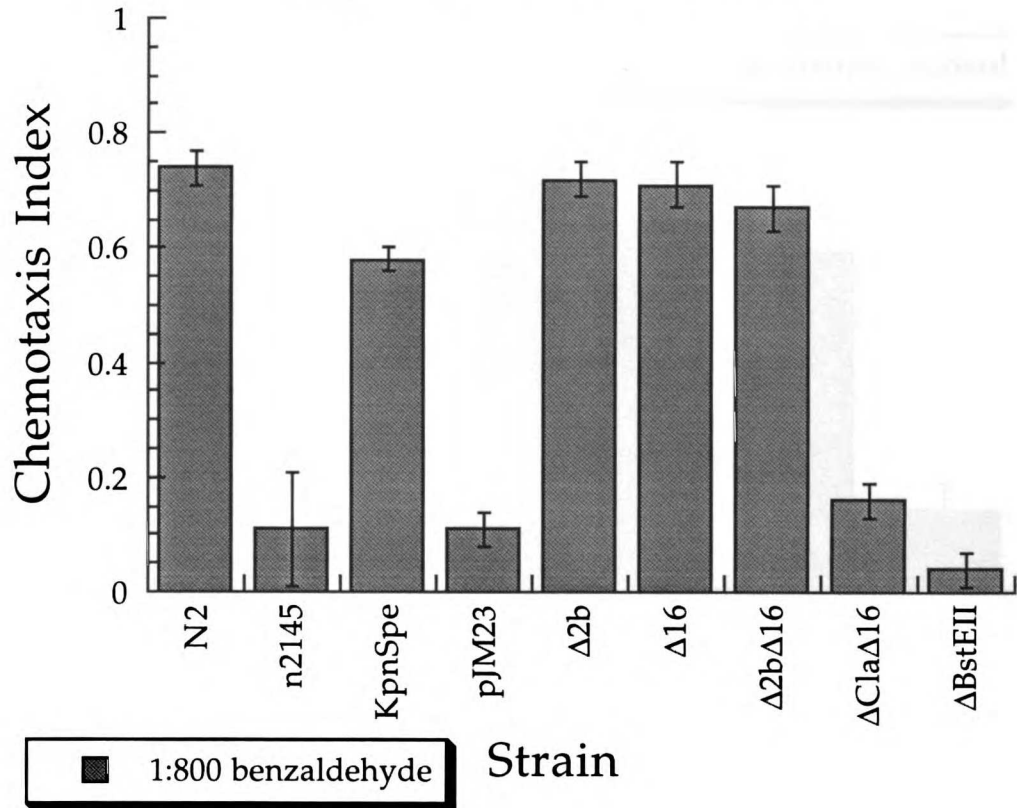


Figure 5-9. Coding and regulatory regions required for *odr-2* rescue. Deletions were made in the rescuing KpnSpe fragment that destroyed specific isoform coding regions or extended deletions previously shown not to affect *odr-2* chemotaxis rescue. These constructs were introduced into *odr-2* (*n2145*) animals and tested for chemotaxis to 1:800 benzaldehyde. N2 and *n2145* are non-transgenic strains. Co-injection marker alone was used as an additional negative control (pJM23).

ODR-2 isoforms can functionally substitute for one another

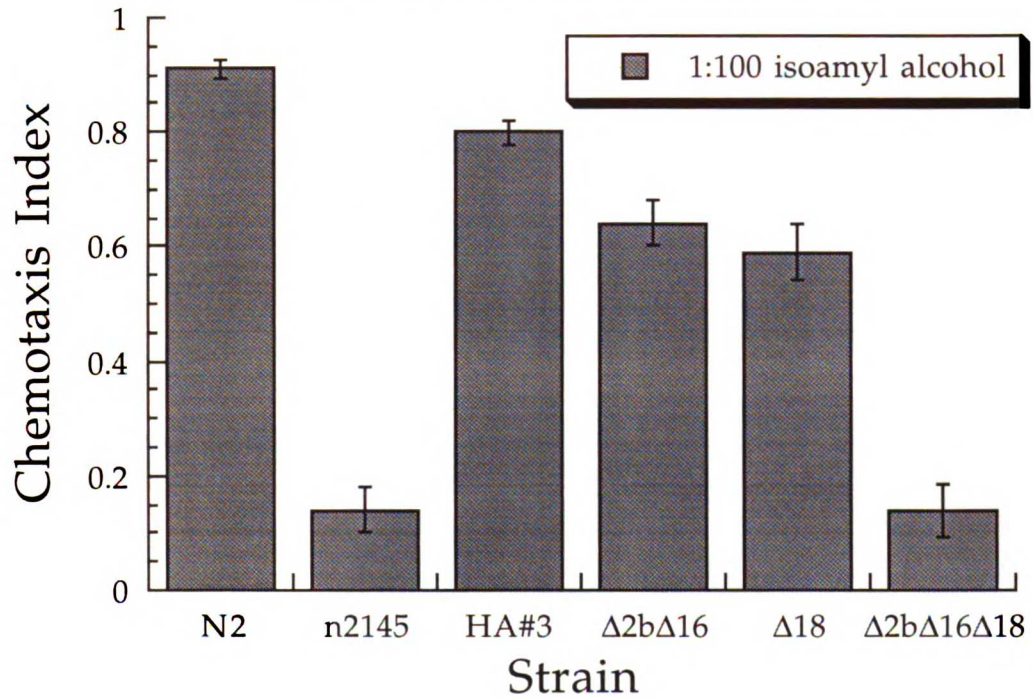
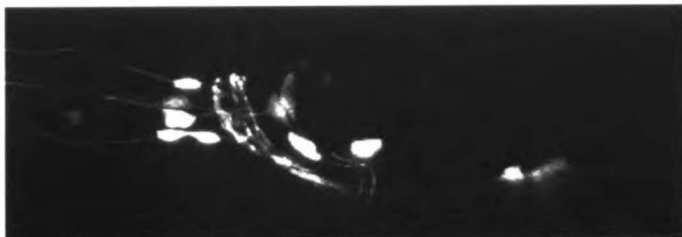
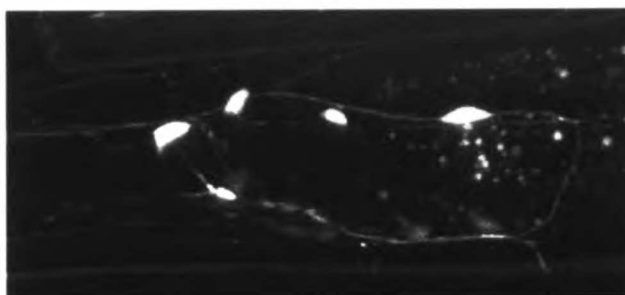


Figure 5-10. ODR-2 isoforms can functionally substitute for one another. Internal deletions that destroyed the alternative coding regions of *odr-2* were made in the rescuing epitope-tagged construct, HA#3. The deletion constructs ablated: isoform 2b and 16 coding regions simultaneously ($\Delta 2b\Delta 16$); the 18 coding region individually ($\Delta 18$); all three alternative isoform coding regions simultaneously ($\Delta 2b\Delta 16\Delta 18$). Each of these clones was tested for rescue of the *odr-2* (*n2145*) isoamyl alcohol chemotaxis defect.

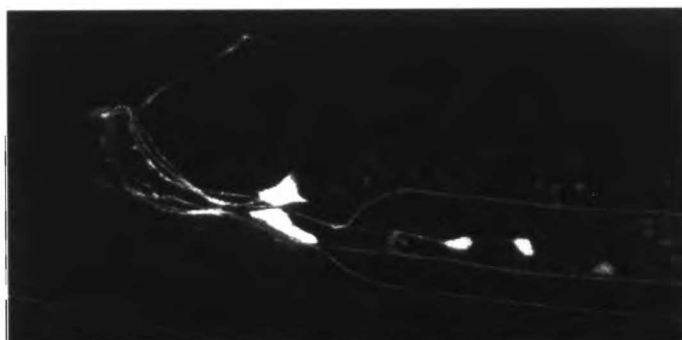
A. *odr-2* (2b)



B. *odr-2* (16)



C. *odr-2* (18)



D. *odr-2* (Sph)



E. *hot-1a*

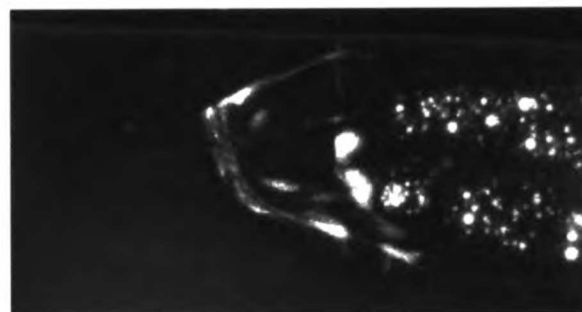


Figure 5-11. Expression of *odr-2* and *hot-1a* GFP fusion constructs. GFP expression in the head region of adult animals were collected as confocal planes and projected onto the images shown; anterior is to the left and dorsal is up. Non-head region neuronal GFP expression was also observed (data not shown). (A), (B), (C), and (E) represent GFP transcriptional fusions driven by sequence upstream of the predicted translation start sites of *odr-2* (2b), *odr-2* (16), *odr-2* (18), and *hot-1a* respectively. (D) *odr-2* (*Sph*) translational GFP expression, driven by regions upstream of isoforms 16 and 18.

The n1939 mutation abolishes *odr-2* function

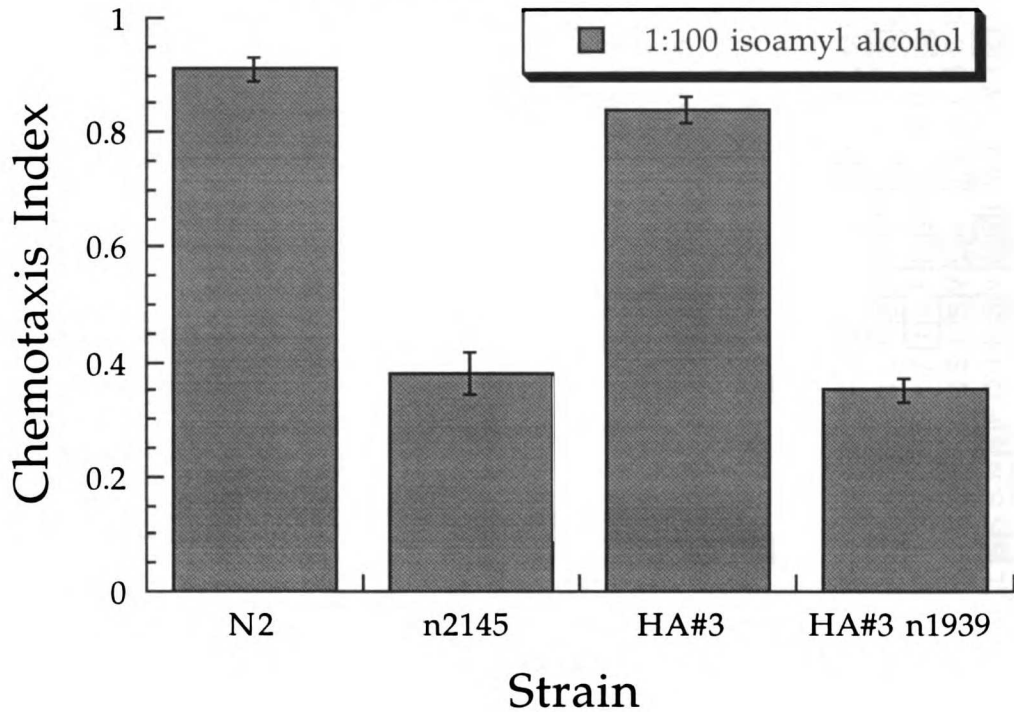


Figure 5-12. The n1939 mutation is sufficient to abolish *odr-2* function. The nonsense mutation in the isoform 2b alternative coding region was introduced into the rescuing epitope-tagged *odr-2* construct, HA#3, and the resulting construct tested for ability to rescue *odr-2* (n2145) chemotaxis to 1:100 isoamyl alcohol.

Figure 5-13

odr-2	1	...	LRLP	CYSCMS	PY	LE	DHYP	YIS	HL	YR	...	KP	LS	FD	TH	CD	KH	37																													
hot-1	1	...	HTAR	CYSCMS	KL	YE	AV	WP	SL	HI	YK	...	RP	NF	TD	CD	DE	37																													
hot-2	1	AGAP	IPRQV	ECYSCMS	LS	YQ	TS	WK	YL	QT	TY	...	YP	KV	FT	DR	CR	DP	43																												
hot-3	1	RF	SCMS	QM	YE	GF	MS	NG	LD	RF	...	RP	NF	SS	QC	DG	35																												
hot-4	1	CA	SA	SV	YL	PL	WS	QL	MH	HY	...	PP	KN	FT	DR	CW	QP	30																											
hot-5	1	CF	SCAS	FE	YR	VL	FD	KD	TS	LS	...	RP	KF	FD	RL	CD	LE	35																											
odr-2	38	S	L	E	T	S	Y	L	Y	S	K	N	C	S	D	M	C	V	T	L	R	I	N	D	V	V	G	G	R	R	R	H	G	...	Y	M	R	G	C	L	S	D	L	78			
hot-1	38	R	I	A	E	G	R	V	P	I	V	H	C	P	T	I	C	V	S	L	F	E	Q	P	N	I	A	G	V	R	I	K	G	...	Y	T	R	G	C	M	S	D	V	78			
hot-2	44	-	N	S	E	R	G	M	P	T	V	M	C	G	S	V	C	V	S	L	M	E	P	D	V	E	A	G	V	F	I	G	F	K	...	H	I	R	G	C	L	D	R	V	84		
hot-3	36	-	M	D	V	T	N	M	H	T	V	P	C	R	T	I	C	L	T	I	Q	Q	N	L	V	M	G	Q	P	T	G	H	R	...	L	Y	M	R	G	C	A	L	T	I	77		
hot-4	31	-	-	-	-	D	S	G	I	G	L	V	P	C	S	A	C	F	T	L	V	E	R	I	D	D	V	S	E	Q	H	G	V	...	-	I	R	G	C	M	D	R	L	67			
hot-5	36	E	M	V	R	G	Y	A	P	V	E	A	C	H	S	T	C	V	T	I	F	E	P	Q	Y	F	G	G	L	Q	S	L	Q	R	P	F	L	Y	I	R	G	C	A	D	H	I	80
odr-2	79	-	H	G	Y	N	H	S	L	I	R	...	T	L	A	E	R	Q	G	C	L	D	T	T	A	R	E	L	F	L	P	T	A	Q	R	Q	E	L	E	P	S	R	-	117			
hot-1	79	L	I	S	G	F	N	Q	T	I	V	T	W	Y	-	R	W	M	H	R	D	S	C	R	P	Y	R	K	K	E	L	F	K	L	G	-	-	E	S	A	D	D	S	T	-	119	
hot-2	85	L	R	H	G	F	N	Q	S	A	L	R	T	H	-	R	F	H	Q	N	H	C	R	T	L	S	R	S	A	L	F	N	P	A	R	-	-	Q	T	D	P	P	A	L	G	126	
hot-3	78	A	R	R	G	L	N	N	H	T	L	S	-	-	M	F	D	R	Y	D	I	C	R	D	M	S	A	S	D	L	F	S	H	-	-	-	-	E	H	A	D	S	Q	R	-	114	
hot-4	68	L	L	F	G	L	D	D	D	V	R	N	I	L	S	A	Y	E	N	Q	R	V	C	R	H	T	D	R	K	L	L	R	L	F	-	-	-	-	P	L	S	G	Q	T	D	-	107
hot-5	81	F	S	S	M	K	D	R	P	I	E	V	E	-	-	F	L	H	R	S	P	I	C	V	K	L	Q	L	S	Q	I	Y	P	Q	-	-	-	-	V	Q	A	N	E	I	-	117	
odr-2	118	-	L	S	L	C	A	C	H	N	N	L	C	N	F	-	-	-	-	-	-	-	S	-	V	S	P	P	C	F	F	I	F	L	F	V	I	L	V	I	F	L	M	R	L	-	152
hot-1	120	-	I	D	V	C	T	C	Y	A	D	H	C	N	G	-	-	-	-	-	-	N	S	A	S	S	I	S	I	V	S	A	L	L	V	L	L	V	I	A	Y	F	L	-	-	153	
hot-2	127	D	V	Q	L	C	S	C	Y	G	D	R	C	N	S	-	-	-	-	-	-	T	I	M	T	S	S	I	F	I	V	F	L	L	V	F	L	H	R	L	L	Y	-	-	162		
hot-3	115	-	I	R	V	C	S	C	L	G	D	R	C	N	S	-	-	-	-	-	-	A	I	S	T	S	N	C	Q	S	L	S	V	L	A	L	V	A	L	S	S	L	L	F	151		
hot-4	108	-	V	T	F	C	S	C	N	G	D	F	C	N	E	H	D	M	L	R	E	L	S	S	N	S	F	Q	I	H	S	V	L	L	V	A	T	W	I	L	L	F	150				
hot-5	118	-	V	Q	V	C	S	C	D	K	D	G	C	N	F	D	S	I	N	-	-	D	S	T	S	K	Y	N	S	I	F	I	V	S	A	F	L	F	G	F	Y	F	V	F	158		

Figure 5-13. Sequence alignment of the ODR-2 family of proteins. The ten conserved cysteines are numbered. Locations of introns are noted by vertical lines. Residues identical in half or more of the family members are boxed and shaded. For *hot-1/2/4/5* there are no potential in-frame start methionines upstream of the listed coding regions, and probable upstream splice acceptor sites are noted. With *hot-2*, it is unclear which of the two possible splice sites upstream of the Ly-6 domain is used, so both are marked. Amino terminal sequence of HOT-1A (MLLVDDHIIR NRRKIPDTPK RSYSNPYDTF VKLLIVVALA PKGVEASGER IYDETNYQGG NLPYK) and HOT-5A (MRQLPSILLI LVYFIRSVEL LK) has been determined from identified cDNAs.

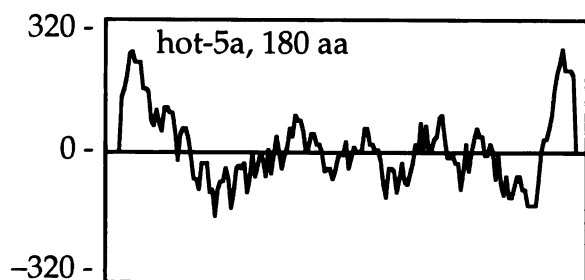
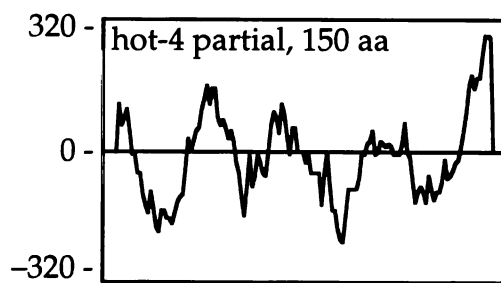
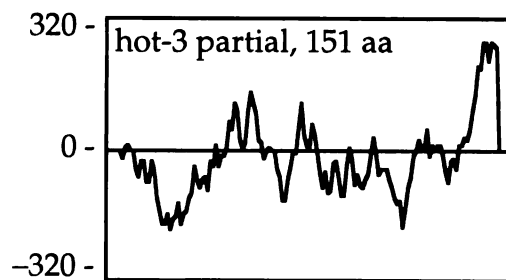
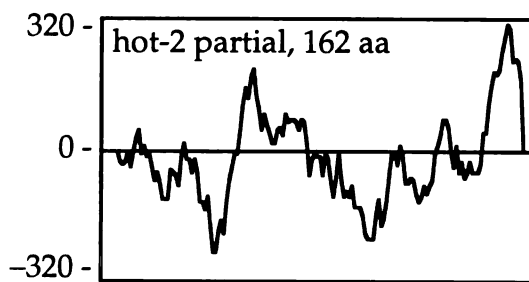
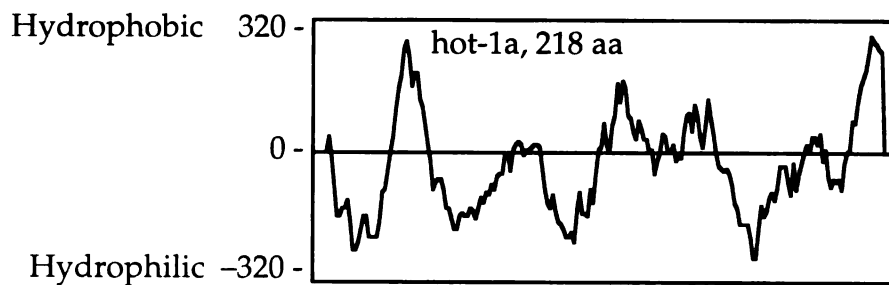


Figure 5-14. Hydrophobicity plots of the *odr-2* paralogs in *C. elegans*. Analysis was by the method of Kyte-Doolittle, such that positive and negative deflections reflect hydrophobic and hydrophilic character respectively (Kyte and Doolittle, 1982). The sequence of the five *odr-2* paralogs were predicted from genomic sequence information. The amino terminus sequence of HOT-1a was deduced from a cDNA isolated by RT-PCR, while that of Hot-5a was inferred from an expressed sequence tag provided by Y. Kohara. Amino terminal sequences of Hot-2, 3, and 4 have not been identified. Note that all of the predicted proteins are hydrophobic at the extreme carboxy terminus, while both identified amino terminal sequences possess significant hydrophobic character, consistent with the possibility of GPI anchorage to the plasma membrane.

Perspectives and future directions

When the work described in this dissertation was initiated in 1993, many signaling components in vertebrate olfaction had been identified, including a large family of seven transmembrane receptors, a G protein α subunit, an adenylyl cyclase, and a cyclic nucleotide-gated channel α subunit. Although the presence of these molecules in olfactory neurons was consistent with the biochemical responses observed following odorant treatment, functional evidence that these components were required for olfactory signaling was lacking. Little was known regarding the specificity and sensitivity of the putative olfactory receptors, as none had been definitively shown to respond to odorants in physiological conditions.

Identification of signaling components required for chemosensory behaviors in *C. elegans*

C. elegans is an excellent model system for studying olfaction and olfactory behaviors. Its genetic tractability provides one approach to identify molecules functionally required for chemosensation. However, in 1993, nothing was known about the molecular basis of olfaction in *C. elegans*. Invertebrate olfaction might proceed via G protein-coupled pathways as in vertebrates, by the two-component regulatory systems used in prokaryotes, or by some novel mechanism.

Since then, work in this and other labs has demonstrated that G protein-coupled signaling components are crucial for chemosensory behaviors in *C. elegans*. The molecules required for AWC chemosensory function include a G protein α subunit, guanylyl cyclases, and two subunits of a cyclic nucleotide-gated channel. These components define a pathway analogous to vertebrate olfactory cyclic nucleotide-mediated signaling.

However, a capsaicin/Trp-like putative ion channel, OSM-9, is required for chemotaxis mediated by the AWA sensory neurons. Because phototransduction in *Drosophila* via Trp involves inositol

trisphosphate-mediated signaling, AWA and AWC may utilize distinct second messenger signaling pathways. Interestingly, OSM-9 can play a modulatory role in the AWC neurons that require cyclic nucleotide second messengers. It will be interesting to determine whether IP₃ also modulates vertebrate olfaction, which might explain the controversial reports of IP₃-mediated signaling in vertebrate olfactory neurons (Schild and Restrepo, 1998).

This thesis

The work presented here has contributed to understanding *C. elegans* olfactory signal transduction in a number of ways, and has demonstrated the power of utilizing multiple approaches to studying a given process. Behavioral dissection of chemosensory discrimination, genomic analysis to identify candidate genes, genetic identification of functionally significant molecules, and molecular analysis of a protein of known function have all contributed significantly.

A family of candidate chemosensory receptors was identified in *C. elegans* by examination of the sequenced regions of the genome (Chapter 1). Their structural similarity to seven transmembrane G protein-coupled receptors, large number, and high diversity suggested similar mechanisms of sensory perception in *C. elegans* and vertebrate olfaction.

A notable difference between the two systems is that while only a single type of olfactory receptor is expressed in each vertebrate olfactory neuron, *C. elegans* chemosensory neurons can express multiple receptors. This difference likely reflects the requirements of a simple nervous system with a limited number of chemosensory neurons (Chapter 1). Expression of multiple receptors also provides a molecular basis for the ability of a single type of chemosensory neuron to discriminate between multiple odorants, which was also demonstrated in this thesis (Chapter 4).

odr-10 was originally isolated based on its selective inability to respond to the odorant diacetyl. Significantly, it represents the first identified olfactory receptor with a known physiologically

relevant ligand (Chapters 2 and 3). Its ability to respond to diacetyl, and not to butanone or 2,3-pentanedione, demonstrates that at least one olfactory receptor possesses a high degree of ligand selectivity. Future work will determine whether such specificity is a general feature of other olfactory receptors in both vertebrates and invertebrates.

While the genes described above represent signal transduction molecules whose roles had already been suspected based on analysis of vertebrate olfaction, the cloning of *odr-2* demonstrates the ability of genetics to identify novel molecules required for olfactory responses. *odr-2*, which is required for behaviors mediated by AWC, is exceptional in the specificity of its mutant phenotype despite its widespread neuronal expression. Furthermore, *odr-2* does not appear to be expressed in the AWC chemosensory neurons. These findings suggest that unlike the previously identified molecules, which probably function in the initial perception of odors, ODR-2 may act in non-chemosensory neurons that are part of the neural circuit that mediates chemosensory behavior. Further characterization of *odr-2* may lead to a better understanding of how neurons downstream of the olfactory receptor neurons contribute to chemotactic behavior.

Future directions

With many chemosensory transduction components already identified, future work will likely instead focus on studying how signaling is regulated. Work in this thesis suggests that odorant-specific downregulation during olfactory discrimination occurs within a chemosensory neuron. Likewise, olfactory adaptation is odorant-specific between stimuli sensed by the same neuron (Colbert and Bargmann, 1995). What are the mechanistic bases of these processes within a chemosensory neuron? Genetic approaches towards addressing these questions might include isolating mutants that are specifically defective in adaptation or cross-saturation.

Despite the significant progress made in understanding *C. elegans* olfactory signaling, little is known about how initial odorant perception is processed to produce behavior. The known neuroanatomy is one place to start. However, laser ablation of individual types of interneurons

immediately downstream of the chemosensory neurons does not abolish chemotaxis (Cori Bargmann, personal communication). This result reveals functional redundancy of the downstream interneurons and may represent a form of parallel distributed processing. Ablation of multiple classes of interneurons could identify the neuronal network used for chemosensory processing.

One difficulty in studying neuronal signaling in *C. elegans* has been the inability to monitor a response other than the final outcome of behavior. It has not been possible to determine the intra-neuronal effects of a genetic or physical perturbation that prevents chemotaxis. However, advances in electrophysiological recordings from identified *C. elegans* chemosensory neurons may provide insight into neural processing (Goodman et al., 1998). Another approach may be to visualize calcium concentration changes within the intact animal (Tim Yu, personal communication). These approaches may identify which neurons are involved in generating chemosensory behavior, what changes occur upon odorant stimulation, and possible mechanisms for processing.

The molecules that mediate chemosensory processing in *C. elegans* interneurons are likely to be identified genetically, perhaps by screening for chemotaxis defects in conjunction with abnormal calcium imaging in response to odorant stimulation. Difficulties include the possibility that genes required in the chemosensory neuronal network might be broadly required in the *C. elegans* nervous system, and that the mutant phenotypes may not be specific to chemosensory behaviors.

Because of its restricted mutant phenotype, the *odr-2* gene may be a good starting point for genetic analysis of the chemosensory circuit. First, it must be confirmed that *odr-2* functions in interneurons associated with chemosensory neurons. This might be addressed by mosaic analysis or by attempting chemotaxis rescue by expressing *odr-2* using promoters specific to candidate downstream interneurons. Genetic screens for suppressors of the *odr-2* mutant phenotype may identify molecules that functionally interact with ODR-2. A biochemical approach would be to

screen for proteins that directly bind ODR-2, followed by reverse genetic analysis of candidate interacting proteins.

C. elegans is uniquely suited for molecular investigation of neuronal network function. The combination of a defined nervous system, variety of behavioral responses, forward and reverse genetic tractability, nearly complete genomic sequence identification, and rapid progress in electrophysiological techniques will allow description of behavior in unprecedented detail. Because many key components of sensory signal transduction and neuronal cell biology have been conserved from invertebrates to mammals, future research using this simple nematode is certain to reveal general principles in nervous system function.

Bibliography

- Albrecht JC, Nicholas J, Cameron KR, Newman C, Fleckenstein B, and Honess RW. Herpesvirus saimiri has a gene specifying a homologue of the cellular membrane glycoprotein CD59. (1992) *Virology* 190: 527-30.
- Altschul SF, Gish W, Miller W, Myers EW, and Lipman DJ. Basic local alignment search tool. (1990) *J Mol Biol* 215: 403-10.
- Antony AC, and Miller ME. Statistical prediction of the locus of endoproteolytic cleavage of the nascent polypeptide in glycosylphosphatidylinositol-anchored proteins. (1994) *Biochem J* 298: 9-16.
- Aoufouchi S, Yelamos J, and Milstein C. Nonsense mutations inhibit RNA splicing in a cell-free system: recognition of mutant codon is independent of protein synthesis. (1996) *Cell* 85: 415-22.
- Apanovitch DM, Slep KC, Sigler PB, and Dohlman HG. Sst2 is a GTPase-activating protein for Gpa1: purification and characterization of a cognate RGS-Galpha protein pair in yeast. (1998) *Biochemistry* 37: 4815-22.
- Bakalyar HA, and Reed RR. Identification of a specialized adenylyl cyclase that may mediate odorant detection. (1990) *Science* 250: 1403-6.
- Balasubramanian S, Lynch JW, and Barry PH. Calcium-dependent modulation of the agonist affinity of the mammalian olfactory cyclic nucleotide-gated channel by calmodulin and a novel endogenous factor. (1996) *J Membr Biol* 152: 13-23.
- Baloh RH, Tansey MG, Golden JP, Creedon DJ, Heuckeroth RO, Keck CL, Zimonjic DB, Popescu NC, Johnson E, Jr., and Milbrandt J. TrnR2, a novel receptor that mediates neurturin and GDNF signaling through Ret. (1997) *Neuron* 18: 793-802.
- Bamezai A, and Rock KL. Overexpressed Ly-6A.2 mediates cell-cell adhesion by binding a ligand expressed on lymphoid cells. (1995) *Proc Natl Acad Sci U S A* 92: 4294-8.
- Bargmann CI, Hartweg E, and Horvitz HR. Odorant-selective genes and neurons mediate olfaction in *C. elegans*. (1993) *Cell* 74: 515-27.
- Bargmann CI, and Horvitz HR. Chemosensory neurons with overlapping functions direct chemotaxis to multiple chemicals in *C. elegans*. (1991) *Neuron* 7: 729-42.
- Bargmann CI, Thomas JH, and Horvitz HR. Chemosensory cell function in the behavior and development of *Caenorhabditis elegans*. (1990) *Cold Spring Harb Symp Quant Biol* 55: 529-38.
- Behrendt N, Ploug M, Patthy L, Houen G, Blasi F, and Dano K. The ligand-binding domain of the cell surface receptor for urokinase-type plasminogen activator. (1991) *J Biol Chem* 266: 7842-7.
- Behrendt N, Ronne E, and Dano K. Domain interplay in the urokinase receptor. Requirement for the third domain in high affinity ligand binding and demonstration of ligand contact sites in distinct receptor domains. (1996) *J Biol Chem* 271: 22885-94.

- Belluscio L, Gold GH, Nemes A, and Axel R. Mice deficient in G_{olf} are anosmic. (1998) *Neuron* 20: 69-81.
- Ben-Arie N, Lancet D, Taylor C, Khen M, Walker N, Ledbetter DH, Carrozzo R, Patel K, Sheer D, Lehrach H, and North MA. Olfactory receptor gene cluster on human chromosome 17: possible duplication of an ancestral receptor repertoire. (1994) *Hum Mol Genet* 3: 229-35.
- Benovic JL, Pike LJ, Cerione RA, Staniszewski C, Yoshimasa T, Codina J, Caron MG, and Lefkowitz RJ. Phosphorylation of the mammalian beta-adrenergic receptor by cyclic AMP-dependent protein kinase. Regulation of the rate of receptor phosphorylation and dephosphorylation by agonist occupancy and effects on coupling of the receptor to the stimulatory guanine nucleotide regulatory protein. (1985) *J Biol Chem* 260: 7094-101.
- Berghard A, and Buck LB. Sensory transduction in vomeronasal neurons: evidence for G_{α_o} , $G_{\alpha_{12}}$, and adenylyl cyclase II as major components of a pheromone signaling cascade. (1996) *J Neurosci* 16: 909-18.
- Berghard A, Buck LB, and Liman ER. Evidence for distinct signaling mechanisms in two mammalian olfactory sense organs. (1996) *Proc Natl Acad Sci U S A* 93: 2365-9.
- Berman DM, Wilkie TM, and Gilman AG. GAIP and RGS4 are GTPase-activating proteins for the G_i subfamily of G protein alpha subunits. (1996) *Cell* 86: 445-52.
- Betzl C, Lange G, Pal GP, Wilson KS, Maelicke A, and Saenger W. The refined crystal structure of alpha-cobratoxin from *Naja naja siamensis* at 2.4-A resolution. (1991) *J Biol Chem* 266: 21530-6.
- Boekhoff I, and Breer H. Termination of second messenger signaling in olfaction. (1992) *Proc Natl Acad Sci U S A* 89: 471-4.
- Boekhoff I, Inglese J, Schleicher S, Koch WJ, Lefkowitz RJ, and Breer H. Olfactory desensitization requires membrane targeting of receptor kinase mediated by beta gamma-subunits of heterotrimeric G proteins. (1994a) *J Biol Chem* 269: 37-40.
- Boekhoff I, Kroner C, and Breer H. Calcium controls second-messenger signalling in olfactory cilia. (1996) *Cell Signal* 8: 167-71.
- Boekhoff I, Michel WC, Breer H, and Ache BW. Single odors differentially stimulate dual second messenger pathways in lobster olfactory receptor cells. (1994b) *J Neurosci* 14: 3304-9.
- Boekhoff I, Schleicher S, Strotmann J, and Breer H. Odor-induced phosphorylation of olfactory cilia proteins. (1992) *Proc Natl Acad Sci U S A* 89: 11983-7.
- Boekhoff I, Tareilus E, Strotmann J, and Breer H. Rapid activation of alternative second messenger pathways in olfactory cilia from rats by different odorants. (1990) *Embo J* 9: 2453-8.
- Boekhoff I, Touhara K, Danner S, Inglese J, Lohse MJ, Breer H, and Lefkowitz RJ. Phosducin, potential role in modulation of olfactory signaling. (1997) *J Biol Chem* 272: 4606-12.
- Bohm SK, Grady EF, and Bunnnett NW. Regulatory mechanisms that modulate signalling by G-protein-coupled receptors. (1997) *Biochem J* 322: 1-18.
- Borisy FF, Ronnett GV, Cunningham AM, Juilfs D, Beavo J, and Snyder SH. Calcium/calmodulin-activated phosphodiesterase expressed in olfactory receptor neurons. (1992) *J Neurosci* 12: 915-23.

- Bourne HR. How receptors talk to trimeric G proteins. (1997) *Curr Opin Cell Biol* 9: 134-42.
- Bradley J, Li J, Davidson N, Lester HA, and Zinn K. Heteromeric olfactory cyclic nucleotide-gated channels: a subunit that confers increased sensitivity to cAMP. (1994) *Proc Natl Acad Sci U S A* 91: 8890-4.
- Brakenhoff RH, Gerretsen M, Knippels EM, van Dijk M, van Essen H, Weghuis DO, Sinke RJ, Snow GB, and van Dongen GA. The human E48 antigen, highly homologous to the murine Ly-6 antigen ThB, is a GPI-anchored molecule apparently involved in keratinocyte cell-cell adhesion. (1995) *J Cell Biol* 129: 1677-89.
- Breer H, Boekhoff I, and Tareilus E. Rapid kinetics of second messenger formation in olfactory transduction. (1990) *Nature* 345: 65-8.
- Brenner S. The genetics of *Caenorhabditis elegans*. (1974) *Genetics* 77: 71-94.
- Bruch RC, and Medler KF. A regulator of G-protein signaling in olfactory receptor neurons. (1996) *Neuroreport* 7: 2941-4.
- Brunet LJ, Gold GH, and Ngai J. General anosmia caused by a targeted disruption of the mouse olfactory cyclic nucleotide-gated cation channel. (1996) *Neuron* 17: 681-93.
- Buck L, and Axel R. A novel multigene family may encode odorant receptors: a molecular basis for odor recognition. (1991) *Cell* 65: 175-87.
- Buj-Bello A, Adu J, Pinon LG, Horton A, Thompson J, Rosenthal A, Chinchetru M, Buchman VL, and Davies AM. Neurturin responsiveness requires a GPI-linked receptor and the Ret receptor tyrosine kinase. (1997) *Nature* 387: 721-4.
- Carr WE, Gleeson RA, and Trapido-Rosenthal HG. The role of perireceptor events in chemosensory processes. (1990) *Trends Neurosci* 13: 212-5.
- Chen J, Makino CL, Peachey NS, Baylor DA, and Simon MI. Mechanisms of rhodopsin inactivation in vivo as revealed by a COOH-terminal truncation mutant. (1995) *Science* 267: 374-7.
- Chen Q, and Konopka JB. Regulation of the G-protein-coupled alpha-factor pheromone receptor by phosphorylation. (1996) *Mol Cell Biol* 16: 247-57.
- Chen TY, and Yau KW. Direct modulation by Ca(2+)-calmodulin of cyclic nucleotide-activated channel of rat olfactory receptor neurons. (1994) *Nature* 368: 545-8.
- Chess A, Simon I, Cedar H, and Axel R. Allelic inactivation regulates olfactory receptor gene expression. (1994) *Cell* 78: 823-34.
- Classon BJ, and Coverdale L. Mouse stem cell antigen Sca-2 is a member of the Ly-6 family of cell surface proteins. (1994) *Proc Natl Acad Sci U S A* 91: 5296-300.
- Coburn CM, and Bargmann CI. A putative cyclic nucleotide-gated channel is required for sensory development and function in *C. elegans*. (1996) *Neuron* 17: 695-706.
- Codias EK, Fleming TJ, Zacharchuk CM, Ashwell JD, and Malek TR. Role of Ly-6A/E and T cell receptor-zeta for IL-2 production. Phosphatidylinositol-anchored Ly-6A/E antagonizes T cell receptor-mediated IL-2 production by a zeta-independent pathway. (1992) *J Immunol* 149: 1825-52.

Colbert HA, and Bargmann CI. Odorant-specific adaptation pathways generate olfactory plasticity in *C. elegans*. (1995) *Neuron* 14: 803-12.

Colbert HA, and Bargmann CI. Environmental signals modulate olfactory acuity, discrimination, and memory in *Caenorhabditis elegans*. (1997) *Learning & Memory* 4: 179-191.

Colbert HA, Smith TL, and Bargmann CI. OSM-9, a novel protein with structural similarity to channels, is required for olfaction, mechanosensation, and olfactory adaptation in *Caenorhabditis elegans*. (1997) *J Neurosci* 17: 8259-69.

Cole GM, and Reed SI. Pheromone-induced phosphorylation of a G protein beta subunit in *S. cerevisiae* is associated with an adaptive response to mating pheromone. (1991) *Cell* 64: 703-16.

Cray C, Keane RW, Malek TR, and Levy RB. Regulation and selective expression of Ly-6A/E, a lymphocyte activation molecule, in the central nervous system. (1990) *Brain Res Mol Brain Res* 8: 9-15.

Davies A, and Lachmann PJ. Membrane defence against complement lysis: the structure and biological properties of CD59. (1993) *Immunol Res* 12: 258-75.

Davis S, Aldrich TH, Stahl N, Pan L, Taga T, Kishimoto T, Ip NY, and Yancopoulos GD. LIFR beta and gp130 as heterodimerizing signal transducers of the tripartite CNTF receptor. (1993) *Science* 260: 1805-8.

Dawson TM, Arriza JL, Jaworsky DE, Borisy FF, Attramadal H, Lefkowitz RJ, and Ronnett GV. Beta-adrenergic receptor kinase-2 and beta-arrestin-2 as mediators of odorant-induced desensitization. (1993) *Science* 259: 825-9.

Dhallan RS, Yau KW, Schrader KA, and Reed RR. Primary structure and functional expression of a cyclic nucleotide-activated channel from olfactory neurons. (1990) *Nature* 347: 184-7.

Dohlman HG, Apaniesk D, Chen Y, Song J, and Nusskern D. Inhibition of G-protein signaling by dominant gain-of-function mutations in Sst2p, a pheromone desensitization factor in *Saccharomyces cerevisiae*. (1995) *Mol Cell Biol* 15: 3635-43.

Dohlman HG, Song J, Ma D, Courchesne WE, and Thorner J. Sst2, a negative regulator of pheromone signaling in the yeast *Saccharomyces cerevisiae*: expression, localization, and genetic interaction and physical association with Gpa1 (the G-protein alpha subunit). (1996) *Mol Cell Biol* 16: 5194-209.

Dulac C, and Axel R. A novel family of genes encoding putative pheromone receptors in mammals. (1995) *Cell* 83: 195-206.

Durbec P, Marcos-Gutierrez CV, Kilkenny C, Grigoriou M, Wartiovaara K, Suvanto P, Smith D, Ponder B, Costantini F, Saarma M, Sariola H, and Pachnis V. GDNF signalling through the Ret receptor tyrosine kinase. (1996) *Nature* 381: 789-93.

Dwyer ND, Troemel ER, Sengupta P, and Bargmann CI. Odorant receptor localization to olfactory cilia is mediated by ODR-4, a novel membrane-associated protein. (1998) *Cell* 93: 455-466.

Fadool DA, and Ache BW. Plasma membrane inositol 1,4,5-trisphosphate-activated channels mediate signal transduction in lobster olfactory receptor neurons. (1992) *Neuron* 9: 907-18.

- Falke JJ, Bass RB, Butler SL, Chervitz SA, and Danielson MA. The two-component signaling pathway of bacterial chemotaxis: a molecular view of signal transduction by receptors, kinases, and adaptation enzymes. (1997) *Ann Rev Cell Dev Biol* 13: 457-512.
- Fire A, Harrison SW, and Dixon D. A modular set of *lacZ* fusion vectors for studying gene expression in *Caenorhabditis elegans*. (1990) *Gene* 93: 189-98.
- Firestein S, Darrow B, and Shepherd GM. Activation of the sensory current in salamander olfactory receptor neurons depends on a G protein-mediated cAMP second messenger system. (1991) *Neuron* 6: 825-35.
- Firestein S, Picco C, and Menini A. The relation between stimulus and response in olfactory receptor cells of the tiger salamander. (1993) *J Physiol* 468: 1-10.
- Firestein S, Shepherd GM, and Werblin FS. Time course of the membrane current underlying sensory transduction in salamander olfactory receptor neurones. (1990) *J Physiol* 430: 135-58.
- Fleming TJ, and Malek TR. Multiple glycosylphosphatidylinositol-anchored Ly-6 molecules and transmembrane Ly-6E mediate inhibition of IL-2 production. (1994) *J Immunol* 153: 1955-62.
- Fleming TJ, O'hUigin C, and Malek TR. Characterization of two novel Ly-6 genes. Protein sequence and potential structural similarity to alpha-bungarotoxin and other neurotoxins. (1993) *J Immunol* 150: 5379-90.
- Fletcher CM, Harrison RA, Lachmann PJ, and Neuhaus D. Structure of a soluble, glycosylated form of the human complement regulatory protein CD59. (1994) *Structure* 2: 185-99.
- Freedman NJ, and Lefkowitz RJ. Desensitization of G protein-coupled receptors. (1996) *Recent Prog Horm Res* 51: 319-51; discussion 352-3.
- Freitag J, Krieger J, Strotmann J, and Breer H. Two classes of olfactory receptors in *Xenopus laevis*. (1995) *Neuron* 15: 1383-92.
- Friedman S, Palfree RG, Sirlin S, and Hammerling U. Analysis of three distinct Ly6-A-related cDNA sequences isolated from rat kidney. (1990) *Immunogenetics* 31: 104-11.
- Friedrich RW, and Korsching SI. Combinatorial and chemotopic odorant coding in the zebrafish olfactory bulb visualized by optical imaging. (1997) *Neuron* 18: 737-52.
- Georgi LL, Albert PS, and Riddle DL. *daf-1*, a *C. elegans* gene controlling dauer larva development, encodes a novel receptor protein kinase. (1990) *Cell* 61: 635-45.
- Goodman MB, Hall DH, Avery L, and Lockery SR. Active currents regulate sensitivity and dynamic range in *C. elegans* neurons. (1998) *Neuron* 20: 763-772.
- Gumley TP, McKenzie IF, Kozak CA, and Sandrin MS. Isolation and characterization of cDNA clones for the mouse thymocyte B cell antigen (ThB). (1992) *J Immunol* 149: 2615-8.
- Gumley TP, McKenzie IF, and Sandrin MS. Tissue expression, structure and function of the murine Ly-6 family of molecules. (1995) *Immunol Cell Biol* 73: 277-96.
- Hanninen A, Jaakkola I, Salmi M, Simell O, and Jalkanen S. Ly-6C regulates endothelial adhesion and homing of CD8(+) T cells by activating integrin-dependent adhesion pathways. (1997) *Proc Natl Acad Sci U S A* 94: 6898-903.

- Hawes BE, Touhara K, Kurose H, Lefkowitz RJ, and Inglesse J. Determination of the G beta gamma-binding domain of phosducin. A regulatable modulator of G beta gamma signaling. (1994) *Journal of Biological Chemistry* 269: 29825-30.
- Hedgecock EM, and Russell RL. Normal and mutant thermotaxis in the nematode *Caenorhabditis elegans*. (1975) *Proc Natl Acad Sci U S A* 72: 4061-5.
- Hekman M, Bauer PH, Söhlemann P, and Lohse MJ. Phosducin inhibits receptor phosphorylation by the beta-adrenergic receptor kinase in a PKA-regulated manner. (1994) *Febs Letters* 343: 120-4.
- Hepler JR, Berman DM, Gilman AG, and Kozasa T. RGS4 and GAIP are GTPase-activating proteins for G_q alpha and block activation of phospholipase C beta by gamma-thio-GTP-G_q alpha. (1997) *Proc Natl Acad Sci U S A* 94: 428-32.
- Herman RK. Touch sensation in *Caenorhabditis elegans*. (1996) *Bioessays* 18: 199-206.
- Herrada G, and Dulac C. A novel family of putative pheromone receptors in mammals with a topographically organized and sexually dimorphic distribution. (1997) *Cell* 90: 763-73.
- Heximer SP, Watson N, Linder ME, Blumer KJ, and Hepler JR. RGS2/G0S8 is a selective inhibitor of G_q function. (1997) *Proc Natl Acad Sci U S A* 94: 14389-93.
- Hicke L, and Riezman H. Ubiquitination of a yeast plasma membrane receptor signals its ligand-stimulated endocytosis. (1996) *Cell* 84: 277-87.
- Hicke L, Zanolari B, and Riezman H. Cytoplasmic tail phosphorylation of the alpha-factor receptor is required for its ubiquitination and internalization. (1998) *Journal of Cell Biology* 141: 349-358.
- Hobert O, D'Alberti T, Liu Y, and Ruvkun G. Control of neural development and function in a thermoregulatory network by the LIM homeobox gene *lin-11*. (1998) *J Neurosci* 18: 2084-96.
- Hobert O, Mori I, Yamashita Y, Honda H, Ohshima Y, Liu Y, and Ruvkun G. Regulation of interneuron function in the *C. elegans* thermoregulatory pathway by the *ttx-3* LIM homeobox gene. (1997) *Neuron* 19: 345-57.
- HogenEsch H, de Geus B, Tielen F, and Rozing J. Constitutive expression of Ly-6.A2 on murine keratinocytes and inducible expression on TCR gamma delta+ dendritic epidermal T cells. (1993) *J Dermatol Sci* 5: 114-21.
- Horowitz MC, Fields A, DeMeo D, Qian HY, Bothwell AL, and Trepman E. Expression and regulation of Ly-6 differentiation antigens by murine osteoblasts. (1994) *Endocrinology* 135: 1032-43.
- Howell S, Lanctot C, Boileau G, and Crine P. A cleavable N-terminal signal peptide is not a prerequisite for the biosynthesis of glycosylphosphatidylinositol-anchored proteins. (1994) *J Biol Chem* 269: 16993-6.
- Hunt TW, Fields TA, Casey PJ, and Peralta EG. RGS10 is a selective activator of G alpha i GTPase activity. (1996) *Nature* 383: 175-7.
- Innamorati G, Sadeghi HM, Tran NT, and Birnbaumer M. A serine cluster prevents recycling of the V2 vasopressin receptor. (1998) *Proc Natl Acad Sci U S A* 95: 2222-6.

- Iwami G, Kawabe J, Ebina T, Cannon PJ, Homcy CJ, and Ishikawa Y. Regulation of adenylyl cyclase by protein kinase A. (1995) *J Biol Chem* 270: 12481-4.
- Jeng CJ, McCarroll SA, Martin TF, Floor E, Adams J, Krantz D, Butz S, Edwards R, and Schweitzer ES. Thy-1 is a component common to multiple populations of synaptic vesicles. (1998) *J Cell Biol* 140: 685-98.
- Jing S, Wen D, Yu Y, Holst PL, Luo Y, Fang M, Tamir R, Antonio L, Hu Z, Cupples R, Louis JC, Hu S, Altmann BW, and Fox GM. GDNF-induced activation of the ret protein tyrosine kinase is mediated by GDNFR-alpha, a novel receptor for GDNF. (1996) *Cell* 85: 1113-24.
- Jing S, Yu Y, Fang M, Hu Z, Holst PL, Boone T, Delaney J, Schultz H, Zhou R, and Fox GM. GFRalpha-2 and GFRalpha-3 are two new receptors for ligands of the GDNF family. (1997) *J Biol Chem* 272: 33111-7.
- Jokiranta TS, Tissari J, Teleman O, and Meri S. Extracellular domain of type I receptor for transforming growth factor-beta: molecular modelling using protectin (CD59) as a template. (1995) *FEBS Lett* 376: 31-6.
- Jones DT, and Reed RR. Golf: an olfactory neuron specific-G protein involved in odorant signal transduction. (1989) *Science* 244: 790-5.
- Juif DM, Fulle HJ, Zhao AZ, Houslay MD, Garbers DL, and Beavo JA. A subset of olfactory neurons that selectively express cGMP-stimulated phosphodiesterase (PDE2) and guanylyl cyclase-D define a unique olfactory signal transduction pathway. (1997) *Proc Natl Acad Sci U S A* 94: 3388-95.
- Kanse SM, Kost C, Wilhelm OG, Andreassen PA, and Preissner KT. The urokinase receptor is a major vitronectin-binding protein on endothelial cells. (1996) *Exp Cell Res* 224: 344-53.
- Kaplan JM, and Horvitz HR. A dual mechanosensory and chemosensory neuron in *Caenorhabditis elegans*. (1993) *Proc Natl Acad Sci U S A* 90: 2227-31.
- Kieffer B, Driscoll PC, Campbell ID, Willis AC, van der Merwe PA, and Davis SJ. Three-dimensional solution structure of the extracellular region of the complement regulatory protein CD59, a new cell-surface protein domain related to snake venom neurotoxins. (1994) *Biochemistry* 33: 4471-82.
- Kim JY, Soede RD, Schaap P, Valkema R, Borleis JA, Van Haastert PJ, Devreotes PN, and Hereld D. Phosphorylation of chemoattractant receptors is not essential for chemotaxis or termination of G-protein-mediated responses. (1997) *J Biol Chem* 272: 27313-8.
- Kleene SJ. Origin of the chloride current in olfactory transduction. (1993) *Neuron* 11: 123-32.
- Kleene SJ. High-gain, low-noise amplification in olfactory transduction. (1997) *Biophys J* 73: 1110-7.
- Kleene SJ, and Gesteland RC. Calcium-activated chloride conductance in frog olfactory cilia. (1991) *J Neurosci* 11: 3624-9.
- Klein RD, Sherman D, Ho WH, Stone D, Bennett GL, Moffat B, Vandlen R, Simmons L, Gu Q, Hongo JA, Devaux B, Poulsen K, Armanini M, Nozaki C, Asai N, Goddard A, Phillips H, Henderson CE, Takahashi M, and Rosenthal A. A GPI-linked protein that interacts with Ret to form a candidate neurturin receptor. (1997) *Nature* 387: 717-21.

- Koch WJ, Inglese J, Stone WC, and Lefkowitz RJ. The binding site for the beta gamma subunits of heterotrimeric G proteins on the beta-adrenergic receptor kinase. (1993) *Journal of Biological Chemistry* 268: 8256-60.
- Koelle MR. A new family of G-protein regulators - the RGS proteins. (1997) *Curr Opin Cell Biol* 9: 143-7.
- Koelle MR, and Horvitz HR. EGL-10 regulates G protein signaling in the *C. elegans* nervous system and shares a conserved domain with many mammalian proteins. (1996) *Cell* 84: 115-25.
- Komatsu H, Mori I, Rhee JS, Akaike N, and Ohshima Y. Mutations in a cyclic nucleotide-gated channel lead to abnormal thermosensation and chemosensation in *C. elegans*. (1996) *Neuron* 17: 707-18.
- Korty PE, Brando C, and Shevach EM. CD59 functions as a signal-transducing molecule for human T cell activation. (1991) *J Immunol* 146: 4092-8.
- Kramer RH, and Siegelbaum SA. Intracellular Ca²⁺ regulates the sensitivity of cyclic nucleotide-gated channels in olfactory receptor neurons. (1992) *Neuron* 9: 897-906.
- Krause M, and Hirsh D. A trans-spliced leader sequence on actin mRNA in *C. elegans*. (1987) *Cell* 49: 753-61.
- Kroner C, Boekhoff I, and Breer H. Phosphatase 2A regulates the responsiveness of olfactory cilia. (1996) *Biochim Biophys Acta* 1312: 169-75.
- Kurahashi T. The response induced by intracellular cyclic AMP in isolated olfactory receptor cells of the newt. (1990) *J Physiol* 430: 355-71.
- Kurahashi T, and Kaneko A. High density cAMP-gated channels at the ciliary membrane in the olfactory receptor cell. (1991) *Neuroreport* 2: 5-8.
- Kurahashi T, and Menini A. Mechanism of odorant adaptation in the olfactory receptor cell. (1997) *Nature* 385: 725-9.
- Kurahashi T, and Shibuya T. Ca²⁺-dependent adaptive properties in the solitary olfactory receptor cell of the newt. (1990) *Brain Res* 515: 261-8.
- Kurahashi T, and Yau KW. Co-existence of cationic and chloride components in odorant-induced current of vertebrate olfactory receptor cells. (1993) *Nature* 363: 71-4.
- Kyte J, and Doolittle RF. A simple method for displaying the hydropathic character of a protein. (1982) *J Mol Biol* 157: 105-32.
- LeClair KP, Palfree RG, Flood PM, Hammerling U, and Bothwell A. Isolation of a murine Ly-6 cDNA reveals a new multigene family. (1986) *Embo J* 5: 3227-34.
- Lee PH, and Goetz FW. Characterization of a novel cDNA obtained through differential-display PCR of phorbol ester-stimulated ovarian tissue from the brook trout (*Salvelinus fontinalis*). (1998) *Mol Reprod Dev* 49: 112-8.
- Levy NS, Bakalyar HA, and Reed RR. Signal transduction in olfactory neurons. (1991) *J Steroid Biochem Mol Biol* 39: 633-7.

- Liman ER, and Buck LB. A second subunit of the olfactory cyclic nucleotide-gated channel confers high sensitivity to cAMP. (1994) *Neuron* 13: 611-21.
- Liu M, Chen TY, Ahamed B, Li J, and Yau KW. Calcium-calmodulin modulation of the olfactory cyclic nucleotide-gated cation channel [published erratum appears in *Science* 1994 Dec 23;266(5193):1933]. (1994) *Science* 266: 1348-54.
- Low MG. The glycosyl-phosphatidylinositol anchor of membrane proteins. (1989) *Biochim Biophys Acta* 988: 427-54.
- Lowe G, and Gold GH. Nonlinear amplification by calcium-dependent chloride channels in olfactory receptor cells. (1993) *Nature* 366: 283-6.
- MacNeil I, Kennedy J, Godfrey DI, Jenkins NA, Masciantonio M, Mineo C, Gilbert DJ, Copeland NG, Boyd RL, and Zlotnik A. Isolation of a cDNA encoding thymic shared antigen-1. A new member of the Ly6 family with a possible role in T cell development. (1993) *J Immunol* 151: 6913-23.
- Mao M, Yu M, Tong JH, Ye J, Zhu J, Huang QH, Fu G, Yu L, Zhao SY, Waxman S, Lanotte M, Wang ZY, Tan JZ, Chan SJ, and Chen Z. RIG-E, a human homolog of the murine Ly-6 family, is induced by retinoic acid during the differentiation of acute promyelocytic leukemia cell. (1996) *Proc Natl Acad Sci U S A* 93: 5910-4.
- Matsunami H, and Buck LB. A multigene family encoding a diverse array of putative pheromone receptors in mammals. (1997) *Cell* 90: 775-84.
- McLatchie LM, Fraser NJ, Main MJ, Wise A, Brown J, Thompson N, Solari R, Lee MG, and Foord SM. RAMPs regulate the transport and ligand specificity of the calcitonin-receptor-like receptor. (1998) *Nature* 393: 333-339.
- Mello CC, Kramer JM, Stinchcomb D, and Ambros V. Efficient gene transfer in *C.elegans*: extrachromosomal maintenance and integration of transforming sequences. (1991) *Embo J* 10: 3959-70.
- Mombaerts P, Wang F, Dulac C, Chao SK, Nemes A, Mendelsohn M, Edmondson J, and Axel R. Visualizing an olfactory sensory map. (1996) *Cell* 87: 675-86.
- Mori I, and Ohshima Y. Neural regulation of thermotaxis in *Caenorhabditis elegans*. (1995) *Nature* 376: 344-8.
- Nakamura T, and Gold GH. A cyclic nucleotide-gated conductance in olfactory receptor cilia. (1987) *Nature* 325: 442-4.
- Newell PC, Europe-Finner GN, Liu G, Gammon B, and Wood CA. Signal transduction for chemotaxis in *Dictyostelium amoebae*. (1990) *Semin Cell Biol* 1: 105-13.
- Ngai J, Chess A, Dowling MM, Necles N, Macagno ER, and Axel R. Coding of olfactory information: topography of odorant receptor expression in the catfish olfactory epithelium. (1993a) *Cell* 72: 667-80.
- Ngai J, Dowling MM, Buck L, Axel R, and Chess A. The family of genes encoding odorant receptors in the channel catfish. (1993b) *Cell* 72: 657-66.

- Noel LS, Champion BR, Holley CL, Simmons CJ, Morris DC, Payne JA, Lean JM, Chambers TJ, Zaman G, Lanyon LE, Suva LJ, and Miller LR. RoBo-1, a novel member of the urokinase plasminogen activator receptor/CD59/Ly-6/snake toxin family selectively expressed in rat bone and growth plate cartilage. (1998) *J Biol Chem* 273: 3878-83.
- Ohkura N, Inoue S, Ikeda K, and Hayashi K. The two subunits of a phospholipase A2 inhibitor from the plasma of Thailand cobra having structural similarity to urokinase-type plasminogen activator receptor and LY-6 related proteins. (1994) *Biochem Biophys Res Commun* 204: 1212-8.
- Pace U, Hanski E, Salomon Y, and Lancet D. Odorant-sensitive adenylate cyclase may mediate olfactory reception. (1985) *Nature* 316: 255-8.
- Palfree RG. Ly-6-domain proteins--new insights and new members: a C-terminal Ly-6 domain in sperm acrosomal protein SP-10. (1996) *Tissue Antigens* 48: 71-9.
- Palfree RG, Sirlin S, Dumont FJ, and Hammerling U. N-terminal and cDNA characterization of murine lymphocyte antigen Ly-6C.2. (1988) *J Immunol* 140: 305-10.
- Parmentier M, Libert F, Schurmans S, Schiffmann S, Lefort A, Eggerickx D, Ledent C, Mollereau C, Gerard C, Perret J, Grootegoed A, and Vassart G. Expression of members of the putative olfactory receptor gene family in mammalian germ cells. (1992) *Nature* 355: 453-5.
- Pei G, Tiberi M, Caron MG, and Lefkowitz RJ. An approach to the study of G-protein-coupled receptor kinases: an in vitro-purified membrane assay reveals differential receptor specificity and regulation by G beta gamma subunits. (1994) *Proc Natl Acad Sci U S A* 91: 3633-6.
- Pelosi P. Perireceptor events in olfaction. (1996) *J Neurobiol* 30: 3-19.
- Perkins LA, Hedgecock EM, Thomson JN, and Culotti JG. Mutant sensory cilia in the nematode *Caenorhabditis elegans*. (1986) *Dev Biol* 117: 456-87.
- Pitcher J, Lohse MJ, Codina J, Caron MG, and Lefkowitz RJ. Desensitization of the isolated beta 2-adrenergic receptor by beta-adrenergic receptor kinase, cAMP-dependent protein kinase, and protein kinase C occurs via distinct molecular mechanisms. (1992a) *Biochemistry* 31: 3193-7.
- Pitcher JA, Inglese J, Higgins JB, Arriza JL, Casey PJ, Kim C, Benovic JL, Kwatra MM, Caron MG, and Lefkowitz RJ. Role of beta gamma subunits of G proteins in targeting the beta-adrenergic receptor kinase to membrane-bound receptors. (1992b) *Science* 257: 1264-7.
- Plesner T, Behrendt N, and Ploug M. Structure, function and expression on blood and bone marrow cells of the urokinase-type plasminogen activator receptor, uPAR. (1997) *Stem Cells* 15: 398-408.
- Ploug M, and Ellis V. Structure-function relationships in the receptor for urokinase-type plasminogen activator. Comparison to other members of the Ly-6 family and snake venom alpha-neurotoxins. (1994) *Febs Lett* 349: 163-8.
- Premont RT, Inglese J, and Lefkowitz RJ. Protein kinases that phosphorylate activated G protein-coupled receptors. (1995) *Faseb J* 9: 175-82.
- Probst WC, Snyder LA, Schuster DI, Brosius J, and Sealfon SC. Sequence alignment of the G-protein coupled receptor superfamily. (1992) *DNA Cell Biol* 11: 1-20.

- Ranganathan R, and Ross EM. PDZ domain proteins: scaffolds for signaling complexes. (1997) *Curr Biol* 7: R770-3.
- Ressler KJ, Sullivan SL, and Buck LB. A zonal organization of odorant receptor gene expression in the olfactory epithelium. (1993) *Cell* 73: 597-609.
- Ressler KJ, Sullivan SL, and Buck LB. Information coding in the olfactory system: evidence for a stereotyped and highly organized epitope map in the olfactory bulb. (1994) *Cell* 79: 1245-55.
- Restrepo D, Boekhoff I, and Breer H. Rapid kinetic measurements of second messenger formation in olfactory cilia from channel catfish. (1993) *Am J Physiol* 264: C906-11.
- Restrepo D, Miyamoto T, Bryant BP, and Teeter JH. Odor stimuli trigger influx of calcium into olfactory neurons of the channel catfish. (1990) *Science* 249: 1166-8.
- Riesgo-Escovar J, Raha D, and Carlson JR. Requirement for a phospholipase C in odor response: overlap between olfaction and vision in *Drosophila*. (1995) *Proc Natl Acad Sci U S A* 92: 2864-8.
- Roayaie K, Crump JG, Sagasti A, and Bargmann CI. The G alpha protein ODR-3 mediates olfactory and nociceptive function and controls cilium morphogenesis in *C. elegans* olfactory neurons. (1998) *Neuron* 20: 55-67.
- Roldan AL, Cubellis MV, Masucci MT, Behrendt N, Lund LR, Dano K, Appella E, and Blasi F. Cloning and expression of the receptor for human urokinase plasminogen activator, a central molecule in cell surface, plasmin dependent proteolysis [published erratum appears in *EMBO J* 1990 May;9(5):1674]. (1990) *Embo J* 9: 467-74.
- Ryba NJ, and Tirindelli R. A new multigene family of putative pheromone receptors. (1997) *Neuron* 19: 371-9.
- Sambrook J, Fritsch EF, and Maniatis T (1989). *Molecular Cloning: A Laboratory Manual*. (Cold Spring Harbor, NY: Cold Spring Harbor Press).
- Sautter A, Zong X, Hofmann F, and Biel M. An isoform of the rod photoreceptor cyclic nucleotide-gated channel beta subunit expressed in olfactory neurons. (1998) *Proc Natl Acad Sci U S A* 95: 4696-4701.
- Schild D, and Restrepo D. Transduction mechanisms in vertebrate olfactory receptor cells. (1998) *Physiol Rev* 78: 429-66.
- Schleicher S, Boekhoff I, Arriza J, Lefkowitz RJ, and Breer H. A beta-adrenergic receptor kinase-like enzyme is involved in olfactory signal termination. (1993) *Proc Natl Acad Sci U S A* 90: 1420-4.
- Schroder S, and Lohse MJ. Inhibition of G-protein betagamma-subunit functions by phosphodiesterase-like protein. (1996) *Proc Natl Acad Sci U S A* 93: 2100-4.
- Sengupta P, Chou JH, and Bargmann CI. *odr-10* encodes a seven transmembrane domain olfactory receptor required for responses to the odorant diacetyl. (1996) *Cell* 84: 899-909.
- Sengupta P, Colbert HA, and Bargmann CI. The *C. elegans* gene *odr-7* encodes an olfactory-specific member of the nuclear receptor superfamily. (1994) *Cell* 79: 971-80.

- Sicard G, and Holley A. Receptor cell responses to odorants: similarities and differences among odorants. (1984) *Brain Res* 292: 283-96.
- Sklar PB, Anholt RR, and Snyder SH. The odorant-sensitive adenylate cyclase of olfactory receptor cells. Differential stimulation by distinct classes of odorants. (1986) *J Biol Chem* 261: 15538-43.
- Stahl N, and Yancopoulos GD. The tripartite CNTF receptor complex: activation and signaling involves components shared with other cytokines. (1994) *J Neurobiol* 25: 1454-66.
- Stanford WL, Bruyns E, and Snodgrass HR. The isolation and sequence of the chromosomal gene and regulatory regions of Ly-6A.2. (1992) *Immunogenetics* 35: 408-11.
- Stanford WL, Haque S, Alexander R, Liu X, Latour AM, Snodgrass HR, Koller BH, and Flood PM. Altered proliferative response by T lymphocytes of Ly-6A (Sca-1) null mice. (1997) *J Exp Med* 186: 705-17.
- Strader CD, Fong TM, Tota MR, Underwood D, and Dixon RA. Structure and function of G protein-coupled receptors. (1994) *Annu Rev Biochem* 63: 101-32.
- Su B, Waneck GL, Flavell RA, and Bothwell AL. The glycosyl phosphatidylinositol anchor is critical for Ly-6A/E-mediated T cell activation. (1991) *J Cell Biol* 112: 377-84.
- Sulston J, Du Z, Thomas K, Wilson R, Hillier L, Staden R, Halloran N, Green P, Thierry-Mieg J, Qiu L, Dear S, Coulson A, Craxton M, Durbin R, Berks M, Metzstein M, Hawkins T, Ainscough R, and Waterston R. The *C. elegans* genome sequencing project: a beginning. (1992) *Nature* 356: 37-41.
- Suzuki A, Shioda N, Maeda T, Tada M, and Ueno N. A mouse TGF-beta type I receptor that requires type II receptor for ligand binding. (1994) *Biochem. Biophys. Res. Commun.* 198: 1063-1069.
- Tanaka M, Marunouchi T, and Sawada M. Expression of Ly-6C on microglia in the developing and adult mouse brain. (1997) *Neurosci Lett* 239: 17-20.
- Terrill WF, and Dusenbery DB. Threshold chemosensitivity and hypothetical chemoreceptor function of the nematode *Caenorhabditis elegans*. (1996) *Journal of Chemical Ecology* 22: 1463-1475.
- Thompson JD, Higgins DG, and Gibson TJ. CLUSTAL W: improving the sensitivity of progressive multiple sequence alignment through sequence weighting, position-specific gap penalties and weight matrix choice. (1994) *Nucleic Acids Res* 22: 4673-80.
- Treanor JJ, Goodman L, de Sauvage F, Stone DM, Poulsen KT, Beck CD, Gray C, Armanini MP, Pollock RA, Hefti F, Phillips HS, Goddard A, Moore MW, Buj-Bello A, Davies AM, Asai N, Takahashi M, Vandlen R, Henderson CE, and Rosenthal A. Characterization of a multicomponent receptor for GDNF. (1996) *Nature* 382: 80-3.
- Troemel ER, Chou JH, Dwyer ND, Colbert HA, and Bargmann CI. Divergent seven transmembrane receptors are candidate chemosensory receptors in *C. elegans*. (1995) *Cell* 83: 207-18.
- Troemel ER, Kimmel BE, and Bargmann CI. Reprogramming chemotaxis responses: sensory neurons define olfactory preferences in *C. elegans*. (1997) *Cell* 91: 161-9.

- Trupp M, Arenas E, Fainzilber M, Nilsson AS, Sieber BA, Grigoriou M, Kilkenny C, Salazar-Grueso E, Pachnis V, Arumae U, Sariola H, Saarma M, and Ibanez CF. Functional receptor for GDNF encoded by the c-ret proto-oncogene. (1996) *Nature* 381: 785-8.
- Tsunoda S, Sierralta J, Sun Y, Bodner R, Suzuki E, Becker A, Socolich M, and Zuker CS. A multivalent PDZ-domain protein assembles signalling complexes in a G-protein-coupled cascade. (1997) *Nature* 388: 243-9.
- Udenfriend S, and Kodukula K. How glycosylphosphatidylinositol-anchored membrane proteins are made. (1995) *Annu Rev Biochem* 64: 563-91.
- van de Rijn M, Heimfeld S, Spangrude GJ, and Weissman IL. Mouse hematopoietic stem-cell antigen Sca-1 is a member of the Ly-6 antigen family. (1989) *Proc Natl Acad Sci U S A* 86: 4634-8.
- van den Berg CW, Cinek T, Hallett MB, Horejsi V, and Morgan BP. Exogenous glycosyl phosphatidylinositol-anchored CD59 associates with kinases in membrane clusters on U937 cells and becomes Ca²⁺-signaling competent. (1995) *J Cell Biol* 131: 669-77.
- Vassar R, Chao SK, Sitcheran R, Nunez JM, Vosshall LB, and Axel R. Topographic organization of sensory projections to the olfactory bulb. (1994) *Cell* 79: 981-91.
- Vassar R, Ngai J, and Axel R. Spatial segregation of odorant receptor expression in the mammalian olfactory epithelium. (1993) *Cell* 74: 309-18.
- von Heijne G. A new method for predicting signal sequence cleavage sites. (1986) *Nucleic Acids Res* 14: 4683-90.
- von Heijne G. Signals for protein targeting into and across membranes. (1994) *Subcell Biochem* 22: 1-19.
- Vowels JJ, and Thomas JH. Multiple chemosensory defects in *daf-11* and *daf-21* mutants of *Caenorhabditis elegans*. (1994) *Genetics* 138: 303-16.
- Wang F, Nemes A, Mendelsohn M, and Axel R. Odorant receptors govern the formation of a precise topographic map. (1998) *Cell* 47-60.
- Ward S. Chemotaxis by the nematode *Caenorhabditis elegans*: identification of attractants and analysis of the response by use of mutants. (1973) *Proc Natl Acad Sci U S A* 70: 817-21.
- Ward S, Thomson N, White JG, and Brenner S. Electron microscopical reconstruction of the anterior sensory anatomy of the nematode *Caenorhabditis elegans*. (1975) *J Comp Neurol* 160: 313-37.
- Ware RW, Clark D, Crossland K, and Russell RL. The nerve ring of the nematode *Caenorhabditis elegans*: sensory input and motor output. (1975) *J. Comp. Neur.* 162: 71-110.
- Watson N, Linder ME, Druey KM, Kehrl JH, and Blumer KJ. RGS family members: GTPase-activating proteins for heterotrimeric G-protein alpha-subunits. (1996) *Nature* 383: 172-5.
- Wei Y, Lukashev M, Simon DI, Bodary SC, Rosenberg S, Doyle MV, and Chapman HA. Regulation of integrin function by the urokinase receptor. (1996) *Science* 273: 1551-5.
- Weth F, Nadler W, and Korsching S. Nested expression domains for odorant receptors in zebrafish olfactory epithelium. (1996) *Proc Natl Acad Sci U S A* 93: 13321-6.

White JG, Southgate E, Thomson JN, and Brenner S. The structure of the nervous system of the nematode *Caenorhabditis elegans*. (1986) *Philos. Trans. R. Soc. London [Biol]* 314: 1-340.

Williams AF, Tse AG, and Gagnon J. Squid glycoproteins with structural similarities to Thy-1 and Ly-6 antigens. (1988) *Immunogenetics* 27: 265-72.

Winberg ML, Mitchell KJ, and Goodman CS. Genetic analysis of the mechanisms controlling target selection: Complementary and combinatorial functions of netrins, semaphorins, and IgCAMs. (1998) *Cell* 93: 581-591.

Wrana JL. TGF-beta receptors and signalling mechanisms. (1998) *Miner Electrolyte Metab* 24: 120-30.

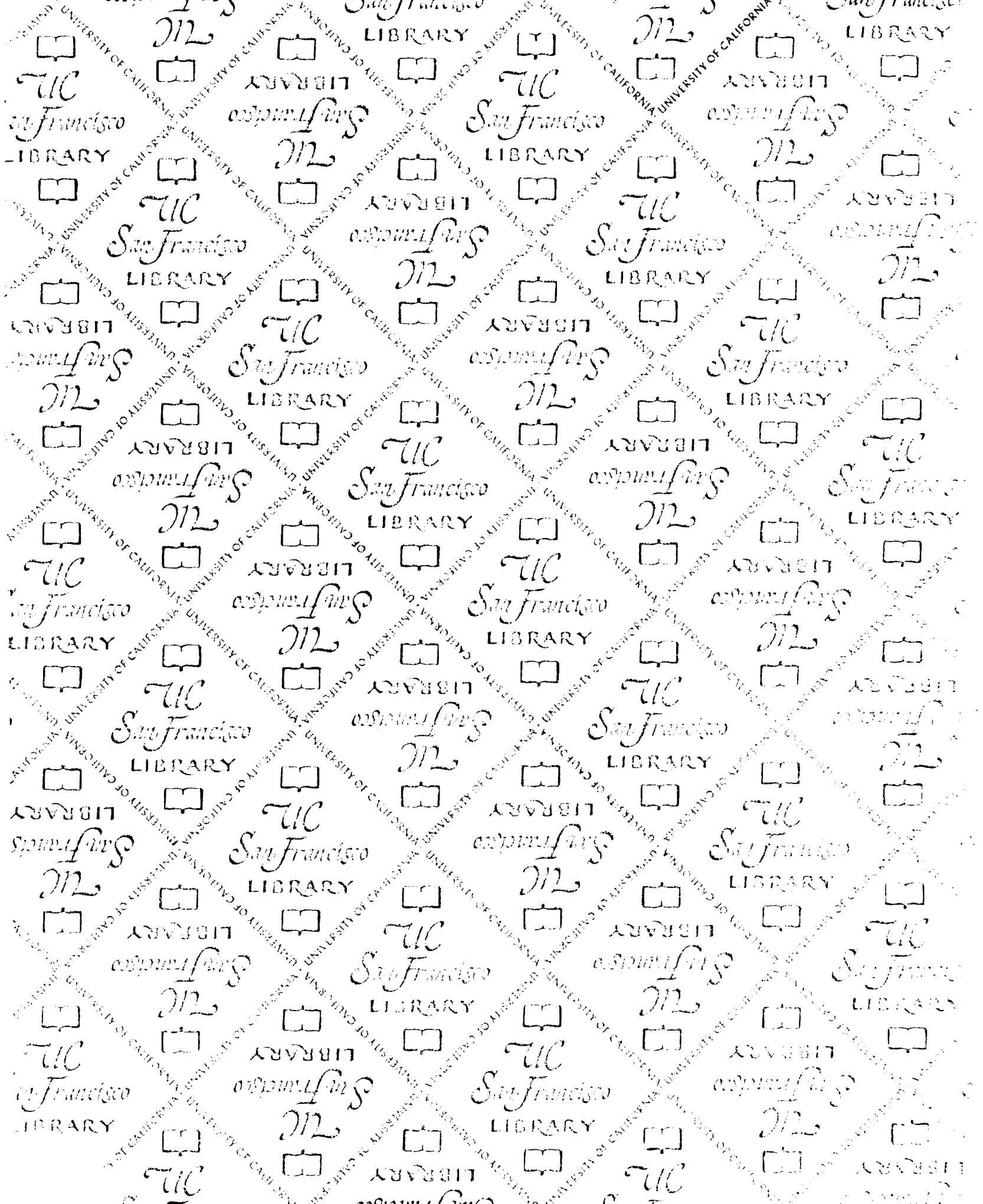
Wright RM, John E, Klotz K, Flickinger CJ, and Herr JC. Cloning and sequencing of cDNAs coding for the human intra-acrosomal antigen SP-10 [published erratum appears in *Biol Reprod* 1990 Nov;43(5):following 903]. (1990) *Biol Reprod* 42: 693-701.

Yan C, Zhao AZ, Bentley JK, Loughney K, Ferguson K, and Beavo JA. Molecular cloning and characterization of a calmodulin-dependent phosphodiesterase enriched in olfactory sensory neurons. (1995) *Proc Natl Acad Sci U S A* 92: 9677-81.

Yan Y, Chi PP, and Bourne HR. RGS4 inhibits G_q-mediated activation of mitogen-activated protein kinase and phosphoinositide synthesis. (1997) *J Biol Chem* 272: 11924-7.

Yu S, Avery L, Baude E, and Garbers DL. Guanylyl cyclase expression in specific sensory neurons: a new family of chemosensory receptors. (1997) *Proc Natl Acad Sci U S A* 94: 3384-7.

Zhao H, Ivic L, Otaki JM, Hashimoto M, Mikoshiba K, and Firestein S. Functional expression of a mammalian odorant receptor. (1998) *Science* 279: 237-42.



For reference

Not to be taken from the room.

